Filamentous phage-derived nano-rods for applications in diagnostics and vaccines

A thesis presented in partial fulfillment of the requirements for the degree of

Doctor of Philosophy

In

Biochemistry

at Massey University, Palmerston North

New Zealand

Sadia Sattar

2013

Dedicated to my parents

Acknowledgements

"In the name of Allah, the Most Gracious, the Most Merciful"

First of all I would like to acknowledge my supervisor Dr. Jasna Rakonjac for her continuous support and critical evaluation of my work throughout my PhD. Indeed it was due to her encouragement and innovative thinking that polished my skills and enabled me to do well. I would also like to thank my cosupervisor Dr. Kathryn Stowell for her valuable feedback. A special thanks to my lab fellows Nicholas Bennett, Wesley Wen, Carel Jobsis and Julian Spagnuolo at helipad. I would also like thank the staff at Institute of Fundamental Sciences; their cooperation and kindness will be treasured always.

I would like to extend my gratitude to my sweet friends Sophia Khanum, Shazrah Salam and Amber Faisal for their continuous support, understanding, cooperation and care; they indeed made things easier for me at the time of stress by just being around apart from giving me valuable suggestions during my research and writing this thesis.

I would like to say thanks to Sadia Tahir, Saima Ejaz and Tina Sehrish for being a sweet part of my social circle in New Zealand. Their presence was treasured and valued always.

A special thanks to my family.

My parents remained a source of contentment for me always, particularly during this course of study. My father's continuous encouragement, support and suggestions for my study throughout these five years is remarkable, I must say **Abbu** very few people can do what you have done for me and the entire family!! You are my biggest inspiration to excel further, thank you so much for being what you are. A special thanks to my **Ammi** for letting me pursue my dream of higher education and bearing my absence with patience, I know mom it was tough for you!

Not to forget the support of my sisters Tanzeela, Adeela, Nadia, and Asia along with the continuous encouragement of my brothers Ibrahim, Ismail, Ishaq and Yaqoob. Lastly I would like to say thanks to my nephew Zaid, and my nieces Eesha, Ayesha Mariyam and cute Rania for their lovely smiles in stressful days.

Abstract

Filamentous bacteriophage, as their name indicates are filament-like bacterial viruses. The F-pilus-specific filamentous phage of *Escherichia coli*, Ff (f1, M13 and fd) are resistant to heat, pH extremes and detergents. Their structural properties and amenability to engineering using recombinant DNA technology have enabled their extensive use in modern biotechnology. For example, Ff can be functionalized by displaying up to five different proteins and peptides on their surface. Ff phage have been successfully employed in diagnostic devices. Moreover, direct use as antigen-carriers is also a subject of interest in vaccine development. However, use of Ff-phage vaccines and in the at-home diagnostic devices is controversial, mainly because of their ability to replicate in gut *E. coli*, and possibility of mobilization and horizontal gene transfer of antibiotic resistance or virulence factor-encoding genes transfer among the gut and environmental bacteria. Moreover, the large length-to-diameter ratio of the virion (1000 nm x 6 nm) impairs diffusion of filamentous phage through complex matrices and could restrict use of filamentous phage in lateral flow diagnostic devices.

To overcome both of these problems we have constructed much shorter, rod-like functionalized particles (50 nm x 6 nm), named “Ff-nano”, which do not carry any genes. The properties of these short particles were investigated, showing that they have superior resistance to heating in the presence of ionic detergent sodium dodecyl sulphate (SDS) in comparison to the full-length phage of the same virion composition. The Ff-nano particles displaying a bacterial Fibronectin-Binding (FnB) protein as fusion to virion protein pIII, localized in five copies at one of the two ends of the virion, were produced and purified. These functionalized nanorods were tested in two applications: as detector particles in a dip-stick-type lateral flow device and as antigen carrier in a vaccine trial. The FnB-displaying nanorods were able to quantitatively detect fibronectin in solution. In the vaccine trial, the Ff-nano particles elicited a weak response to the FnB displayed at a low-copy-number at the nanorod end. In contrast, the response to the major protein pVIII was strong, indicating that the multi-copy display of antigenic peptides along the rod, as fusion to the major coat protein pVIII, is required for using the Ff-nano effectively as vaccine carriers.

Contents

List of Figures

List of Tables

Chapter 1

Literature Review

1.1 Biology of Filamentous Phage: Introduction

Filamentous bacteriophage, as their name implies, are long, filament-like viruses almost 1-2 μm in length and 6-7 nm in diameter. They belong to genus Inovirus and family Inoviridae (King et al., 2011), predominantly infecting Gram-negative bacterial genera such as *Escherichia* (Marvin and Hohn, 1969), *Salmonella*, *Yersinia*, *Pseudomonas*, *Xanthomonas*, *Thermus*, *Neisseria* and *Vibrio* (Calendar and Abedon, 2005; Rakonjac et al., 2011; Russel, 2006). There are only two reports of filamentous phage infecting Gram-positive bacterial species such as *Clostridium acetobutylicum* and *Propionibacterium freudenreichii* (Chopin et al., 2002; Kim and Blaschek, 1991).

Filamentous phage contain collapsed circular single stranded DNA genome that is encapsidated as a two-stranded helix in a long flexible tube composed of repeating subunits of a single major coat protein (Marvin and Hoffmann-Berling, 1963; Newman et al., 1977). The ends of the tube are sealed by two different pairs of minor coat proteins (Figure 1.2) (Model and Russel, 1988; Rowitch et al., 1988). The length of the particle is determined by the size of DNA it encapsulates as well as DNA conformation within the capsid (Marvin, 1990). However, relative efficiency of initiation or termination to elongation of the particle also plays a crucial role in determining the virion length (Lopez and Webster, 1983; Rakonjac and Model, 1998). Filamentous phage genomes are small, with only nine to eleven closely packed genes and an intergenic region (IG) which holds information for DNA replication and assembly of virions (Beck and Zink, 1981; Makowski, 1994; Russel and Model, 1989).

Unlike other bacterial viruses, filamentous phage are assembled and released at the bacterial membranes without killing or lysing the host cell. (Hoffmann-Berling and Mazé, 1964) some of filamentous phage even play critical role in host virulence and biofilm formation as reported for phage CTXϕ of *Vibrio cholerae* (Waldor and Mekalanos, 1996) and Pf4 of *Pseudomonas aeruginosa* (Rice et al., 2008).

Filamentous phage that infect male (F+) strains of *Escherichia coli* are among the best studied filamentous viruses. Most of current knowledge about filamentous phage physiology and genetics is derived from the studies on F pilus-specific phage including f1, M13 and fd (Hoffmann-Berling and Mazé, 1964; Loeb, 1960). Their genomes are 98% identical and they are collectively referred to as Ff phage (Beck et al., 1978; Beck and Zink, 1981; van Wezenbeek et al., 1980). They are also among the most productive of filamentous phage with titres going up to 10^{13} /ml. (Brown and Dowell, 1968; Rakonjac et al., 2011). Ff phage infect their host species by interacting to the tip of primary receptor, the F conjugative pilus, which then retracts bringing the phage to the cell surface so that the infection can proceed (Loeb, 1960; Model and Russel, 1988). Ff replicate as plasmid-like extra-chromosomal replicons called episomes using rolling circle mode of DNA replication, followed by release of virions from infected cells by secretion.

Fully assembled progeny phage particles are released into the culture supernatant approximately 10-15 minutes after infection (Hofschneider and Preuss, 1963) with an exponential production rate of 1000 phage /cell, for first 40 minutes. Later phage release becomes linear with time, as bacteria enter stationary phase. As the infected host population continues to divide and grow indefinitely upon passaging, the phage production continues at a steady rate. Ff infection results in increase of host generation time that result in producing a region of lower cell density by infected cells on a lawn of non-infected cells. These areas of low cell density are recognized on a bacterial lawn as visible, albeit turbid plaques. Many filamentous phage replicate too poorly to affect the host generation time and these phage do not produce visible plaques; hence their visual detection is not possible. Unless otherwise mentioned, the description of phage structure, replication and assembly would be referring to Ff phage collectively.

Although the lysogenic integration in host chromosome is a defining characteristic of temperate bacteriophage which have an alternative lytic cycle, genomes of many filamentous phage, which are non-lytic by their nature, can also integrate into bacterial chromosomes and form "lysogens". These phage, called temperate filamentous phage, follow different strategies for integration, excision and replication of their genome. The common property of the filamentous phage lysogens is that host survives both the "integrated" as well as "induced" states (Kuo et al., 1987). Several Gram-negative

pathogens associated with human diseases usually contain one or more chromosomally integrated filamentous bacteriophage (Gonzalez et al., 2002; King et al., 2011; Mooij et al., 2007). The best studied example of this chromosomal integration and pathogenic contribution is CTXφ phage of *Vibrio cholerae* that encodes major virulence factor of this pathogen, the Cholera toxin (CtxAB) (McLeod et al., 2005; Rakonjac, 2001; Val et al., 2005). In contrast to Ff, the titres upon induction of such lysogenic phage are low (10^6 for CTXφ) (Davis et al., 2000), therefore their detection by plaque formation is difficult. Low productivity is not a generalized principle for all filamentous phage lysogens. Lysogens of Cf1t (*Xanthomonas campestris pv. citri*) and Pf4 (*P. aeruginosa* PA01) produce high titres upon induction (10^{10}) (Kuo et al., 1987; Rakonjac, 2001; Rice et al., 2008). Table 1.1 enlists some examples of different modes of filamentous bacteriophage lifestyles.

Ff filamentous bacteriophage have found enormous applications since they were first discovered. As they have single stranded DNA genome they have been used as DNA sequencing vectors (Vieira and Messing, 1982) as well as model system, for the discovery and study of rolling circle mode of DNA replication (Dotto and Zinder, 1984), *in vitro* translation (Konings et al., 1975; Model and Zinder, 1974), protein targeting to membranes (Chang et al., 1979; Davis et al., 1985), and secretion of proteins from Gram-negative bacteria (Kazmierczak et al., 1994; Linderoth et al., 1997). They have found extensive application in combinatorial technologies. Owing to phage display technology, they are also employed in production of recombinant therapeutic antibodies (Hoogenboom et al., 1998) and in nanotechnology for nucleation of inorganic crystals and quantum dots to synthesize nano-wires as well as other complex nano-shapes (Bhaviripudi et al., 2007; Mao et al., 2003; Mao et al., 2004)

Table 1.1 Filamentous bacteriophage and their life styles*

Name	Host	Temperate	Plaque formation	Titre**	Virulence-associated	Reference
f1* **	*Escherichia coli*	No	Yes	High	No	(Loeb, 1960)
fd* **	*Escherichia coli*	No	Yes	High	No	(Marvin and Hoffmann-Berling, 1963)
M13* **	*Escherichia coli*	No	Yes	High	No	(Hofschneider and Preuss, 1963)
Ike	*Escherichia coli*	No	Yes	High	No	(Khatoon et al., 1972)
If1	*Escherichia coli*	No	Yes	High	No	(Meynell and Lawn, 1968)
If2	*Escherichia coli*	No	Yes	High	No	(Meynell and Lawn, 1968)
MDA	*Neisseria meningitidis*	Yes	Not indicated	Not indicated	Yes	(Bille et al., 2005)
Pf1	*Pseudomonas aeruginosa*	No	Yes	High	No	(Takeya and Amako, 1966)
Pf4	*Pseudomonas aeruginosa*	Yes	Yes	Medium	Yes	(Webb et al., 2004)
Pf5	*Pseudomonas aeruginosa*	Yes	Not indicated	Low	Yes	(Mooij et al., 2007)
CUS1	*Escherichia coli* O18:K1:H7	Yes	No	Low	Yes	(Gonzalez et al., 2002)
CUS2	*Yersinia pestis* biovar *orientalis*	Yes	No	Low	Yes	(Gonzalez et al., 2002)
CTXφ	*Vibrio Cholera*	Yes	No	Low	Yes	(Waldor and Mekalanos, 1996)
Lf	*Xanthomonas campestris pv. Campestris*	No	Yes	High	No	(Tseng and 1990)
B5	*Propionibacte-rium freudenreichii*	No	Yes	Not indicated	No	(Chopin et al., 2002)

*Table adopted from (Bennett, 2010) with permission.

** Titre= highest serial dilution of phage stock that gives a positive signal.

***The three F-pilus-specific filamentous phage of *E. coli* are referred to as Ff phage and used interchangeably. Their genomic sequence is 98% identical.

1.2 Ff Filamentous Bacteriophage Genome

Ff filamentous bacteriophage (f1, fd and M13) contain ssDNA genome of around 6400 nucleotides, that consists of nine closely packed open reading frames (ORFs) encoding 11 proteins (Beck et al., 1978; Beck and Zink, 1981; Hill et al., 1991) and a non-coding intergenic region (IG). IG region contains origin of replication for (+) and (-) strand synthesis and an imperfect 32-base-pair hairpin containing packaging signal (PS) (Dotto and Zinder, 1983; Schaller et al., 1969) (Figure 1.1). All gene products are essential for virus replication and encapsulation (Hohn et al., 1971; Rapoza and Webster, 1995). Phage genes I and II carry internal translational initiation sites that encode in-frame restart proteins XI and X, respectively.

Phage genes can be divided in to three main categories. Category one includes genes whose product is required for the phage DNA replication and formation of ssDNA complex that serves as a packaging substrate (*gII*, *gX* and *gV*). The second category includes genes that are required for phage assembly and release from the host cell (*gI*, *gXI* and *gIV*). Third and last category includes the phage genes whose protein products are structural components of phage capsid (*gIII*, *gVI*, *gVII*, *g VIII* and *gIX*) (Table 1.2).

All phage genes are transcribed simultaneously resulting in steady accumulation of phage proteins. The two operons (*gII-gV-gVII-gIX-gVIII* and *gIII-gVI-gI-gIV*) are transcribed in the same direction with (+) strand corresponding to sense strand. There are only two terminators one at the end of each operon, preventing read-through (Rakonjac, 2001). The differential expression of phage proteins is ensured by differences in ribosomal binding site strengths and accessibilities, as well as varied promoter regulations (Blumer et al., 1987; Blumer and Steege, 1989). Phage proteins pII and pVII are required in lower amounts. An inherently defective translation initiation site in *gVII* mRNA leads to its controlled production and is coupled to its upstream gene (Ivey-Hoyle and Steege, 1989, 1992), whereas transcription of *gII* is limited by a weak rho-dependent termination signal at the beginning of the gene. Greater amount of infrequently used codons in the mRNA of *gII* further ensures less protein product. On the other hand are genes whose protein products are required in large quantities such as *gVIII* and *gV*. Transcription from multiple nested promoters in

each operon results in high amount of transcripts from genes closer to terminators. These transcripts are processed by varied RNA processing mechanisms utilizing RNaseE that stabilize corresponding RNAs, but not the RNAs of the low-abundance genes in the operons (Goodrich and Steege, 1999; Stump and Steege, 1996). Overall, these regulatory mechanisms result in high production of ssDNA-binding protein pV and major coat protein pVIII.

In later stages of infection, when pV accumulates to a greater concentration, it binds to a specialized tetraplex structure in mRNAs encoding *gII* and *gX* (Oliver et al., 2000) repressing their translation and reducing the pII and pX protein levels in the host cell which in turn results in lowered production of phage DNA replicative forms (Fulford and Model, 1988a, b; Mullis et al., 1986) shifting the balance towards formation of ssDNA-pV complex and phage assembly. As a result of this negative feedback loop on pII and pX translation by pV, a dynamic balance between phage DNA and protein production is maintained; where DNA synthesis is balanced by phage assembly and secretion as well as host cell division.

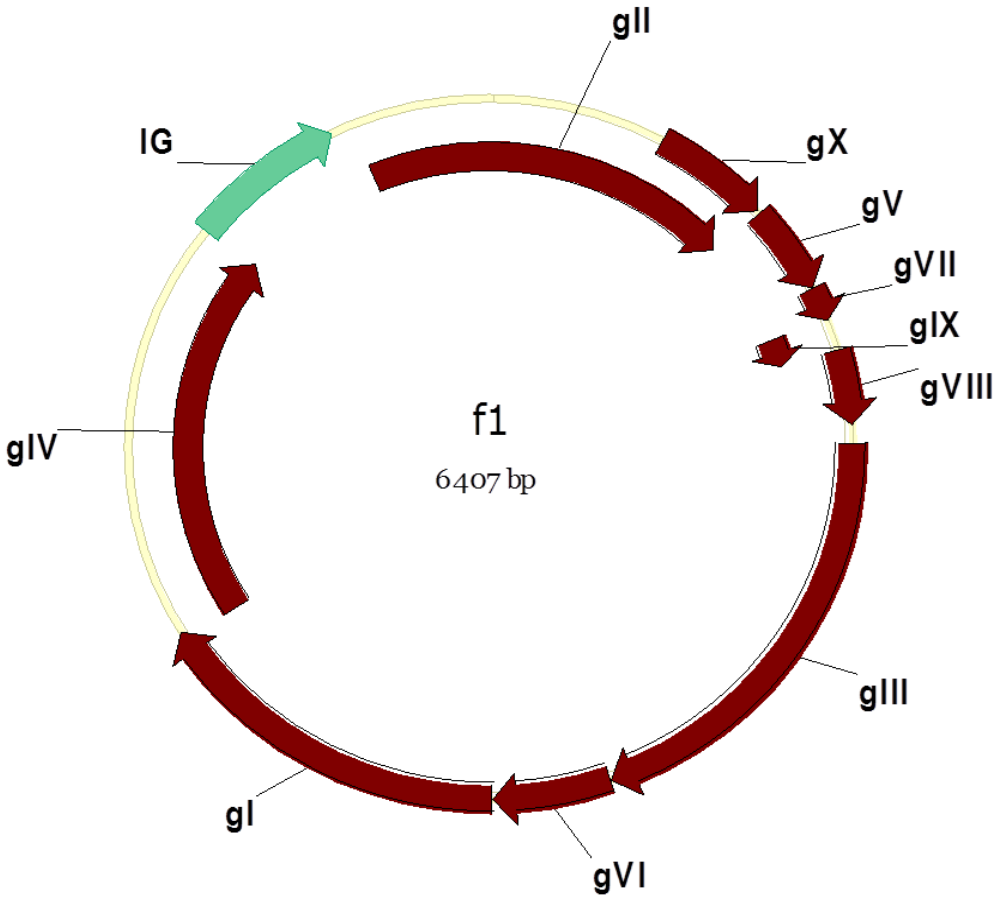

Figure 1.1 Map of f1 genome. The positions of genes are indicated. IG; Intergenic region marked between *gII* and *gIV*. Genes are symbolized by a lowercase "g" as a prefix to the appropriate roman number (e.g. *gIII*) Phage protein products are symbolized by a lowercase "p" as a prefix (e.g. pIII; Table 1.2).

Table 1.2 Ff filamentous phage genes/proteins and their properties

Gene	Protein	Size (aa)*	Function	Location
gI	pI	348	Inner membrane assembly protein	Inner membrane
	pXI	108	Inner membrane assembly protein	Inner membrane
gII	pII	410	Replication protein of Rep family (Strand transferase)	Cytoplasm
	pX	111	Replication	Cytoplasm
gIII	pIII	406	Minor virion protein	Virion end (distal end)
gIV	pIV	405	Assembly (outer membrane channel)	Outer membrane
gV	pV	87	Replication (ssDNA complex)	Cytoplasm
gVI	pVI	113	Minor virion protein	Virion end (distal end)
gVII	pVII	33	Minor virion protein	Virion end (proximal end)
gVIII	pVIII	50	Major coat protein (virion)	Virion filament
gIX	pIX	32	Minor virion protein	Virion end (proximal end)

*Amino acids

1.3 Structure of Filamentous Phage Virion

The structure of filamentous phage was resolved using X-ray diffraction, atomic force as well electron microscopy (Figure 1.2). Filamentous phage are long tube-like viruses with a fixed diameter of 6-7 nm. The length of the virion is determined by the amount of the packaged DNA. A typical 6400 nucleotide ssDNA is packaged in to almost 930 nm long tube (Russel, 2006) whereas a small microphage variant of 221 nucleotides is packaged as a 50 nm particle (Specthrie et al., 1992). There is no fixed limit to how much DNA can be packaged as in the case of icosahedral viruses, however filamentous phage particles carrying two sets of 6.4kb genome produce very fine plaques indicating their poor production. Larger phage almost twenty-fold longer than wild-type phage can be produced by mutants of minor coat proteins required for initiation (pVII/pIX) or termination (pIII/ pVI) of assembly (Lopez and Webster, 1983; Rakonjac and Model, 1998) but some of these are non-infectious and vulnerable to mechanical damage (e.g. from vortexing) (Russel et al., 2004).

In all Ff virions, the virus coat is composed of five proteins (pIII, pVI, pVIII, pVII, pIX). The protein tube that surrounds the ssDNA genome is composed of 2700 copies of helically arranged single major coat protein pVIII only 50-aminoacids in length (Newman et al., 1977; Pratt et al., 1969). Both ends of the filament are distinguishable as indicated by electron micrographs (Figure 1.2). The end where assembly starts referred as proximal end of virion is composed of two small proteins pVII and pIX (33 and 32 amino acids long respectively); in absence of either hardly any phage particles are formed. The distal end which is required for infection and stability is composed of pIII and pVI (406 and 113 amino acids respectively) (Endemann and Model, 1995; Gailus and Rasched, 1994; Grant et al., 1981a; Grant et al., 1981b; Gray et al., 1978; Rakonjac et al., 2011; Rakonjac and Model, 1998).

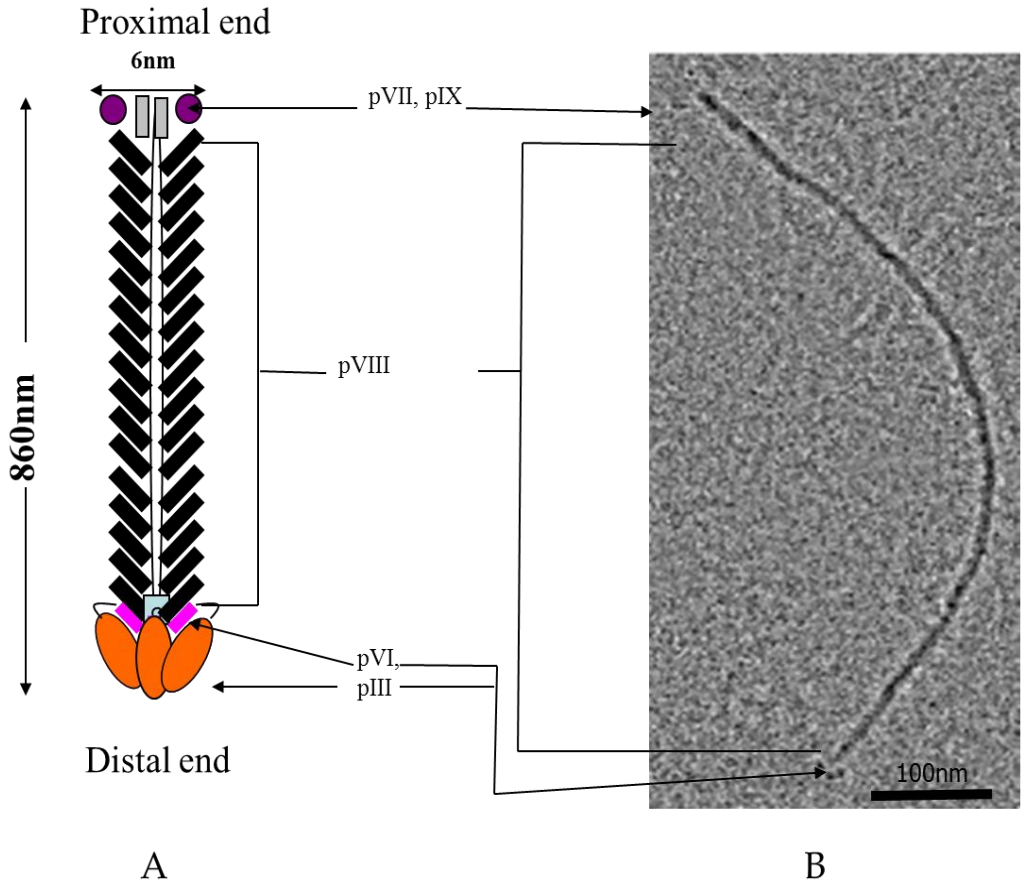

Figure 1.2 Structure of filamentous phage virion. **A).** Schematic representation of the virion. **B)** Electron Micrograph of the Ff phage. Proximal end of virion contains minor coat proteins pVII and pIX. Major coat protein pVIII forms the main cylinder of virion filament. Minor coat proteins pIII and pVI form the capping complex at the distal end of the virion. Transmission electron micrograph was adopted from (Gray et al., 1979) with permission.

1.3.1 Major Coat Protein pVIII

The long flexible capsid tube of filamentous phage is composed mainly of repeated units of a small protein, product of gene VIII, called pVIII. The structure, orientation composition and arrangement of pVIII in solution as well as in virion is extensively studied mainly because of its role in discovery and characterization of mechanism of protein integration in lipid bilayer (Hemminga et al., 1993); employing sophisticated techniques such as X-ray fiber diffraction and solid-state NMR (Opella et al., 2008) .

In Ff phage the mature product of *gVIII* is 50 amino acids in length with a 23 amino acid signal sequence which directs it to SecYEG/ YidC translocator (Samuelson et al., 2001). This signal sequence is cleaved upon insertion in to the membrane (Russel and Model, 1982). Each pVIII molecule overlaps like a fish-scale with its neighbors to form a right handed helix, with each subunit oriented at 20° angle from the main virion axis (Marvin, 1998b). Each pVIII molecule has three regions; an N-terminal acidic domain, a central hydrophobic section and a C-terminal basic domain (Model and Russel, 1988) (Figure 1.3). All pVIII molecules are integrated in inner bacterial membrane prior to assembly using C-terminal hydrophobic trans-membrane helix, with a C-terminal tail in cytoplasm and N-terminal portion in the periplasm (Rakonjac et al., 2011; Vos et al., 2009; Wickner, 1975). Inside membrane as well as in virion first 4-5 negatively charged N-terminal residues are unstructured, whereas the remaining part is a slightly curved α- helix (Makowski and Russel, 1997). The N-terminal disordered segment is exposed on the surface, whereas C-terminal basic residues are on the interior of the tube, interacting with DNA phosphates (Greenwood et al., 1991 ; Hunter et al., 1987; Marvin, 1978) .

Interactions between hydrophobic mid-sections of adjacent pVIII molecules as well as between amphipathic regions of N-terminal portion of one subunit and hydrophobic regions of C-terminal helix of neighboring subunit are basis for holding the virion together (Roth et al., 2002) (Figure 1.3B). In Ff filamentous phage pVIII subunits are arranged in a five-start helix (Class I of symmetry of helical viruses) with 2-fold screw axis. Each ring in virion tube carries five pVIII subunits (5-fold rotation axis) (Caspar and Makowski, 1981; Marvin et al., 2006) (Figure 1.3).

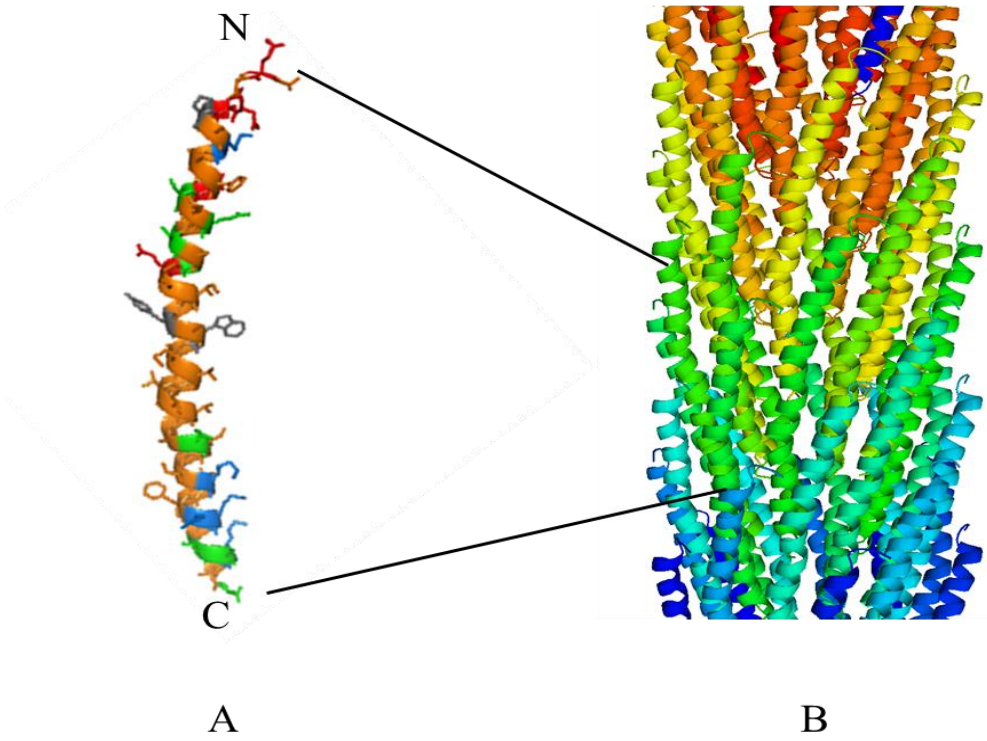

Figure 1.3 Ribbon model of major coat protein pVIII. A). Arrangement of various amino acid residues in pVIII monomer; hydrophobic (green), positively charged (blue), hydrophilic residues (orange) and negatively charged residues are represented in red, **N** and **C** termini are indicated. **B)** Arrangement of pVIII monomers within the virion capsid; pVIII molecules overlap within the virion filament as fish-scales making a shingle like array of α-helices.

Images are obtained from coordinates of the RSCB PDB accession number 2cOw using PyMOL (DeLano, 2006; Marvin et al., 2006) adopted from (Bennett, 2010; Rakonjac et al., 2011) with permission.

1.3.2 Minor Coat Proteins

As indicated by electron micrographs, each end of virus has a distinct morphology. The proximal end of virus particle which is extruded first during the phage secretion from *E. coli* is composed of 3-5 copies of two minor coat proteins, pVII and pIX. The distal end of the filament required for both the termination of assembly and infection of the host is composed of five copies of two minor coat proteins, pIII and pVI.

Minor Coat Proteins pVII and pIX

In contrast to pVIII, very little is known about the ends of filament, probably due to high length to width ratio of the long filament. In Ff both pVII and pIX are small ribosomally translated proteins only 33 and 32 amino acids in length, respectively, and are located at the proximal end of the virion (Figure 1.2). Both are integral membrane proteins prior to assembly; however they are synthesized without a signal sequence and are thought to spontaneously integrate in membrane (Endemann and Model, 1995; Grant et al., 1981b). The detailed structure of these proteins is not resolved; however they are predicted to be hydrophobic α helices just like pVIII, which suggests that they interact with pVIII through hydrophobic interactions in a similar fashion as adjacent pVIII residues interact with each other (Marvin, 1998a). The exact arrangement of these proteins in the virion is not known. Genetic analysis indicates that C-terminal residues in these proteins interact with the packaging signal (an ssDNA hairpin loop at one of the termini of the packaging substrate, the pV-DNA complex). They are required for initiation of assembly and in their absence the only virions that are formed are derived from recycled pVII and pIX of the incoming phage that infected the cell (Russel and Model, 1989; Webster and Lopez, 1985). Since the N-termini of both of these proteins have been used to display antibody variable regions, this suggests that they are exposed to or at least are near to the surface of the virion. Furthermore, the inserted sequence results in targeting and display only if it is fused to an upstream (heterologous) N-terminal signal sequence, which becomes cleaved by signal peptidase during the SecYEG-dependent transport, displaying the inserted (displayed) protein at the very N-terminus (Gao et al., 2002; Gao et al., 1999; Huang et al., 2005).

Minor Coat Protein pIII and pVI

The distal end of the virion, also referred to as a 'cap' is somewhat pointed and appear to contain lollipop-like knobbed structures (Gray et al., 1981). Total number of each of the two proteins pIII and pVI remained a matter of debate. Electron micrograph data by Gray et al. (1979)combined with an overestimate of pIII molecular weight in older literature suggested that there were three pIII molecules in the cap complex (Gray et al., 1979). Once the genome sequence became available, the correct calculation of molecular weight calculations (~ 46 KDa) suggested at least five pIII molecules at this end (Grant et al., 1981b). This is now confirmed by the ZnS-labeling of the pIII termini using the ZnS nanocrystal-nucleating peptide displayed at pIII N-terminus that showed five ZnS quantum dots at the pIII virion end (Lee et al., 2002). Since pIII and pVI are equimolar in the virion cap (Grant et al., 1981b), five molecules of pVI are expected to be present at this end, thus maintaining the five-fold symmetry of pVIII arrangement in the virion tube (Rakonjac et al., 2011). Both pIII and pVI are integral membrane proteins prior to their incorporation in the virion (Boeke and Model, 1982; Endemann and Model, 1995). This end mediates virion entry as well as exit from the host cell and is also required for virion stability (resistance to ionic detergents).

PVI is larger (113 amino acids) than pVII and pIX, yet it is largely hydrophobic. Like all other capsid proteins, pVI is a trans-membrane protein prior to its integration in the virion, however it is synthesized without a signal sequence and is thought to be targeted to the host inner membrane in a SecA-independent manner (Endemann and Model, 1995). The protein is predicted to contain three trans-membrane α helices, with N-terminal in the periplasm and C-terminal in the cytoplasm (Krogh et al., 2001). Intact phage particles do not react with antibodies specific to the C-terminus of pVI, indicating that this portion is probably buried inside the virion (Endemann and Model, 1995). However, it was shown that pVI fusions at the C-terminus can be incorporated in the virion with low efficiency, indicating at least some portion of protein is surface-exposed. Both proteins, pIII and pVI can be isolated together as a complex from phage particles (Gailus and Rasched, 1994). Since pVI is degraded in cells that lack pIII, it is evident that these proteins interact with each other in the membrane, however pIII/pVI complex could not be detected from the infected cells (Rakonjac et al., 1999), indicating that proteins undergo some conformation change when incorporated in the

virion that imparts additional stability to the pIII/pVI complex in the virion (Calendar and Abedon, 2005). Moreover, pVI is also essential to incorporate pIII in the virion (Rakonjac et al., 1999) and to form stable phage particles, as its absence results in production of long unstable polyphage (Lopez and Webster, 1983).

PIII has received a lot more attention than pVI, probably because of its role in phage infection and its extensive use as a display platform in phage display technology (Kay et al., 1996; Russel et al., 2004; Smith and Petrenko, 1997). The structure of pIII is resolved in detail and in contrast to other phage coat proteins it is hydrophilic. It is largest of the virion coat proteins and is synthesized with an 18 amino acid N-terminal signal sequence and requires SecYEG bacterial export channel for membrane insertion (Rapoza and Webster, 1993) . Mature pIII is approximately 42 kDa protein, 406 amino acids in length. Protein folds in three distinct domains, two N-terminal domains named N1and N2 and a C-terminal (C) domain, each separated by glycine-rich flexible linkers (Figure 1.4).

The trans-membrane C-terminal domain, 149 residues in length, contains a 15-residue hydrophobic α helix (membrane anchor) that, upon assembly termination, becomes buried inside the phage particle. The retention of pIII in the host membrane is dependent upon the overall hydrophobicity of the domain and not the exact sequence (Boeke and Model, 1982; Davis et al., 1985; Davis and Model, 1985; Marvin, 1998a; Rakonjac et al., 1999). Prior to assembly into the virion, apart from the C-terminal membrane anchor and the 5 C-terminal residues that are in cytoplasm, most of the protein extends in to periplasm. The C-terminal 132-residues are essential for pIII incorporation into filamentous phage and termination of assembly process from host cell, whereas 93 residues on C-terminal are required for phage release from the virion (Crissman and Smith, 1984; Makowski and Russel, 1997; Rakonjac et al., 1999; Stengele et al., 1990). Phage genomes with *gIII* deletions or carrying 83 residues of C-terminal domain result in production of phage particles that are not released from the host cell, instead they tether along the bacterium surface as long filaments. These filaments are likely to break-off by mechanical shearing and do not contain pIII, hence they are unstable and disassemble by detergents such as Sarkosyl (Rakonjac et al., 1999). It is also known that C-terminal domain has an essential role in phage infection.

Phage particles carrying 83 residues of the C-domain coupled to both N-domains were found to be non-infectious, as well as particles containing 93 and 110 residues of the C-domain fused to N1N2. The shortest C-domain segment that can mediate infection is 121 nucleotides in length (Bennett and Rakonjac, 2006).

The two N-terminal domains of pIII are required for filamentous phage infection and are responsible for knob-like appearance on the tip of phage. These 'knobs' represent N1N2 domains that interact with each other (Armstrong et al., 1981) and can be removed by subtilisin treatment, rendering the remaining particle (that contains the complete C-domain) non-infectious. Moreover, N1N2 domains are found to be separated from the phage body by flexible linkers (Gray et al., 1979). When N1-N2 portion of pIII is expressed separately from the rest of the protein, it forms a compact complex, as determined by X-ray crystallography as well as NMR spectroscopy (Armstrong et al., 1981; Boeke et al., 1982; Crissman and Smith, 1984; Holliger et al., 1999; Lubkowski et al., 1998; Riechmann and Holliger, 1997; Stengele et al., 1990) (Figure 1.4). Moreover, X-ray crystallography resolved a complex between N1N2 domains of pIII and Tol A protein, the phage co-receptor in the periplasm (Lubkowski et al., 1999). In contrast to N1, the N2 domain is found to interact with the primary phage receptor, the F-pilus (Caro and Schnös, 1966). This N2 - F-pilus interaction results in a conformational change that dissociates N1-N2 complex and exposes the N1–Tol A binding site that is present at the interface between N1 and N2, and is covered by N1 before F-pilus binding (Deprez et al., 2005).

The N1N2 domains are not required for resistance of the virion cap to detergent, consistent with their loose attachment to the virion cap. It is not yet resolved whether C-terminal domain of pIII alone or its complex with pVI is responsible to impart resistance to detergents and cause both the excision from the membrane during termination of assembly process and membrane insertion during infection. However they form a tight complex at the cap end of virion, that remains stable even after virion dissociation with a combination of surfactants (deoxycholate) and organic solvents (chloroform) (Gailus and Rasched, 1994). Structural modeling suggests similarity of the C-domain to the α-helical pore-forming toxins such as diphtheria toxin (Bennett and Rakonjac, 2006).

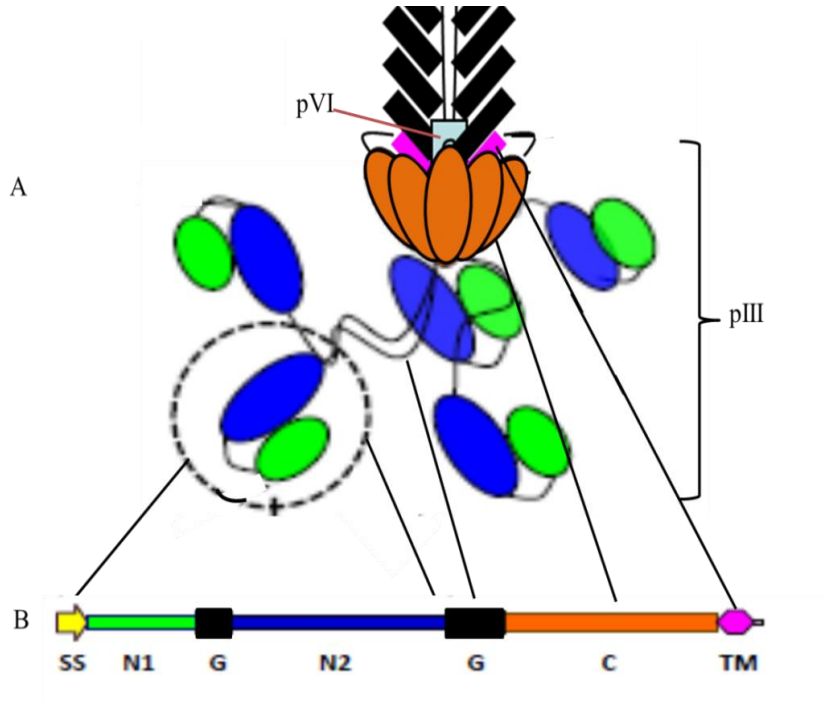

Figure 1.4 Schematic presentation of pIII. **A).** Arrangement of pIII domains in virion; **B)** Domain organization of pIII pre-protein, N1, N2 and C domains of pIII, SS; signal sequence, G; glycine-rich flexible linkers. Same domains are presented in mature virion in corresponding colors. Figure adapted from (Rakonjac et al., 2011) with permission.

1.4 Morphogenetic Proteins: pI, pXI, pIV

Products of *gene I*, *gene XI*, and *gene IV* (pI, pXI and pIV respectively) are required for the assembly of filamentous phage, but are not present in the intact virion (Russel, 1991), nor are they required for DNA replication (Pratt and Erdahl, 1968). pI is a 348-amino-acid integral membrane protein synthesized without a signal sequence. It possess a centrally located hydrophobic trans-membrane α-helix that serves as a membrane anchor to direct pI to membrane in a SecA-dependent manner (Rapoza and Webster, 1993). Protein pI spans the membrane with 75 residue C-terminal domain in the periplasm, and N-terminal 250-amino acid domain in the cytoplasm (Guy-Caffey et al., 1992). This N-terminal cytoplasmic domain has a putative ATP-binding domain that is essential for assembly. The detailed analysis of protein is hampered due to its extreme toxicity to host cells; however it has been shown to be required for making phage-specific "adhesion zones" where both inner and outer membranes of host *E. coli* are in contact. These contact sites, referred to as exit sites, are essential for assembly (Feng, 2000; Horabin and Webster, 1988). Translation initiated from an internal ATG in *gI* results in pXI, whose sequence is exactly the same as the C-terminal domain of pI; covering the membrane anchor and the periplasm domain, however it lacks the internal cytoplasmic domain. pXI is 108 amino acids in length and is essential for phage assembly, however its function is not yet known (Haigh and Webster, 1999).

PIV is a large protein, around 405 amino acids in length, and is synthesized with a 21 residue signal sequence which is cleaved upon translocation through the inner membrane. This protein makes a large 14 subunit barrel-like complex in the outer membrane, around 13.5 nm in diameter and 12 nm high (Opalka et al., 2003). This barrel can be differentiated into three stacked rings (N, M and C) and a central pore that is interrupted by a septum in the middle ring. The internal diameter of channel is around 8.8 nm, sufficient diameter to transport 6-7 nm filamentous phage particle (Marciano et al., 2001). This diameter, however, could be a limiting factor in pVIII display of large protein domains. pIV is homologous to several Gram-negative transport channels "secretins" (Bayan et al., 2006). Together with pI and pXI in the inner membrane, pIV in the outer membrane forms the assembly-secretion site for the concurrent assembly and transport of phage particles across the bacterial membranes.

1.5 DNA Metabolism Proteins: pII, pX and pV

The product of *gII* is 410 amino acids-long protein designated as pII. Parental DNA strand which is converted to double strand DNA by host enzymes is called replicative form and acts as template for the synthesis of pII, which is the first protein synthesized after the filamentous phage infection in the host bacterium. It is a site-specific strand-transferase of the Rep family that is essential for replication of the positive strand, which is packaged into the virion. Therefore pII is required for infection cycle, as the initial RF form cannot produce positive strand ssDNA for packaging without this protein (Greenstein and Horiuchi, 1989; Horiuchi, 1997). Phage pX, a 111 amino-acid protein, is synthesized as an internal translation initiation product of *gII*, starting at codon 300 which is in the same frame as *gene II* ATG, hence it has same sequence as the C-terminal third of pII and is essential for balance of DNA replication and ssDNA packaging (Fulford and Model, 1984; Makowski and Russel, 1997; van Wezenbeek et al., 1980)

Protein pV, usually referred to as ssDNA-binding protein, is an 87 amino acid-long cytoplasmic protein. The pV dimer has largely β-strand structure, having five antiparallel β-sheets and two antiparallel β-ladder loops. During the late stages of phage life cycle, pV accumulates to a concentration that allows dimerization. Dimer has a high affinity for ssDNA, to which it binds a dimer. This binding collapses circular ssDNA into a quasi-duplex by each pV monomer binding one DNA strand. Assembly of this pV-ssDNA complex (that occurs in the cytoplasm) starts from the hairpin loop, "zipping" the ssDNA circle into a rod that serves as a packaging substrate for assembly into the filamentous virions (Alberts et al., 1972; Oey and Knippers, 1972). Coating of phage ssDNA by pV also blocks the negative strand origin of replication, thereby preventing its conversion to RF-form (Pratt and Erdahl, 1968; Salstrom and Pratt, 1971).

1.6 Ff Phage Life Cycle

Ff filamentous phage replicate as episomes in the host cells, which result in production of large phage progeny. Unlike lysogenic phage, Ff phage genomes do not encode the

lysis regulatory proteins. The life cycle of Ff filamentous phage can be divided in to three distinct stages: infection, replication and assembly with simultaneous secretion of phage particles from the host cells. Each section involves different phage proteins.

1.6.1 Infection

Ff Filamentous phage infection is mediated by a complex series of trans-membrane transactions which is poorly understood, apart from identifying host receptors, tip of F-pilus and periplasm domain III of protein TolA. The infection process begins with the adsorption of filamentous phage to the tip of primary host receptor; the F-pilus that is long, filamentous cell surface appendage resembling Ff phage themselves. There are several different kinds of pili used by different filamentous phage. Ff filamentous phage use conjugative F-pili which themselves are involved in horizontal gene transfer between bacteria (Loeb, 1960; Marvin and Hoffmann-Berling, 1963; Silverman, 1997). The initial adsorption to the F-pilus is mediated by one of the two N-terminal domains (N2) of pIII (Deng and Perham, 2002) (Figure 1.5). Filamentous phage binding to F-pilus was thought to mediate the pilus retraction, however it is now known whether they are dynamic structures continuously assembling and disassembling on their own, or whether disassembly is triggered by phage binding (Clarke et al., 2008). Once phage is bound to the pilus tip it starts retracting, bringing the phage closer to secondary receptor in periplasm (Jacobson, 1972). The secondary receptor for Ff filamentous phage is highly conserved inner- membrane protein complex of Gram-negative bacteria called TolQRA complex (Click and Webster, 1998). TolQRA is a component of Tol-Pal complex involved in maintenance of cell membrane integrity during cell division in Gram-negative bacteria (Cascales et al., 2007). TolA is integrated in inner membrane and is known to interact with two other proteins (TolQ & TolR) to make a complex (Webster, 1991). Absence of any of the proteins of TolQRA complex renders host cell resistant to phage infection, which indicates necessity of this complex for infection process (Click and Webster, 1997; Click and Webster, 1998; Sun and Webster, 1986). Binding of pIII N2 domain to the pilus mediates a conformation change in pIII N1-N2 complex (Eckert et al., 2005), thereby releasing N1 domain from N2 and exposing the interface residues between two domains to allow N1 interaction with domain III of TolA protein in TolQRA complex (Deng and Perham, 2002; Lubkowski et al., 1999; Riechmann and Holliger, 1997). The exact chain of events that

follows the pilus contraction up till interaction of pIII N1 domain with TolA is unknown. TolQRA complex mediates depolymerization as well as insertion of phage coat proteins into the inner bacterial membrane and translocation of ssDNA across the membrane into the cytoplasm by a poorly understood mechanism (Armstrong et al., 1983; Russel et al., 2004; Russel et al., 1988). It is also evident that three C-terminal α helical domains (two hydrophilic and one hydrophobic anchor) and two N-terminal domains (N1, N2) covalently linked with each other at a specific distance are indispensable for phage infection (Bennett and Rakonjac, 2006; Krebber et al., 1997; Spada et al., 1997). Any phage having insertion of domains in between N and C terminal domains are poorly infective (Heilpern and Waldor, 2003) (Figure 1.5).

1.6.2 Replication

Once the virus ssDNA (the (+) strand) enters the cytoplasm of host cell, the complementary strand is replicated and the resulting circular double-stranded DNA is converted in to a supercoiled form called the replicative form (Mullis et al., 1986) . Host RNA polymerase uses the (+) strand as a template to synthesize a 20 nucleotide primer which initiates at the negative (-) strand origin of replication in non-coding intergenic region (IG) of viral ssDNA (Brutlag et al., 1971; Geider and Kornberg, 1974; Higashitani et al., 1996; Horiuchi, 1997). The priming site ((-) strand origin of replication) consists of two hairpins that are separated by a stretch of single-strand DNA (labeled as B and C in Figure 1.6). First hairpin resembles -35 promoter sequence (B) whereas second has a -10 motif (C) in its structure, mimicking the double-stranded promoters to which the RNA polymerase normally binds to initiate transcription (Horiuchi, 1997). Host RNA polymerase binds to this promoter-mimic with higher affinity in comparison to regular promoter sequences within the bacterial genome (Higashitani et al., 1997), however this (-) origin of replication is not absolutely essential for initiation of (-) replication, as RNA primer can be synthesized at other places in phage genome with low efficiency (Kim et al., 1981) . The short 20 nucleotide RNA primer is used by host DNA polymerase to synthesize the (+) strand. After synthesis the new strand is ligated by host ligase and double-stranded DNA is supercoiled by gyrase thus converting it to replicative form (Mullis et al., 1986) which acts as a template for (+) strand replication and phage gene expression (Figure 1.6).

Further replication of RF requires the synthesis of pII, a phage encoded endonuclease-topoisomerase. pII makes a nick at specific site in the IG region called (+) strand origin of replication and binds to the 5' end, hence allowing host DNA polymerase to bind free 3' end and start rolling-circle mode of DNA replication that results in synthesis of (+) strand of viral DNA using (-) strand as a template and displacement of the "old" ssDNA circle (Asano et al., 1999; Greenstein et al., 1988; Horiuchi, 1997; Meyer and Geider, 1982). Plus-strand origin of replication is absolutely required for initiation as well as termination of replication (Greenstein and Horiuchi, 1989; Horiuchi, 1997), even point mutations in this region result in 10,000 fold decrease in positive strand synthesis (Dotto et al., 1981; Dotto and Zinder, 1984). The (+) strand origin of replication (*ori*) consists of two regions designated as I and II (figure 1.5). Region I is the core region for the initiation of (+) strand replication as it contains the pII nicking site (5780), as well as initiation and termination sites as two hairpin loops (D and E; figure 1.5). The region II of (+) strand *ori* is also required; however mutations in this region are tolerated. Once the new (+) strand is synthesized the old strand is displaced through the strand-transfer reaction by pII, which is then recycled and converted to RF or later in the life cycle coated by pV to serve as a packaging substrate for phage assembly (Figure 1.5 and 1.6).

As the phage DNA replication progresses there is an exponential increase of phage proteins in host cytoplasm which results in accumulation of phage single-strand DNA binding protein pV. Once pV reaches a threshold concentration it starts binding newly synthesized ssDNA (+) strands, thereby preventing their conversion to replicative forms (Alberts et al., 1972; Cavalieri et al., 1976; Mullis et al., 1986; Pratt et al., 1974). PV also has a regulatory function as it inhibits *gII* and *gX* mRNA translation (Michel and Zinder, 1989). Back to back binding of pV dimers collapses ssDNA in to a rod like structure, with packaging signal protruding out as a hairpin loop and is the only region of ssDNA that is exposed to exterior (Bauer and Smith, 1988; Gray, 1989). This pV-ssDNA complex appearing like a flexible filament in electron micrographs is the substrate for phage assembly (Bauer and Smith, 1988; Gray, 1989). Packaging or morphogenetic signal directs the pV-ssDNA complex to the phage export machinery in the inner and outer membrane of host bacterium.

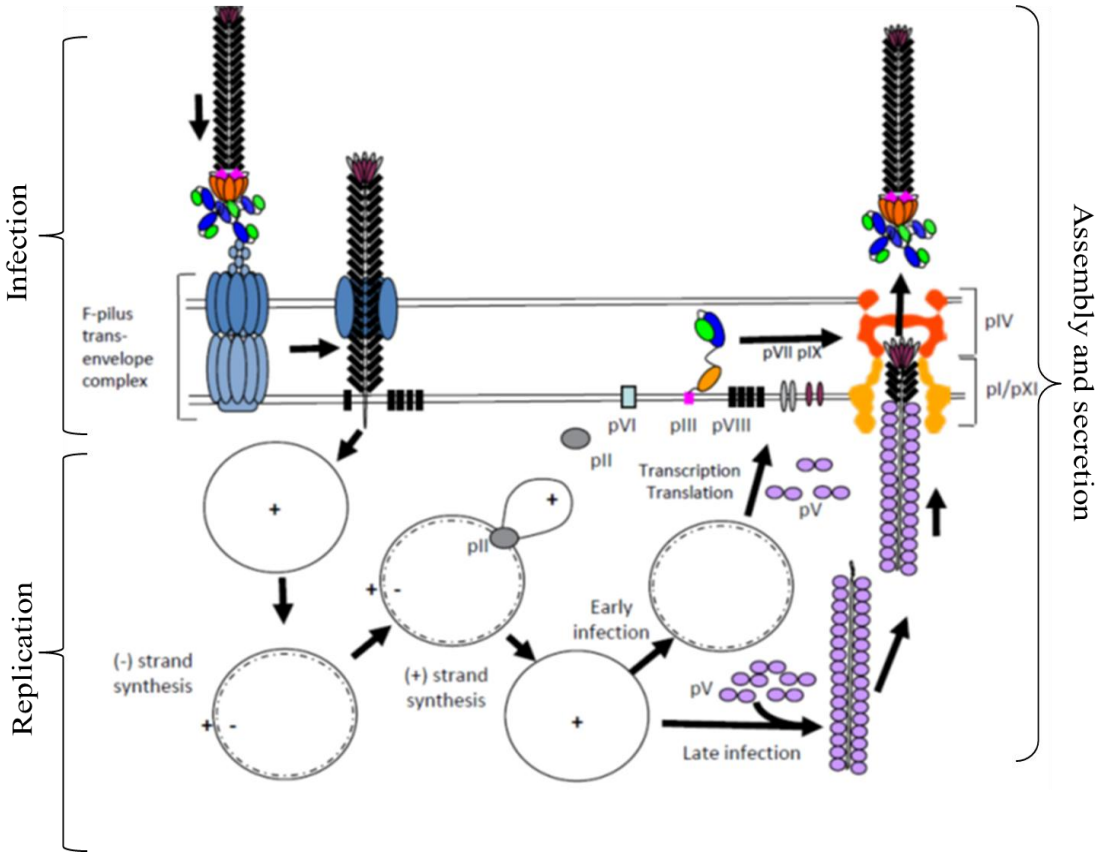

Figure 1.5 Schematic overview of filamentous phage life cycle. Phage pIII interacts with F-pilus on bacterial surface and injects its ssDNA into host cytoplasm (Infection). This ssDNA is converted to replicative form by the action of host RNA ad DNA polymerases. (+) strand after coating with pV (ssDNA binding protein) is converted to pV-ssDNA complex that contains an exposed hairpin loop, the packaging signal. Meanwhile, all proteins required for assembly and virion capsid formation are synthesized from the RF form as a template and directed to membrane. The ssDNA-pV complex is directed to assembly complex composed of pI, pXI and pIV. As the complex reaches inner membrane component of assembly machinery (pI/pXI), the pV molecules are replaced by pVIII residues. Once the complete genome is coated with pVIII, termination proteins pIII and pVI are added and the virion is released from the host cell. Figure adapted from (Rakonjac et al., 2011) with permission.

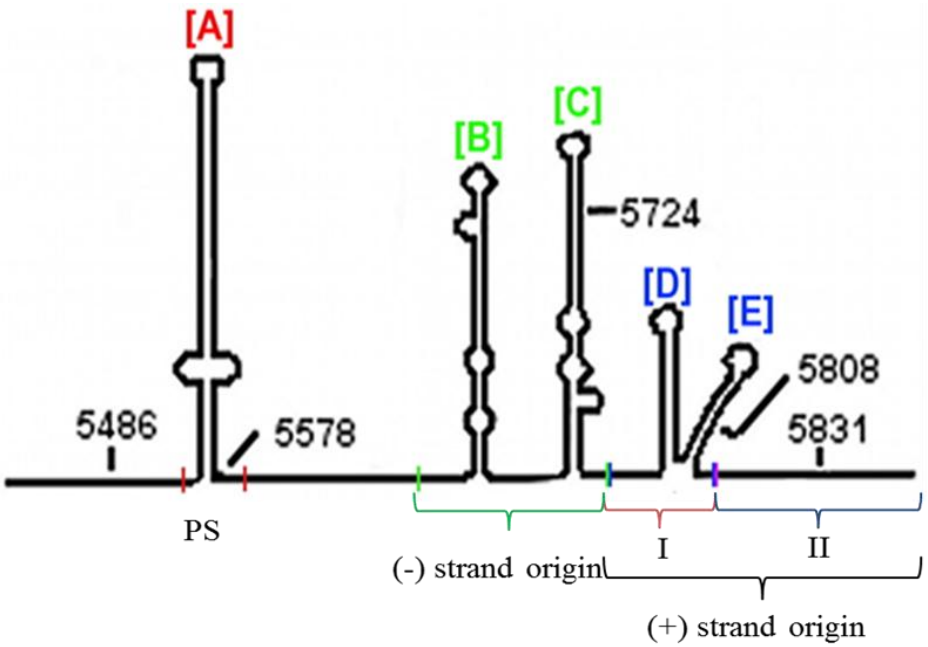

Figure 1.6 Secondary structure of filamentous phage intergenic region (IG). The IG region of phage is composed of packaging signal (PS; [A] hairpin loop), (-) strand origin of replication ([B] and [C] hairpin loops) and (+) strand origin of replication (region I containing [D] and [E] hairpin loops and region II. B and C; promoter mimic for *E. coli* RNA polymerase binding to synthesize a primer. (+) strand is divided in to two sections I and II. Section I (loops D and E) contains pII nicking site as well as initiator ad terminator sequences. Section II stabilizes binding of pII. Numbers represent nucleotide sequence of f1 according to (Hill et al., 1991).

1.6.3 Assembly and Secretion of Filamentous Phage Virions

In contrast to headed phage that assemble spontaneously in the host cell cytoplasm, filamentous phage assemble at the host cell membranes by a secretory process and phage are released into the culture medium as they assemble (Figure 1.5). This secretory process takes place at adhesion zones in the bacterial membranes and can be divided in to five stages: pre-initiation, initiation, elongation and termination (Russel et al., 2004). Five virion proteins involved in this process, are integral membrane proteins before the start of phage assembly and are transferred from the membrane into a lipid-free virion during assembly.

Before the phage assembly can start, specialized sites called adhesion zones are formed at the bacterial membranes, presumably through interaction between the inner membrane components of assembly machinery (pI/pXI) and outer membrane component (pIV) during pre-initiation phase of assembly process. These adhesion zones serve as assembly sites where inner and outer membranes of bacterial host can be seen in close contact with each other, and in the case of filamentous phage and other secretory systems, they are a consequence of a compact trans-envelop assembly complexes (Lopez and Webster, 1985). Phage assembly/secretion complex is composed of three morphogenetic proteins: pI, a presumed ATPase and its restart truncated form pXI in the inner membrane whereas pIV in outer membrane. The C-terminal domains of pI and pXI interact with N-terminal of pIV in the host periplasm independent of all other phage proteins (Marciano et al., 1999). Whereas pIV is known to form a large gated channel in the outer membrane (Opalka et al., 2003) pI and pXI are also presumed to make a large multimeric complex (5-6 copies of each) in the inner membrane. This complex in absence of other phage proteins causes membrane depolarization, suggesting that it acts a channel (Horabin and Webster, 1986; Horabin and Webster, 1988). Interaction of two complexes (pI/pXI and pVI) results in formation of a large export/assembly channel at assembly sites (Feng et al., 1999).

Initiation of Ff assembly requires the presence of pV-ssDNA complex in cytoplasm, minor coat proteins pVII and pIX integrated in to the membrane as well as pI/pXI/pIV assembly complex in the membrane (Feng et al., 1999). The packaging signal (PS) protruding from pV-ssDNA complex then interacts with pI cytoplasmic domain and C-terminal end of minor coat proteins pVII/pIX, starting the assembly process by

removal of pV dimers from the complex, and adding pVIII, presumably through pI/pXI action (Rapoza and Webster, 1995; Russel, 1991). Host-encoded small cytoplasmic protein thioredoxin also interacts with pI presumably conferring processivity to elongation process (thioredoxin is required for f1, but not M13 assembly). As the ssDNA traverses bacterial membrane, pV dimers are successively removed and replaced by pVIII embedded in the membrane. The particle is extruded through the assembly complex as it is coated with pVIII molecules. At the end of the assembly process, pIII and pVI are added to the virion. Addition of these two proteins at the terminal end of nascent phage particle brings about some conformational change that releases the particle from the assembly site (Rakonjac and Conway, 2006; Rakonjac et al., 1999). A certain minimal portion of pIII is required for phage release from the bacterial cells, however this fragment is shorter than the one required for the phage entry (Bennett et al., 2011; Rakonjac et al., 1999) (Section 1.3.2) (Figure 1.5).

1.7 Applications of Ff Filamentous Phage

Filamentous bacteriophage had been the vehicle for basic understanding of fundamental molecular biology processes such as DNA replication, translation and transcription. They have also found extensive application as DNA sequencing vectors due to their ability to produce ssDNA at a high amount. In mid-eighties filamentous phage applications entered a new era with the discovery of phage display technology.

1.7.1 Phage Display Technology

Phage display technology was introduced in 1985 by George Smith who fused a portion of *Eco*RI endonuclease gene to the filamentous phage minor coat protein pIII and demonstrated its affinity enrichment from a mixture of phage population using an immobilized polyclonal antibody against *Eco*RI endonuclease (Smith, 1985). These experiments introduced two important concepts. First, large phage libraries (10^8) with each phage particle expressing a unique random peptide can be synthesized using recombinant DNA technology and peptides binding immobilized ligands can be affinity purified using a technique called biopanning (Parmley and Smith, 1988). Second, each identified peptide can be amplified as the technique provides a direct link

between the displayed proteins (phenotype) and the DNA encoding them that is packaged inside the virion (genotype).

Few years later the display idea was exploited to assemble first combinatorial phage display random peptide libraries (Cwirla et al., 1990; Devlin et al., 1990; Scott and Smith, 1990). Not only peptides but functional proteins can also be displayed on the surface of filamentous phage (Bass et al., 1990; McCafferty et al., 1990). Phage display found its extensive use in peptide and antibody libraries. Peptide libraries are most frequently employed to identify peptides with specific binding affinity for important cellular receptors (Arap et al., 1998; Lowman et al., 1991; Wrighton et al., 1996) whereas antibody libraries are used to identify recombinant monoclonal antibodies having affinity for therapeutic targets such as tumor antigens (Schier et al., 1995). In addition to these major applications phage display is also employed to identify high affinity protease inhibitors (Roberts et al., 1992), transcription factors with altered recognition sites (Rebar and Pabo, 1994) as well as immunogenic peptides from antigens of interest (Delacruz et al., 1988; Minenkova et al., 1993; Willis et al., 1993). A new addition to the enormous potential of phage display technology is its recent application in nanotechnology. Selection of phage displayed peptides that nucleate specific nanocrystals, including metal salts, alloys, semiconductors or quantum dots has enabled the synthesis of complex nanostructures like nanowires and nano rings (Huang et al., 2005; Lee et al., 2002; Mao et al., 2003; Mao et al., 2004).

Selection of Phage Coat Protein and Display Formats

All five coat proteins of Ff filamentous phage have been used for the display of foreign peptides (Gao et al., 1999; Hufton et al., 1999; McCafferty et al., 1990). Proteins at the proximal end of the virion (Figure 1.2) pVII and pIX have been used for successful display of antibody fragments at their N-termini. Since both pVII and pIX are directed to the membrane by inherent hydrophobicity, in a SecYEG-independent manner, the insertion of foreign peptide requires addition of a signal sequence for their incorporation in to the virion (Gao et al., 1999). In contrast to others virion proteins, pVI that interacts with pIII at the distal end of virion only allows display at the C-terminus. This is particularly useful for the display of cDNA-encoded peptides as

addition of stop codon at the end of cDNA does not interfere with the display, hence pVI is useful for expression cloning used to study protein-protein interactions (Jespers et al., 1996; Jespers et al., 1995).

PVIII, the major coat protein, and pIII at the distal end of the virion filament are so far the most extensively used filamentous phage coat proteins in phage display. Both pIII and pVIII are synthesized with an N-terminal signal sequence which is cleaved upon protein insertion in to the bacterial membranes and N-termini of mature proteins are located in the periplasm before insertion in to virion. Both proteins span bacterial membranes by a single C-terminal hydrophobic membrane helix – also called the membrane anchor. Upon their insertion in to the virion, N-termini of both these proteins are exposed to the surface. Therefore, in order to display any peptide on these two proteins it needs to be cloned in-frame, in between the signal sequence and N-terminal of the mature protein.

PVIII Display

The major coat protein pVIII is present in around 2700 copies on surface of the wild-type f1 virion (the number depending on the size of encapsidated ssDNA). The number of peptide copies that can be displayed on the surface of filamentous phage using pVIII as a display platform depends on the length of the peptide. If foreign peptide is to be displayed on each copy of pVIII then it should be maximum of 7 residues (Iannolo et al., 1995). Longer peptides can be displayed, but efficiency of display becomes sequence-dependent. However, larger peptides and even the entire proteins can be displayed on pVIII if wild-type pVIII is supplied along with the recombinant fusion-pVIII molecules, to allow assembly of virion. These mixed virions require two copies of *gVIII* in the same cell, one encoding the wild-type pVIII and one encoding the peptide-pVIII fusion. These two can be expressed either from the same episome (e.g. a phage 8+8 vector) or from two different episomes (e.g. a helper phage and a phagemid/plasmid vector). Phagemid vectors are specialized plasmid vectors that contain phage intergenic sequence ((+) and (-) origins of replication and packaging signal) along with its plasmid origin, as well as recombinant pVIII coding sequence suitable for inserting coding sequence for display (Barbas III et al., 2001). When *E. coli* containing a phagemid is infected with a helper phage, phagemid is replicated

using the f1 origin of replication and packaged as ssDNA into the virion, generating viral particles containing phagemid DNA which are called phagemid particles (Ji et al.) or transducing particles (TDPs) (Russel and Model, 1989). Wild-type pVIII is encoded by helper phage. The phagemid/helper phage system results in production of mosaic, having a mix of wild-type as well as recombinant pVIII molecules in the capsid (Mead, 1988). Mosaic display options are available for pIII- and pVI-based display as well (Smith and Petrenko, 1997).

PIII Display

The minor coat protein pIII, present in 5 copies at distal end of virion, is the protein of choice in the display of most peptides and proteins, mostly because of its tolerance to the insertion of large peptides and the rich choice of vectors (Russel et al., 2004). PIII is most frequently expressed from phagemid rather than phage vectors, as protein domains fused to pIII sometimes result in decreased infectivity of the resulting virions. Phagemid vectors have an additional advantage of expression from an inducible promoter, which is particularly desirable as pIII chimeras are often toxic to host cells. Such phagemids are used in combination with two types of helper phage. One type of helper phage encodes wild type pIII, resulting in mosaic virions containing less than one copy of pIII-fusion protein per virion due to preferential incorporation of wild type pIII over the chimeric one into the virions. The other type of helper phage carry *gIII* deletion resulting in expression of five copies of pIII-fusion protein per phage (de Wildt et al., 2002; Griffiths et al., 1993; Rakonjac et al., 1997).

1.7.2 Application of Filamentous Phage in Diagnostics

In recent years phage display technology has found immense applications in immunology, pharmacology and drug discovery. Phage particles expressing peptides with specific affinity to ligands have been employed in *in-vivo* and *in-vitro* diagnostic techniques of transfusion medicine research as well as for mapping vasculature in organ-specific manner (Siegel et al., 2003). Functionalized phage particles carrying specific peptides with high binding affinity for tumor cell surface receptors (α_v integrin) have been used to target tumor vasculature in a variety of tumor types (carcinoma, sarcoma, melanoma) in tissue culture and mouse model (Lee et al., 2007; Rasmussen et al., 2002). Phage-displayed tumor homing peptides have also been coupled to chemotherapy drugs to improve their therapeutic index. Successful degeneration of the tumor treated with phage peptide-drug conjugate was observed due to inhibition of primary tumor growth and metastasis in comparison to the tumors given non conjugated drug (Arap et al., 1998). Functionalized phage particles were also employed to agglutinate blood cells that bear specified antigen *in-vitro*, a technique in which phage-peptide conjugates are used as blood bank typing reagents (Siegel et al., 1997). This was particularly useful because the phage reagent can replicate in *E. coli* host, lowering the cost of production, and have greater sensitivity as only a dozen phage particles expressing appropriate peptide were sufficient to produce a positive reaction. Another advantage given by phage-displayed antibodies as blood bank typing reagents was their specificity which eliminated false positive reactions. Similar technique was used for fingerprinting the serum antibodies in prostate cancer patients which lead to the identification of specific tumor antigen (Mintz et al., 2002). Moreover, intra-nasal administration of filamentous phage particles expressing anti-β amyloid antibody fragment as a pIII fusion to mouse model enabled *in-vivo* detection of Alzheimer's disease amyloid plaques in brain tissue for the first time (Frenkel and Solomon, 2002).

Full-length phage particles displaying short peptide loops have been used in lateral flow dip stick devices for non-competitive immunodetection of small molecules as an alternative to antibodies (González-Techera et al., 2007). A more sophisticated system for detection of small molecules, named Phage Anti-Immune complex Assay (PHAIA) by the authors, was developed using phage display (Kim et al., 2009). This system

detects antigen indirectly, by specifically recognizing antibody-antigen complex, but not the free antibody. In this approach, phage displaying specific peptides is first selected by screening of random peptide phage display libraries using the antibody-small molecule complex as bait, and counter-selecting against a free antibody or the small molecule. The phage displaying a peptide recognizing insecticide-monoclonal antibody complex was used to detect extremely low amount of insecticide molecules in environmental samples, as well as in urine, as a biomarker to assess human exposure to insecticides. It was also adapted to onsite detection of these molecules in a dipstick format (Kim et al., 2009).

Besides these successful reports, the commercial use of filamentous phage in diagnostics has not commenced as yet. This could be due to their poor diffusion and restricted mobility through membranes and matrices owing to their large size and filamentous structure. Furthermore, functionalized phage or phagemid particles that display peptides of interest are recombinant viruses (GMOs) and their use poses potential health and ecological problems, increasing the regulatory hurdles that need to be overcome before their use outside of laboratory containment.

1.7.3 Application as Recombinant Vaccine Carriers

Filamentous phage had been routinely used to study the immunogenic potential of desired peptides displayed as recombinant fusions to either major coat protein pVIII or minor coat protein pIII on their surface. Since their first use as immunogenic carriers (Delacruz et al., 1988) they are now known to possess several desirable properties to act as a model system to study antibody response. To date filamentous phage have been reported as successful in phage based vaccine preparation in the mouse for rabies (Houimel and Dellagi, 2009), HIV (Berardinis et al., 2003), melanoma (Eriksson et al., 2007; Eriksson et al., 2009), Alzheimer's disease (Frenkel et al., 2003), herpes simplex virus (Grabowska et al., 2000) and candidiasis (Wang et al., 2006; Yang et al., 2007). They are highly immunogenic, producing high antibody titres even after single administration without any adjuvant (De Berardinis and Haigwood, 2004; van Houten et al., 2006). Their particulate nature, size, shape, virion composition and associated bacterial lipopolysaccharides make them suitable candidates to elicit long-lasting immunity (Grabowska et al., 2000). Their ability to resist high temperatures as well as variable pH adds to their suitability as vaccine carries for example landscape pVIII

epitope libraries are able to retain measureable specific bind ability for more than six months at room temperature and more than six weeks at 63 ºC (Brigati et al., 2008). These properties are particularly desirable when generating vaccines for underdeveloped countries as it bypasses the need of refrigeration and ease of storage and shipping. Immune response to phage is mainly T helper cell dependent (Gaubin et al., 2003; Hashemi et al., 2010; Ulivieri et al., 2008; Wan et al., 2005; Willis et al., 1993) however high cross linking of pVIII residues may lead to the production of antibody secreting cells (Henry et al., 2011). They can also be engineered to target antigen presenting cells specifically (Sartorius et al., 2011). Immune response is shown to be better focused to the immunogenic peptides if they are expressed on the surface of bacteriophage rather than conventional carriers, probably due to the limited surface exposed residues of coat proteins available to generate immune response (van Houten et al., 2006) .

Despite these tempting properties, the use of filamentous phage as vaccine carriers is limited to trials in animal models, mainly because they are live viruses and vaccine preparation using live virus as a vector has a limited chance of regulatory approval. Even the use of inactivated filamentous phage particles is of concern due to easy unspecific uptake of filamentous phage by epithelial cells. This is a particular problem, as bacteriophage can easily enter the vasculature and their distribution to brain and other vital organs is very clearly documented (Dabrowska et al., 2005; Frenkel and Solomon, 2002).

1.8 Microphage / Nanophage

In filamentous bacteriophage genome spontaneous duplication of (+) strand origin of replication by homologous recombination results in the production of short defective phage particles, after about 40 passages through bacterial host in the absence of plaque purification (La Farina et al., 1987). In these genomes that contain duplicate origins, replication starts at first (+) strand origin (*ori1*) and continues until pII encounters 2nd positive origin (*ori2*) and recognizes it as a terminator. The resulting replication product size corresponds to the region between the two duplicated (+) origins. Since virion length is determined by the genome length it carries, these short genomes are packaged in to small phage particles, however production of these particles is

inefficient and represents only 0.1% of the total phage progeny. These phage particles cannot replicate at their own as they do not contain complete set of genes required for the production of essential proteins. They are consequently dependent upon co-infection with a helper phage for their replication and assembly (La Farina et al., 1987; Rakonjac et al., 2011).

Plasmids having filamentous phage intergenic region {(+) and (-) strand replication origins as well as packaging signal (PS)} are packaged as phagemid particles or transducing particles when infected with suitable helper phage (Cleary and Ray, 1981; Dente et al., 1983; Russel et al., 1986). Using the same principle a plasmid was engineered to carry duplicated origin of replication that produced very small filamentous phage particles upon infection with helper phage (Specthrie et al., 1992). The plasmid used for engineered production of microphage particles (pLS7) carried phage packaging signal flanked by two positive origins of replication (Figure 1.7). The first origin (*ori1*) was a wild type origin able to function both as initiator as well as terminator. The second origin (*ori2*) had a 29 nucleotide deletion that removed the pII binding site and could only act as a terminator, allowing the strand-transferase reaction which releases the (+) strand corresponding to the replicated region. PII binds to first origin of replication (*ori1*) makes a nick and starts replication that proceeds through packaging signal. Then it encounters the second origin (*ori2*) of replication that can only act as a terminator, makes another nick and ligates the two ends of displaced (+) strand between the two origins, releasing a short circular ssDNA (200 nt in length). This small circular ssDNA was shown to successfully package as a phage particle using an appropriate helper phage (Specthrie et al., 1992). The system produced two types of particles; full-length helper phage particles and small nanophage particles called “microphage” (Specthrie et al., 1992). Since the length of phage particles is determined by the size of ssDNA enclosed these microphage particles were only 50 nm in length with a usual diameter of 6-7 nm. However the system was found to be of low efficiency with microphage population making only 3% of the total phage population (Figure 1.8).

In 2009 the original microphage production system was improved, leading to the increase in efficiency of microphage production; moreover a method for their purification away from full-length helper phage particles was also developed (Bennett,

2010) . The new system was efficient in terms of production and purity of the microphage particles in comparison to original publication; however the purification technique still had a poor yield for technological applications. These particles are now renamed as ‘nanophage’ due to their nanometer length scale.

Nanophage particles are short and compact and they have an appearance of rods, as opposed to flexible filaments of full-length phage particles. They carry short circular ssDNA of 200 nt and are incapable of replicating at their own; furthermore, they do not contain any coding sequences. Despite being short in length they appear to retain the same composition and arrangement of all capsid proteins present in full-length phage particles (Bennett, 2010). It is therefore predicted that they can be used in all the applications of phage display in which the full-length phage particles are used. Table 1.3 shows a comparison of nanophage properties with full-length phage particles.

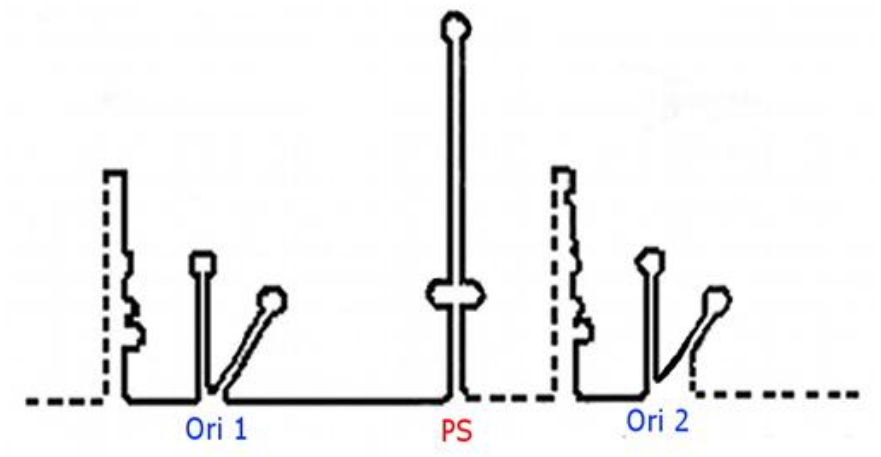

Figure 1.7 Engineered origin of replication for microphage (nanophage) production. *Ori1*; wild type positive origin of replication capable initiating as well as terminating rolling circle mode of ssDNA replication. PS; packaging signal, *Ori2*; mutated positive origin of replication acting as terminator only. Figure adapted from (Specthrie et al., 1992) with permission.

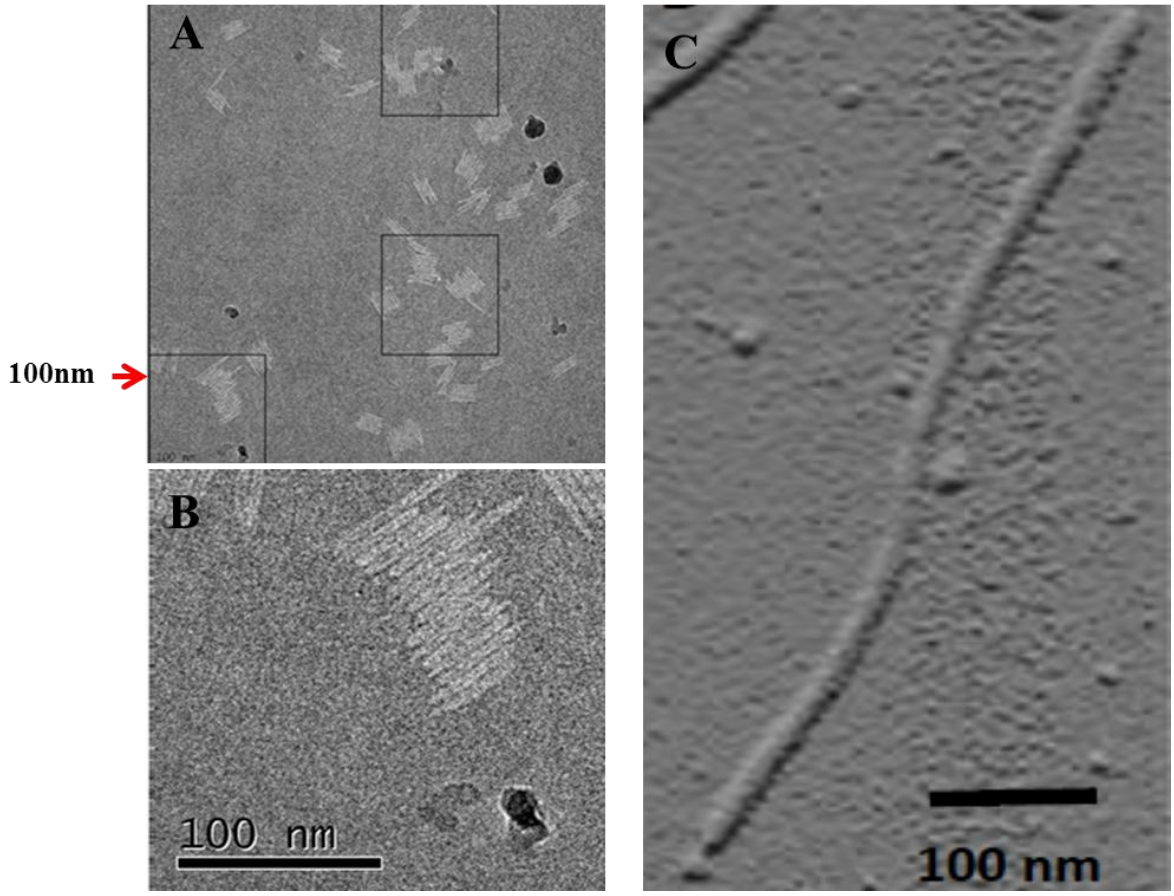

Figure 1.8 Electron micrographs of nanophage particles. A) & B) Negatively stained electron micrograph image of nanophage particles. The sample was prepared using Uranyl Acetate. Bar corresponds to 100 nm. Image adopted from (Bennett, 2010; Rakonjac et al., 2011). C) Full-length Ff virion in 100 nm scale, atomic force electron micrograph image adopted from (Rakonjac et al., 2011) with permission.

Table 1.3 Comparison of nanophage properties with full-length Ff phage particles

Properties	Wild-type (full-length) filamentous phage	Nanophage
Particle size	860 nm	50 nm
Length of packaged ssDNA	6.4 Kb	0.221 Kb
Replication	Positive and negative strand replication	Positive strand replication only
Episome	Full-length phage genome	Plasmid carrying phage packaging signal and duplicated (+) strand origin of replication
Genes	All genes required for the production of phage particles	No genes, carries only modified IG region of phage
Production	High efficiency (10^{12} /ml)	Low efficiency (10^{10}/ml)
Purification	Separation from *E. coli* cells and small molecules in the culture supernatant	Requires additional techniques for separation from full-length helper phage (Bennett, 2010); this study (Chapter 3)
Infectivity	Replicates and releases progeny upon entry into *E. coli*	Cannot replicate without a helper phage
Display and applications	Extensively used (Section 1.7)	No reports of applications to date

1.9 Aims of the Project

Despite the versatility of filamentous phage and enormous potential to be used in biomedical applications (Section 1.7), the use of these particles for out-of-containment human and animal applications is still in trial phase. For direct therapeutic and diagnostic applications antibodies, peptides or other molecules selected by phage display library screening must be expressed in other systems. Part of the reason why phage themselves are not used in biomedical applications is that they are live viruses and are genetically modified Ff phage are also defined by the New Zealand Hazardous Organisms and New Organisms Act as genetically modified organisms, preventing their application outside of laboratory containment. Filamentous phage carry genetic material that allows their propagation in gut *E. coli* and often encode antibiotic resistance markers; this increases the potential for horizontal gene transfer of antibiotic resistance among bacterial gut community. Furthermore, filamentous phage have been shown to unspecifically deliver their DNA into eukaryotic nuclei (Larocca et al., 1999). These potential risks in turn slim the chances for regulatory approval and consumer acceptance of filamentous phage use outside of laboratory environment. Finally, filamentous phage applications in diagnostics, such as in lateral flow devices, are restricted due to their filamentous structure and tendency to cluster and entangle. These properties result in their poor and non-uniform diffusion through membranes, and pose a difficulty in their penetration through matrices. The nanophage particles lack all these drawbacks; nevertheless they have all other properties, like temperature, detergent and pH extreme tolerance that make filamentous phage a desirable bio-nanoparticle for medical and non-medical applications (Section 1.8). Current study was designed to convert the nanophage production system into a display system and to explore the potential of nanophage particles in biomedical applications, with three specific aims:

1) To improve production and purification of the nanophage and convert the nanophage production system into a display system, to obtain functionalized bio-nanoparticles (Chapter 3).

2) To assess the potential of functionalized nanophage particles for use in lateral flow diagnostic devices (Chapter 4).

3) To assess the potential of the nanophage particles to serve as vaccine carriers to elicit antibody response against a displayed vaccine target (Chapter 5).

Chapter 2

Materials and Methods

2.1 Bacterial Strains and Growth Conditions

All bacterial strains used in this study are listed in Table 2.1. *E. coli* strains are derivatives of laboratory strain K12.

Table 2.1 Bacterial strains

Strains	Genotype	Source/Reference
Escherichia coli		
TG1	*supE44* Δ*(hsdM-mcrB)5* (rk^- mk^- $McrB^-$) *thi* Δ*(lac-proAB)* F' [*traD36 lacI*^{q} Δ*(lacZ)M15 proA*$^+$*B*$^+$].	(Carter et al., 1985)
K561	*HfrC* λ^+ *relA1 spoT1 T2*^{R} *(ompF627 fadL701) ΔlacZ lac1*^{q}	The Rockefeller University (Zinder-Model) collection
K1030	*HfrC* λ^- *relA1 spoT1 T2*^{R} *(ompF627 fadL701) supD zed508::Tn10*	The Rockefeller University (Zinder-Model) collection
K2092	*TG1 supD zed508::Tn10*	J. Rakonjac, unpublished
K2091	*K561 supD zed508::Tn10*	J. Rakonjac, unpublished
***Streptococcus pyogenes* D734**	M-type 22 clinical isolate (wild-type)	The Rockefeller University Lancefield collection

All *Escherichia coli* strains were propagated in Difco™ 2xYT (Yeast Extract Tryptone) liquid medium (Becton-Dickinson (BD) and Company USA) at 37 ºC with continuous shaking (200 rpm) unless otherwise stated, or on 2xYT agar plates (1.2% Bacto-Agar from BD). The medium was supplemented with suitable antibiotics where necessary sourced from Sigma-Aldrich (Australia). Antibiotics were used at following concentrations; Chloramphenicol (Cm) 25µg/ml, Ampicillin 100µg/ml and Kanamycin (Km) at 30µg/ml, unless otherwise indicated.

All cultures were stored long-term at -80 ºC in 7% (v/v) Dimethyl sulfoxide (DMSO). For short-term storage (up to two weeks) solid culture plates were stored at 4 ºC.

Post vaccination challenge was performed using group A *Streptococcus pyogenes* strain D734 (M type 22; from which the FnB domain was derived). The strain was cultured in Todd-Hewitt broth (Becton Dickinson) in sealed yellow cap tubes at 37 ºC without shaking. To check the β-hemolysis *S. pyogenes* was grown on Columbia sheep blood agar plates sourced from Fort Richard. Plates were incubated overnight at 37 ºC in sealed chambers maintaining anaerobic conditions.

2.2 Plasmids, Oligonucleotides, Phage and Recombinant DNA Methods

Plasmids and oligonucleotides used in this study are listed in Tables 2.2 and 2.3, respectively.

Table 2.2 Plasmids

Plasmids	Parent	Description	Resistance	Reference
pNJB2	pACYC184	*tac*-gII fusion inserted into the *Sac*II/*Ava*I-cleaved pACYC184	Tet	(Bennett, 2005)
pNJB07	PCR4 Blunt	Contains repaired nanophage origin of replication from pLS7	Km & Amp	(Bennett, 2010)
pSS3	pNJB07	Deleted Km resistance gene	Amp	This study
pVCSM13 (pDH)	VCSM13 phage	Deleted phage origin of replication and packaging signal	Km	Gagic and Rakonjac unpublished,
pMAL-c2X		pMAL-c2X expression cloning vector.	Amp	New England Biolabs
pSS4	pMAL-c2X	FnB domain from *sof22* gene (*S. pyogenes* strain D734) inserted in frame with the N-terminal tag MBP	Amp	This study
pDJ04	pDJ01	Contains *sof22* gene (encoding the FnB domains) from *S. pyogenes* (M type 22, D734)	Cm	(Jankovic et al., 2007)

Table 2.3 Oligonucleotides used for cloning

Name	Sequence	Restriction sites
JR438	TCCCCCGCGGGAGGTCATGGACCGATTGTC	*Sac*II
JR439	TCCCCCCGGGCTCGTTATCAAAGTGGAAGA AGC	*Xma*I
NJB6001	GTTCCTTTCTATTCTCACTCCGCGGCCCAG CCGGCCATGGGATATCAGGCGGC	*Sac*II *Nco*I, *Eco*RV
NJB6003	GCCATGGGATATCAGGCGGCCGCTCCCGG GGGCGCTGAAACTGTTGAAAGTTGTT	*Xma*I
SS31	CGCGGATCCATTGTCGATATCGTCGAAGAT ACT	*Bam*HI
SS32	CCCAAGCTTTTACTCGTTATCAAAGTGGAA GAAGC	*Hind*III

2.2.1 Recombinant Methods and Construction of Recombinant Plasmids and Phage

General molecular biology techniques were carried out as described in Sambrook and Russell (Sambrook et al., 1989) . Restriction Endonucleases used in this study were sourced from New England Biolabs Inc. (USA), Roche Molecular Biochemicals (Germany) and Invitrogen Life Technologies Inc. (USA). Oligonucleotides used for cloning, sequencing and PCR reactions (Table 2.3) were manufactured by Integrated DNA Technologies Inc. (USA). High-fidelity DNA polymerases, PWO (Roche) and PRIMESTAR (Takara, Japan) were used for PCR amplifications destined for cloning. For all other PCR amplifications *Taq* DNA polymerase was used.

2.2.2 Plasmid DNA Isolation

Plasmids used in study are listed in Table 2.2. Small scale plasmid DNA preparations were carried out using High Pure Plasmid Isolation kit (Invitrogen Life Technology Inc.; USA) that utilizes modified alkaline lysis method (Bimboim and Doly, 1979). For large scale preparation of plasmids High Pure Plasmid Midiprep kit from Invitrogen Life Technology Inc. was used. Two milliliters of stationary phase *E. coli* culture

containing the respective plasmid was harvested for a miniprep, and 25 ml culture for a midiprep. DNA extraction was performed as per manufacturer's instructions. Briefly, cells were disrupted by alkaline lysis, followed by protein precipitation using potassium acetate (3 M, pH 5.5). The lysate was poured in to the pre-packed Anion-exchange column fitted with the filtration cartridge unit. Impurities were removed by washing the column and DNA was eluted with the elution buffer (100mM Tris-HCl, pH 8.5). For minipreps, the DNA was eluted in 50 µL of buffer or water and was used in experiments without further processing. However in midipreps, the DNA was eluted in 5 mL of buffer and had to be concentrated by isopropanol precipitation. The obtained pellet was suspended in 200 µL of buffer (10mM Tris-HCl pH 8.0).

2.2.3 Construction of Rnano3FnB Phage Displaying the Fibronectin Binding (FnB) Domain of *Streptococcus pyogenes*

The display helper phage Rnano3FnB was constructed in two steps by direct phage cloning: first, the helper phage Rnano was modified for the ease of cloning by inserting a 45 nucleotide fragment corresponding to MCS of phage display vector pHEN2 (Goffinet et al., 2008) in between the signal sequence and mature part of pIII by overlap extension PCR using primers NJB6001//NJB6003. The resulting phage was called Rnano3 (Table 2.4; Figure 2.1). In the second step, a DNA fragment encoding FnB domain (453 nucleotides) were PCR-amplified from pDJ04 (Jankovic et al., 2007) using primers JR438//JR439 (Table 2.3) and cloned in to *Sac*II/*Xma*I fragment of Rnano3 (Table 2.4). This phage, Rnano3FnB, was used as a helper phage, to produce nanophage displaying FnB domains on pIII. It was expected that the nanophage and helper phage display 5 copies of the pIII-FnB fusion per virion, however a lower copy number was displayed on purified particles, as determined by the Western blotting (Fig. 5.24, Chapter 5) due to proteolytic degradation in the periplasm of *E. coli* where the FnB portion is located, and during purification of virions. The stocks of the helper phage and purified nanophage were prepared and titrated as described in Sections 2.3.1 - 2.3.2.

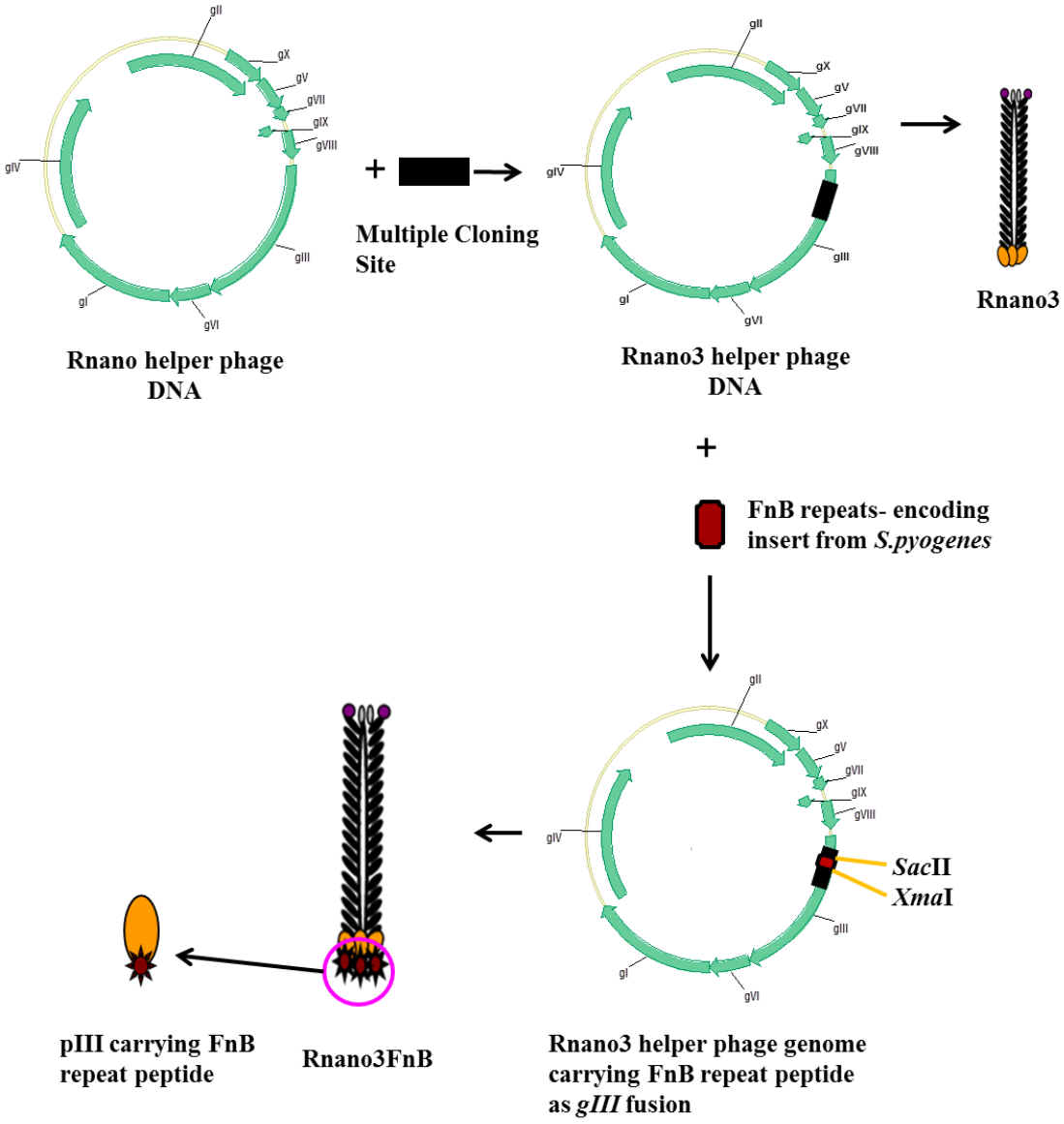

Figure 2.1 Schematic presentation of construction of Rnano3FnB from Rnano.

2.2.4 Construction of MBP-FnB Fusion

FnB domain was PCR-amplified using Rnano3FnB as template. Amplification primers SS31 and SS32 contained *Bam*HI and *Hind*III restriction sites, respectively (Table 2.3) and ligated to *Bam*HI/*Hind*III-digested expression vector pMAL-c2X (New England Biolabs) downstream of *malE* gene that encodes maltose-binding protein (MBP). The resulting recombinant plasmid, pSS4, encoded an MBP-FnB fusion.

2.3 Phage Strains and General Phage Growth and Quantification Methods

Phage strains used in this study are listed in Table 2.4.

Table 2.4 Phage strains

Phage	Genotype	Reference
f1	Wild type	(Loeb, 1960)
VCSM13	M13 pA15*ori* Kan^R *IR*	Stratagene (USA)
R408	f1 *ΔPS gIX(T30A) IRI gtrxA2*	(Russel et al., 1986)
R408-3	R408 containing 45 nucleotides corresponding to MCS of phage display vector pHEN2	This work
Rnano	f1 *ΔPS IX (T30A) IRI gtrxA2* $gVIII^{am}$ ($E25^{am}$)	(Bennett, 2010)
Rnano3	Rnano containing 45 nucleotides corresponding to MCS of phage display vector pHEN2	This work
Rnano3FnB	Rnano3 containing FnB domain (inserted into *Sac*II and *Xma*I cloning sites)	This work

2.3.1 Preparation of Phage Stocks

All phage and phagemid stocks were prepared by infecting an exponential phase culture ($O.D_{600}$ = 0.2) of appropriate bacterial strain, with a phage at multiplicity of infection (m.o.i) of 50 for 30 min at 37 ºC. The culture was further incubated for 4 h at 37 ºC with continuous shaking at 200 rpm to allow for phage and phagemid growth. At

the end of incubation the culture was centrifuged at 6000g for 15 min to remove bacterial cells from supernatant. To remove any residual bacterial cells, the supernatant was either filtered through a 0.2 µm-pore membrane or heated at 65 ºC for 20 min. Phage stocks were titrated as described in the Section 2.3.2 whereas phagemid stocks were titrated as explained in Section 2.3.3 and stored at 4 ºC (Sambrook et al., 1989).

2.3.2 Titration of Infectious Phage Particles

Phage f1, R408 and VCSM13 were titrated on strains K561 or TG1, whereas phage Rnano, Rnano3 and Rnano3FnB (containing an amber mutation in *gVIII*) were titrated on suppressor strains K2091 or K2092. Briefly, 10 µl drops of phage dilutions were placed on soft agar containing 0.2 ml of overnight culture of appropriate bacterial strain. After the absorption of the phage drop plates were incubated at 37 ºC overnight. Plaques in the area of absorbed phage were counted to determine the approximate number of phage particles. The titre was expressed as plaque forming units per ml (pfu /ml).

2.3.3 Titration of Phagemid Particles

Phagemid particles carrying Amp^R marker in phage stocks were titrated on *E. coli* strain K1030 (Table 2.1). Double-layer plates were prepared using 2xYT liquid medium supplemented with 100 µg /ml ampicillin. After solidification these plates were overlaid by another layer of 2xYT without any antibiotic just before use to allow in-agar infection of K1030 cells prior to exposure to ampicillin. Plates were incubated at 37 ºC overnight, and ampicillin resistant colonies were counted next day. The titre of phagemid particles is given as colony forming units / milliliters (cfu /ml).

2.3.4 Quantification of Virions by Agarose Gel Electrophoresis of Phage Particles

To quantify nanophage or full-length helper phage, SDS-disassembled virions were subjected to electrophoresis and the amount of released DNA was quantified. Briefly, the virions were disassembled in SDS–containing buffer (1% SDS, 1 × TAE, 5 % glycerol, 0.25 % BPB) at 70 ºC for 20 min and subjected to electrophoresis in 1.2 % agarose gel in 1×TAE buffer. After electrophoresis, the ssDNA released from disassembled virions was stained with ethidium bromide and quantified by densitometry (Rakonjac and Model, 1998). The amount of ssDNA in any band is not

linearly proportional to the intensity of fluorescence therefore each gel contained a set of twofold dilutions of purified f1 ssDNA, which were used for calibration (Chapter 3, Figure 3.2). Gel was photographed by a CCD camera (Biorad, USA). Image gauge V4.0 and Microsoft Excel were used for quantitative analysis. Second order polynomial function was used to fit the standard curve. Amount of ssDNA was converted to the genome equivalents based on the molecular weight of ssDNA genome. Molecular weight was in turn calculated from base composition and length of virion.

Native virion agarose electrophoresis was used to detect and separate the intact virions of the full-length (helper) phage and nanophage, for analysis and purification (as described in 2.4.2). Position of native phage on agarose gel was determined by soaking gel in 0.2M NaOH for 1h, followed by neutralization with 0.45M Tris pH 7.0 and staining with ethidium bromide.

2.4 Growth, Concentration and Purification of Nanophage

2.4.1 Differential PEG Precipitation

Nanophage (or microphage) are short filamentous phage particles, 50 nm in length, in contrast to full-length Ff phage particles that are 860 nm in length. The system adapted for efficient production and purification of nanophage is a modification of the system published by Specthrie *et al* 1992 (Bennett, 2010). An exponentially growing culture of K1030 carrying pNJB07 (nanophage-producing plasmid) (Table 2.4) was infected with appropriate helper phage (Rnano3 or Rnano3FnB) at m.o.i of 50. The culture was incubated for 1h at 37 ºC without shaking to allow infection with helper phage. Incubation was continued overnight at 37 ºC with shaking at 200 rpm. Next day cells were spun down (7000 rpm/20 min/4 ºC) and the supernatant containing nanophage and helper phage was subjected to differential PEG precipitation to separate full-length helper phage from the nanophage particles.

In the first step “Low-PEG precipitation” of helper phage was performed at a final PEG 8000 concentration of 2.5% w/v and 0.5 M NaCl, overnight at 4 ºC. Precipitated helper phage was collected by centrifugation at 10,000 rpm for 45 min at 4 ºC. Supernatant containing nanophage was transferred to sterile containers, whereas the

helper phage-rich pellet was suspended in TBS (50mM Tris, 150mM NaCl, pH 7.0). In the supernatant PEG concentration was increased from 2.5% to 15% ("High PEG") to precipitate the nanophage, and was incubated overnight at 4 ºC. The following day the nanophage-rich precipitate from "High PEG" was collected by centrifugation (10,000/45 min/4 ºC) and suspended in TBS. Both helper phage- and nanophage-rich fractions were subjected to subsequent detergent purifications (Sarkosyl/Triton X-100) followed by low-PEG or high-PEG precipitation, respectively, to solubilize any membrane lipids or cell wall peptidoglycan and associated proteins that precipitated with phage. These detergent purification steps allowed the concentration of nanophage fraction to 1ml volume (Bennett, 2010).

2.4.2 Phage Preparative Agarose Gel electrophoresis

Separation of helper phage from nanophage by differential PEG precipitation is not complete. The nanophage fraction contains a considerable amount of helper phage in it. Nanophage were purified away from helper phage based on the large difference in size, by a preparative agarose gel electrophoresis of native virions, The gel fraction containing the nanophage band was excised and the nanophage particles were separated from agarose using a spin filter device (Bennett, 2010). The filtrate was precipitated overnight in High PEG (15% PEG and 0.5 M NaCl) and nanophage pellet was dissolved in appropriate volume of TE buffer. Improvement of the system for optimum production and purification of nanophage will be discussed in Chapter 3.

2.4.3 Electroelution of Phage Particles

The phage bands corresponding to full-length and nanophage particles were excised from the preparative agarose gel using a sharp scalpel blade. These gel slices were transferred to dialysis tubes (Novagen, D-tube dialyzer Maxi, MWCO 12-14 kDa; product number 71510-3) containing 500 µl of sterile 1 × TAE buffer. These tubes were then placed in electrophoresis chamber in sterile 1 × TAE buffer and electrophoresed overnight. Next day gel slice was removed and phage particles (full-length or nanophage particles) were PEG precipitated overnight at 4 ºC. The PEG precipitate was dissolved in appropriate amount of 1 × PBS and stored at -80 ºC until further used.

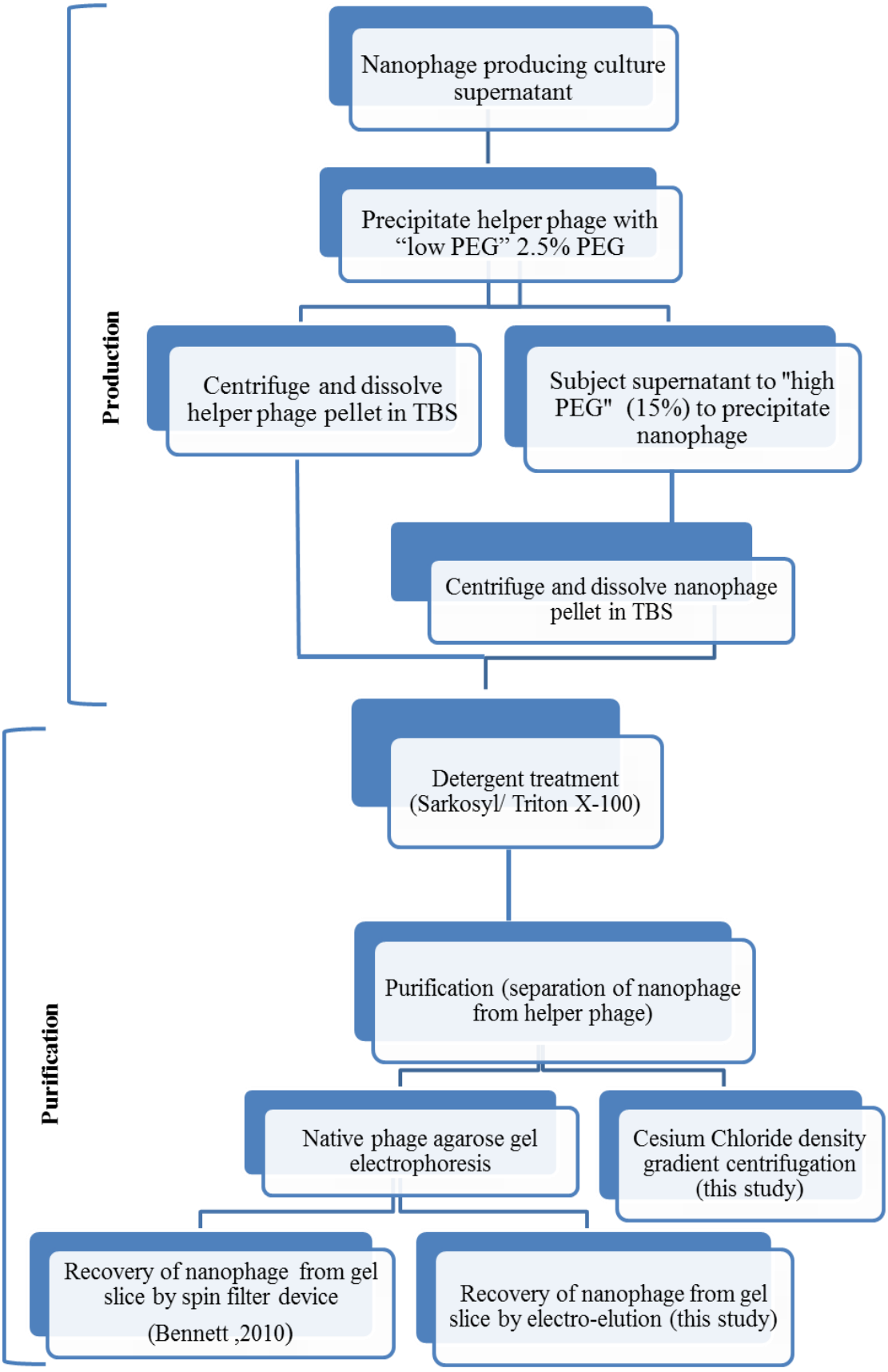

Figure 2.2 Outline of the nanophage production and purification protocol.

2.4.4 Cesium Chloride Density Gradient Purification of Phage Particles

Purification of full-length (helper) and nanophage, after differential precipitation and Sarkosyl/Triton x 100 treatment, was also performed using cesium chloride (CsCl) density gradient centrifugation instead of preparative agarose, in an attempt to increase the yield. After detergent treatment 100 µl phage were suspended in 2.5 ml of NET buffer (0.1 M NaCl, 1mM EDTA, and 0.01 M Tris-HCl, pH 7.6), 1.5 g solid CsCl was added and volume was made up to 4 ml with the NET buffer, to obtain a final concentration of 0.375 g/ mL. Centrifugation was carried out for 18 h at 110,000 g. Full-length phage were extracted by direct removal of grey band using a 25 gauge syringe needle, using a protocol outlined in Sambrook and Russell (Sambrook et al., 1989). Another band running very close to helper phage band was observable after the CsCl centrifugation of the nanophage, however it was not confirmed whether or not it corresponded to nanophage particles. Therefore, to collect nanophage, 150-250 µl fractions were collected and visualized using agarose electrophoresis of native virions. The fractions having clear nanophage band and no full-length phage band on the gel were titrated to determine the amount of helper phage (Chapter 3, Section 3.2.2). Titration accurately quantifies residual phage, otherwise undetectable in agarose gels.

2.5 Protein Purification and Detection

2.5.1 Purification of MBP-FnB Fusion

The recombinant plasmid expressing MBP-FnB fusion (pSS4, Table 2.2) was transformed into *E. coli* TG1 strain. The cells in exponential growth phase ($O.D._{600}$ = 0.2) were induced with 0.3 mM IPTG (isopropyl-β-D-thio-galactopyranoside; Merck) for 1h. The cells were pelleted and lysed by sonication in the presence of the column buffer (20 mM Tris-HCl, 200 mM NaCl, 1 mM EDTA). The MBP-FnB fusion was purified by affinity chromatography using a column packed with matrix containing covalently linked amylose as a ligand (New England Biolabs). After loading of the column with the cell lysate, the column was washed with the column buffer. The MBP-FnB fusion was then eluted using soluble maltose (10 mM). The MBP-FnB protein expression and purification was monitored using SDS-PAGE followed by staining with Coomassie Blue or western blotting.

2.5.2 Detection of Proteins by SDS-PAGE and Western Blotting

Proteins from purified phage samples, culture supernatants and cell lysates were separated by SDS-PAGE using glycine gel system (Laemmli, 1970), transferred to nitrocellulose filters and then detected using appropriate antibodies. R164, polyclonal rabbit anti-pIII antibody, was used to detect pIII (Rakonjac and Model, 1998). Anti-rabbit antiserum conjugated to alkaline phosphatase was used as secondary antibody, which in turn was detected using Nitro Blue Tetrazolium (NBT) and 5-Bromo-4-Chloro-3-Indolyl Phosphatase (BCIP) in alkaline buffer (Blake et al., 1984). TBS (30 mM Tris, 150mM NaCl, pH8.0, 0.05% Tween 20) was basic buffer used in western blotting. Blocking buffer contained 5% skim milk powder.

2.6 ELISA Assays

Three types of ELISA assays were used in this thesis. First, for testing of phage-displayed FnB repeat's binding to fibronectin, phage ELISA assay was used. Second, for confirmation of MBP-FnB recognition, an indirect ELISA assay was used. Finally, for evaluation of the vaccination, ELISA assay was used to detect antibodies against FnB domain in the serum of immunised animals.

2.6.1 Phage ELISA Assay

The fibronectin-binding assay was carried out by phage enzyme linked immunosorbent assay (Phage ELISA (Harlow, 1999). The microtitre plate wells (Nunc-Immuno MaxySorp^{TM}, Denmark) were coated overnight at 4 °C, with 20 µg/ml human plasma fibronectin (Sigma, Australia) in 100 µl sodium bicarbonate buffer pH 9.5. The wells were washed once with 300 µl of phosphate buffered saline, 0.05% Tween 20 (PBST). Wells were then blocked with 250 µl of 2% (w/v) Bovine Serum Albumin (BSA) in PBS for 2h at room temperature. Wells were then washed three times with 300µl of PBST. Rnano3FnB full-length phage or nanophage particles (1×10^8) in 100µl of PBS were added to the wells. Negative controls (buffer and protein) were PBS and 2% BSA in PBS, whereas negative phage control was Rnano3 (Table 2.4). The plates were then incubated at room temperature for 2 h. Un-bound phage particles were removed by extensive washing with PBST (300 µl, 7 times). To detect phage particles bound to fibronectin in the wells, 100 µl of rabbit anti-pVIII (polyclonal antibody to M13, fd

and f1, Progen Biotechnik (Germany)) was added at the concentration of 0.1 µg/ml in 1× PBS and incubated for 1h. The wells were then washed five times with 300 µl PBST buffer. Next, wells were incubated with 100 µl of secondary HRP-conjugated anti rabbit antibody at a dilution of 1:2000 and then washed with 300 µl PBST seven times. The HRP bound to the plate was detected with 1-Step™ Turbo TMB-ELISA reagent (Thermo Scientific, Product # 34022). The enzyme reaction was stopped by adding 0.5 M H_2SO_4. The signal was quantified by absorbance at 450 nm.

2.6.2 MBP-FnB – Fibronectin Interactions Analyzed by ELISA

MBP-FnB domain fusion was tested for its functional integrity in ELISA setup. Briefly the microtitre plate wells (Nunc-Immuno MaxySorp™, Denmark) were coated overnight at 4 ºC with MPB-FnB domain fusion (5 µg/100 µl) in sodium carbonate buffer (pH 9.6).Maltose binding protein (MBP) expressed from empty vector (pMAL-c2X) (Table 2.2) served as negative control. After washing twice with 300 µl PBST (phosphate buffered saline, 0.05% Tween 20) the wells were blocked with 250 µl of 2% (w/v) Bovine Serum Albumin (BSA) for 2 h at 37 ºC. Wells were then washed 3 times with 300 µl of PBST, and incubated with 20 µg/ml human plasma fibronectin (Sigma, Australia) in 100 µl sodium bicarbonate buffer (pH 9.6). Wash wells 3 times with PBST (300 µl) and incubate at room temperature for 1 h with 100 µl of anti-fibronectin antibody (mouse monoclonal, Sino Biological Inc. Beijing China) dilution (1:2000). After 5 washes with PBST the wells were incubated with 100 µl of HRP-conjugated secondary antibody (mouse monoclonal) for 1h at room temperature and then washed with 300 µl PBST seven times. The plate was then developed with 1-Step™ Turbo TMB-ELISA reagent (Thermo Scientific, Product # 34022) for 30 min. The enzyme reaction was stopped by adding 25 µl of 0.5 M H_2SO_4. Absorbance was read at 450 nm.

2.6.3 Evaluation of Antibody Response by ELISA

For detection of phage specific antibodies after the vaccination experiment, the 96 well plate (Nunc-Immuno MaxySorp™, Denmark) was incubated with 1×10^8 phage particles in 50µl of Na_2CO_3 buffer (pH 9.6), whereas for the detection of FnB domain specific antibodies the plates with coated with 1µg of FnB domain (Section 2.5.1) in 50 µl of 1×PBS and incubated overnight at $4^{\circ}C$. Plates were washed twice and blocked

overnight at 4 ºC with 5% skimmed milk in 1×PBST (250 µl/well). Plates were then thoroughly washed (3 times /300 µl 1×PBST) and incubated with 50 µl of two hundred fold serum dilution (1×PBS and 1% BSA) for 1h at room temperature. Plates were then washed 6 times with 300 µl of 1×PBST, and incubated for 1 h at room temperature with 50 µl of 1:2000 fold dilution of biotinylated γ-chain specific goat anti- mouse IgG (Sigma) and biotinylated µ-chain specific goat anti-mouse IgM (Sigma).After washing plates 7 times with PBST, Streptavidin conjugated HRP (50 µl/well) was added to a dilution of 1:2000, and incubated for 1h at room temperature. PBS and 2% BSA in 1×PBS were used as negative controls. Plates were again washed with PBST 6 times and developed with 1-Step^{TM} Turbo TMB-ELISA reagent (Thermo Scientific, Product # 34022) for 30 min. The enzyme reaction was stopped by adding 12.5µl of 0.5M H_2SO_4. Absorbance was read at 450 nm. Antibody titres were determined as inverse value of the highest dilution of antiserum (in a series of two-fold dilutions) that gave a positive signal (above the negative control) in the ELISA assay against the antigen.

2.7 Use of Nanophage in Immunodiagnostic Devices: Dipsticks

2.7.1 Preparation of Dipsticks

To test the potential use of nanophage particles in diagnostics, a dipstick immunoassay was developed. It allows the qualitative determination of analytes. Full-length phage and nanophage displaying FnB domain as pIII fusion (Rnano3FnB) were used as detector probes. As FnB domain binds human fibronectin with high-affinity, fibronectin was the test-analyte for phage-based dip-sticks. Hi-Flow Plus membrane cards, used to make the sticks, were purchased from Millipore Corporation Bedford, USA. These cards contain nitrocellulose membranes casted on a 2 mil (0.001 inch or 0.252 mm-thick) polyester film backing. The membrane cards were cut in to 0.5 cm × 2.5 cm size sticks using automatic-card-cutting tool (BIODOT membrane cutter; SM5000; sheet slitter). The membrane has flow rate of 46 sec / 2.5 cm (total length of the dip-stick). Such membranes are suitable for the fast detection of abundant analyte. The distal end of strip contains 1.5 mm wide absorbent pad (label ‘A’ Figure 2.3), which increases the total volume of the sample that enters the test strip. The reagents for detection were applied to the membrane either before cutting (using a mechanical

dispenser) or by spotting 2 µl of appropriate reagents on the pre-cut strip using a pipette. Undiluted mouse anti-pVIII antibody (1 µg/ µl) was spotted at the control strip (label 'C' Figure 2.3) for the detection of virions that did not bind the test strip. The test strip (label 'T' in Figure 2.3) contained anti-fibronectin antibody (Sino Biological Inc.) or Collagen (Sigma) to detect fibronectin-loaded phage for direct detection assays, or fibronectin for competition assays. The protein-loaded strips were allowed to dry at 37 ºC for 1 h and stored in zip-lock sealed bags in dark place until use.

2.7.2 Assay Procedure

The coated strips were incubated in 50 µl mixture of analyte (fibronectin) and virions displaying FnB domain (Rnano3FnB) or controls without FnB (Rnano3) in 1 x PBS; specific assay concentrations are indicated in chapter 4. Strips were allowed to dry for 1 h at 37 ºC; the bound virions were visualized by western blotting. For western blotting, the strips were incubated in rabbit anti pVIII antibody (0.66 µg/mL) for 1 h at room temperature, followed by 5 washes of 5 min each, with PBST. Anti-rabbit antiserum-conjugated to alkaline phosphatase (Sigma, USA) was used as secondary antibody. The strips were washed again five times with PBST, and developed using Nitro Blue Tetrazolium (NBT) and 5-Bromo-4-Chloro-3-Indolyl Phosphatase (BCIP) in alkaline buffer (Blake, Johnston et al 1984). The details of the trial and optimization procedures as well as troubleshooting will be discussed in Chapter 4.

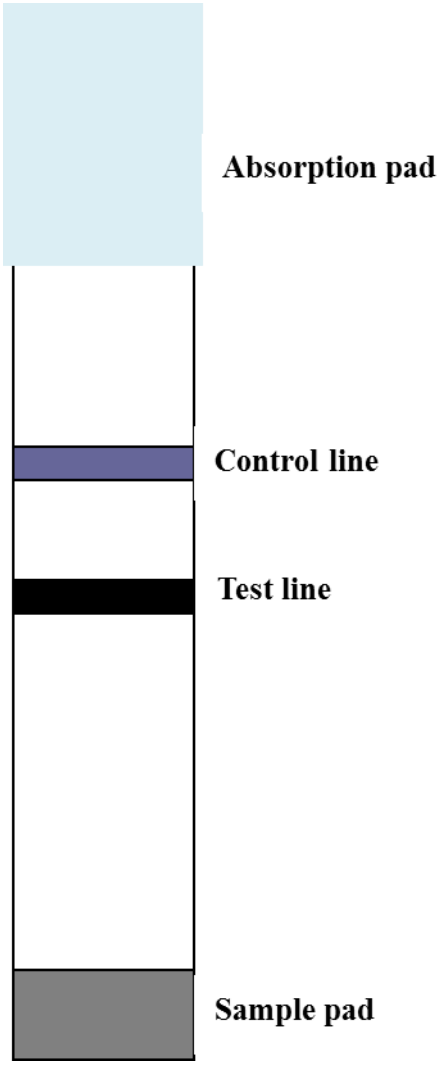

Figure 2.3 Custom-made dipstick device. Sample pad which is dipped in sample solution; test strip to capture any analyte bound with detector probe; control or capture strip to capture unbound probe; Absorption pad (cellulose fiber pad to increase volume of analyte absorbed).

2.7.3 Fluorescein Isothiocyanate (FITC) Labeling of Phage

Fresh fluorescein isothiocyanate solution (1 mg/ml) was prepared in 1 M NaCO3/ NaHCO3 (pH 9.0) buffer. Five hundred microliters of 1×10^{13} phage particles/ml were precipitated using 15% PEG / 0.5 M NaCl for nanophage and 2.5 % PEG / 0.5 M NaCl for full length phage respectively. The precipitate was dissolved in 200 µl of 1 M $NaCO_3$ / $NaHCO_3$ (pH 9.0) buffer. Fifty microliters of FITC solution was added to the phage suspension and incubated for 1 h at room temperature in the dark on a rotor. Reaction was stopped by adding 10 µl of the NH4Cl and phage were precipitated with respective PEG concentration twice. Final PEG pellet was suspended in 100 µl of 1×PBS and stored at 4 ºC in dark until further use.

2.8 Vaccination Protocols

2.8.1 Animals

Four to six week old female BALB/c mice were obtained from Small Animal Production Unit (SAPU), Massey University, and were housed at the same facility in standard cages. The animals were provided with standard rodent chow and water ad libitum. Appropriate ethics approval was obtained for the said research [MUAEC Protocol 11/85, updated 21-9-12]. Mice were confirmed to be sero-negative (no detectable antibody response to the phage virions or FnB domain in ELISA assay) before commencing with vaccination.

2.8.2 Preparation of Large and Nanophage for Immunization

The large scale preparation of nanophage and full-length phage was carried out using the protocols outlined in Sections 2.3.1- 2.4.1. The purification of nanophage and full-length phage used in this vaccination experiment will be discussed in detail in Chapter 3. After final purification and titration the full-length (Table 2.4) were titrated, whereas the nanophage were quantified by densitometry (Sections 2.3.2 and 2.3.4, respectively). All samples were divided into 6 aliquots, each containing 1×10^{10} particles in 100 µl of PBS. All full-length/nanophage samples displaying FnB were stored in 7% DMSO, at -80 ºC until used for immunization.

2.8.3 Immunization of Mice

BALB/c mice (30 animals, four to six week old) were separated in to five groups of 6 mice each, for immunization with a different sample (Table 2.5). Groups I and II were immunised with the full-length phage, Rnano3 and Rnano3FnB, respectively. Groups III and IV were both immunised with the nanophage displaying FnB domain; sample for immunisation of group IV was heat-treated (48 h at 37 $^{\circ}C$) before immunisation. Group V was immunised with sterile buffer (PBS). Groups I and V served as negative controls, whereas group II served as positive control (Table 2.5). Immunisation was carried out through intra-peritoneal route (i.p.). Each mouse in group I and II (full-length phage) was immunized, with 1×10^{10} particles in 100 µl of PBS. Mice in group III and IV (nanophage displaying FnB domain) were immunized with 1×10^{11} particles in 100 µl of PBS. Four booster doses ten days apart were given to each mouse through the same route over a period of 7 weeks (Table 2.5).

Table 2.5 Experimental protocol for immunization

Group[a]	Vaccine[b]
I	Full-length Rnano3
II	Full-length Rnano3 FnB
III	Nanophage Rnano3FnB
IV	Heat treated Rnano3FnB
V	PBS (No phage)

[a] Each group contained 6 BALB/c female mice 4-6 weeks old. All animals within a group were vaccinated with the same vaccine preparation.

[b] Each vaccine was injected intraperitoneally at ten days intervals for 7 weeks. Blood sample was collected on days 0, 10, 20, 30 and 49. On day 51 all mice were challenged intranasally with *S. pyogenes* suspension

2.8.4 Challenge

Ten days after the last booster vaccination, all groups were challenged intra nasally with *S. pyogenes* (D734; M type 22), with 10 - 20 µl of bacterial suspension (1.3×10^7 CFU) per nostril. The bacterial suspension was directly delivered to one of the nostrils using a micro-capillary pipette tip attached to a P20 pipetman. At day 15 post-challenge the animals were euthanized under SOP 09/03 Procedure for Performing Euthanasia in Mice, Rats, Hamsters and Guinea Pigs using CO_2.

2.8.5 Sample Collection

Blood samples were collected prior to first vaccination, before each booster dose and 15 days after the challenge (at the end of the experiment). Following euthanasia, a final blood sample was collected by cardiac puncture. Blood was allowed to clot at room temperature for 2 h. The clot was separated from the serum by centrifugation for 5 min at 2000 rpm; the serum was collected and stored at -20 °C until further use.

To assess bacterial colonisation after challenge, nasal swabs, first three tracheal rings and lung tissue were collected. Nasal swabs were collected using sterile cotton applicators, which were dissolved into 500 µl of Todd Hewitt broth in eppendorf tubes. Lung tissue (entire left lung) was collected and placed into a microfuge tubes containing 500 µl PBS supplemented with protease inhibitor (Roche). The tissue was macerated in the same buffer, and then centrifuged at 1300 rpm for 5 min. The tracheal rings were collected in Todd Hewitt broth and agitated by vortexing for 10 sec to separate bacteria from tissue. All samples were plated on Columbia Blood Agar plates, indicator for *S. pyogenes* through β haemolysis.

2.8.6 Statistical Analysis

The antibody response against phage and FnB domain was detected by ELISA, as described above. Significance of the observed differences in antibody response of various groups was analyzed using Wilcoxon-Mann-Whitney test. Differences were considered significant at $P \leq 0.05$.

Chapter 3

Investigation and Modifications of the Nanophage Production System

3.1 Introduction

The original engineered system for production and partial purification of short particles (50 nm in length) derived from f1 filamentous phage was a low-efficiency system, resulting in poor yields of the short particles (Specthrie et al., 1992). This system was recently modified to increase the efficiency of short particle production, by construction of a novel helper phage and modification of the protocol for purification of the nanophage away from the full-length helper phage (Bennett, 2010). The short phage were named "nanophage", to signify their much smaller (~ $1/20^{th}$) length in comparison to the full-length f1 phage.

In this chapter, the nanophage production system was further investigated, functionalized and improved, with the ultimate aim to develop a high-efficiency system for nanotechnology and biotechnology applications. Furthermore, the resistance of the nanophage to heating in the presence of ionic detergent sodium dodecyl sulfate (SDS) was investigated, in comparison to the full-length filamentous phage.

3.2 Development of an Improved Nanophage Production Protocol

3.2.1 Purification of Nanophage

In the current system of nanophage production (Bennett, 2010) the full length virions were partially separated from the nanophage by differential PEG precipitation and preparative agarose gel electrophoresis of the native virions, followed by purification of the nanophage from a gel slab containing the nanophage band, using centrifugation through a glass wool column to eliminate agarose (Chapter 2; Section 2.4.2). However, the recovery of nanophage from an agarose gel slab using this method was very poor (~ 1%) and the preparation was contaminated with agarose particles. Therefore, it was essential to develop an alternative technique to achieve better recovery of the nanophage particles. In this context, electroelution after agarose gel electrophoresis

was trialed, as well as replacing preparative agarose gel electrophoresis by cesium chloride gradient separation.

3.2.2 Cesium Chloride Gradient Purification

Cesium chloride gradient purification is extensively used for phage purification away from cellular debris, which is co-precipitated together with the phage using PEG/NaCl method. The nanophage have a 20-fold higher ratio of end-caps to the filament proper in comparison to the full-length helper phage. Given that the end-caps and filament proper must have different compositions and therefore very likely different densities relative to each other, it was expected that the resultant density of the full-length phage is different from that of the nanophage. As the cesium chloride gradients have ability to separate molecules with small differences in densities (Meselson and Stahl, 1958), this method could have a potential to separate full-length helper phage from the nanophage. Given that densities of the caps vs. the body of the phage are not known (i.e. it is not known or predictable whether the caps or the body have a higher density), the relative position of the nanophage vs. the long phage in the CsCl gradient could not be predicted.

The 15% PEG fraction after differential PEG precipitation, which is highly enriched for the nanophage, was subjected to the cesium chloride density gradient centrifugation, as outlined in Section 2.4.4. Two distinct grey bands, likely corresponding to the full-length phage and the nanophage, were observed after ultracentrifugation; however the two bands ran very close to each other and it was not possible to extract one of the two bands without disturbing the other. Moreover, the position of nanophage was not known and it was not certain whether the observed second band corresponds to nanophage or not. Therefore fractions of the gradient were collected until both phage bands were removed from the centrifuge tube. A total of 26 fractions, 150-250 µl each, were collected and subjected to native phage agarose gel electrophoresis to locate the position of the nanophage and full-length helper phage in the gradient (Figure 3.1). The nanophage were detected in fractions 17-26 (Figure 3.1, lanes 2-11), whereas the full-length helper phage were identified in fractions 21-26 (Figure 3.1, lanes 7-11). The full-length helper phage and nanophage fractions therefore overlapped; fractions 21 and 22 contained vary small amount of full-length helper phage (Figure 3.1, lanes; 6 and 7) whereas fractions 19 and 20 contained no

detectable full-length helper phage (Figure 3.1, lanes; 4 and 5). Even though full-length helper phage and the nanophage fractions overlapped with each other, the full-length phage were distributed over a narrower range of fractions in comparison to the nanophage. The fractions that contained a strong nanophage band, but very weak or undetectable full-length helper phage band were titrated to determine the amount of residual full-length helper phage (Figure 3.1, lanes 4-6). The titration showed that fractions 19, 20 and 21 still contained helper phage at $2x10^{9}$, $1x10^{10}$ and $2x10^{11}$ particles per fraction respectively, in comparison to the input into the gradient at $1.3x10^{13}$. In summary, the difference in density of the nanophage and the long phage was insufficient for separation by CsCl density gradient centrifugation.

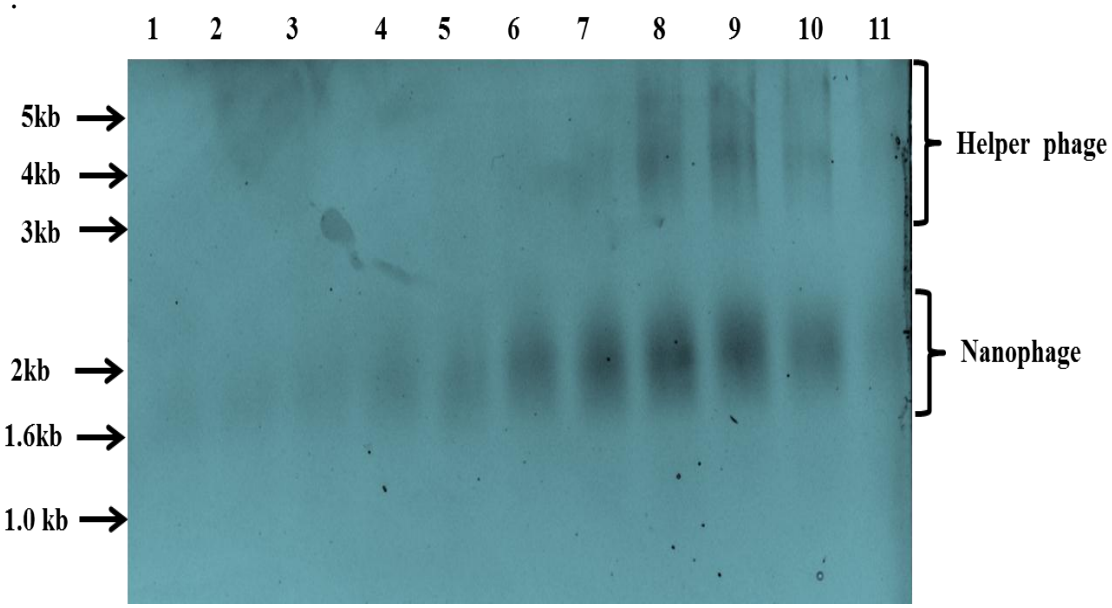

Figure 3.1 Separation of the nanophage and full-length helper phage by CsCl-density gradient ultracentrifugation. Fractions obtained after centrifugation were subjected to agarose gel electrophoresis. Lanes: 1, fraction 16; 2, fraction 17; 3, fraction 18; 4, fraction 19; 5, fraction 20; 6, fraction 21; 7, fraction 22; 8, fraction 23; 9, fraction 24; 10, fraction 25; 11, fraction 26. The fraction numbering is in the high-to-low density direction (bottom-to-top of the tube). Fractions loaded in lanes 4, 5 and 6 were titrated to determine the number of residual full-length helper phage.

3.2.3 Improved Nanophage Recovery after Preparative Agarose Gel Electrophoresis

The protocol developed by N. Bennett (2010) and described in Section 2.4.2 recovered the nanophage from a gel slice by centrifugation through a siliconised glass wool plug, using a home-made spin-filter device. However, the recovery was very poor and almost 99 percent of sample was lost during the procedure. In an attempt to improve the nanophage yield, the recovery of nanophage from the gel slab was performed by electroelution using a D-Tube dialyzer (Novagen) as described in Material and Methods (Section 2.4.3).

Starting from the nanophage-enriched lysate, obtained after differential PEG precipitation, nanophage were separated from the full-length helper phage using preparative native virion electrophoresis (Bennett, 2010), followed by excision of the nanophage-containing band from the gel. Two separate electroelution experiments were performed from the same nanophage-enriched lysate (Figure 3.2; Table 3.1). The eluted nanophage were concentrated by PEG precipitation to obtain the final electro-purified nanophage (EPN) (Figure 3.2, lanes 10 & 11). To detect the residual helper (full-length) phage, the EPN preparation was titrated. It was found that samples still contained large phage; however the number of particles in electroelutions of two different gel slices was 134-fold and 1400-fold lower than in the starting material loaded onto the agarose gel (Table 3.1). The amount of the nanophage in the starting PEG-enriched material and the final electro-purified nanophage was calculated using densitometry analysis of eluted and purified nanophage, using as a standard a series of two-fold dilutions of the wild-type f1 phage of known concentration (Figure 3.2, lanes 1-9). Quantification of the nanophage showed a recovery of 45% and 30% in the two different elutions, relative to the starting material loaded on agarose gel. This is a much higher recovery when compared to electrophoresis in combination with glass-wool extraction or the CsCl gradient purification, both of which resulted in a very poor nanophage recovery.

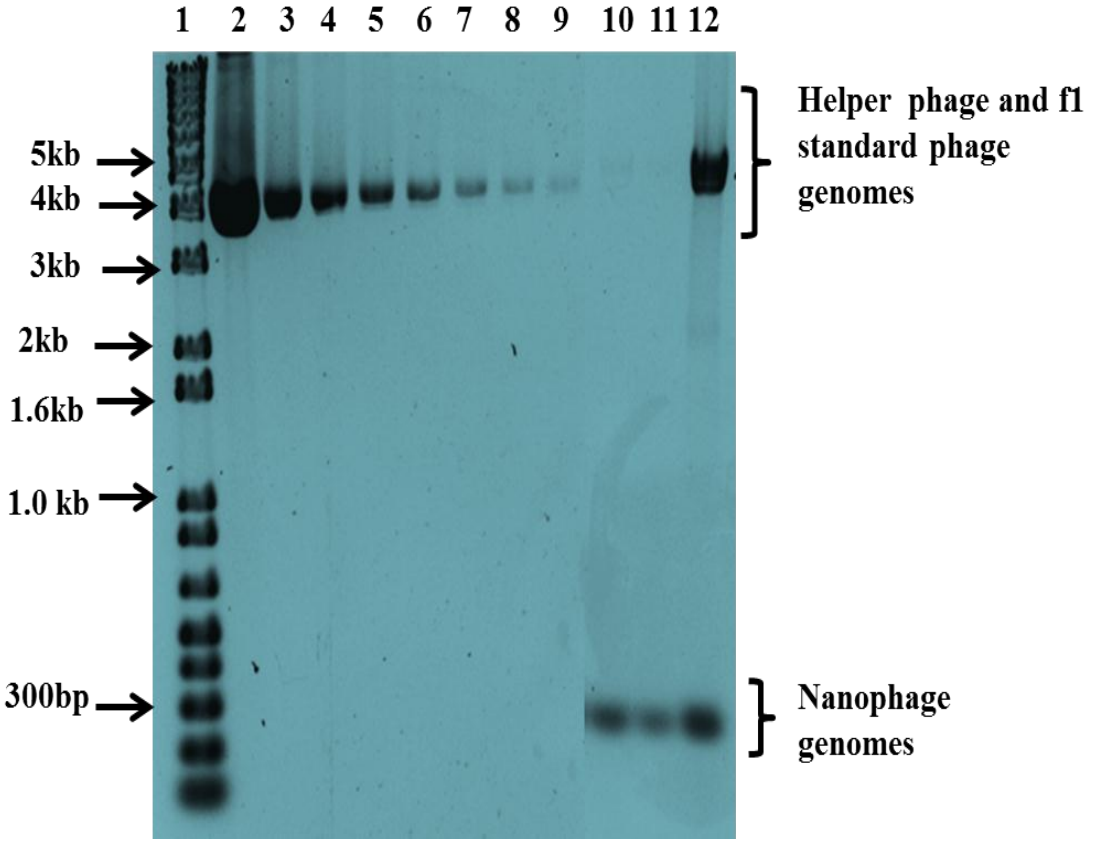

Figure 3.2 Gel used for quantification of electroeluted phage by agarose gel electrophoresis. Lane 1, 1kb+ ladder; 2-9, two fold dilutions of phage standard (f1 wild-type); 10, and 11, EPN1 and EPN2 (5 µl out of 300 µl), respectively (electro-purified nanophage from two different preparative electrophoreses); 12, nanophage-enriched lysate (5 µl out of 1 ml) (material loaded onto the preparative gels from which nanophage in lanes 10 and 11 were eluted).

Table 3.1 Purification of the nanophage by native agarose gel electrophoresis and electroelution

	Nanophage (total number[c])	**Recovery of the nanophage[d]**	**Helper phage (total number[e])**	**Helper: nanophage ratio[f]**	**Fold decrease in helper: nanophage ratio[g]**
Input[a]	6.4×10^{14}	N/A (starting material)	4.5×10^{12}	7.0×10^{-3}	N/A (starting material)
EPN1[b]	2.9×10^{14}	45 %	1.5×10^{10}	5.2×10^{-5}	134
EPN2	1.98×10^{14}	31 %	9.9×10^{8}	5.0×10^{-6}	1400

[a] Starting material - nanophage-enriched lysate obtained by differential PEG precipitation and loaded on the preparative gel.

[b] Electro-purified nanophage from two independent experiments (corresponding to the EPN1 and EPN2 lanes 10 & 11 in Figure 3.2.

[c] Determined by densitometry (Figure 3.2).

[d] Ratio of the nanophage amount in a purified sample to the amount in the input.

[e] Determined by titration.

[f] Determined by dividing the total number of full-length helper phage with the total number of the nanophage particles.

[g] Determined by dividing the "helper**:** nanophage" ratio in purified fractions to the "helper**:** nanophage" ratio in the input.

3.3 Stability of Nanophage to Sodium Dodecyl Sulphate (SDS) at 70 °C

In the course of nanophage analyses by agarose gel electrophoresis, it was observed that the standard protocol for *in vitro* disassembly, heating the virions for 10 min at 70°C in a buffer containing 1% SDS, was not efficient in releasing DNA from the nanophage particles (data not shown). This indicated that the nanophage particles could be more stable to heat/SDS treatment than the full length helper virions, even though both are composed of identical coat proteins (pVIII, pVII, pIX, pIII and pVI) and were assembled within the same *E. coli* cell. To test this hypothesis, a time-course experiment was used to monitor disassembly of approximately equal number (2×10^{12}) full-length helper phage and nanophage at 70 °C in the presence of 1% SDS; one sample was also incubated at 100 °C. Disassembly of the helper (full-length) phage and nanophage virions was monitored through release of ssDNA, which was separated by agarose gel electrophoresis and visualized directly by staining with ethidium bromide (Figure 3.3 A). To identify the ssDNA remaining encapsidated inside the virions that resisted heat/SDS treatment, the virion proteins were stripped off the ssDNA by soaking the gel in an alkaline buffer (NaOH), followed by neutralization and re-staining of the gel by ethidium bromide (Figure 3.3 B).

When the full-length (helper) virions were analyzed, untreated samples did not contain any free ssDNA and all ssDNA was contained within the virion (Figure 3.3, compare the corresponding untreated sample lanes in gels A and B). At the first time-point (5 min) of incubation in SDS buffer at 70 °C, all full-length virion ssDNA was detected as a free form, and none within the virion (Figure 3.3 A). When the nanophage were subjected to the same analysis, some free DNA was observed at the time points 5 min – 20 min, however a large proportion was encapsidated and were only detected after the *in situ* disassembly (Figure 3.3, compare the 70 °C-treated sample lanes (5-20 min) in A *vs*. B). The amount of virion-encapsidated DNA decreased gradually between 5 min and 20 min time points, but was only completely eliminated by incubation at 100 °C. Conversely, the free DNA amount sharply increased at 100 °C, confirming that this is the only treatment that disassembles all nanophage virions (Figure 3.3, compare lane 12 in A *vs*. B). An unexpected free DNA band was detected in all heat-treated nanophage samples; this band did not increase in the intensity upon heating at 100 °C,

hence this represents a virion population that has the same level of stability as the full-length virions. This band is not present in all nanophage samples (data not shown). A faint band of the same size was also detectable in the full-length phage preparation upon treatment at 70 °C (Fig. 3.3A). The full-length phage were purified from the same culture as the nanophage preparation, by the low-PEG precipitation. This is consistent with the helper phage giving rise to shorter particles or "miniphage" if a replicating phage in the culture undergoes duplication of the origin of replication (La Farina et al. (1987); data not shown). These shorter phage would have been enriched for in the nanophage fraction that was obtained by high-PEG precipitation, but not in the low-PEG fraction that poorly precipitates relatively short miniphage. Unequivocal identification of this DNA band requires further analysis by sequencing or Southern Blotting using appropriate probes. It is interesting that these miniphage particles, despite being relatively short, do not demonstrate high resistance to heating in SDS that the nanophage possess.

Overall, this experiment has demonstrated that the nanophage have superior resistance to heating in the presence of ionic detergent SDS in comparison to the full-length phage, given that a good proportion of the particles remains intact during prolonged incubation at 70 °C in the presence of 1% SDS. From the standpoint of understanding filamentous phage structure and physical properties, these findings indicate that the site of action for SDS is likely along the filament, and that perhaps imperfections of pVIII packing due to mechanical bending and twisting, which is observed in the full-length phage, but not the nanophage electron micrographs (Bennett, 2010), may play a role in this. From the technological standpoint, this property may be of interest to nanotechnology or diagnostic applications that involve harsh conditions, such as introduction of chemical modifications or use at high temperature in detergent-containing environment. Further investigation into stability under other conditions (e.g. pH extremes and organic solvents) would provide further information that would be valuable for the nanophage applications.

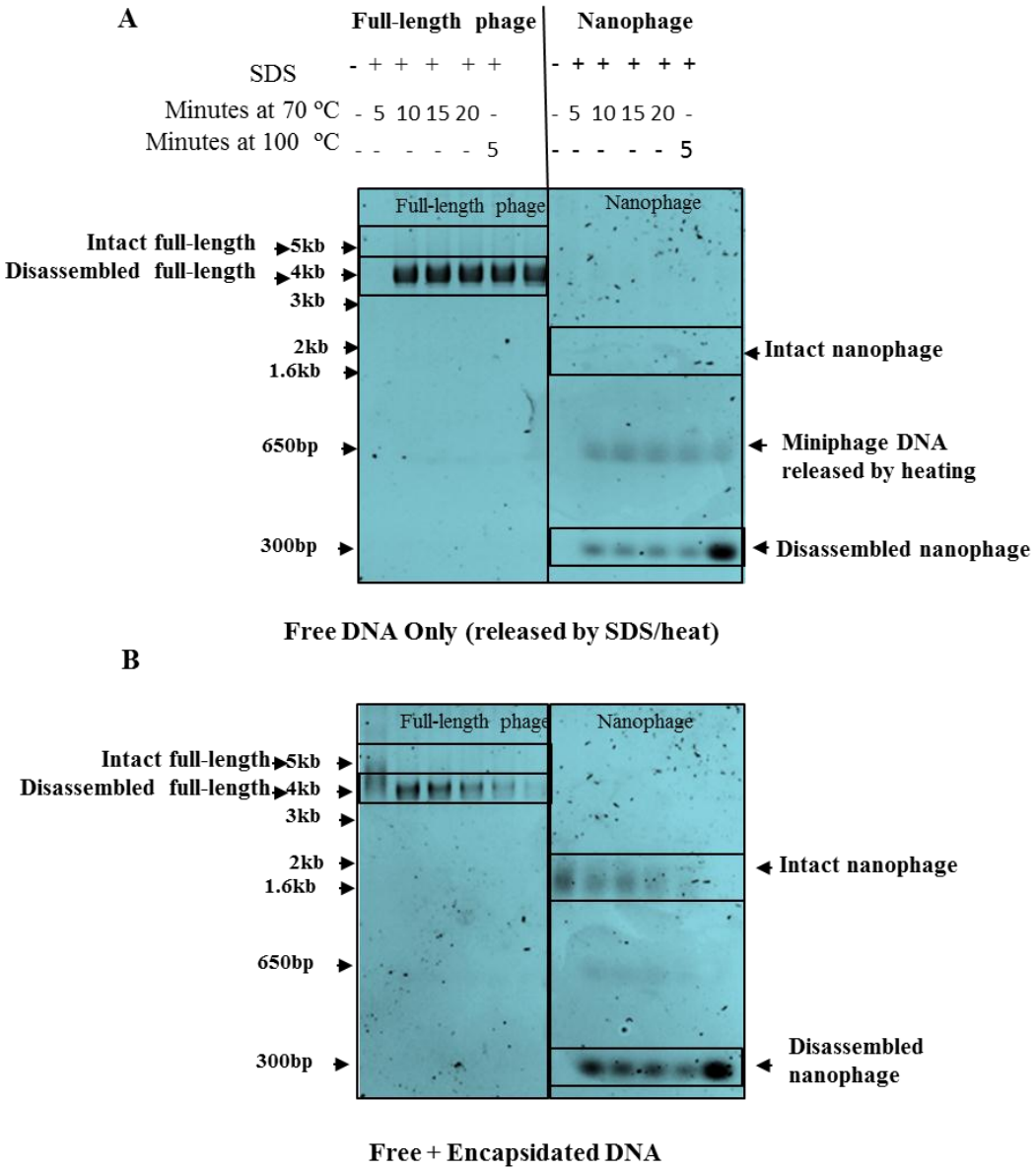

Figure 3.3 Resistance of nanophage to heating in SDS vs. full-length (helper) phage. A. Free DNA, released from the virions by heat/SDS treatment. Virion-encapsulated DNA cannot be detected, as it is not exposed to ethidium bromide. **B**. Same gel as in A, except that the DNA packaged inside the intact (undamaged) virions (in addition to the free DNA) was now visualised by in-gel virion disassembly, followed by staining in ethidium bromide.

Annotation: Treatments for the samples in each lane are indicated above the gel. Arrowheads along the sides of the gel point to the relevant bands of phage DNA: intact full-length or intact nano, the virion-encapsidated DNA inside the SDS-resistant virions; disassembled full-length and disassembled nano, DNA from the SDS/heat-disassembled virion fraction.

3.4 Construction of a Nanophage-Display System

Production of the shortest possible Ff-derived particles requires that shortest possible ssDNA (200 nt) is packaged into a phage-like particle (Bennett, 2010; Specthrie et al., 1992). In order to replicate such a short ssDNA, an engineered plasmid is used as a carrier and template for the nanophage genome replication. This plasmid contains a 200-bp nanophage genome that is replicated from an incomplete positive strand origin of replication, through the packaging signal, and terminated at the second positive strand origin which is initiation-incompetent. The replication from positive origin is initiated and terminated by a rep-family strand-transferase pII, each replication cycle resulting in a 200 nt single-stranded circle that contains a packaging signal. A helper phage provides pII and all other proteins required for replication and packaging of the 200-nt circular ssDNA nanophage genome into the nanophage. As the phage assembly is flexible and can incorporate multiple genomes into one particle, a process that depends on the ratio of the major coat protein (pVIII) to the initiation and termination proteins (pVII/pIX and pIII/pVI), in order to stimulate short particle assembly, a helper phage with decreased relative amount of the major coat protein pVIII was deemed more appropriate than the wild-type for assembly of short particles (Bennett, 2010; Specthrie et al., 1992). The incomplete positive strand origin of replication (segment I only; lacking the segment II) in the nanophage genome warranted use of a helper with a known compensatory mutation in *gII* (pII) that allows replication of positive strand origin of replication that lacks the segment II (Enea and Zinder, 1982). Helper phage R474 that has a mutation in promoter region of the *gVIII*, produces 40% less pVIII than would occur using a phage with a wild-type promoter (Specthrie et al., 1992). However, the mutation in the *gVIII* promoter region of R474 was located within the coding sequence for minor coat protein pVII, causing a missense mutation and resulting in overall decreased helper phage titres which in turn reduced the amount of nanophage produced. N. Bennett (2010) constructed a different helper phage, derived from the "standard" helper phage R408 (containing wild-type promoter of *gVIII* and coding sequence of *gVII*). To decrease the amount of pVIII protein without affecting other genes, a $gVIII^{amber}$ mutation was introduced into R408. In *supD* strains, this mutation is suppressed at a rate of about 50%, leading to significant decrease in pVIII amount. This helper phage was named Rnano (Chapter 2, Table 2.4).

This helper phage was further converted into display vector, by inserting a multiple cloning site between the signal sequence and mature portion of pIII, to obtain a nanophage display vector/helper phage, named Rnano3 (Chapter 2, Figure 2.1). However, Rnano3 forms small plaques; hence the same MCS was also inserted into the standard helper phage R408, to obtain helper phage R408-3. As R408-3 gave somewhat bigger plaques than suppressed Rnano3, there would be a benefit in being able to use that phage rather than the *gVIII*^{am} helper Rnano3. In order to examine whether R408-3 can be used in the nanophage production, the Rnano3 and R408-3 phage were compared in their ability to elicit the nanophage production (Figure 3.4). R408-3 appeared equally efficient in producing nanophage particles as Rnano3; however the R408-3 preparation contained a strong extra band, which was puzzling.

The abundant nanophage production indicated that previous assumption of decreased amount of pVIII favoring the production of nanophage particles may not be valid. The appearance of additional band in the R408-3 preparation was hypothesized to be due to conversion of the nanophage-producing plasmid into a phagemid through deletion of the terminator of f1 origin of replication, an event that must have converted the nanophage production plasmid into a phagemid. Therefore, it was considered less desirable than Rnano3 for use in the nanophage production and the work in Chapters 4 and 5 was carried out using the Rnano3. Retrospectively, this band was identified as virion-encapsidated nanophage DNA of the SDS-resistant nanophage virions (c.f. Fig. 3.3.; data not shown). It is therefore possible to use the R408-3 for the nanophage production instead of Rnano3, due to more focused migration of the native virions in agarose gel electrophoresis in comparison to Rnano3, which gives a diffuse band.

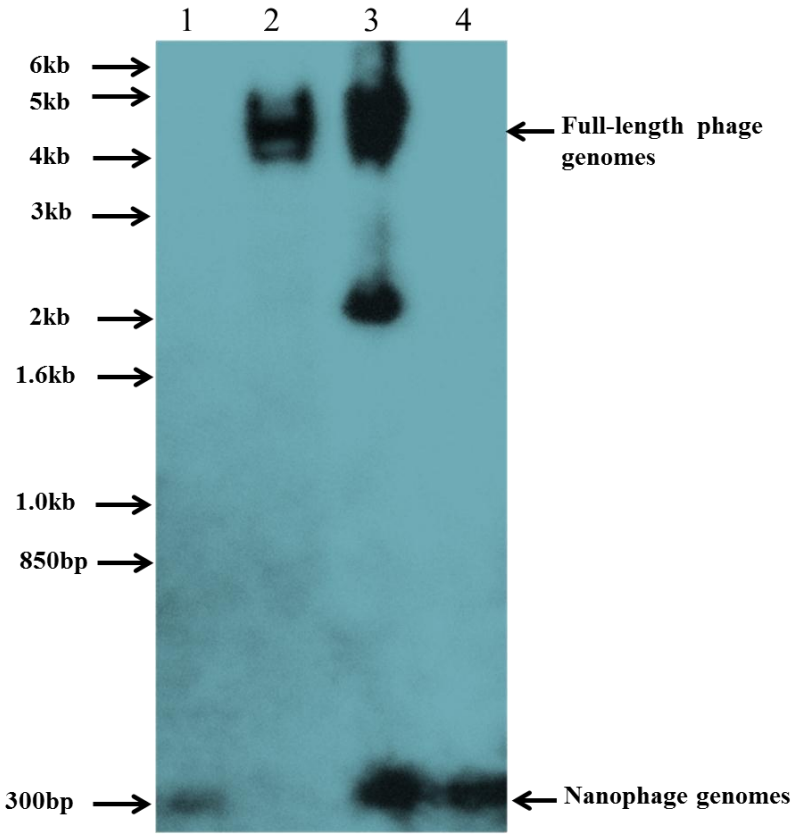

Figure 3.4 Comparison of nanophage particles produced by Rnano3 and R408-3 as helper phage. Preparations enriched for the nanophage ("high-PEG fraction) and the full-length helper phage ("low-PEG fraction) were tested to determine the amount of nanophage produced using Rnano3 vs. R408-3. Virions were disassembled by heating (5 min at 70 °C in the presence of 1% SDS) and the released ssDNA was separated by electrophoresis on an agarose gel. Upon completion of electrophoresis, the phage particles that remained intact after the SDS/heat pre-treatment were dissociated *in situ* by soaking the agarose gel in NaOH buffer. DNA was visualized by Southern blotting using a PCR-generated probe corresponding to the origin of replication and packaging signal (the intergenic (IG) sequence). Lanes: 1 and 4, nanophage-enriched preparations ("high-PEG") produced using Rnano3 and R408-3 helper phage, respectively; 2 and 3, full-length phage-enriched preparations ("low-PEG") produced using helper phage Rnano3 and R408-3, respectively. The arrows indicate 1 Kb Plus double-stranded linear DNA ladder (Life technologies). This standard is not suitable for direct comparison of ssDNA size in nucleotides. It has been used only to measure the progression of electrophoresis and position of bands due to lack of an appropriate ssDNA marker.

3.5 Testing a Helper Phage-Free System for the Nanophage Production

System for nanophage production developed by N. Bennett (2010) generates full length helper phage particles as well as the nanophage particles. The purification procedure developed in the same study (Bennett, 2010) and in this thesis (Chapter 2, Section 2.4.3) removed most of full-length helper phage (as observed by agarose gel electrophoresis), however they were not eliminated completely (Table 3.1). Depending on preparation, full-length helper phage remained in the final purified nanophage preparation (at the frequency range between 10^{-6} and 10^{-5} relative to the nanophage). Although this is much lower than starting nanophage-enriched sample obtained by differential PEG precipitation that contained 10^{-2} helper phage relative to the nanophage, it could still not be tolerated for applications in which live or full-length bacteriophage (virus) particles are required to be excluded due to regulatory requirements or consumer concerns. For its presumed applications in diagnostics and as antigen carriers in vaccines, there was a need to separate nanophage completely from full-length helper phage and completely eliminate helper phage. Furthermore, purification steps required to separate nanophage from the full-length helper phage increase the time and the cost of the nanophage production. To eliminate helper phage from the production system and to obtain high yield of pure nanophage, a system that does not include a helper phage would be desirable.

To achieve a helper phage-free nanophage production system, a specialized helper PLASMID pDH (Gagic D. and Rakonjac J., unpublished) was tested for use in nanophage production instead of the helper phage. This plasmid is derived from a standard helper phage VCSM13 (Stratagene, La Jolla, CA, USA) by deleting f1 origin of replication and packaging signal. The pDH plasmid replicates from a pA15 plasmid origin of replication and carries a kanamycin resistance gene (Km^R), allowing selection and maintenance in the *E. coli* cells as a plasmid (Vieira and Messing, 1987). This helper plasmid was efficiently producing phage proteins as indicated by high-efficiency assembly of the standard phagemid particles (pJARA140) (Beekwilder et al., 1999) (Chapter 2, Section 2.3.1 and 2.3.3), giving phagemid titres of 5.9×10^{9}/mL in the standard growth experiments. It was observed that phagemid titres were two thousand fold higher when cells (K1030//pDH) were grown at 30 ºC (2.6×10^{11}/mL)

than phagemid titres obtained when they were grown at 37 °C, after transformation with pJARA140. Therefore the nanophage production trial using pDH helper plasmid was carried out at 30 ºC in this particular experiment using protocol described in Chapter 2 (Section 2.3.3).

Since both the helper plasmid (pDH) and nanophage producing plasmid (pNJB07) had a *Km*^{R} marker it was not possible to use them together. As pNJB07 contained both the *Amp*^{R} and *Km*^{R} markers, the latter marker was not required for plasmid selection and maintenance. Therefore, gene encoding the *Km*^{R} marker was removed from pNJB07 using two flanking restriction sites for blunt-cutting enzymes, *Sna*BI and *Nae*I. The double digest produced two fragments, of 2965 bp and 1273 bp. The larger fragment contained the nanophage origin of replication and was circularized using T4DNA ligase. The removal of *Km*^{R} was confirmed by sequencing of purified plasmid DNA and by assaying the transformants for their sensitivity to kanamycin. The plasmid, named pSS3, was tested for nanophage production using the helper phage Rnano. The amount of produced nanophage was comparable to that of pNJB07 (Fig. 3.5A & B, lanes 2-5).

Competent cells made from K1030//pDH were transformed with pSS3. The pool of transformed cells was diluted into fresh growth medium pre-heated to 30 ºC and incubated overnight to test the production of nanophage (Chapter 2, Section 2.4). The original nanophage production system (pNJB07//Rnano) and the nanophage producing system with modified nanophage-producing plasmid (pSS3//Rnano) were used as controls (Figure 3.5A & B).

Strong nanophage bands were detected in both control samples, pNJB07//Rnano and pSS3//Rnano after agarose gel electrophoresis of SDS disassembled (Figure 3.5 A; lanes 2-3 and 4-5 respectively) and native virions (Figure 3.5B; lanes 2-3 and 4-5 respectively) visualized after ethidium bromide staining, indicating that pSS3 plasmid was as efficient in nanophage production as pNJB07. However, no DNA bands corresponding to the nanophage genomes were detected in the helper plasmid system (pSS3/pDH) in the nanophage fraction obtained after precipitation with 15% PEG (Figure 3.5 A, lane 7). The fact that the nanophage genomes were not identified in 15% PEG fraction indicated that nanophage genomes were not produced in a measureable quantity in pSS3/pDH (helper phage-less) system.

Overall, this analysis showed that helper plasmid pDH cannot be used for the nanophage production. The most likely reason for this is that the f1 origin of replication in the nanophage origin is truncated, missing the section II that is required for stable interaction with replication protein pII (Dotto et al., 1984). For efficient replication from this truncated origin a particular mutant of the replication protein pII is required, and this mutation is not present in pDH. Therefore, mutation of pII in the helper plasmid system is required for its use in the nanophage production system. The affinity of pII for the positive strand origin of replication is affected by the lack of section II, therefore it was thought that overexpression of the pII in the same cell could potentially compensate for this and, increasing the recognition event of nanophage origin and the replication from the nanophage origin. To test this hypothesis, plasmid pNJB2 (Bennett, 2005) overexpressing wild-type pII was transformed into K1030 cells carrying pSS3 and pDH and subjected to nanophage production procedure (in the presence of 01 mM IPTG that was used to induce *tac*-gII expression) followed by purification/concentration procedure through differential PEG precipitation using the same protocol as for pSS3/pDH and the two controls in which the Rnano3 helper was used. A band of nanophage genomes was identified after agarose gel electrophoresis, indicating production of nanophage particles (Figure 3.5A & B; lane 9). This confers that absence of nanophage production in pSS3/pDH system is the result of inefficient replication of nanophage origin due to low-efficiency binding of pII to the truncated origin of replication. The nanophage bands derived from an equivalent volume of preparation were, however, very weak in comparison with those obtained using the helper phage Rnano3 (Figure 3.5 A & B, lanes 3 and 5 vs. lane 9), indicating much lower nanophage production for the helper plasmid, even when the wild-type pII is overexpressed.

Given that the helper pDH is a plasmid and has no f1 origin of replication, it was not expected to observe full-length phage particles in 2.5 % PEG fraction of helper plasmid system that precipitates full-length phage. Nevertheless, DNA bands of intermediate size between the nanophage and the full-length helper (lanes 6-9) and a band nearly the size of helper phage (lane 8) were observed in 2.5 and 15 % PEG fractions for pSS3/pDH and pSS3/pDH/pNJB2 systems of nanophage production. Although the helper plasmid lacks a packaging signal, it is possible that some small number re-acquired the missing f1 origin of replication and the packaging signal

through recombination with pSS3 (lane 8), or that the nanophage origin plasmid mutated by deletion of the terminator thereby becoming converted into a phagemid (pSS3/I) whose genome is completely packaged inside the virion (lanes 6-9; intermediate-size band). To detect potential pSS3/I-derived phagemid particles (PPs, virions containing complete packaged pSS3/I DNA), which are expected to package Amp^R marker encoded by pSS3 plasmid, the PEG-precipitated fractions were titrated on Amp-containing plates. The titration (Chapter 2, Section 2.3.3) identified PPs carrying *Amp*^{R} marker in pSS3/pDH and pSS3/pDH/pNJB2 systems. The phagemid titre was 2×10^{10}/mL in the low-PEG fraction, and 1.7×10^{11}/mL in high-PEG fraction for pSS3/pDH system whereas 7×10^{10} in low-PEG and 1×10^{11}/mL in high-PEG fraction for pSS3/pDH/pNJB2 system. This analysis confirmed that the nanophage origin had undergone recombination to remove the replication terminator, resulting in replication and packaging of entire plasmid pSS3/I into long phagemid particles, rather than production of the nanophage. Overall, these findings show that recombination needs to be inactivated in the host cells used for the nanophage production to avoid conversion of the nanophage production plasmid into a phagemid, in addition to the use of pII mutant that compensates for the lack of the section II of the plus strand origin in order to achieve efficient replication of nanophage origin from plasmids.

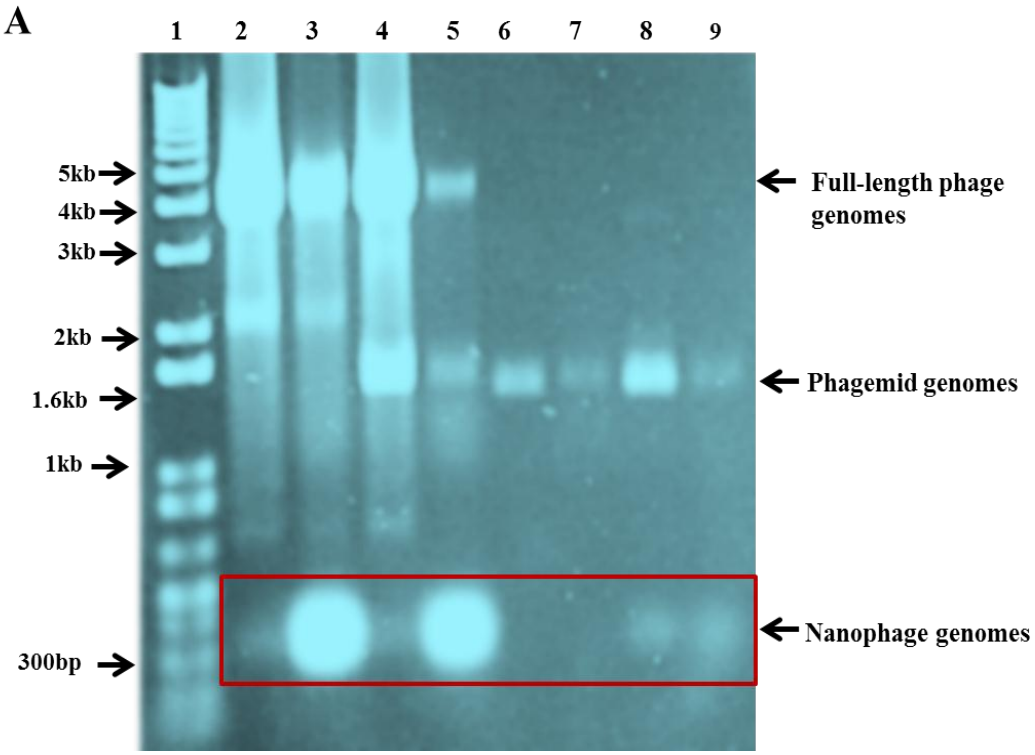
A
1 2 3 4 5 6 7 8 9
5kb
4kb
3kb
2kb
1.6kb
1kb
300bp
Full-length phage genomes
Phagemid genomes
Nanophage genomes

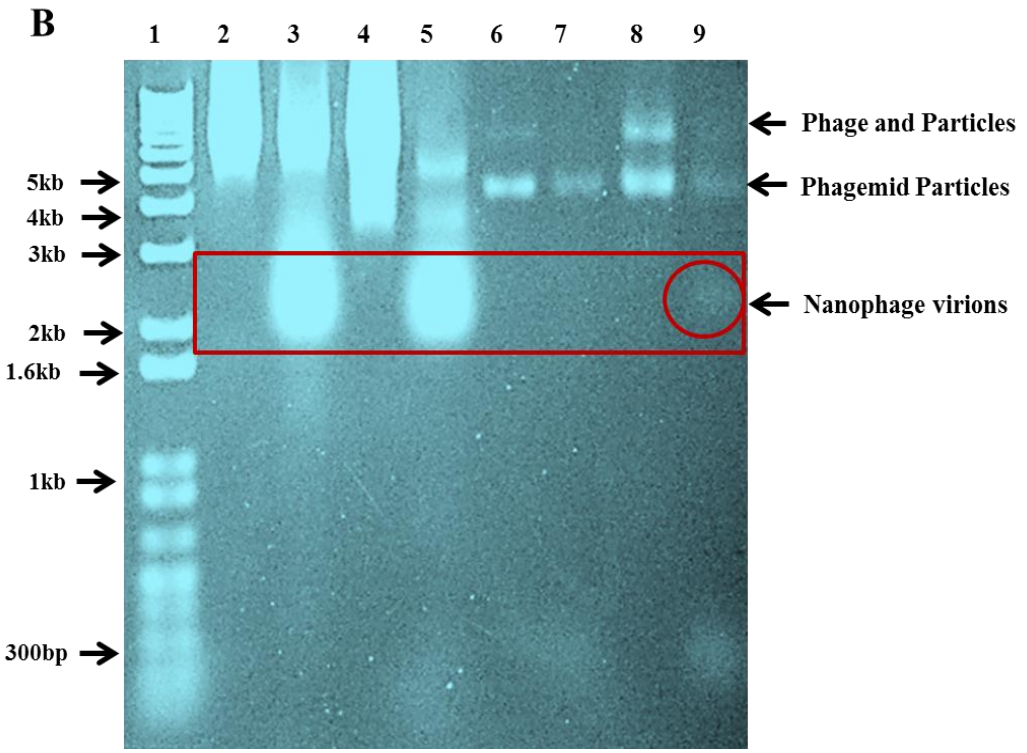
B
1 2 3 4 5 6 7 8 9
5kb
4kb
3kb
2kb
1.6kb
1kb
300bp
Phage and Particles
Phagemid Particles
Nanophage virions

Figure 3.5 Agarose gel electrophoresis of particles produced from the helper phage and helper plasmid systems. **A;** The SDS-disassociated **B;** native phage particles; separated by agarose gel electrophoresis. **A & B**: Lane 1; 1Kb Plus DNA ladder used to mark the position of phage particles and progression of electrophoresis in the absence of a suitable marker. Lanes 2 and 3, respectively, full-length phage (2.5% PEG) and nanophage (15% PEG) fractions obtained with pNJB07/Rnano; 4 and 5, respectively, full-length phage and nanophage fractions obtained using pSS3/Rnano; 6 and 7, respectively, full-length phage and nanophage fractions obtained with pSS3/pDH; 8 and 9, respectively, Full-length and nanophage fractions obtained with pSS3/pDH/pNJB2. Arrows indicate dsDNA fragments of the 1Kb Plus ladder (Life Technologies).

Chapter 4

Applications of Nanophage in Diagnostic assays: ELISA and Dip stick

4.1. Introduction

Use of full length phage particles have been reported in lateral flow dip stick devices for non-competitive immunodetection of small molecules, as an alternative to competitive antibody assays (Gonzalez-Techera et al., 2007). In this technique, called Phage Anti-Immune complex Assay (PHAIA), the probe that are peptides that bind to the antigen-antibody immune complex, but not to the antibody or antigen on their own, were used to recognize the immune complexes. This concept was reported as suitable for in-laboratory and on-site detection of analytes in environmental samples (González-Techera et al., 2007). Currently used filamentous phagemids display vectors, however, are either viruses or plasmids that contain antibiotic resistance markers, and as such are unlikely to be approved for use outside of laboratory containment. Furthermore, the high length-to-diameter ratio in the full-length phage makes them undesirable for lateral flow (dip-stick) assays, as spherical particles are ideally used as detectors in this diagnostic system. In contrast to the current filamentous phage vectors, the nanophage contain only 200 nt of DNA and do not contain any viral or antibiotic resistance genes, therefore their use would overcome regulatory barriers for general use of filamentous phage in lateral flow devices (dip-sticks). Furthermore, their extremely small size (6 nm x 50 nm) and much lower length-to-diameter ratio makes them much more suitable for dip-stick devices.

To test the potential of the nanophage-production system in obtaining nanophage particles that can be used for applications in diagnostics, functionalized nanophage displaying a probe have been produced (Figure 4.1). Detection of the analyte using the probe-displaying nanophage was examined using phage ELISA (Figure 4.2). The displayed probe was Fibronectin-Binding (FnB) domain from a surface protein of *Streptococcus pyogenes* (a multi-domain protein called Serum opacity factor or Sof (Rakonjac et al., 1995) The Sof FnB domain is composed of 4 repeats of a bacterial Fibronectin-binding motif (PF02986) which binds to the F1-F4 repeated domains at the N-terminus of human Fibronectin (Schwarz-Linek et al., 2006). The FnB was

constructed as a pIII fusion in the nanophage-display system (Chapter 2, Section 2.2.3). Fibronectin-binding domain (ligand or detector or probe) has a high affinity for fibronectin (analyte). Whereas in *S. pyogenes* (Group A Streptococcus) infection, binding to Fibronectin is essential for colonization of the human host, when displayed on the phage, FnB domain and its high affinity interaction with fibronectin is useful for applications in high-sensitivity detection assays.

4.2. Fibronectin-binding Activity Assay

For display of the FnB domain in the nanophage production system, the FnB-pIII fusion was constructed in the nanophage-production helper phage-display vector Rnano3 which is used for nanophage production (Chapter 2; Figure 2.1). The resulting construct, Rnano3FnB, was used to produce the full-length (helper) virions and the nanophage particles displaying FnB. A schematic diagram of *E. coli* containing a nanophage production-display system is shown in Figure 4.1.

Phage ELISA

The helper (full-length) virions and the nanophage particles displaying FnB at the pIII end of the virions were produced and purified using native virion gel electrophoresis followed by electroelution, as described in Chapter 3. The phage ELISA was performed as described in Materials and Methods (Section 2.6.1) and is schematically represented in Figure 4.2. Rnano3FnB full length and nanophage particles exhibited efficient binding to immobilized fibronectin as indicated by high ELISA signal in fibronectin coated wells incubated with these phage particles. No ELISA signal over background levels was detected in control wells incubated with nanophage and full-length phage particles without FnB domain (Rnano3) nor in the wells from which fibronectin was omitted (Figure 4.3). ELISA values are presented as average of triplicates. In conclusion, nanophage particles were displaying FnB and hence were able to detect immobilized analyte (fibronectin) as efficiently as the full length phage particles expressing FnB domain as pIII fusion.

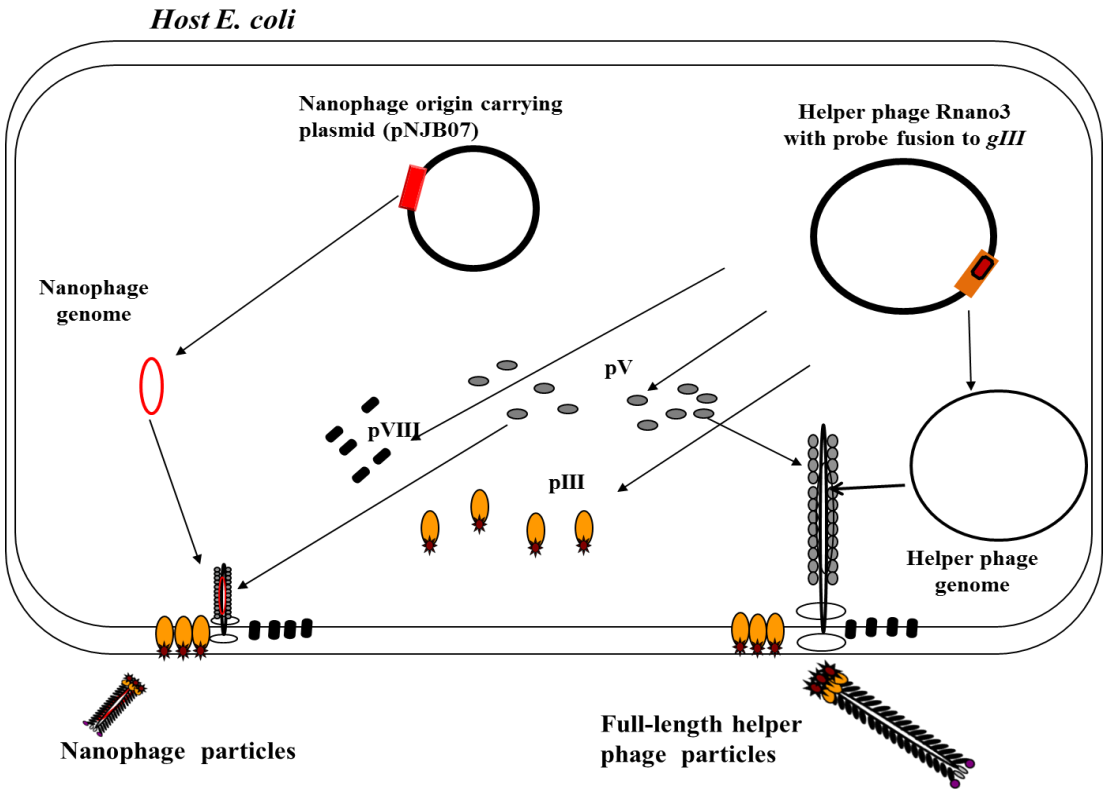

Figure 4.1 Schematic representation of the nanophage production-display system. *E. coli* cell containing the nanophage production plasmid pNJB07 is infected with the helper phage Rnano3 containing fusion of the "probe" to pIII. Upon infection, pII from the helper phage induces replication from the nanophage origin of replication of pNJB07 and also provides all virion proteins and assembly machinery for production of the nanophage virion. All five copies of pIII are fusions to the probe, derived from the helper phage.

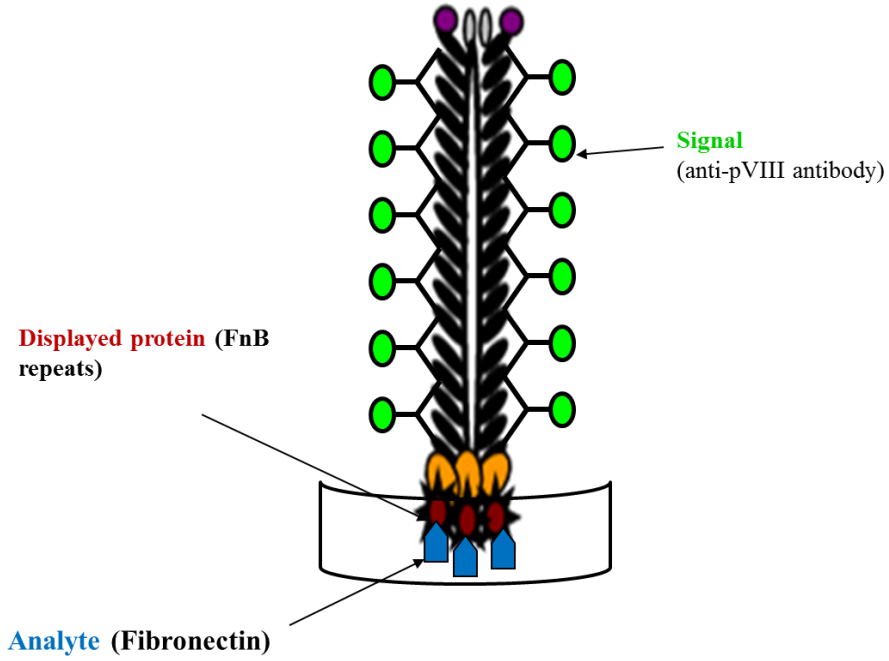

Figure 4.2 Schematic presentation of ELISA assay setup for detecting immobilized analyte (fibronectin). The assays were performed in a 96-well microtitre plate using functionalized full-length phage or nanophage particles.

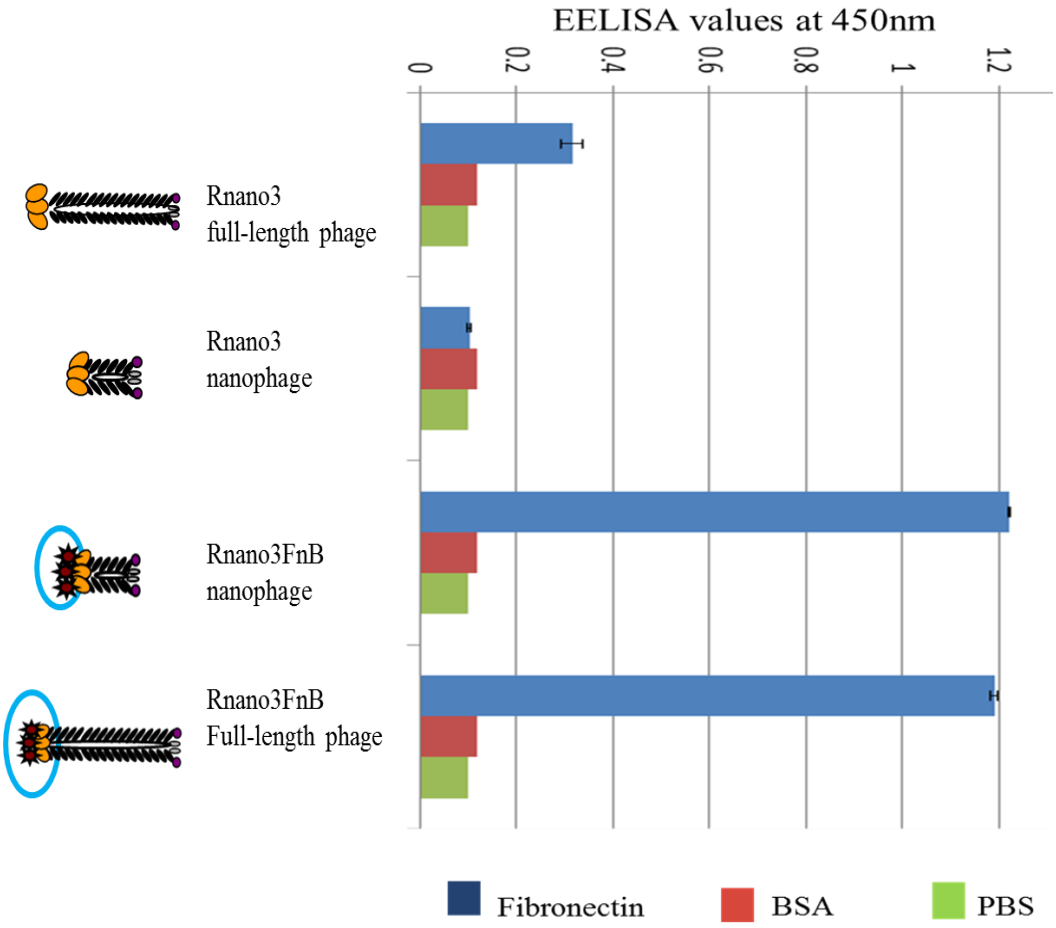

Figure 4.3 Binding of FnB-domain displaying full length and nanophage particles to immobilized analyte (fibronectin) in ELISA setup. A total of 10^8 phage particles were used in each assay, carried out in 96 well plates. Samples: Rnano3 full-length and nanophage particles, Rnano3FnB full length and nanophage particles. BSA was used as negative protein control and PBS as buffer control to check the cross reactivity of primary antibody (anti-pVIII). Data is presented as average of triplicates. Error bars indicate standard deviation.

4.3 Detection of Soluble Analyte in a Sample Solution Using Functionalized Nanophage and Full-length Phage Particles in a Dipstick Format

The nanophage particles demonstrated high signal in detection of immobilized fibronectin (the analyte) in an ELISA setup, showing that they displayed the probe, FnB. To investigate the detection of fibronectin (the analyte) in solution using the nanophage displaying FnB domain as detector (probe) in lateral flow devices, a simple dipstick assay was designed and tested. Hi-flow membrane cards (Millipore), which are designed for the lateral flow assays, were used to make dipsticks. Figure 4.4 shows schematic representation of dipstick assay protocol devised for analyte (fibronectin) detection in a sample solution, using Rnano3FnB particles (Chapter 2; Table 2.4). Instead of printing the T and C lines, the reagents in the initial assay were applied as drops onto the membrane (Figure 4.5A). Since phage were not labeled, western blotting (Chapter 2; Section 2.5.2) was carried out to visualize the phage particles bound to test and control lines. The protocol used is explained in detail in Chapter 2 (Section 2.7). Briefly, Rnano3FnB large or nanophage particles were mixed with analyte (fibronectin) in a well of a 96-well plate in a total volume of 50 µL. Rnano3 full-length phage or nanophage particles produced using Rnano3 helper did not display the FnB domain and were used as negative controls. Dipsticks were allowed to stand in solution for 30 min and then western blotting was carried out to detect the phage particles bound to test and control lines (or spots; depending on the method of application to the membrane).

All phage bound to the analyte (fibronectin) were expected to be found at the test line ‘T’ which contains fibronectin-specific monoclonal antibody. A proportion of phage particles that fail to bind analyte is expected to migrate beyond the test line and to be captured at the control line ‘C’, containing anti pVIII antibody, giving a positive signal in a valid assay (Figure 4.5 A). In the absence of analyte, only control line was expected to give a positive signal. Assays using the Rnano3FnB full-length and nanophage particles, as expected, showed positive signals at both T and C spots, in presence of analyte (fibronectin) in the test solution (Figure 4.5 B, sticks 1 & 3). However, when the assay was carried out using same set of phage but without analyte in the test solution, they still produced a positive signal at test spot (Figure 4.5 B, sticks

2 & 4). Rnano3 phage particles without fibronectin binding domain gave positive signal at the control line only (Figure 4.5 B dipsticks 5 & 6), indicating that the signal in the T spot obtained from the Rnano3FnB phage in the absence of the analyte (fibronectin) was not due to the nonspecific binding of phage to the fibronectin-specific antibodies. As many streptococcal surface proteins interact with the constant domains of antibodies, it was possible that FnB domain was binding to the Fc region of the fibronectin-specific antibody, in the absence of fibronectin. However, when an unrelated antibody of the same class as the fibronectin-specific monoclonal antibody was used at the T line, the Rnano3FnB phage did not bind (data not shown). Therefore, it is most likely that all antibodies, which are purified from serum by affinity chromatography, contain trace amounts of fibronectin bound to the variable domain's antigen binding site. This trace amount of contaminating fibronectin may have been enough to retain FnB domain-displaying phage particles giving a strong signal at the test spot even in absence of fibronectin in the test solution when detected by western blotting (Figure 4.5B, sticks 2 & 4). This is also an indication of high sensitivity of the phage dip-stick assay.

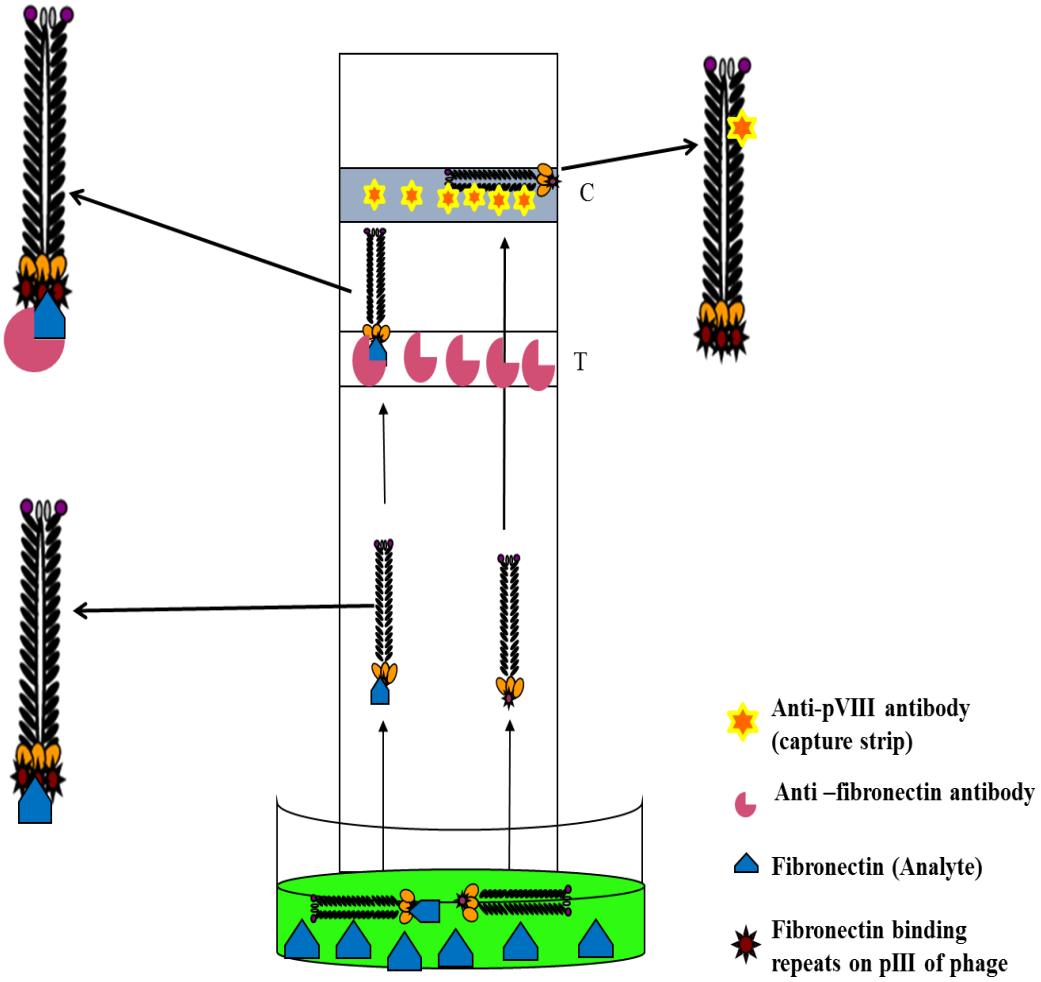

Figure 4.4 Schematic presentation of dipstick immunoassay developed to test the potential of nanophage particles in diagnostics. C: control line indicating a valid assay; T: test line indicating a positive assay.

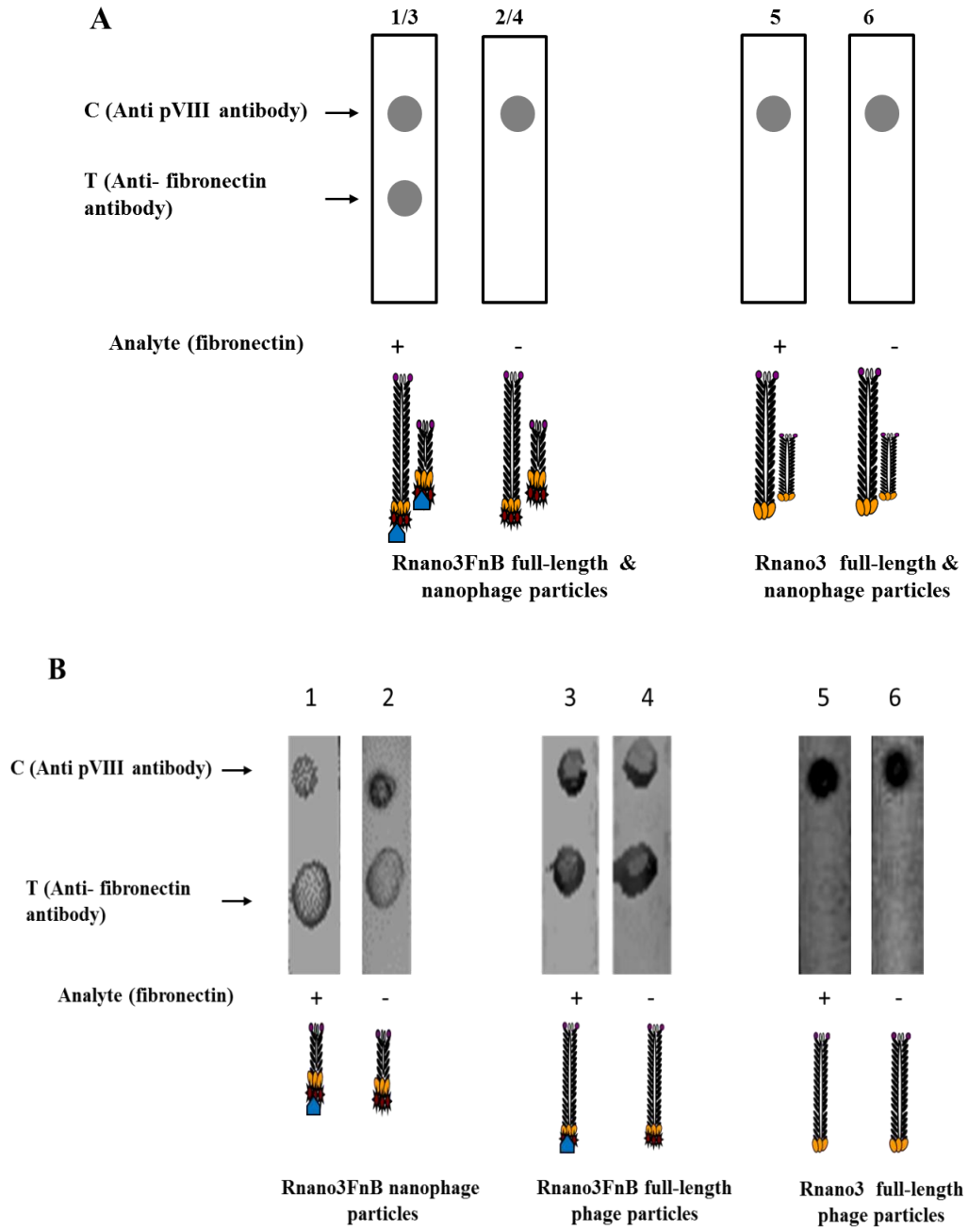

Figure 4.5 Detection of fibronectin in a test solution using a dip-stick assay. Fibronectin-specific monoclonal antibody is spotted at the test (T) spot and phage-specific polyclonal antibody as a control spot (C). A) Expected results of dipstick immunoassay. B) Dip-stick assay for detection of fibronectin with the Rnano3FnB; full-length and nanophage particles gave positive signal even in absence of analyte (sticks 2 & 4); however control Rnano3 gave positive signal at control spot only (sticks 5 & 6). A total of 2×10^{9} phage particles were used in each assay, whereas fibronectin concentration used was 5 µg/50 µl.

4.4 Comparison of FnB-displaying Nanophage with Full-length Phage in a Dip-stick Assay

Nanophage particles were expected to perform better than full-length phage in a lateral flow device like dipstick due to their much lower length-to-diameter ratio, resulting in more desirable hydrodynamic properties. In previous experiment, fibronectin-specific monoclonal antibodies (Sino Biological Inc.) were used at the test spot for detection of fibronectin bound phage particles. However, phage particles displaying no FnB were unexpectedly found to bind to these antibodies fibronectin-specific monoclonal antibodies (Sino Biological Inc.) used at the T spot, even in the absence of analyte. As an alternative to fibronectin-specific monoclonal antibody, the T line was loaded with collagen, which interacts with fibronectin with high affinity. Collagen is known to bind fibronectin with high affinity and is routinely used in sepharose columns to deplete the plasma fibronectin from the serum (Engvall et al., 1981). Therefore it was expected to specifically capture the on the test line 'T' only those FnB-domain-displaying phage particles that contain bound fibronectin. The dipsticks used in this assay contained 1 µg of human type I collagen at the test line T and 1 µg of anti pVIII antibody at control line C. The assay was carried out using unlabeled phage which were detected on sticks by western blotting, as well as fluorescently labelled full-length and nanophage particles detected by phospho-imager. Results obtained with both detection methods exhibited specific binding of the Rnano3FnB (FnB-displaying) nanophage particles to collagen at the T line in presence of fibronectin (Figure 4.6A, sticks 3 & 7, 4.6 B; sticks 3& 6), however the full-length FnB-displaying phage had some residual binding to the collagen T line when detected by western blotting (Figure 4.6A, stick 8). The nanophage particles were found to perform better relative to the full-length phage as there was no background in nanophage dipstick strips when detected by western blotting. Moreover, the lateral flow of nanophage particles was found to be much better than large phage even though 10 fold higher numbers of the nanophage particles relative to full-length virions were used in this assay (Figure 4.6 A, sticks 4 & 8). Rnano3 full-length and nanophage particles exhibited binding to control line only, indicating the lack of unspecific phage binding of phage to collagen (Figure 4.6, sticks 5-6 & 1-2 respectively).

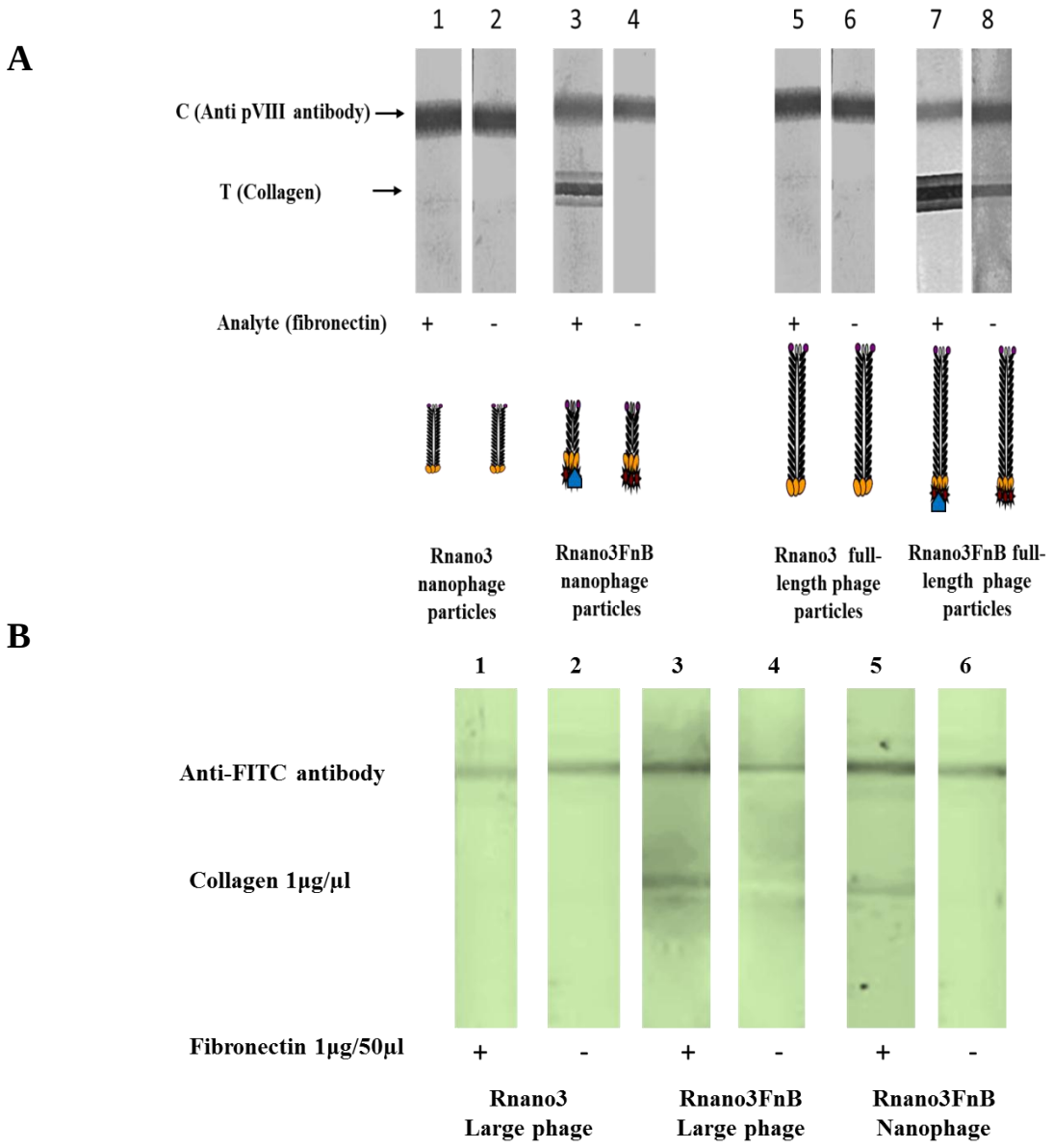

Figure 4.6 Dipstick assay for nanophage using collagen as fibronectin control reagent on test line. A) Sticks were dipped in 50 µl of test solution containing 5 µg of fibronectin and 1×10^{10} full-length phage particles for both Rnano3 and Rnano3FnB sticks 5-6 & 7-8 respectively. Concentration of nanophage particles used was 1×10^{11} for both Rnano3 and Rnano3FnB, sticks 1-2 & 3-4 respectively. Sticks contained 1 µg collagen at the test (T) line and 1 µg of pVIII-specific (phage-specific) antibody at the control line (C). **B)** Dipsticks contained 1 µg of anti-FITC antibody at the control line and 1 µg of collagen at the test line. Phage particles labelled with Fluorescein Isothiocyanate (FITC) were mixed with 1µg of fibronectin in 50 µl test solution. A total of 1×10^{10} full-length phage particles for both Rnano3 and Rnano3FnB and 1×10^{11} for Rnano3FnB nanophage were used in the assay. Signal was detected using Phospho-imager (FUJI).

4.5. Quantitative Measurement of Analyte Using Dipstick Competition Assay

Fibronectin quantification in serum samples can be indicative of several diseases such as proliferative vitreoretinopathy (PVR) (Weller et al., 1988) and platelet thrombus formation (Tomasini-Johansson and Mosher, 2009). Fibronectin-specific antibodies (Sino Biologicals Inc.) used at the test spot for detection of fibronectin bound phage particles displaying FnB were unexpectedly found to bind to these phage particles even in the absence of analyte (Figure 4.5). Therefore, in order to test the ability of nanophage detector probes for quantitative detection of fibronectin in a sample solution, a dipstick competition assay was developed. Figure 4.7 gives a schematic presentation of the competition assay. Fibronectin was spotted on test (T) line of the nitrocellulose membrane. Sticks were dipped in solution containing constant number of phage particles but two-fold serial dilutions of fibronectin, starting from 1 µg. In this competition assay, phage particles bound to analyte from the sample solution will not bind the test line. As the concentration of analyte decreases in the test solution, more phage particles are expected to bind to the analyte on the test (T) line, resulting in an increased signal from highest to lowest concentration of fibronectin (analyte). This was observed for assay dipsticks. At the highest concentration of fibronectin (1 µg; Figure 4.8) the signal at the test line was the weakest, whereas highest signal was observed when there was no fibronectin in the test solution (0 µg fibronectin; Figure 4.8, stick 5 Figure 4.8). The control Rnano3 nanophage particles produced signal only at the C line (Figure 4.8, stick 6).

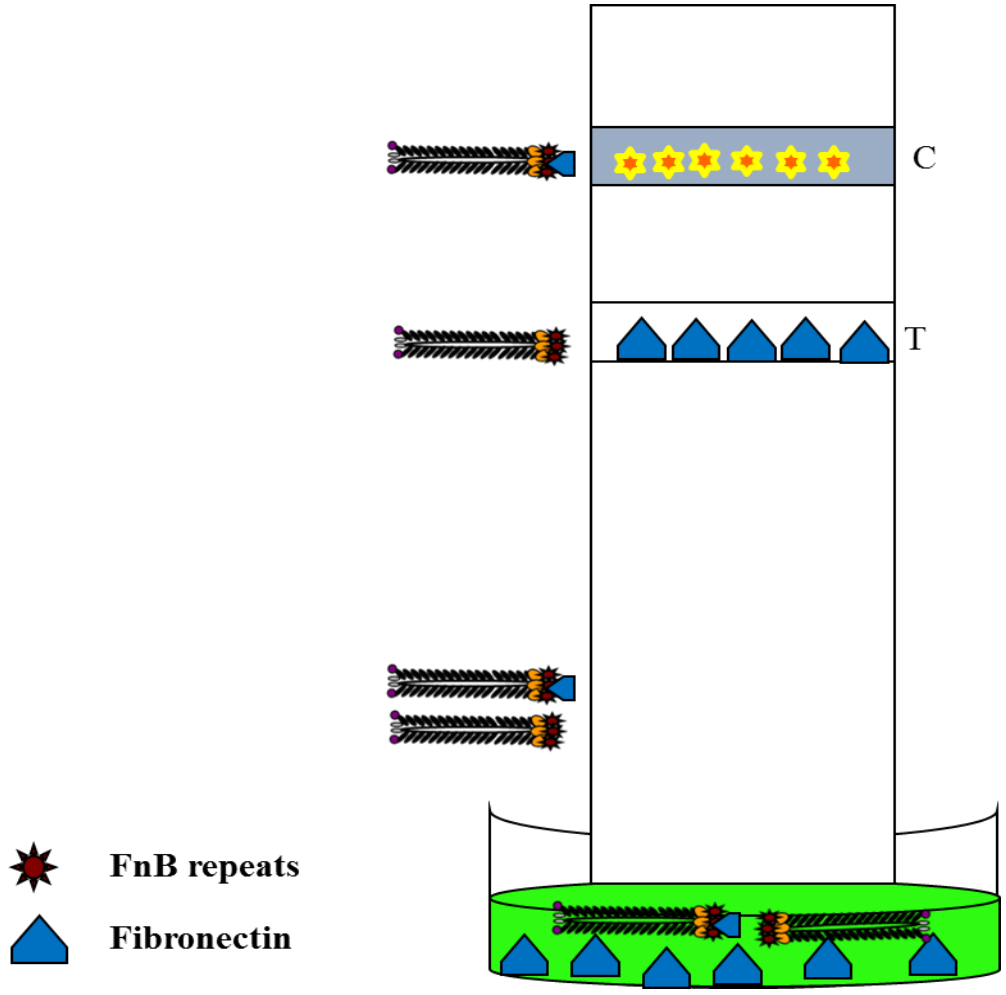

Figure 4.7 Schematic presentation of dipstick competition assay for quantitative detection of fibronectin using nanophage particles. All phage particles bound to analyte in the test solution will be retained at 'C', the control line, whereas the phage particles that are not bound to fibronectin are retained at test line 'T'.

A

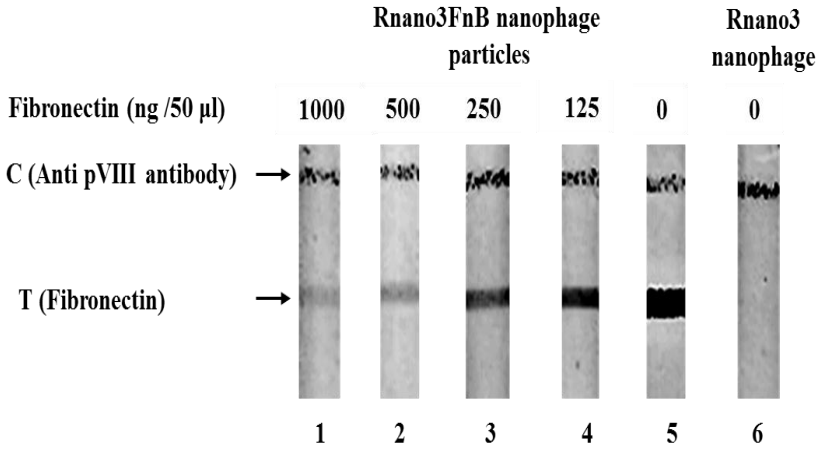

B

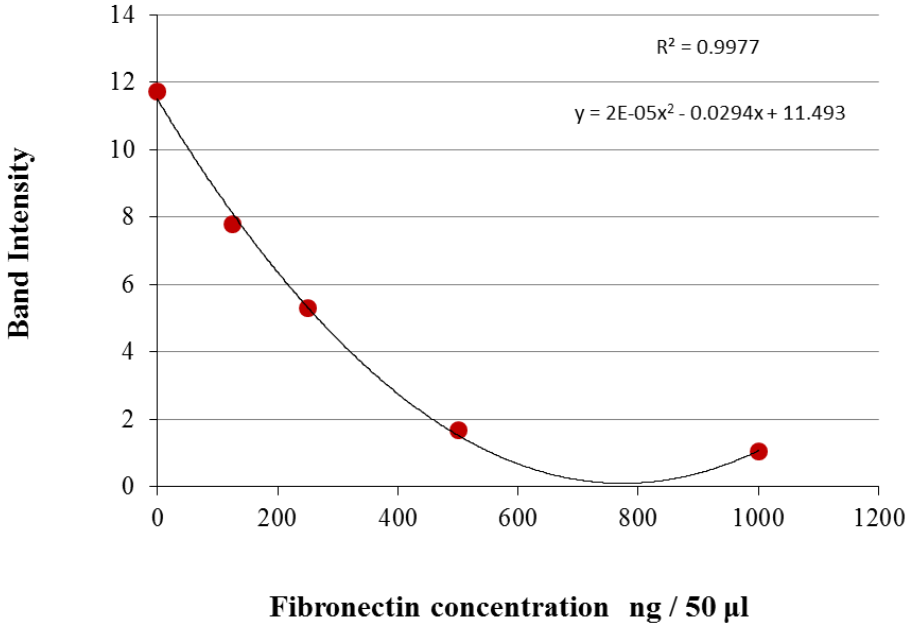

Figure 4.8 Dipstick analyte competition assay for nanophage particles. Sticks contained 1µg of each of fibronectin at the test line (T) and anti pVIII antibody at the control line (C). The sample solution contained serial two fold dilutions of analyte (fibronectin). **A**) Strips 1-5 were dipped in the sample solution containing a gradient of fibronectin concentration; 1000, 500, 250, 125, or 0 ng fibronectin / 50 µl of test solution. Strip 6, Rnano3 control nanophage without FnB domain, dipped in 1×PBS only (no analyte). B) Plot of the signal intensity at the test (T) line vs. fibronectin concentration in the test solution. The T line signal intensity was determined by densitometry. The X-axis indicates fibronectin amount in the total volume of analyst solution (50 µl), whereas Y-axis indicates band intensity.

4.6. Quantitative Measurement of Analyte Using Non-Competitive Assay in Dipstick Format

A non-competitive detection of analytes in the dip-stick format is more desirable than competitive detection due to high sensitivity. In order to examine the limit of analyte detection using the nanophage dip-stick assay, direct detection using collagen at the test (T) line instead of fibronectin-specific monoclonal as outlined in Figure 4.4. Briefly, serial 2-fold dilutions of analyte (fibronectin) starting from 1 µg per assay (50 µl) were mixed with a constant number of Rnano3FnB nanophage particles (1×10^{11} per assay). Sticks containing 1µg of collagen at the test (T) line and 0.5µg of anti-pVIII antibody at the control (C) line were allowed to stand in the solution for 30 minutes. In this direct assay, phage particles bound to analyte in sample solution will bind the test (T) line, hence the intensity of the signal at that line is expected to positively correlate with the concentration of analyte. This was observed in assay dipsticks (Figure 4.9A); at the highest concentration of fibronectin (1 µg) the signal at the test line was the strongest, whereas the weakest signal was observed the lowest concentration (3.9 ng; Figure 4.9A, stick 9). The control Rnano3 nanophage particles that do not display FnB domain produced signal only at the C line (Figure 4.9A, sticks 11 and 12).

Densitometric analysis (Figure 4.9B) of signal at the test line indicated a second order polynomial dependence between the pixel density of the signal and analyte concentration over a range of concentrations between 62.4 ng and 500 ng. This range is much broader than the physiological concentration of fibronectin in the human serum which is 259-400 ng/µl. Assay was found to be highly sensitive in general, as it could detect fibronectin concentrations as low as 3.9 ng.

The result of these dipstick immunoassays confirmed that nanophage particles displaying high-affinity analyte-binding antibodies, proteins or peptides on at the pIII end of the particles can be used to detect the cognate analyte in the solution.

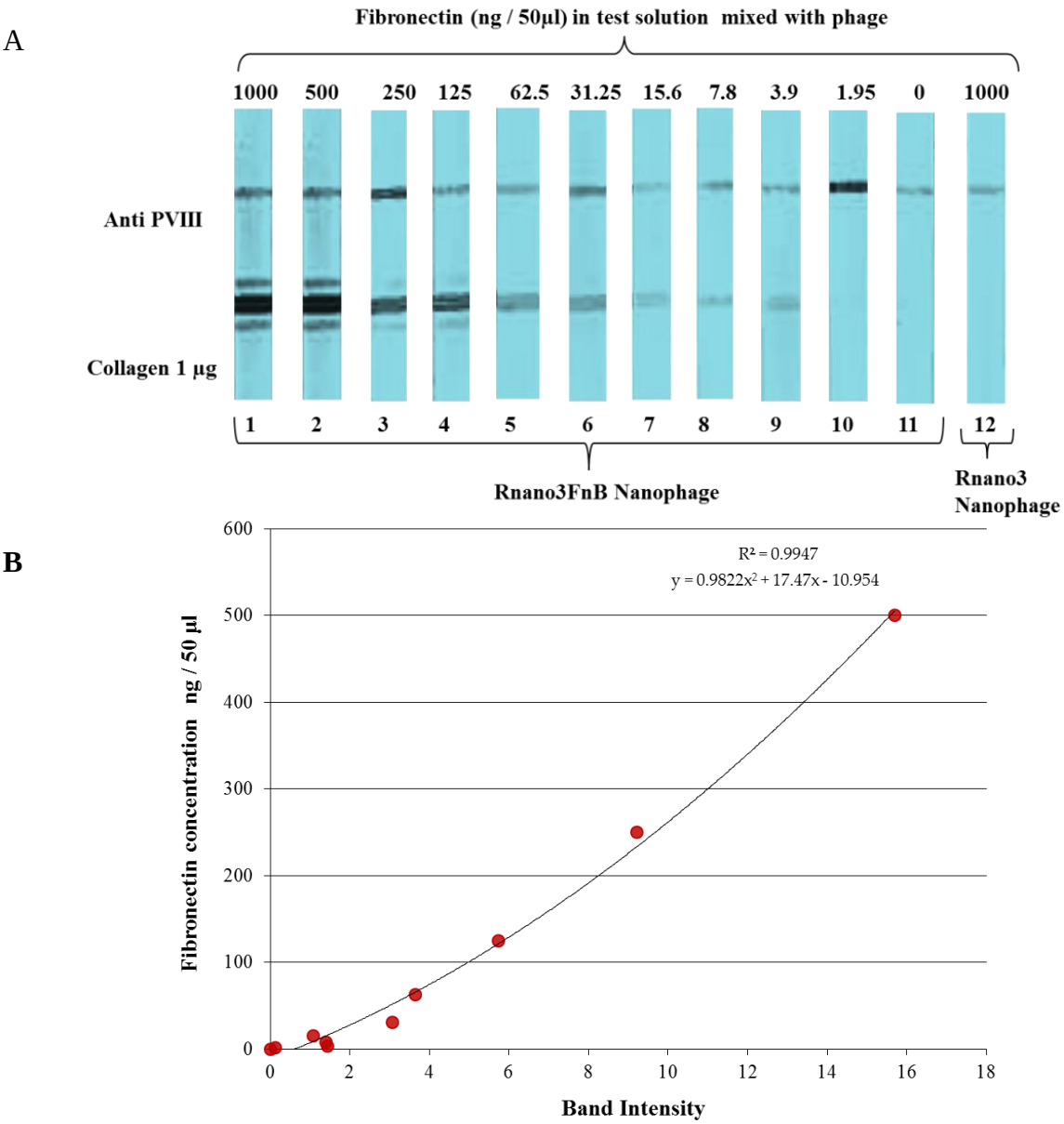

Figure 4.9 Non-competitive detection of analyte in dipstick format using nanophage particles. A) Sticks contained 1 µg of collagen at the test line (T) and 0.5 µg anti pVIII antibody at the control line (C). Sample solutions contained serial two fold dilutions of the analyte (fibronectin). Strips 1-11 were dipped into a series of solutions containing a serial two-fold dilutions fibronectin concentration starting with 1000 ng (in 50 µl as indicated above the strips. The control strip 12 was dipped into the solution containing Rnano3 nanophage (that does not display FnB domain) and 1000 ng of fibronectin in 50 µl. **B)** Plot of the signal intensity at the test (T) line vs. fibronectin concentration in the test solution. The T line signal intensity was determined by densitometry. The X-axis indicates fibronectin amount in the total volume of analyst solution (50 µl), whereas Y-axis indicates band intensity.

Chapter 5

Application of Nanophage in Vaccine Design

5.1 Introduction

Filamentous phage have been reported to elicit strong antibody response, even when applied in low doses and in the absence of adjuvant (van Houten et al., 2010). This is possibly because of high copy-number and highly repetitive arrangement of the major coat protein in the filamentous virion and particulate nature of the phage, allowing phage to serve both as an antigen carrier and adjuvant. Furthermore, it has been shown that immune response is better focused on the antigens conjugated to filamentous phage, relative to the same antigens conjugated to the standard antigen carriers (van Houten et al., 2006). However, despite these advantages over the standard antigen carriers, application of bacteriophage as antigen carriers in human vaccination is just at the proof of concept stage, mainly because of the consumer and regulatory concerns stemming from the fact that Ff bacteriophage are viruses and are capable of replicating within *E. coli* that is part of the gut microbial community (Dabrowska et al., 2005). The recombinant phage used in vaccination are genetically modified organisms; their genomes in most cases contain antibiotic resistance markers that can be transferred to commensal and pathogenic bacteria within the gut; they have also been shown to be taken up un-specifically by eukaryotic cells, resulting in delivery of viral DNA into the nucleus and integration into the chromosome (Larocca et al., 1999). In this chapter, I report that nanophage can be used as vaccine carriers, removing some of the concerns mentioned above, linked to the use of the full-length phage as vaccine carriers.

Nanophage are nanoparticles that are not capable of replicating without a helper phage, yet they retain their ability to act as display scaffold in the same fashion as full-length phage particles (this study, Chapter 4). They have an additional advantage of increased heat and detergent resistance over the full-length phage and are non-toxic and non-infectious (this study, Chapter 3, Section 3.3). Because of these advantages, nanophage could be a viable option for use outside laboratory containment, as vaccine carriers. To

examine whether immunogenic properties of the nanophage are similar to those of the full-length phage, the functionalised nanophage displaying FnB domain as fusion to pIII were purified and tested for induction of antibody response, in comparison to equivalently functionalised full-length phage. Fibronectin binding domain (antigen) is derived from the Serum opacity factor, shown previously to be a virulence factor in *Streptococcus pyogenes* (Group A Streptococci or GAS). The FnB domain mediates tissue invasion by these pathogenic bacteria through interaction with fibronectin from the extracellular matrix (Courtney et al., 1999). The FnB domain has been shown to generate protective immune response against *S. pyogenes* challenge in a mouse model, when administered in conjunction with standard antigen carriers (Schulze et al., 2001).

5.2 Large-scale Purification of Nanophage and Full-length Phage Particles for Immunization

For vaccine development, large-scale preparation of both full-length and nanophage was undertaken, using protocols developed in Chapter 3. The full-length (helper) phage and nanophage were concentrated from 8 L of bacterial culture by differential PEG precipitation (Chapter 2, Section 2.4.1). Crude PEG precipitated phage preparations contain a large amount of bacterial lipopolysaccharides (Huang et al., 2000) and other bacterial debris which renders it unfit for vaccine administration. To remove these impurities, phage stocks were treated with detergents triton X-100 and Sarkosyl and importantly purified further away from remaining impurities and the full-length phage by the native virion agarose gel electrophoresis followed by electroelution (Chapter 3, Section 2.4.3). All buffers and equipment used in electroelution were sterilized. The purified full-length and nanophage particles were suspended in sterile phosphate buffer saline (PBS). After final purification, both full-length and nanophage particles were quantified by phage titration and densitometric analysis, respectively (Chapter 2, Section 2.3.4). Purified nanophage samples used in vaccination contained a small number of remaining full-length phage that could not be eliminated by preparative virion electrophoresis and electroelution (5 full-length phage particles per million nanophage particles; Chapter 3, Section 3.2.3).

5.3 Gauging the Nano- and Full-length Particles for Vaccine Trial

To compare fibronectin binding activity of full-length and nanophage particles, capture ELISA was performed using fibronectin-coated wells (Chapter 2, Section 2.6.1; Chapter 4, Section 4.2, Fig. 4.2). A titration of fibronectin-binding activity of the FnB-displaying nanophage and full-length phage preparations was carried out to identify the dilutions of nanophage particle preparations giving comparable fibronectin binding activity to full-length phage particles. This in turn was used to decide the relative numbers of nanophage and full-length phage particles required for immunization. When the ELISA titration data was compared to the number of particles in particular assays, it was observed that in this particular preparation, the FnB-displaying nanophage particles had 10-fold lower fibronectin binding activity per particle than FnB-displaying full-length phage. Therefore, a 10-fold excess of the nanophage particles (1×10^{11} nanophage particles in 100 µl of 1X PBS) was used for immunization in comparison to full-length phage particles (1×10^{10} full-length phage particles in 100 µl of 1 × PBS). With respect to the relative concentrations of phage coat protein pVIII, this corresponds to overall 1:2 ratio in the nanophage vs. full length phage vaccine samples, given that the length ratio of the nanophage to full-length phage is approximately 1:20.

5.4 Vaccination Trial Design and Immunization Schedule

To evaluate the antigenic potential of nanophage particles in comparison to full-length phage particles, a vaccine trial in a mouse model was carried out. Thirty female BALB/c mice (4 to 6 weeks of age) were divided into five groups of (group I-V). Each group was given an intraperitoneal injection of a vaccine in PBS, without any adjuvant or emulsifier (Figure 5.1). Group I and II animals were injected with the full-length (helper) phage, either with no displayed antigen (LongRnano3) or displaying FnB domain (LongRnano3FnB), whereas group III was immunized with nanophage particles displaying FnB domain (ShortRnano3FnB). Phage purification was carried out at 4 ºC and the samples were stored at -80 ºC, to protect the displayed FnB domain from degradation by *E. coli*-derived proteases present in the phage preparations. However, a vaccine that could survive the “cold chain” disruption by periodic

exposure to ambient temperature, in particular in the tropical regions, would be valuable for applications in areas that have no access to refrigeration. This is why group IV was included in the trial in order to evaluate antigenic properties of the nanophage vaccine after prolonged disruption of the cold chain. To obtain the vaccine sample, nanophage particles displaying FnB domain (WarmShortRnano3FnB) were pre-incubated at 37 ºC for 48 h prior to injection. Group V was injected with PBS only. Fibronectin binding domain (FnB) is highly conserved in various *S.pyogenes* fibronectin binding proteins. Several of them are already shown in literature to possess strong immunogenic potential when administered in a mouse model with standard adjuvants and carriers, therefore FnB domain-only positive control was not used in this study. Since Rnano3 full-length and nanophage particles were expected to induce similar immune response only, Rnano3 full-length phage vaccine was included in the trial as negative control.

For the nanophage preparations (groups III and IV) each animal was immunized with 1×10^{11} particles suspended in 100 µl of PBS, whereas for full-length phage particles (groups I and II) 1×10^{10} phage particles were used in same volume of buffer.

After first immunization, four booster doses, each ten days apart, were administered through the same route over a period of 7 weeks. Blood samples were collected from tail veins before 1st vaccination and 10 days after each vaccine dose. Serum was separated from blood and stored at -20 ºC for antibody analysis. Ten days after the final booster vaccination, all groups were challenged intranasally with *S. pyogenes.* The bacterial suspension was directly delivered to one of the nostrils. At 10th day post challenge all mice were humanely euthanized under SOP 09/03 Procedure for Performing Euthanasia in Mice, Rats, Hamsters and Guinea Pigs using CO_2, approved by the Massey University Ethics Committee. A final blood sample was collected from euthanized animals by cardiac puncture. Nasal swabs, tracheal rings and lungs were collected to assess vaccine ability to minimise bacterial colonization (Chapter 2, Section 2.8).

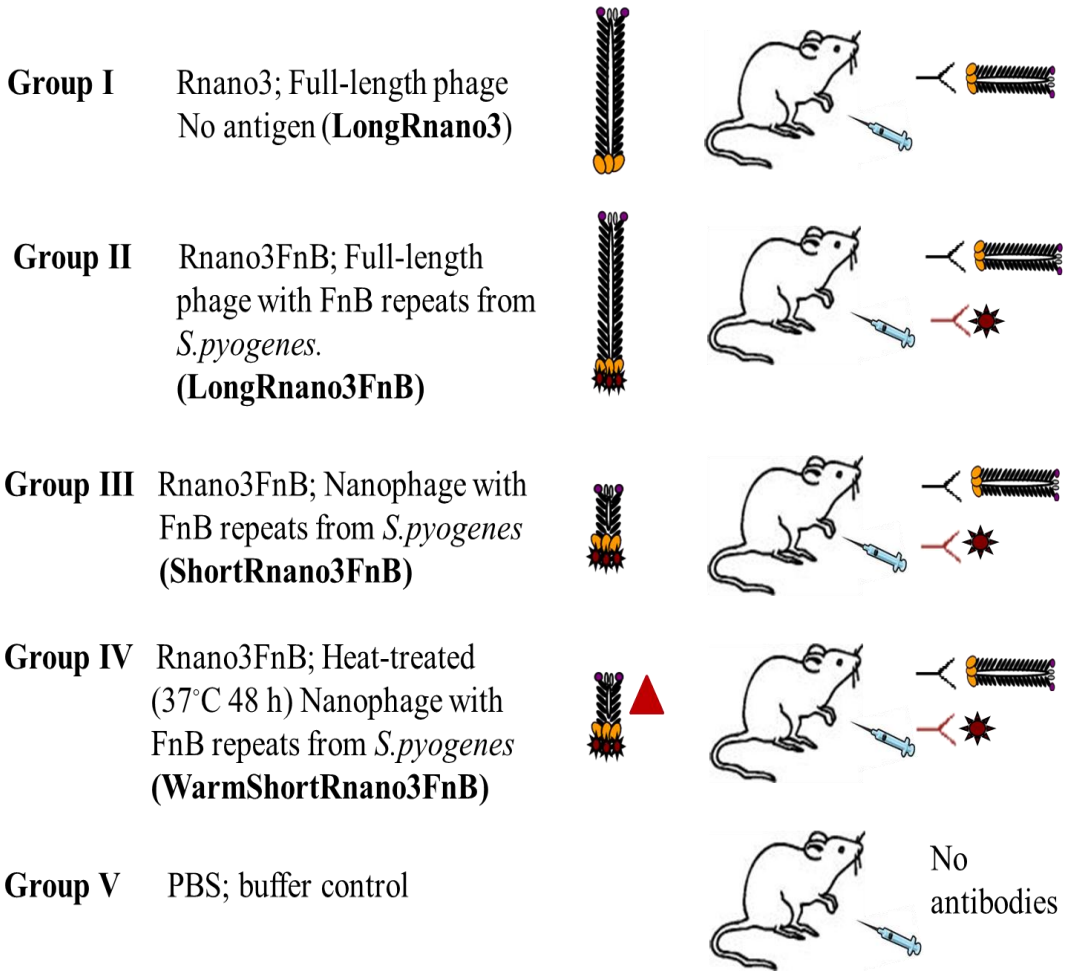

Figure 5.1 Schematic presentation of vaccine trial design. Group I was expected to produce only anti-phage antibodies (**Y**) whereas groups II, III and IV were expected to produce two types of antibodies; antibodies against phage proteins (**Y**), and antibodies against FnB domain (**Y**) expressed as pIII fusion on both full-length and nanophage particles. Group V was expected to be negative for both phage-specific and FnB-domain-specific antibodies. Note the changed terminology of group names for ease of description.

5.5 Immune Response against Phage Proteins

5.5.1 Phage-specific Humoral Immune Response

Serum isolated from experimental animals ten days after the final booster dose was analysed by ELISA against immobilised phage for the presence of phage-specific humoral immune response (Figure 5.2). All antibody titres were determined as inverse value of the highest dilution of antiserum (in a series of two-fold dilutions) that gave a positive signal in the ELISA assay.

All phage-vaccinated groups (I-IV) exhibited a significant IgG antibody response against phage proteins when compared to the control mice vaccinated with PBS buffer (group V; $\boldsymbol{p < 0.05}$). This increase was highly significant for group I (P = 0.005) and II (P = 0.0058) mice vaccinated with full-length phage without and with FnB domain respectively. IgG antibody titres of nanophage vaccine groups III (P = 0.006) and IV (P = 0.025) were also significantly higher than control group (V). However group IV mice exhibited lowest IgG antibody titre in comparison to other groups, probably due to observed large intra-group variance in response of individual animals to inoculated phage. Nanophage vaccine groups (III, IV) exhibited significantly lower phage-specific IgG antibody response (P = 0.037) when compared to full-length phage vaccine groups (Figure 5.2), which was expected as nanophage has 20 fold less pVIII per phage particle in comparison to full-length phage, hence antigen receptors on the surface of B cells are expected to be cross-linked to a comparatively lower extent, resulting in less vigorous activation and overall immune response.

Despite the high background observed for IgM antibody in ELISA, a significant increase in phage-specific IgM was evident for groups I and II (P = 0.006, P= 0.005), whereas titre for group III was marginally significant P = 0.05. IgM titre for group IV mice vaccinated with heat treated nanophage particles was non-significant (P = 0.211) in comparison to control group V **($\boldsymbol{p > 0.05}$)** (Figure 5.3). Serum IgA was at background level for all groups as compared to control.

In conclusion, nanophage vaccine groups (III and IV) induced good phage-specific serum antibody response for IgG; IgM response was marginally significant for group

III only, whereas IgA titre was non-significant for both nanophage vaccine groups when compared to group V vaccinated with PBS buffer. It indicated that nanophage is immunogenic however the immune response induced by nanophage vaccine groups was significantly lower than full-length phage vaccine groups (I and II); Figure 5.4 shows a comparison of three antibodies in all five groups.

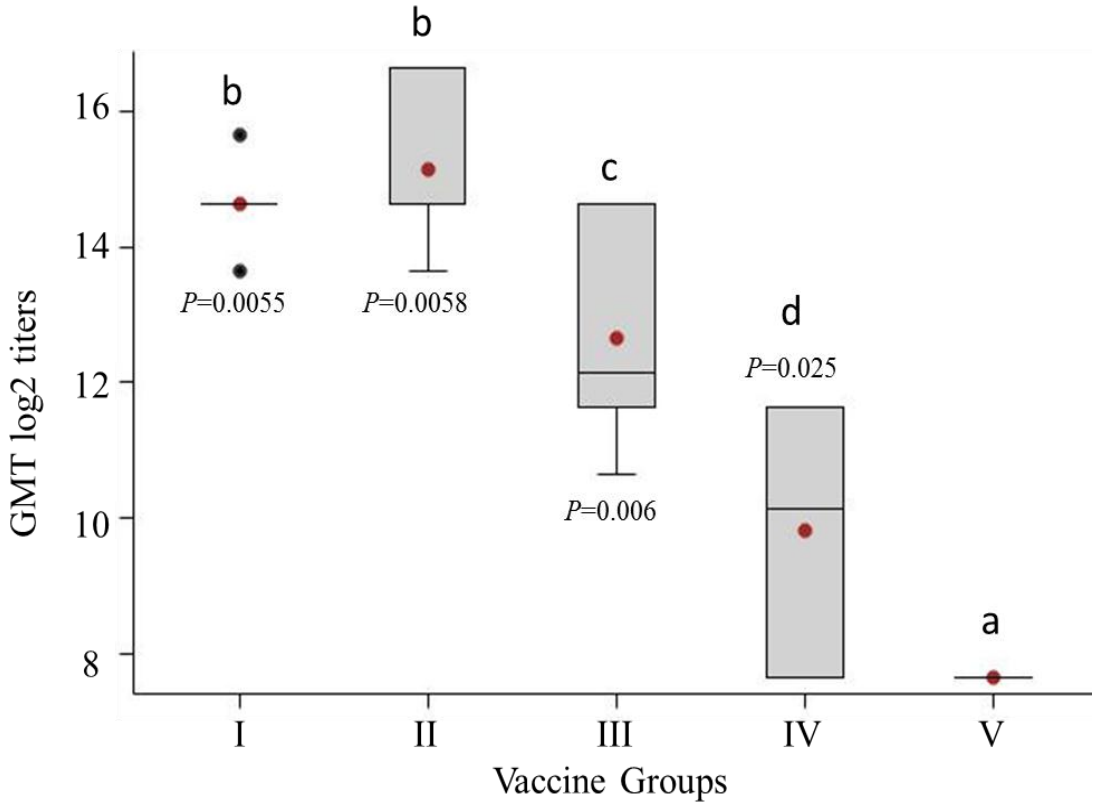

Figure 5.2 Phage-specific IgG, inter-group comparison. I and II, full-length phage vaccines labeled as LongRnano3 and LongRnano3FnB in Figure 5.1; III, nanophage vaccine ShortRnano3FnB (without heat treatment); IV, nanophage vaccine incubated at 37 ºC for 48 h (WarmShortRnano3FnB); V, control group (vaccinated with PBS buffer) (see Figure 5.1 for group labels). Y-axis indicates geometric mean titre (GMT) of antibodies obtained by serum titration (log for base 2). The upper and lower borders of the box represent first and third quartiles, respectively. The horizontal line drawn within the box marks the median. The red dot (●) shows the sample mean. The whiskers (standard deviation from the mean) are drawn to the most extreme points that lie within the fences. Outliers are marked as black dots (●). Lowercase letters (a, b and c) at the top of bars denote groups with significant difference from each other ($p \leq 0.05$; Wilcoxon-Mann-Whitney test).

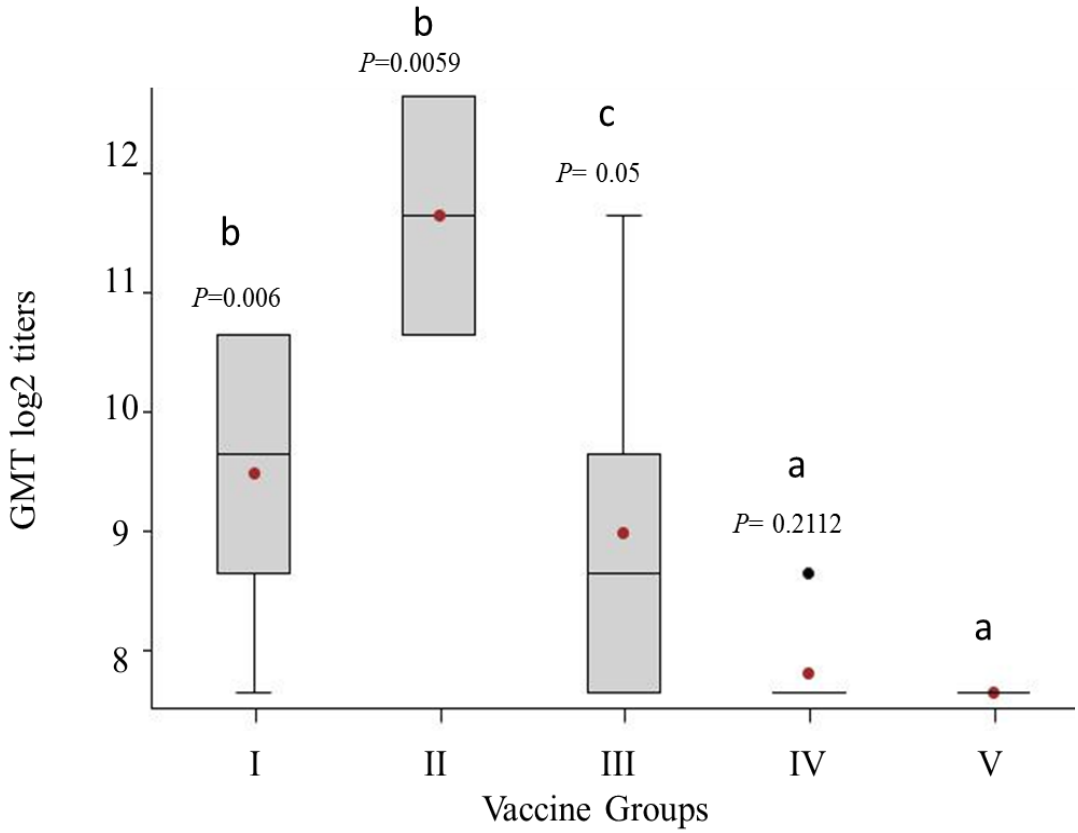

Figure 5.3 Phage-specific IgM antibody inter-group comparisons. I and II, full-length phage vaccines LongRnano3 and LongRnano3FnB respectively; III, nanophage vaccine ShortRnano3FnB (without heat treatment); IV, nanophage vaccine incubated at 37 ºC for 48 h (WarmShortRnano3FnB); V, control group (vaccinated with PBS buffer) (see Figure 5.1 for group labels) . Y-axis indicates GMT (log for base 2) titres of antibodies obtained by serum titration. The upper and lower borders of the box represent first and third quartiles, respectively. The horizontal line drawn within the box marks the median. The red dot (●) shows the sample mean. The whiskers (standard deviation from the mean) are drawn to the most extreme points that lie within the fences. Outliers are marked as black dots (●). Lowercase letters (a, b and c) at the top of bars denote groups with significant difference from each other ($p \leq 0.05$; Wilcoxon-Mann-Whitney test).

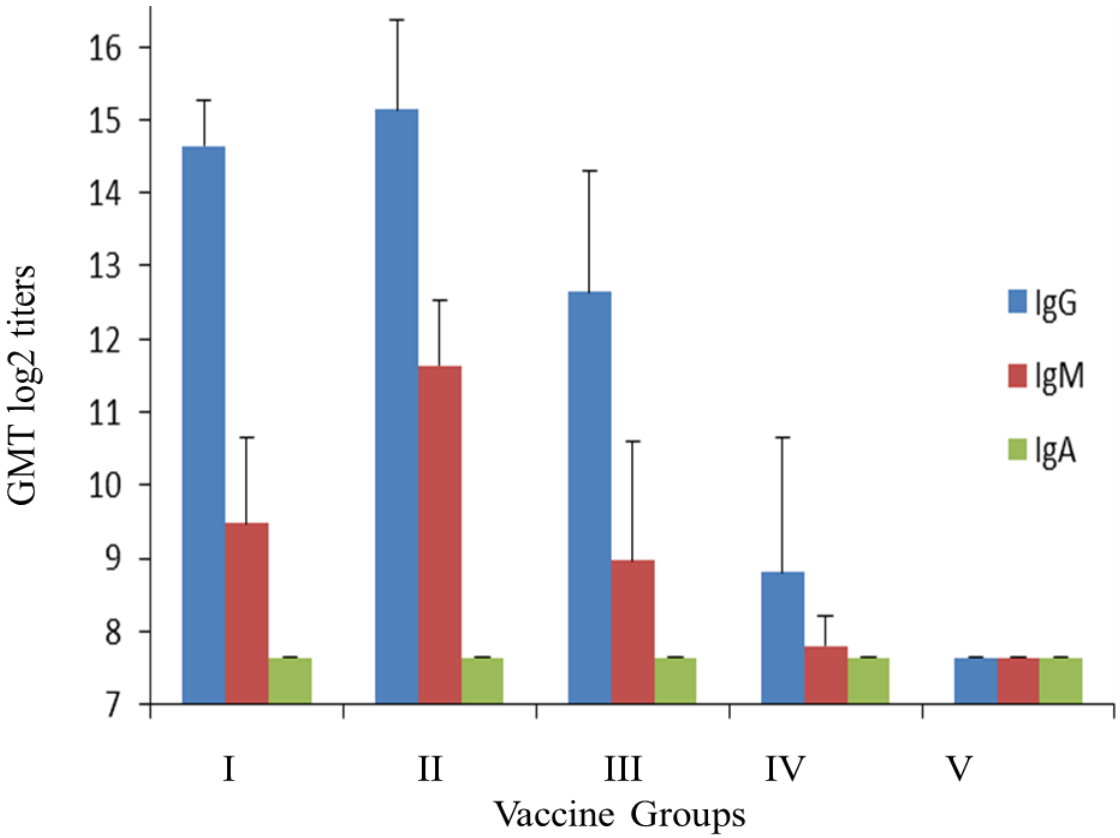

Figure 5.4 Comparison of phage-specific IgG, IgM and IgA response. X-axis indicates vaccine groups; I and II, full-length phage vaccines (LongRnano3 and LongRnano3FnB); III, nanophage vaccine ShortRnano3FnB (without heat treatment); IV, nanophage vaccine incubated at 37 ºC for 48 h (WarmShortRnano3FnB); V, control group (vaccinated with PBS buffer). Y-axis indicates GMT (log for base 2) of antibodies obtained by serum titration. Error bars represent standard deviation.

5.5.2 Phage-specific IgG Antibody Subclasses

As described in the previous section, phage-specific general IgG antibody response was significantly higher for all vaccine groups (I-IV) in comparison to control (group V). In order to determine which IgG subclass dominated immune response, a phage-specific IgG subclass profile for sera of all vaccinated groups was determined. **IgG1** antibody response was significantly higher in all vaccination groups as compared to control (Figure 5.5). Full-length phage vaccine groups (I & II) exhibited low intra-group variation whereas mice vaccinated with nanophage vaccines (III & IV) exhibited a high intra-group variation. This variance was highest for group IV mice that received the 37 ºC-treated nanophage vaccine ($P = 0.05$).

The phage-specific **IgG2a** antibody response was significant for groups I, II and III (Figure 5.6); however group IV vaccinated with the 37 ºC-treated nanophage vaccine exhibited marginally significant ($P = 0.0503$) rise as compared to group V (PBS control). This was probably due to a large intra-group variance in immune response, with two mice being non-responsive to the given vaccine dose. Similarly, a significantly high phage-specific **IgG2b** titre was observed for groups I and II ($P = 0.006$), as compared to group V, whereas increase in titre of IgG2b for nanophage vaccine group III was marginally significant ($P = 0.0508$) whereas for group IV it was statistically non-significant ($P = 0.211$). In addition, group III exhibited large intra-group variance (Figure 5.7).

Phage-specific **IgG3** for all vaccination groups was at a background level for all vaccine groups (data not shown).

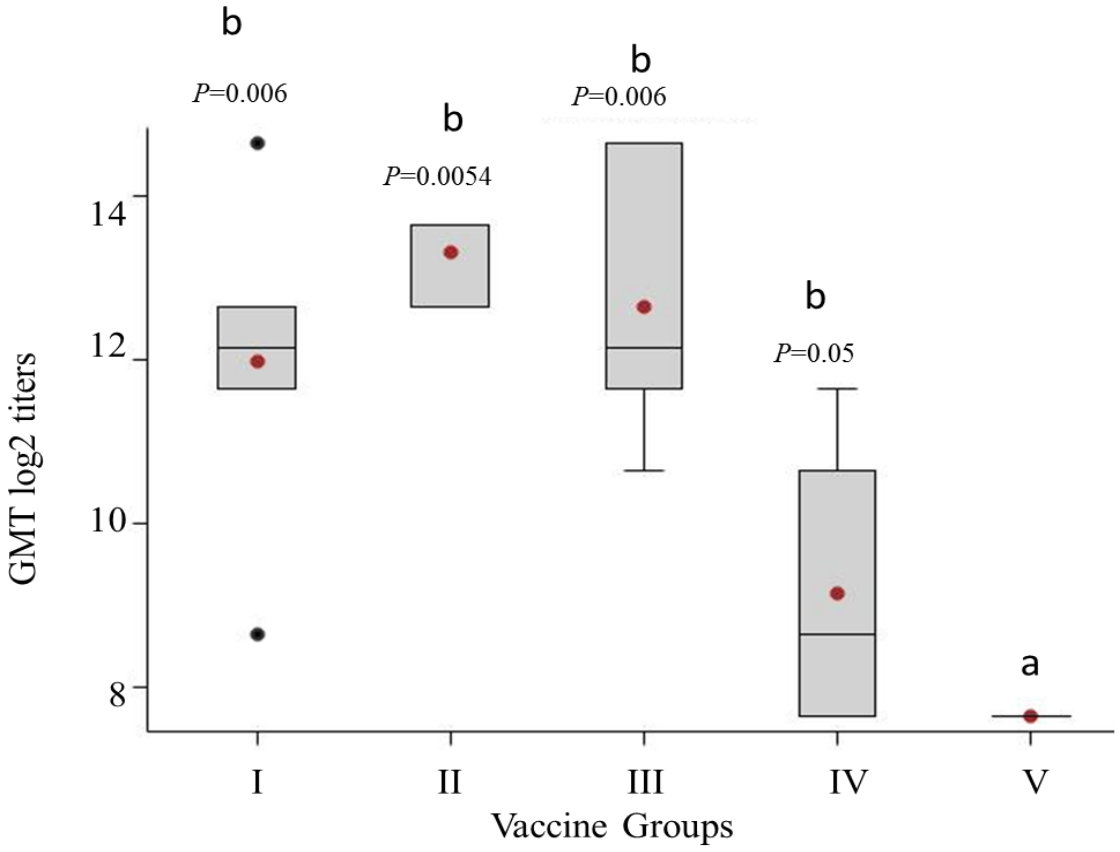

Figure 5.5 Phage-specific IgG1 antibodies. I and II, full-length phage vaccines LongRnano3 and LongRnano3FnB respectively; III, nanophage vaccine ShortRnano3FnB (without heat treatment); IV, nanophage vaccine kept at 37 ºC for 48 h (WarmShortRnano3FnB); V, control group (vaccinated with PBS buffer) (see Figure 5.1 for group labels) . Y-axis indicates GMT (log for base 2) of antibodies obtained by serum titration. The upper and lower borders of the box represent first and third quartiles, respectively. The horizontal line drawn within the box marks the median. The red dot (●) shows the sample mean. The whiskers (standard deviation from the mean) are drawn to the most extreme points that lie within the fences. Outliers are marked as black dots (●). Lowercase letters (a, b and c) at the top of bars denote groups with significant difference from each other ($p \leq 0.05$; Wilcoxon-Mann-Whitney test).

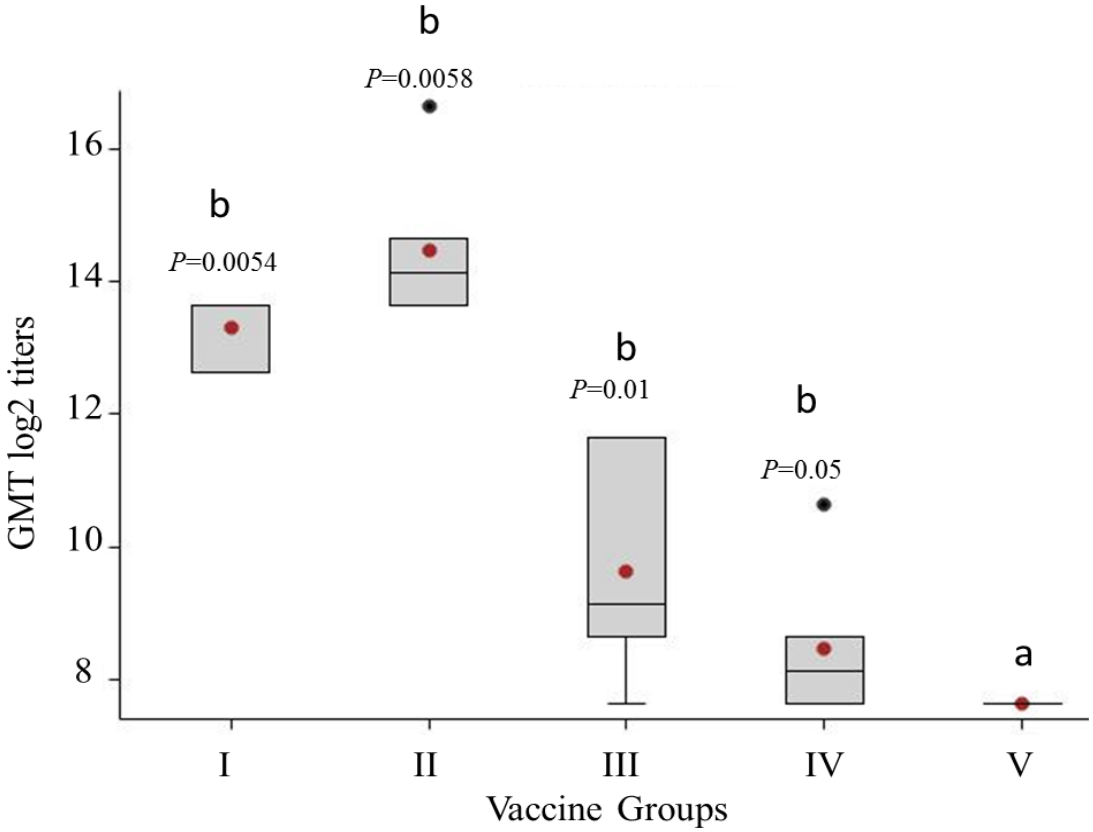

Figure 5.6 Phage-specific IgG2a antibody responses. I and II, full-length phage vaccines LongRnano3 and LongRnano3FnB respectively; III, nanophage vaccine ShortRnano3FnB (without 37 ºC incubation); IV, nanophage vaccine incubated at 37 ºC for 48 h (WarmShortRnano3FnB); V, control group (vaccinated with PBS buffer) (see Figure 5.1 for group labels) .Y-axis indicates GMT (log for base 2) of antibodies obtained by serum titration. The upper and lower borders of the box represent first and third quartiles, respectively. The horizontal line drawn within the box marks the median. The red dot (●) shows the sample mean. The whiskers (standard deviation from the mean) are drawn to the most extreme points that lie within the fences. Outliers are marked as black dots (●). Lowercase letters (a, b and c) at the top of bars denote groups with significant difference from each other ($p \leq 0.05$; Wilcoxon-Mann-Whitney test).

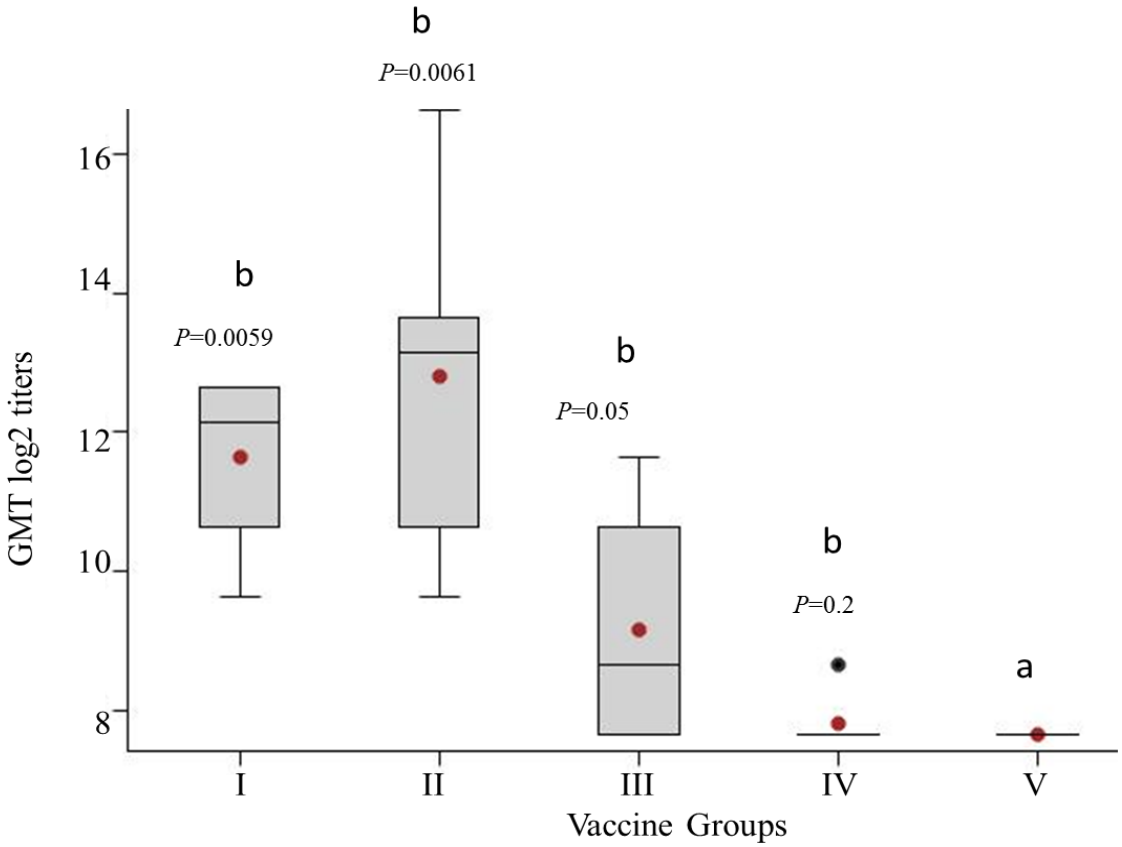

Figure 5.7 Phage-specific IgG2b antibody responses. I and II, full-length phage vaccines LongRnano3 and LongRnano3FnB respectively; III, nanophage vaccine ShortRnano3FnB (without a 37 ºC incubation); IV, nanophage vaccine incubated at 37°C for 48 h (WarmShortRnano3FnB); V, control group (vaccinated with PBS buffer) (see Figure 5.1 for group labels) .Y-axis indicates GMT (log for base 2) antibody titres obtained after serum titration. The upper and lower borders of the box represent first and third quartiles, respectively. The horizontal line drawn within the box marks the median. The red dot (●) shows the sample mean. The whiskers (standard deviation from the mean) are drawn to the most extreme points that lie within the fences. Outliers are marked as black dots (●). Lowercase letters (a, b and c) at the top of bars denote groups with significant difference from each other ($p \leq 0.05$; Wilcoxon-Mann-Whitney test).

5.5.3 Variation in Phage-specific IgG Subclass Antibody within Each Vaccine Group

The phage-specific IgG1, IgG2a and IgG2b antibodies were relatively higher in comparison to IgG3 for all vaccine groups. The IgG1 characterizes a Th2 response, whereas the IgG2a and IgG2b are characteristic of a Th1 immune response. When each subtype titre was compared with others in the same group for the full-length phage vaccine groups (I and II), it was found that phage-specific IgG2a subtype of IgG was higher than IgG1 (**IgG2a > IgG1 = IgG2b > IgG3**). This was significant for group II (P = 0.031), but marginally non-significant for group I (P = 0.071) (Figure 5.8A and B). It indicated an incline towards T helper cell 1 response in full-length phage vaccines.

For the nanophage-immunized group III and IV, phage-specific IgG1 antibody response was higher than IgG2a (**IgG1 > IgG2a = IgG2b > IgG3**), this difference was statistically significant for group III (P = 0.027) whereas non-significant (P = 0.33) for group IV mice. It indicated that immune response to nanophage was mainly Th2 response. A large intra-group variance for both group III and IV (Figure 5.9A and B) was evident.

All phage-specific IgG subclasses were at background level for group V mice (data not shown). A comparison of all IgG subtypes in all groups is given in Figure 5.10. Based on the profiles of phage-specific IgG subclasses, immunization induced a mix of Th1 and Th2 responses, nanophage eliciting a marginally Th2 (IgG1) prevalent response, whereas the full-length phage-induced response was Th1-dominant.

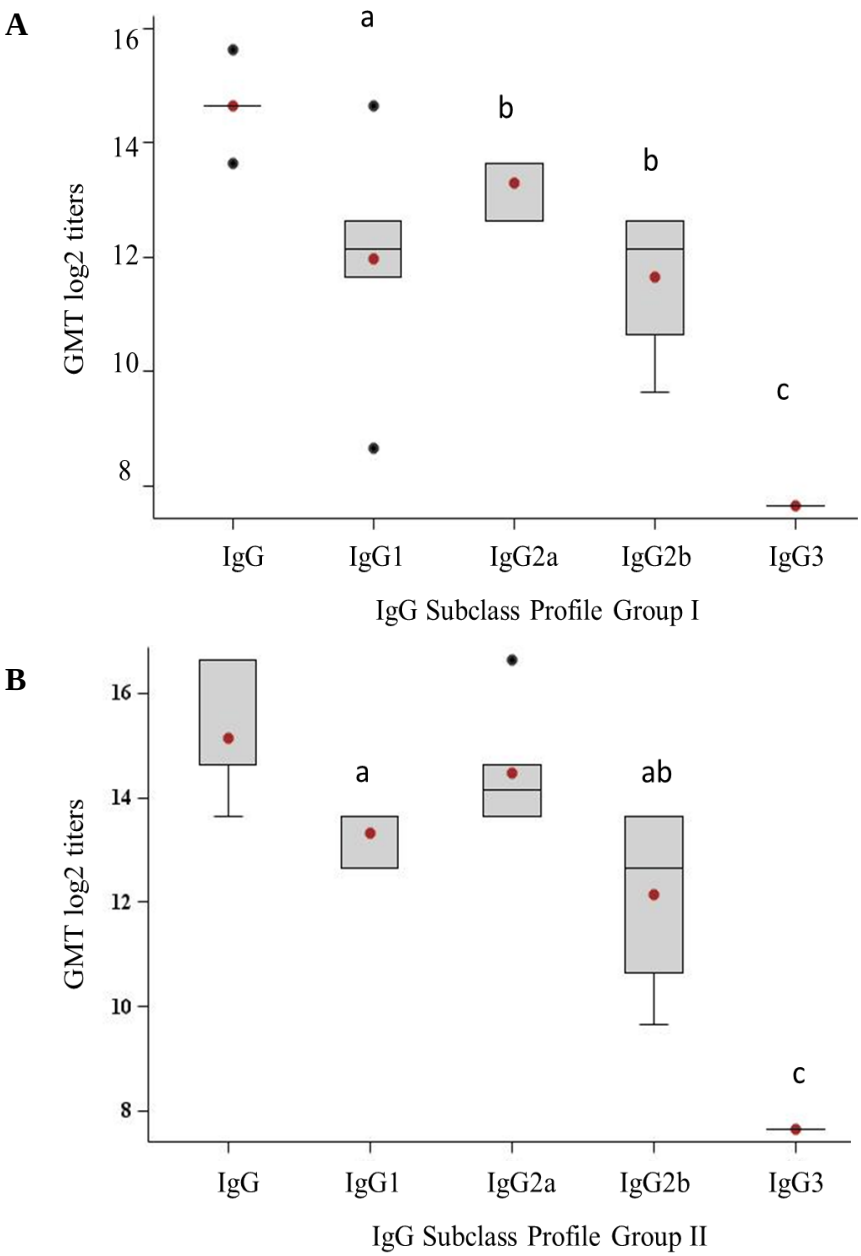

Figure 5.8 In-group comparisons of phage-specific IgG subtypes in full-length phage vaccines. A, group I; **B**, group II, full-length vaccines (LongRnano3 and LongRnano3FnB, respectively).Y-axis indicates GMT (log for base 2) titres obtained after titration of serum. The upper and lower borders of the box represent first and third quartiles, respectively. The horizontal line drawn within the box marks the median. The red dot (●) shows the sample mean. The whiskers (standard deviation from the mean) are drawn to the most extreme points that lie within the fences. Outliers are marked as black dots (●). Lowercase letters at the top of bars represent significant differences at $p \leq 0.05$ (Wilcoxon-Mann-Whitney test).

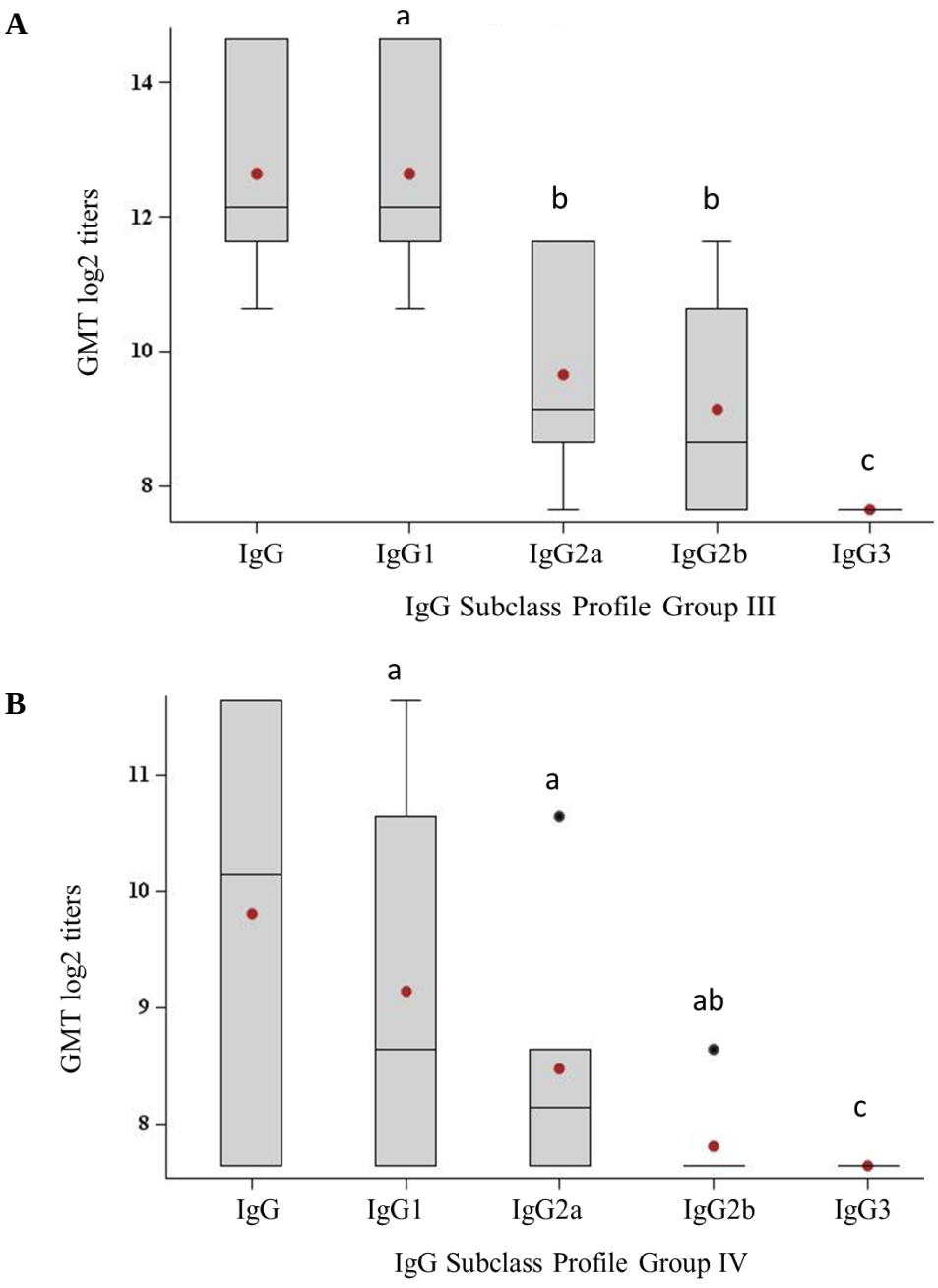

Figure 5.9 In-group comparison of phage-specific IgG subtypes in the nanophage vaccine groups. A, group III; **B**, group IV, nanophage vaccines (ShortRnano3 and WarmShortRnano3FnB, respectively). Y-axis indicates GMT (log for base 2) obtained after titration of serum. The upper and lower borders of the box represent first and third quartiles, respectively. The horizontal line drawn within the box marks the median. The red dot (●) shows the sample mean. The whiskers (standard deviation from the mean) are drawn to the most extreme points that lie within the fences. Outliers are marked as black dots (●). Lowercase letters at the top of bars represent significant differences at $p \leq 0.05$ (Wilcoxon-Mann-Whitney test).

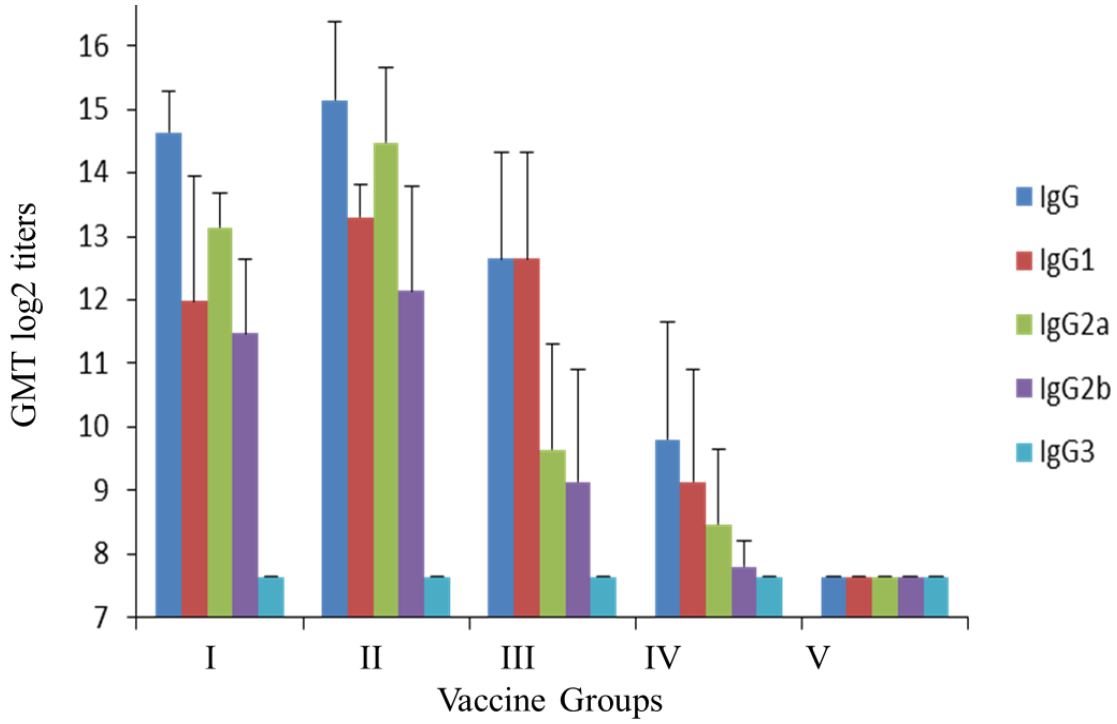

Figure 5.10 Phage-specific IgG subtype profile in all vaccine groups. I and II, full-length vaccines (LongRnano3 and LongRnano3FnB); III, nanophage vaccine ShortRnano3FnB (without heat treatment); IV, nanophage vaccine kept at 37 ºC for 48 h (WarmShortRnano3FnB); V, control group (vaccinated with PBS buffer).Y-axis indicates GMT (log for base 2) titres of antibodies obtained after serum titration. Data is presented as an average of each antibody response for all six mice. Error bars represent standard deviation.

5.5.4 Phage-specific IgG Subclass Profile of Individual Mice in Each Vaccine Group

All vaccination groups exhibited a significant rise in phage-specific IgG antibodies, as discussed above. However, two nanophage-vaccinated groups showed high intra-group variation in the IgG subclasses. This variation affects the overall statistical significance of a group. Therefore, it was essential to determine whether observed significance was due to the low efficacy of the nanophage vaccine or due to immune status of individual mice in each group. In order to do so, IgG subtype profiles for individual animals in each group were analyzed.

All mice in full-length phage vaccine groups I and II (LongRnano3 and LongRnano3FnB, respectively), were responsive to vaccine treatment (Figure 5.11A and B), exhibiting a uniform rise in antibody titres for all IgG subtypes, apart from animal number 2 in group I, that had a relatively lower titre of the IgG1 subclass, animals 4 and 5 that had a lower titre of IgG2b subclass. However, in groups vaccinated with nanophage vaccines, a large individual variation in vaccine response was observed. In group III, two animals were highly responsive (Figure 5.12A); three exhibited moderate increase in antibody responses for almost all IgG subtypes, whereas one mouse was barely responsive above the background level. In Group IV three animals were poorly responsive to vaccine treatment whereas other three were moderate in response (Figure 5.12B). These findings indicate that variation observed in immune response was obtained due to the individual mice immune status. Group V (vaccinated with PBS) mice had no increase in antibody response in any of the animals.

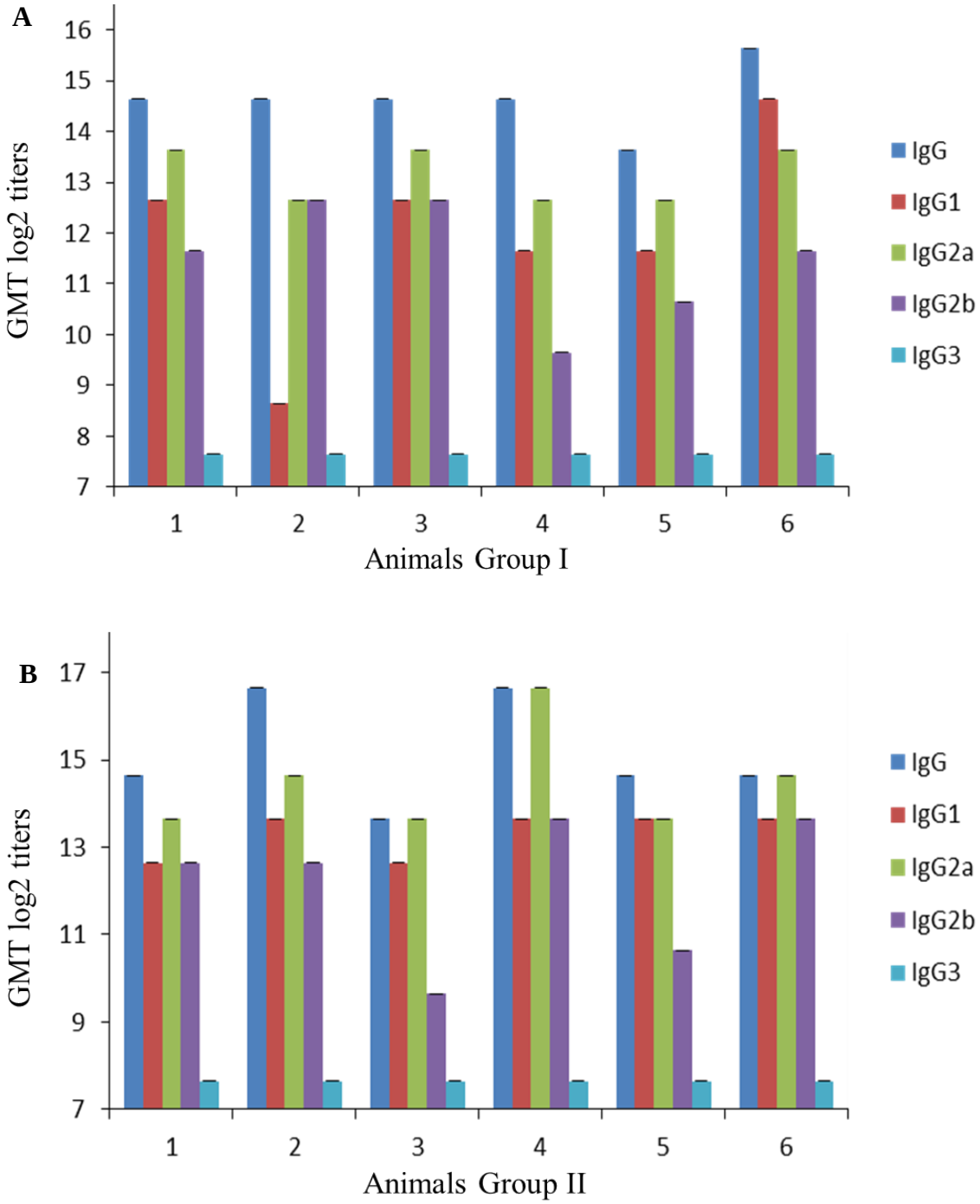

Figure 5.11 Phage-specific IgG subtype profile in individual animals in full-length phage vaccinated animals. A. group I full-length phage vaccine (LongRnano3), **B**, group II, full-length phage vaccine (LongRnano3FnB); X-axis indicates individual animals (1-6), whereas y-axis indicates GMT (log for base 2) titres of antibodies obtained after serum titration. Error bars represent standard deviation.

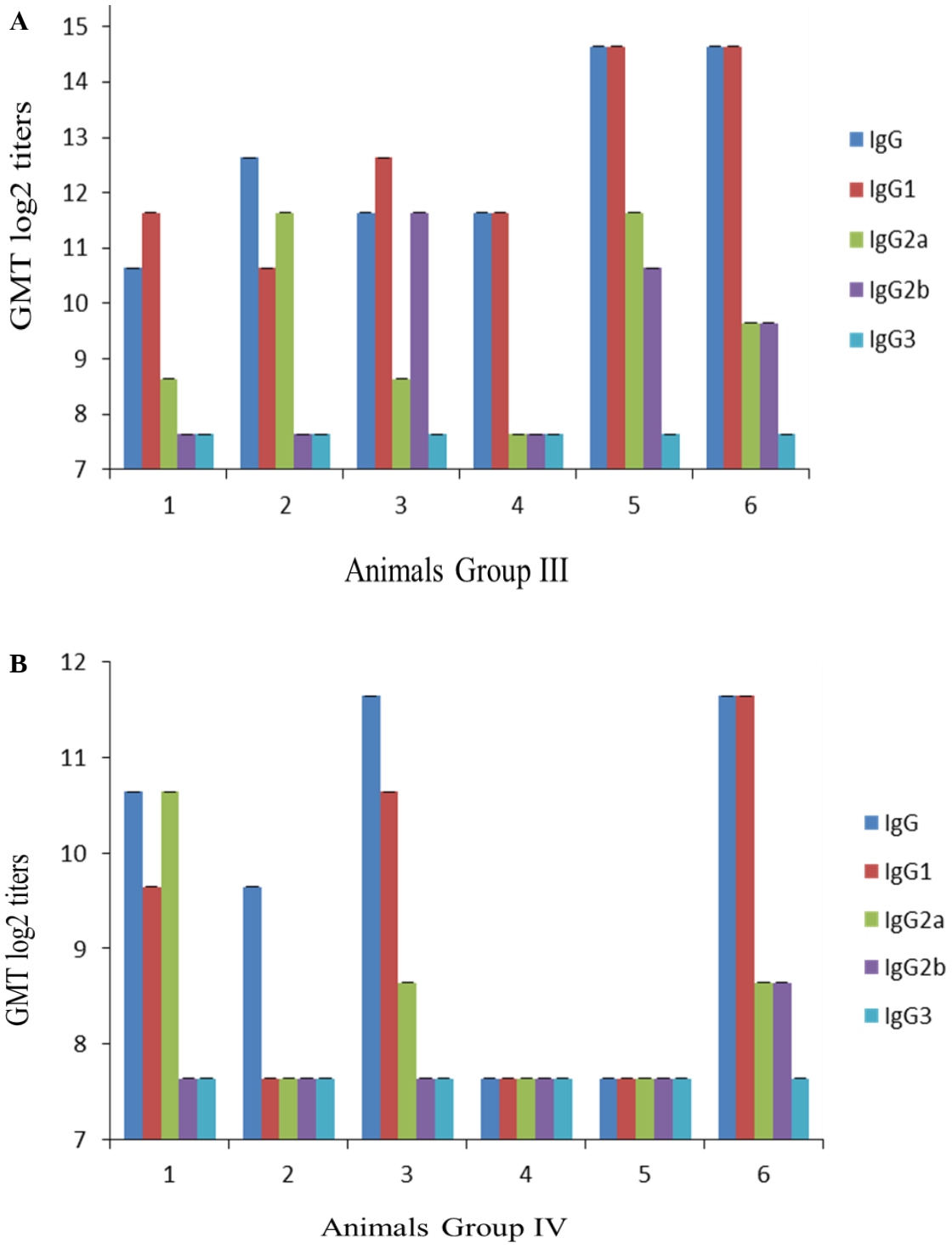

Figure 5.12 Phage-specific IgG subtype profile in individual animals in the nanophage vaccine groups. A. group III, nanophage vaccine ShortRnano3FnB (without heat treatment); **B**. group IV, nanophage vaccine kept at 37 ºC for 48 h (WarmShortRnano3FnB); X-axis indicates individual animals (1-6), whereas y-axis indicates GMT (log for base 2) of antibodies obtained after serum titration. Error bars represent standard deviation.

5.6 Immune Response Against Phage-displayed Fibronectin Binding Domain of *Streptococcus pyogenes*

5.6.1 Experimental Design

Fibronectin binding domain from *S.pyogenes* was expressed as pIII fusion in both full-length and nanophage particles (Chapter 2, Section 2.2.3). The nucleotide sequence encoding FnB domain was seamlessly fused in between signal sequence and mature part of phage pIII in the helper phage used for nanophage and full-length phage production for vaccine trial. The only *gIII* available in the cells assembling the phage was encoded by the chimeric *FnB-gIII* construct. Given that there are five copies of pIII in the virion, each phage particle was expected to express five copies of FnB domain, one fused to each of the five pIII molecules. The display of FnB domain on the phage particles was confirmed using immobilised fibronectin in phage ELISA. Both full-length and nanophage particles with FnB domain exhibited high ELISA signal in comparison to phage particles carrying wild type pIII. The immune response to FnB domain expressed on both full-length and nanophage particles were examined by ELISA assay, using immobilised MBP-FnB fusion as an antigen. Background signal in this assay was very high, suggesting that the serum contained some level of Fn-specific antibodies which are associated with the serum fibronectin, resulting in binding of Fn-specific antibodies to FnB domain via serum fibronectin as a bridge. All antibody titres were determined as inverse value of the highest dilution of antiserum (in a series of two-fold dilutions) that gave a positive signal in the ELISA assay.

5.6.2 FnB Domain-specific General IgG for All Vaccination Groups

It was expected that group II immunized with functionalized full-length phage particles displaying FnB domain as well as group III and IV, immunized with FnB-displaying nanophage particles, would produce FnB domain-specific antibodies. The nature of response against FnB domain was expected to be different from that being produced against phage because the dominant antigen in phage is the highly repetitive major coat protein, vs. FnB domain was displayed at a maximum of 5 copies at one end of the phage (Figure 5.1). The response to FnB domain was indeed weaker than that to the phage. Only two of the three groups (group II and III) produced antibodies against displayed FnB domain (145 amino acids). Increase in antibody titre of IgG class was

significant in case of group II with all mice exhibiting an average titre of IgG against FnB domain of 9.14 (P = 0.01; Figure 5.13). In contrast, the increase in the immune response to FnB domain was statistically non-significant for group III (P = 0.101). This may have been due to a large intra-group variance in FnB domain-specific antibody response observed for group III, in which out of six animals, three were non-responsive and one was moderately responsive, whereas the remaining two exhibited reasonably high titre of antibodies against FnB domains (Figure 5.13). IgM and IgA titres were at background levels for all groups (data not shown). Group I, the full-length phage that did not display FnB domain, was used as control to measure the statistical significance of the antibody response. IgG titre against FnB domain for group IV given the WarmShortRnano3FnB vaccine (the nanophage incubated at 37 °C for 48 h) was at background levels.

Both the full-length phage and the nanophage particles were precipitated overnight from bacterial culture medium using PEG 8000. Since bacterial culture medium contains cellular debris and therefore numerous *E. coli* proteases, it is likely that the FnB domain moiety of the FnB-pIII fusion was proteolytically degraded during incubation. This was confirmed by SDS-PAGE and western blotting analysis (Figure 5.14). This degradation was more pronounced in case of nanophage particles, with the FnB-pIII fusion being 1/10 of the pIII signal, in contrast to the full-length phage where the fusion to pIII ratio was approximately 1:1. Some proteolytic degradation is expected, as the FnB domain is intrinsically unfolded and is therefore expected to be highly susceptible to proteolysis by *E. coli* proteases during assembly in the periplasm and purification. Increased degradation of FnB-pIII fusion in the nanophage in comparison to the full-length phage is very likely due to the second overnight PEG precipitation step in the nanophage purification protocol (Figure 5.14). Since all groups given the phage vaccine exhibited a statistically significant response against phage proteins, the intra-group variance against FnB domain exhibited by group III mice was most likely due to a combination of low amount of antigen due to abovementioned proteolysis and uneven age of the animals used in the experiment (4 to 6 weeks). Group IV mice immunised by the FnB-domain-displaying nanophage vaccine, incubated at 37 ºC for 48h were negative for FnB domain-specific antibodies. Although the vaccine preparations were subjected to extensive purification steps, they are still likely to contain a minimal amount of proteases that are active at 37 °C,

resulting in further FnB domain peptide degradation in group IV. All groups had significant antibody titres against phage proteins (Section 5.5).

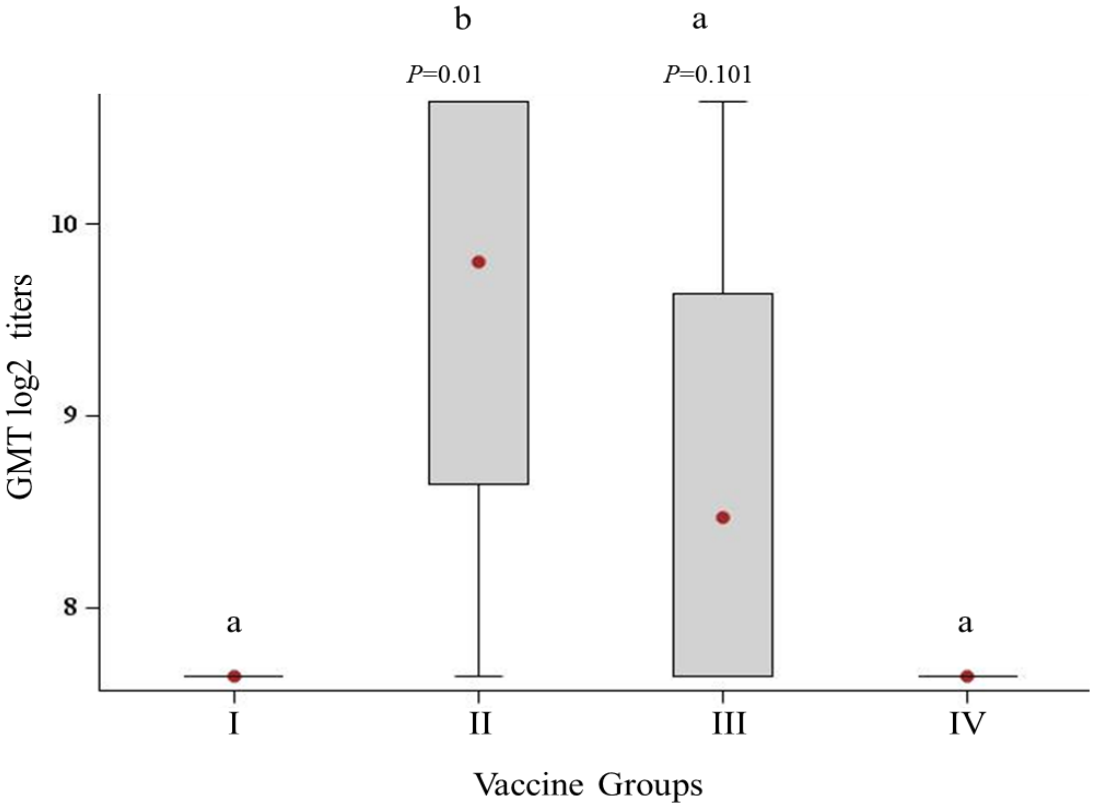

Figure 5.13 IgG antibodies (all subclasses) against FnB domain. I and II, full-length vaccines (LongRnano3 and LongRnano3FnB); III, nanophage vaccine ShortRnano3FnB (without heat treatment); IV, nanophage vaccine kept at 37 ºC for 48 h (WarmShortRnano3FnB); V, control group (vaccinated with PBS buffer). Y-axis indicates GMT (log for base 2) of antibodies obtained after serum titration. The upper and lower borders of the box represent first and third quartiles, respectively. The horizontal line drawn within the box marks the median. The red dot (●) shows the sample mean. The whiskers (standard deviation from the mean) are drawn to the most extreme points that lie within the fences. Outliers are marked as black dots (●). Lowercase letters (a, b and c) at the top of bars denote groups with significant difference from each other ($p \leq 0.05$; Wilcoxon-Mann-Whitney test).

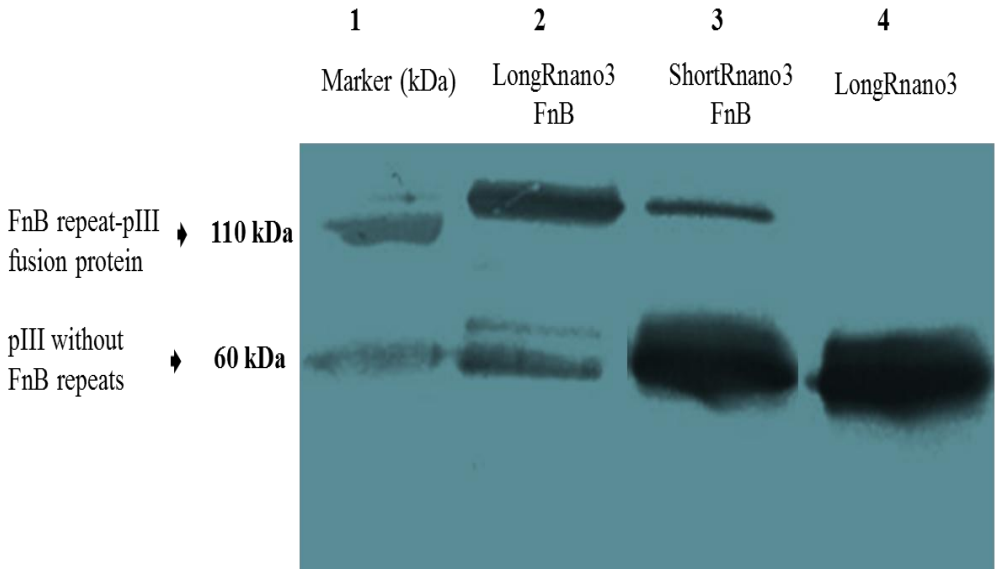

Figure 5.14 Western-blotting detection of FnB-pIII fusion in the full-length phage and nanophage. A polyclonal rabbit anti-pIII antibody (Rakonjac and Model, 1998) was used for blotting. Lane I Molecular mass marker in kDa; lane 2 , functionalized full-length phage used for vaccination (LongRnano3FnB); lane 3 nanophage vaccine ShortRnano3FnB; lane 4, full-length phage Rnano3 without FnB domain (LongRnano3).

5.6.3 FnB Domains-specific IgG Subclass Antibody Response

Only the full-length FnB-displaying vaccine (group II; LongRnano3FnB) and the nanophage FnB-displaying vaccine (group III; ShortRnano3FnB) elicited a measureable response against FnB domain, albeit the immune response for group III was not statistically significant. In order to determine the type of immune response activated by each of these vaccines, IgG subclass profile for both positive groups (II and III) was determined.

Antibody titres indicated that IgG response against FnB domain was mainly IgG1 driven. The **IgG1** response was significant (P = 0.012) for group II vaccinated with full-length (LongRnano3FnB) phage whereas non-significant (P = 0.1) for group III (ShortRnano3FnB) (Figure 5.15). Group II exhibited a slight increase **IgG2a** antibody titres however it was statistically non-significant (P = 0.1) (Figure 5.16). **IgG2b** and **IgG3** titres were at background levels for both groups (II and III) (data not shown).

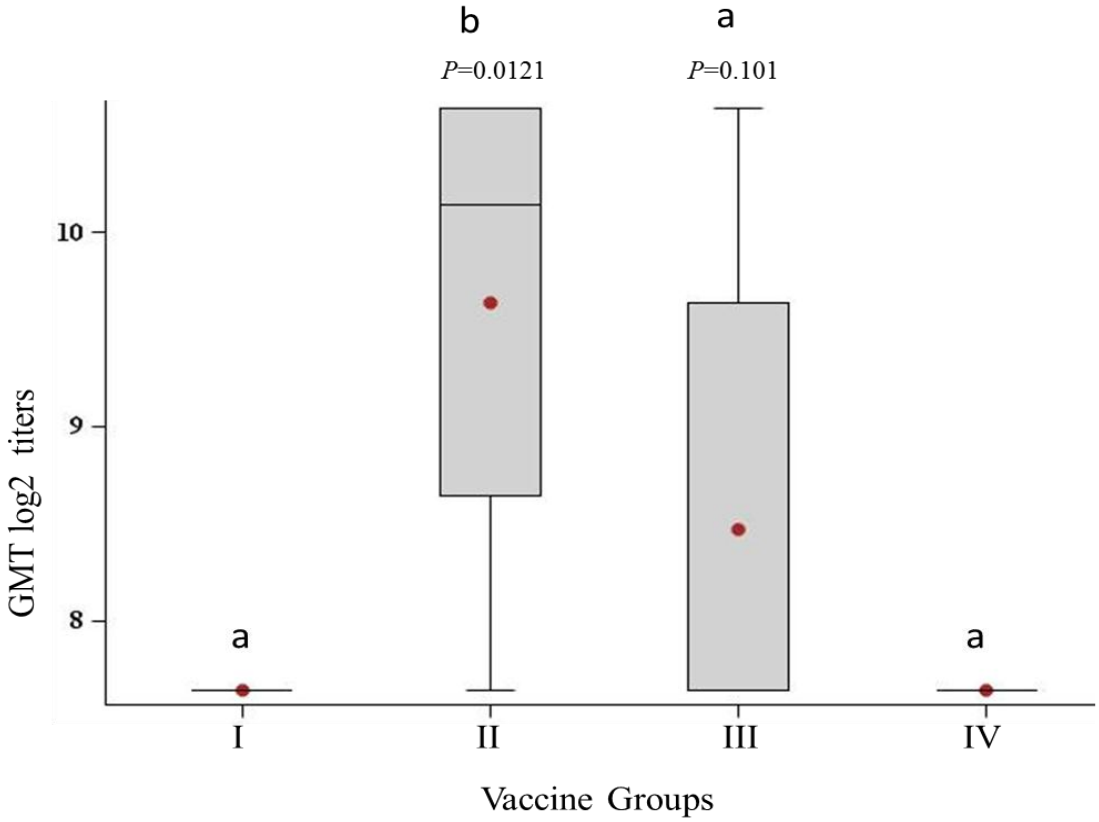

Figure 5.15 IgG1 antibodies against FnB domain. I and II, full-length vaccines (LongRnano3 and LongRnano3FnB); III, nanophage vaccine ShortRnano3FnB (without heat treatment); IV, nanophage vaccine kept at 37 ºC for 48 h (WarmShortRnano3FnB); V, control group (vaccinated with PBS buffer). Y-axis indicates GMT (log for base 2) of antibodies obtained by serum titration. The upper and lower borders of the box represent first and third quartiles, respectively. The horizontal line drawn within the box marks the median. The red dot (●) shows the sample mean. The whiskers (standard deviation from the mean) are drawn to the most extreme points that lie within the fences. Outliers are marked as black dots (●). Lowercase letters (a, b and c) at the top of bars denote groups with significant difference from each other ($p \leq 0.05$; Wilcoxon-Mann-Whitney test)

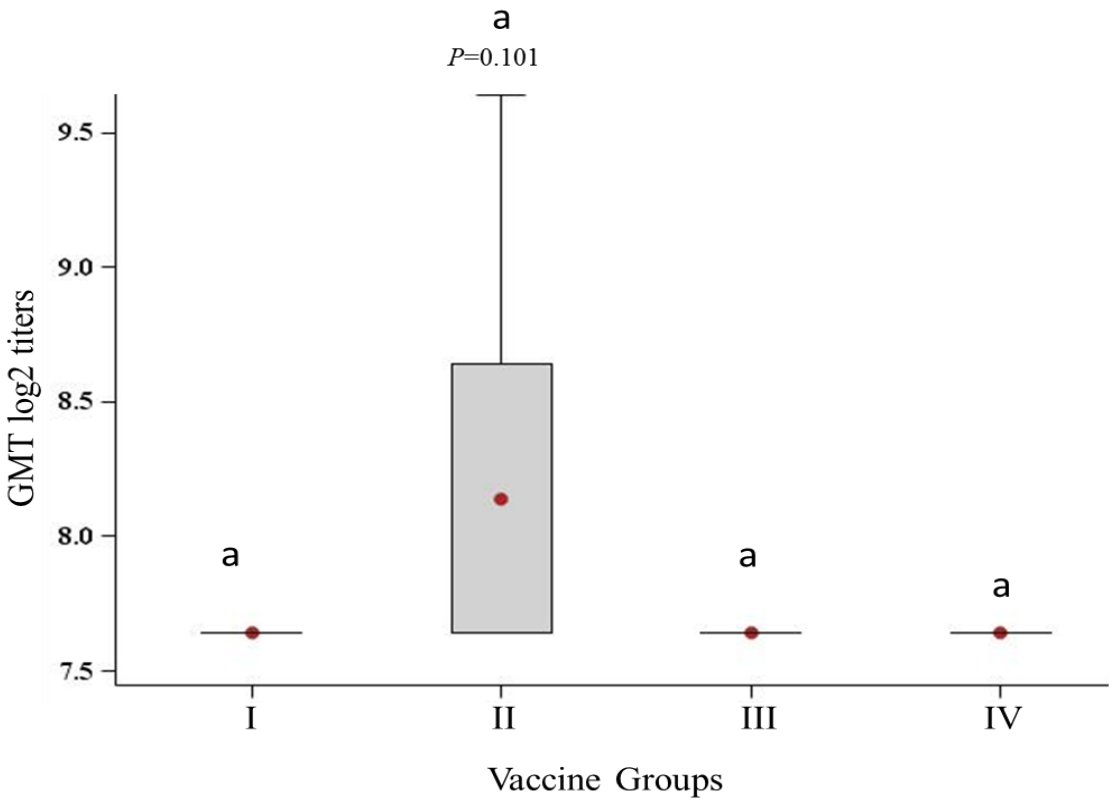

Figure 5.16 IgG2a antibodies against phage-displayed FnB-domain. I and II, full-length vaccines (LongRnano3 and LongRnano3FnB); III, nanophage vaccine ShortRnano3FnB (without heat treatment); IV, nanophage vaccine kept at 37 ºC for 48 h (WarmShortRnano3FnB); V, control group (vaccinated with PBS buffer). Y-axis indicates GMT (log for base 2) of antibodies obtained by serum titration. The upper and lower borders of the box represent first and third quartiles, respectively. The horizontal line drawn within the box marks the median. The red dot (●) shows the sample mean. The whiskers (standard deviation from the mean) are drawn to the most extreme points that lie within the fences. Outliers are marked as black dots (●). Lowercase letters (a, b and c) at the top of bars denote groups with significant difference from each other ($p \leq 0.05$; Wilcoxon-Mann-Whitney test)

5.6.4 Variation in FnB Domain-specific IgG Subclass Antibody Response within Each Vaccine Group

Overall immune response against FnB domain expressed as pIII fusion on both full length and nanophage particles was low. Functionalized full-length phage particles of (group II) triggered a significant response against FnB domain. With respect to IgG subclasses, group II animals exhibited a good increase in titres for both IgG1 and IgG2a, however IgG1 titre was significantly higher than IgG2a (P = 0.0267) followed by IgG2b and IgG3 (**IgG1>IgG2a= IgG2b>IgG3**). This indicated that immune response against FnB domain generated by full length phage particles was predominantly Th2 response (Figure 5.17).

Group III (the FnB-displaying nanophage) exhibited low serum IgG antibody titre which was mainly IgG1. IgG2a and IgG2b titres were at background levels. Even though IgG1 was the only subtype with a value increased relative to the background level, this increase was not statistically significant (P= 0.1) (Figure 5.18). A comparison of all IgG subtypes for all vaccine groups is given in Figure 5.19.

In conclusion, antibody response against FnB domain elicited by immunization with nanophage particles displaying FnB domain (ShortRnano3FnB) was statistically non-significant when compared with phage that did not display FnB domain (group I). Because of the large in-group variance, antibody titres against FnB domain of individual animals in group II and III are compared in Figure 5.20A and 5.20B respectively. Four out of six mice in group II produced antibodies against FnB domain; one was moderately responsive, whereas one was at background level for all IgG subtypes (Figure 5.20 A). In case of group III (the FnB-displaying nanophage) only two animals produced antibodies of all subtypes against FnB-domain, whereas other four were at background levels, which made the overall increase in titre of the FnB domain-specific antibodies is statistically non-significant for group III (Figure 5.20B).

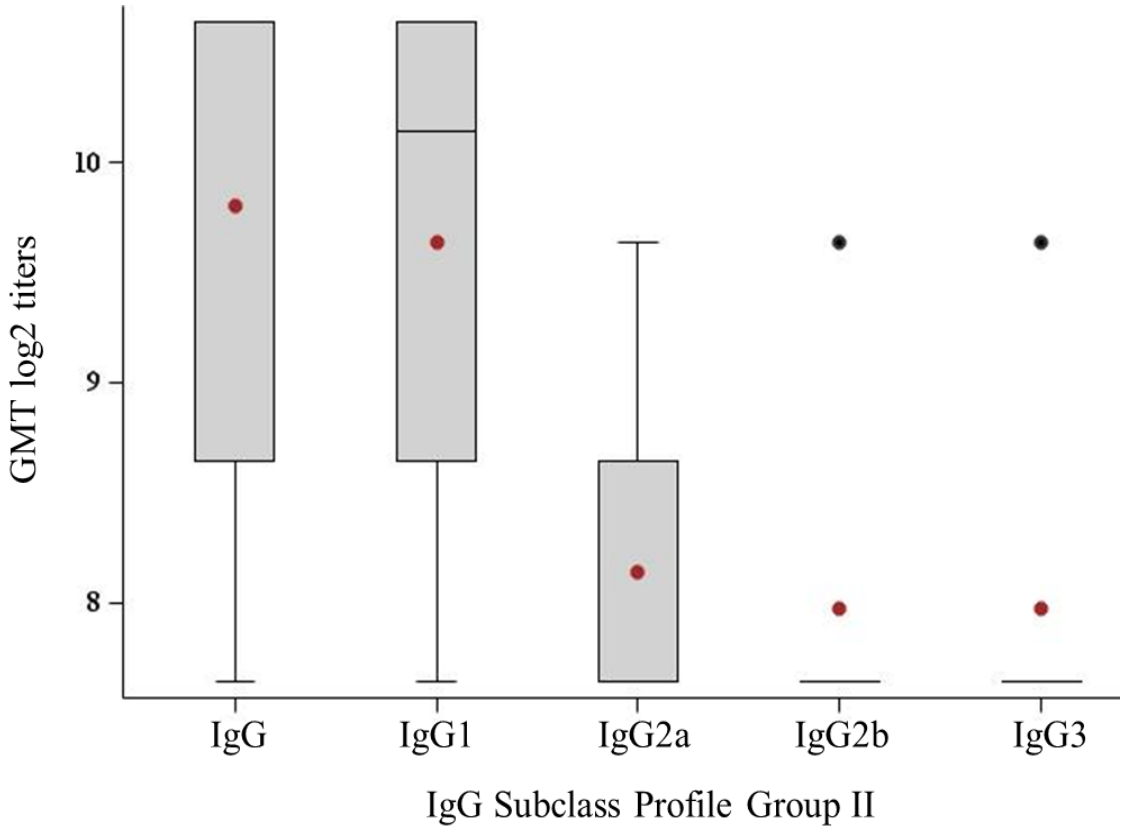

Figure 5.17 Comparison of FnB domain-specific IgG subtypes in group II. Full-length phage vaccine (LongRnano3FnB); X-axis indicates individual IgG subtypes in group II; Y-axis indicates GMT (log for base 2) of antibodies obtained by serum titration. The upper and lower borders of the box represent first and third quartiles, respectively. The horizontal line drawn within the box marks the median. The red dot (●) shows the sample mean. The whiskers (standard deviation from the mean) are drawn to the most extreme points that lie within the fences. Outliers are marked as black dots (●). Lowercase letters at the top of bars represent significant differences at $p \leq 0.05$ (Wilcoxon-Mann-Whitney test).

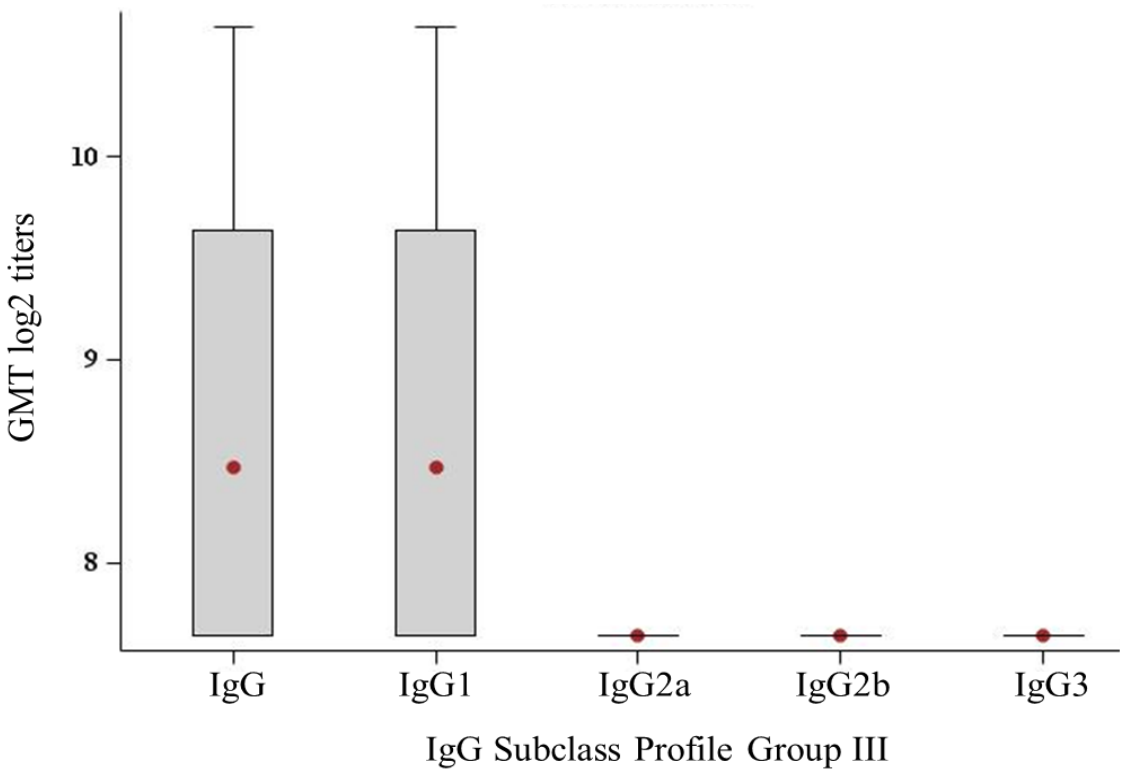

Figure 5.18 Comparison of FnB domain-specific IgG subtypes in group III. Group III vaccinated with functionalized nanophage vaccine (ShortRnano3FnB). X-axis indicates IgG subtypes, whereas Y-axis indicates GMT (log for base 2) of antibodies obtained after serum titration. The width of each box shows the number of animals which is constant in all groups. The upper and lower edges of the box represent first and third quartiles, respectively. The horizontal line drawn within the box marks the median. The red dot (●) shows the sample mean. The whiskers (standard deviation) are drawn to the most extreme points that lie within the fences. Observations outside the fences are marked as black dots (●).

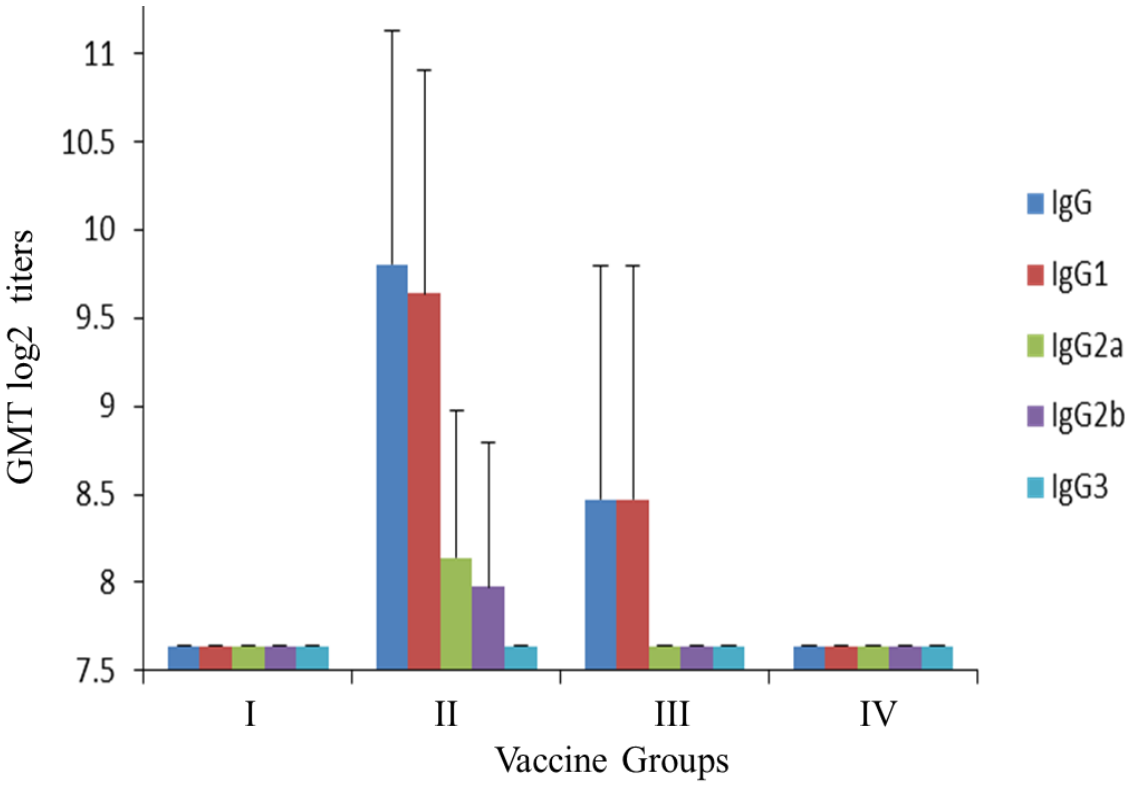

Figure 5.19 FnB domain-specific IgG subtype profile in all vaccine groups. I and II, full-length phage vaccines (LongRnano3 and LongRnano3FnB); III, nanophage vaccine ShortRnano3FnB (without heat treatment); IV, nanophage vaccine kept at 37 ºC for 48 h (WarmShortRnano3FnB); V, control group (vaccinated with PBS buffer). Y-axis indicates GMT (log for base 2) titres of antibodies obtained by serum titration. Data is presented as an average of each antibody response for all six mice. Error bars represent standard deviation.

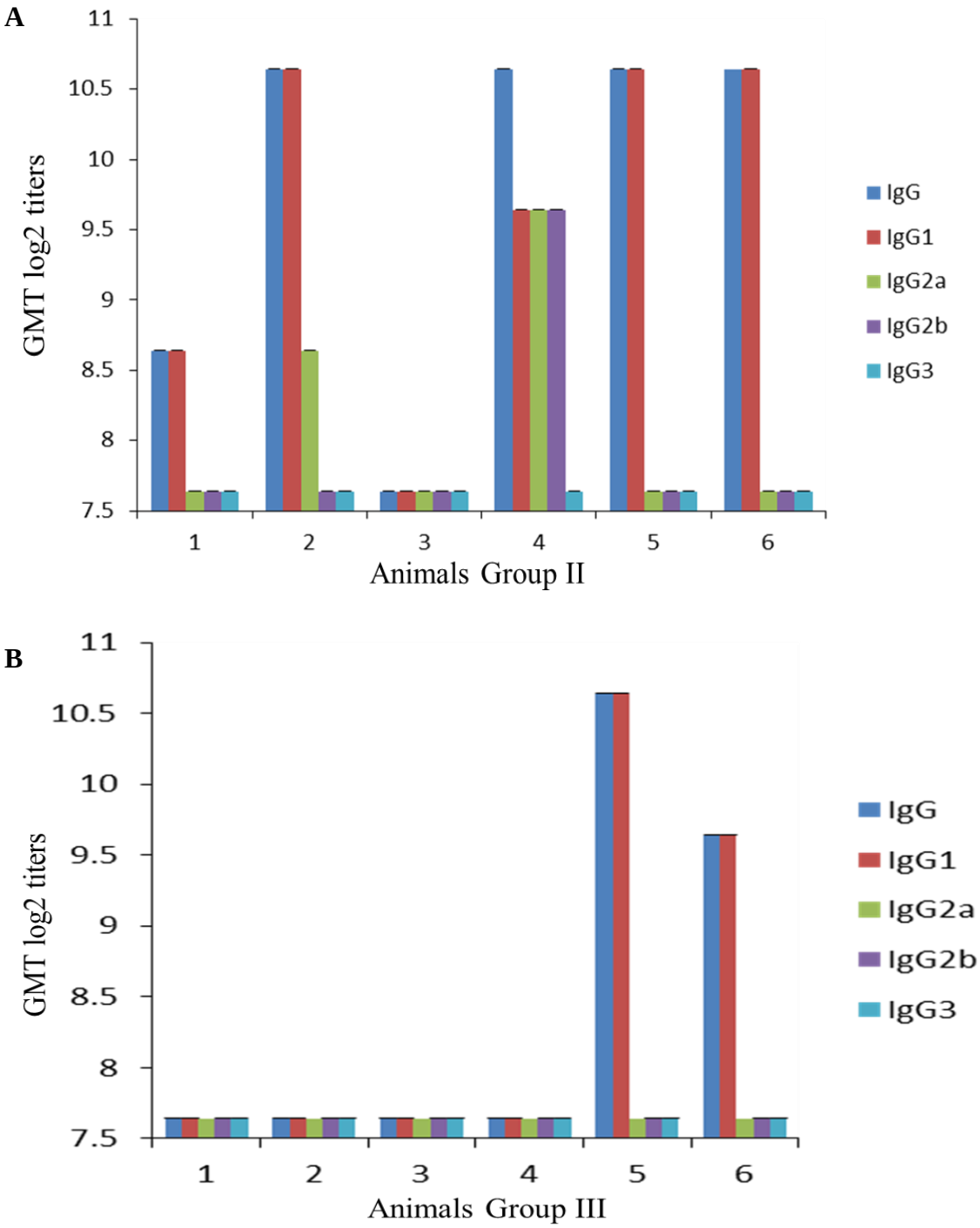

Figure 5.20 FnB domain-specific IgG subtype profile in individual animals. A: Group II, full-length phage vaccine (LongRnano3FnB); B: group III, (ShortRnano3FnB) nanophage vaccine (without temperature treatment). X-axis indicates individual mice whereas y-axis indicates GMT (log for base 2) titres of antibodies obtained by serum titration.

5.7 Comparison of Anti-Phage and Anti-FnB Domain General IgG Antibody Response of Individual Mice in Different Groups

Animals vaccinated with full-length phage particles that do not display FnB domain (LongRnano3) showed antibody response against the major phage protein pVIII, but not against the FnB domain. For this group, the FnB-specific IgG was at background levels (similar to the PBS-immunized animals) whereas phage-specific IgG was significantly high. Group I was used as reference for measuring the significance of antibody titres against phage-displayed FnB domain (Figure 5.21A).

Group II vaccinated with full-length FnB-displaying phage particles (LongRnano3FnB) exhibited significant increase in both phage-specific and FnB domain-specific IgG antibodies ($P = 0.0058$, $P = 0.01$). All mice in group II showed a uniformly increased phage-specific IgG, however IgG response to FnB domain for two out of six animals was poor (Figure 5.21B). The overall increase in FnB domain–specific antibody titre for group II was statistically significant in comparison to control group ($P = 0.01$).

Group III mice vaccinated with nanophage particles (ShortRnano3FnB) exhibited uniformly high titres for phage-specific IgG antibody; however they showed a statistically non-significant response against FnB domain when compared to control group I ($P = 0.1$). Four mice having high phage-specific antibodies were negative for IgG antibody against FnB domain, indicating that the amount of displayed FnB domain may not have been sufficient to elicit significant antibody response due to proteolysis of intrinsically unstructured FnB domain during purification protocol (Figure 5.22A). IgG antibody response against FnB domain for the nanophage (group III; ShortRnano3FnB) was significantly lower than for the full-length phage (group II; LongRnano3FnB).

Group IV mice vaccinated with Rnano3FnB exposed to 37 ºC for 48 h exhibited a comparatively low titre for IgG antibodies against phage proteins; however this response was significantly higher than that of control group V (Figure 5.22B). The antibody titre for phage-displayed FnB domain was essentially at background level for all mice in group IV when compared to group I mice.

Group V that received the PBS buffer was negative for both phage-specific and FnB-domain-specific IgG antibodies.

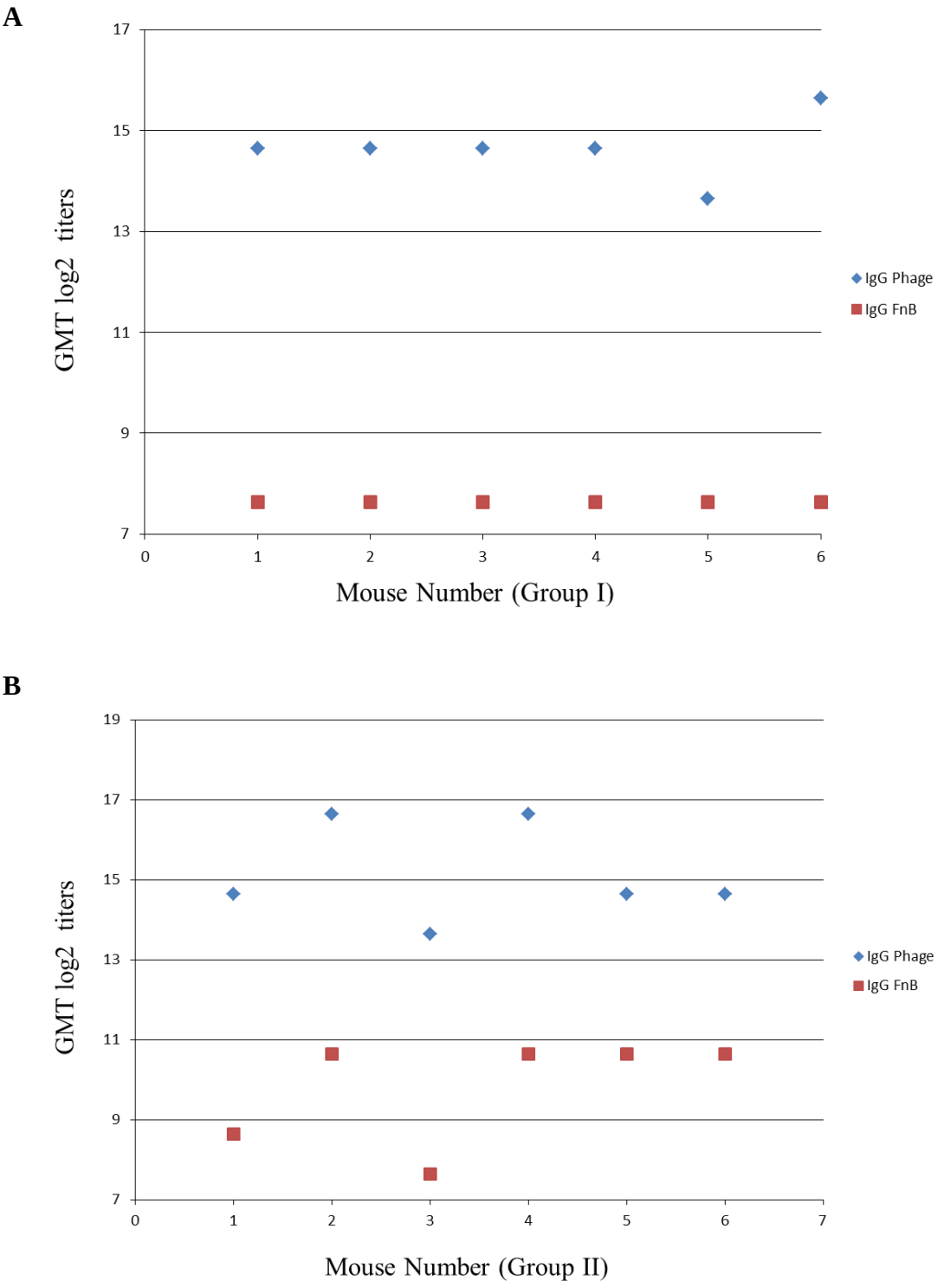

Figure 5.21 Comparison of anti-phage IgG and anti-FnB domain IgG antibodies in individual animals in full-length phage vaccine groups. A. group I, full-length phage vaccine (LongRnano3); **B**, Group II, functionalized full-length phage vaccine (LongRnano3FnB); X-axis indicates animal number (1-6) in respective groups whereas y-axis indicates GMT (log for base 2) titres obtained after serum titration.

A

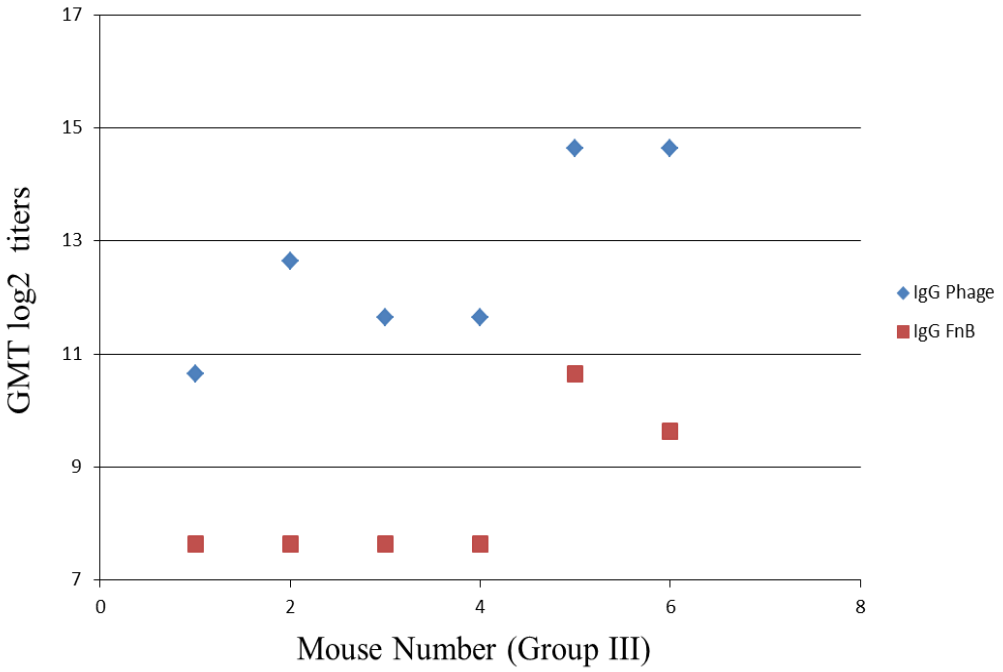

B

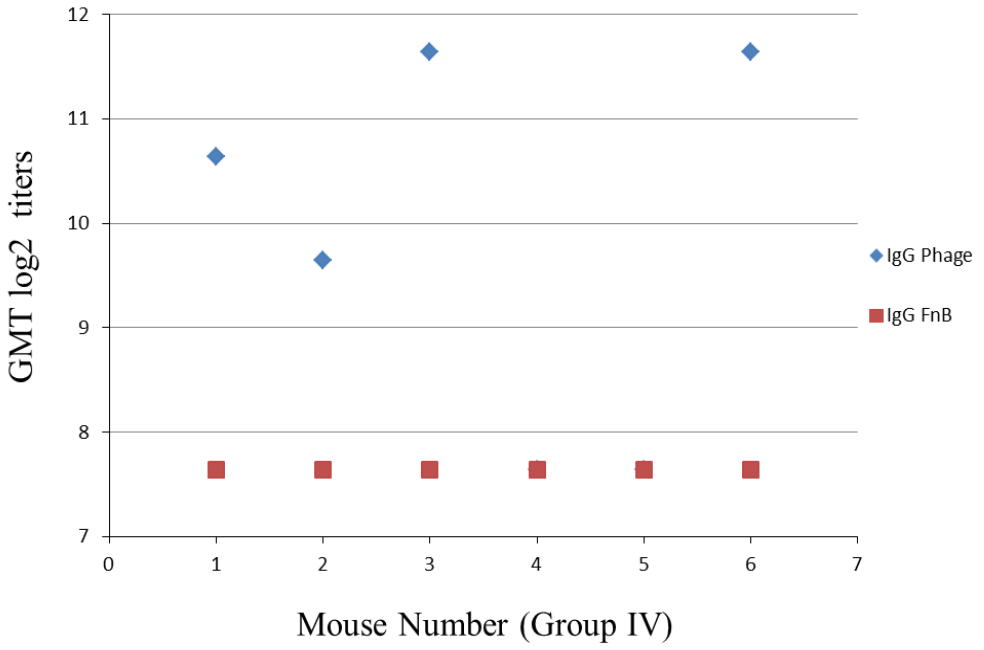

Figure 5.22 Comparison of anti-phage IgG and anti-FnB domain IgG antibodies in individual animals in nanophage vaccine groups. A. Group III, nanophage vaccine ShortRnano3FnB (without heat treatment); **B**, Group IV, nanophage vaccine kept at 37 ºC for 48 h (WarmShortRnano3FnB; X-axis indicates animal number (1-6) in respective groups whereas y-axis indicates GMT (log for base 2) titres obtained after serum titration.

5.8 Comparison of Antibody Response against Displayed FnB domain

Nanophage particles carrying FnB domain peptides as pIII fusions, when used as vaccine carriers (group III) were able to generate statistically significant antibody response against phage proteins when compared to control group. However this response was significantly lower than full-length phage vaccine group II (P = 0.037) (Figure 5.22).

The IgG antibody response against expressed peptide (FnB domain) was significant for only full-length phage vaccine group II (P = 0.01); whereas increase in IgG antibody titre for nanophage vaccine group III was statistically non-significant (P = 0.101) in comparison to control groups (Section 5.6.2). When general IgG antibody titres of functionalized full-length phage vaccine group (II) were compared to nanophage vaccine group, a marginally significant difference was observed (P = 0.6) (Figure 5.23), indicating that two groups slightly differed in antibody titres against expressed peptides. The overall antibody response against FnB domain was lower in comparison to antibody response against phage proteins, consistent with a low copy-number of FnB domain relative to the virion proteins, in particular the major coat protein pVIII which is present in ~2700 copies per virion in the full-length phage and ~125 copies per virion in the short phage.

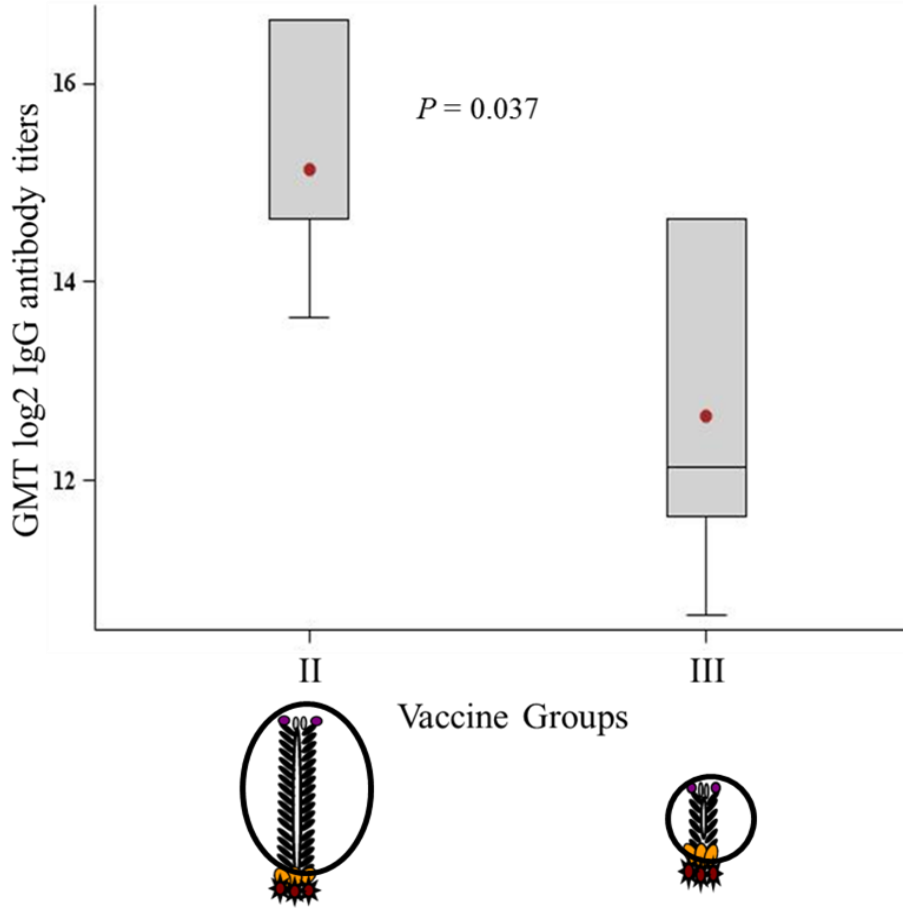

Figure 5.23 Comparison of IgG antibody responses against phage proteins in full-length and nanophage vaccine groups. Group II, full-length phage vaccine LongRnano3FnB, group III; nanophage displaying FnB without heat treatment, X-axis indicates vaccine groups, whereas Y-axis indicates GMT (log for base 2) of antibodies obtained by serum titration. The upper and lower edges of the box represent first and third quartiles, respectively. The horizontal line drawn within the box marks the median. The red dot **(●)** shows the sample mean. The whiskers (standard deviation) are drawn to the most extreme points that lie within the fences. P values at the top of bars represent differences between two groups at $p \leq 0.05$ (Wilcoxon-Mann-Whitney test).

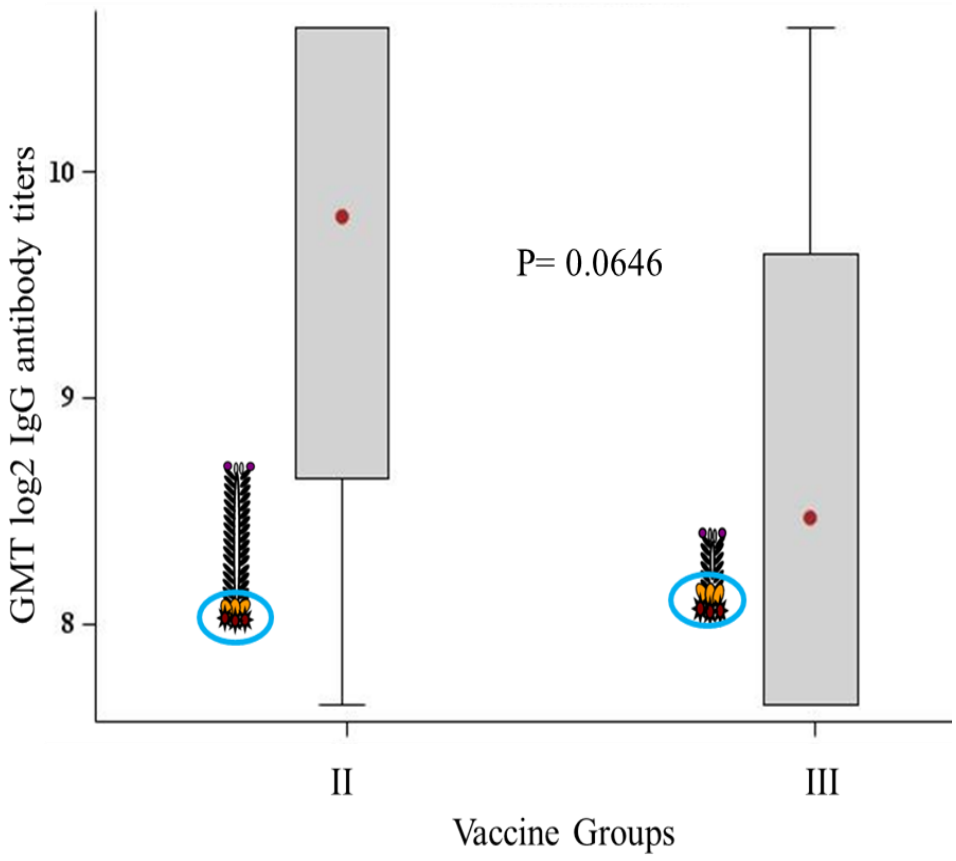

Figure 5.24 Comparison of IgG antibodies against FnB domain in full-length and nanophage vaccine groups. Group II, full-length phage vaccine LongRnano3FnB, group III; nanophage displaying FnB without heat treatment (ShortRnano3FnB), X-axis indicates vaccine groups, whereas Y-axis indicates ELISA values (OD 450 nm) at 200 fold serum dilutions. The width of each box shows the number of animals which is constant in all groups. The upper and lower edges of the box represent first and third quartiles, respectively. The horizontal line drawn within the box marks the median. The red dot **(●)** shows the sample mean. The whiskers (standard deviation) are drawn to the most extreme points that lie within the fences. P values at the top of bars represent differences between two groups at $p \leq 0.05$ (Wilcoxon-Mann-Whitney test).

To examine whether FnB domain expressed as pIII fusion on phage surface are intact in purified full-length and nanophage particles, western blot was carried out. A uniform expression of FnB domain on all five copies of pIII in each phage particle was expected. However it was observed (Figure 5.14) that a considerable fraction of pIII contained no FnB domain portion. This in turn indicated degradation of the FnB domain during production and assembly (in the periplasm of *E. coli*) and purification procedures (PEG precipitation). The low number of FnB domain per particle and small number of particles displaying FnB domain are the likely reason for poor response against it when the nanophage were used for immunization. Use of protease inhibitors and display of antigen along the virion, as fusion to the major coat protein pVIII that is present in the nanophage virion in a high number of copies (125 *vs* 5 for pIII) will be required to obtain an increased immune response to this antigen.

5.9 Challenge Studies

At day 50, ten days after the last booster dose of vaccines, all groups were challenged intranasally with *S .pyogenes* from which the FnB domain used in immunisation was derived (D737; M type 22). The animals were challenged, with 10-20 µl of bacterial suspension (1.3×10^7 CFU) per nostril. The animals were monitored for the infection symptoms for 15 days post challenge (Chapter 2 Sections 2.8.4-2.8.5). However, the strain was not pathogenic to mice. None of the animals tested showed any symptoms of infection, including the PBS-immunised control group. Furthermore, bacteria were cleared successfully, as no *S. pyogenes* were recovered from the tracheal rings and nasal swabs. Therefore, the challenge studies were inconclusive as it could not be established that immune response against FnB domain of *S. pyogenes* was protective or not.

Chapter 6

Discussion

6.1 Introduction

The research presented in this thesis was carried out with the specific aim of improving the production and purification techniques for the nanophage particles, and to carry out preliminary testing of their potential for use in diagnostics and as peptide carriers to elicit antibody response in vaccine development. The project will be discussed in two sections. First section will discuss the outcome of the optimization of the nanophage production and purification system, whereas second section will discuss the results of application of these nanophage particles to diagnostics and vaccine trial.

6.2 Improved Purification Technique for Nanophage Particles

The current nanophage production system produces two types of particles; the nanophage particles as well as full length helper phage particles (Bennett, 2010). As discussed in Chapter 1, Section 1.8 in this thesis, for potential applications of these nanophage particles in human and animal models, the nanophage preparations need to be free from live virus that is capable of replicating inside the gut *E. coli*, which is vital to get regulatory approvals. They also need to be concentrated enough for any particular *in vitro* and *in vivo* application. The purification technique described by (N. Bennett, 2010) had very poor recovery of the nanophage particles (Chapter 3 Section 3.2.3); moreover the purified nanophage preparations contained a considerable fraction of agarose in them, which was not desirable (unpublished data). In order to improve the yield as well as purity standard of nanophage particles, two purification methods were investigated; i) cesium chloride (CsCl) density gradient centrifugation and ii) preparative agarose gel electrophoresis followed by electro-elution (Chapter 3 Sections 3.2.2 & 3.2.3). The CsCl density gradient centrifugation was based on hypothesis that the nanophage will be separated from the full-length (helper) particles as a distinct band, owing to differences in their densities. Two distinct bands were indeed observed

after the CsCl density gradient, however they were very close to each other and extraction of one band without disturbing the other was not possible. The gradient was collected in fractions and ran on gel to identify the fractions containing pure nanophage particles. The purest nanophage fractions apparently free from helper phage particles in gel electrophoresis were found, through helper phage titration, to nevertheless still contain considerable residual full-length phage particles (Chapter 3 Section 3.2.2). Moreover, it was not desirable to pool the nanophage fractions obtained from cesium gradient as each fraction had variable contamination with helper phage. Overall, the final amount of the nanophage particles recovered after CsCl density gradient centrifugation was very low.

Electroelution was trialed as an alternative to achieve better recovery as well as purification away from the full-length (helper) phage. It was already established that nanophage particles separate very well from the full-length (helper) phage particles in agarose gel electrophoresis due to their large difference in size and charge (Bennett, 2010), therefore gel electrophoresis gives a better separation of nanophage particles from full length helper phage. Moreover, as a band in the preparative agarose gel, the nanophage are already concentrated in a much smaller volume as compared to extracted fractions of a CsCl gradient. Extraction of phage from agarose gels was, however, the bottleneck of this method that had a very low recovery (1%) of the nanophage particles by using filtration (Bennett, 2010). In order to increase the efficiency of extraction, the electroelution was used instead of filtration. This method resulted in high nanophage recovery ratio, nearly ~45 %. This was in agreement with the findings of (Yoon et al., 2013) that demonstrated the use of electroelution to separate Hepatitis B core antigen capsids of two different sizes (36 nm and 32 nm) with almost similar recovery percentage.

Ideally, this protocol would have removed all full-length phage, which are undesirable contamination. Electro-purification of the nanophage resulted in up to ~1000-fold enrichment of the nanophage over the full-length phage. Despite the wide separation of the full-length phage from the nanophage bands that could not have allowed mixing of these two types of particles, the very large amount of the full-length phage loaded onto the gel (~10^{12} per lane) most likely resulted in a uniform low-level contamination of the chamber and the gel with the long phage. Alternatively, the liquid crystal nature of

the filamentous phage at a high concentrations resulted in cross-contamination of the nanophage with the full-length phage. The contamination with the helper phage decreased slightly when agarose concentration was low (0.8%) and the electrophoresis was run at low voltage for a long time; however the contamination was not completely eliminated. It is demonstrated by Huang *et al* 2008 (Huang et al., 2008) that at high phage concentrations ($>10^{12}$) and salt concentration equal to the one used in the current purification protocol (140 mM NaCl) filamentous phage tend to adhere together in the form of tangled filaments or bundles. This was confirmed by TEM imaging of the purified nanophage sample EPN1 (Figure 6.1) which clearly shows the nanophage particles sticking with each other as well as with full-length helper phage, making long thread like structures. This may have been the reason of helper phage contamination of gel electroeluted nanophage preparations which can be improved by increasing the salt concentrations in the nanophage samples before preparative agarose gel electrophoresis. However, increasing salt concentration results in altering ionic balance and hence hampers phage mobility in agarose gel.

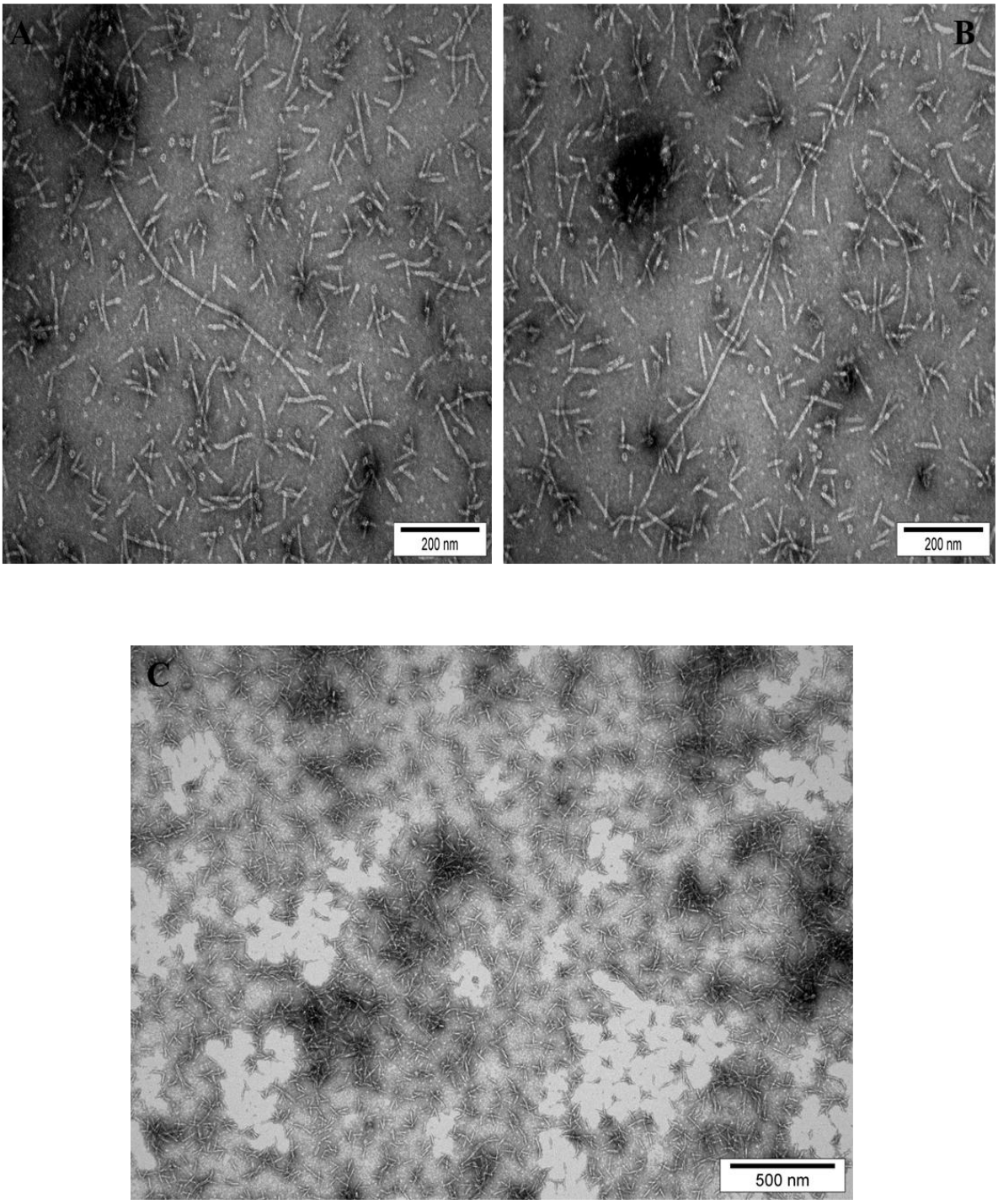

Figure 6.1 Transmission Electron Micrographs (TEM) of purified nanophage sample EPN1. The samples were negatively stained using Uranyl acetate. Bar corresponds to 200nm **(A & B)** and 500nm **(C).**

6.3 Stability of Nanophage Particles

The mechanism of filamentous phage dissociation in the presence of ionic detergent Sodium Dodecyl-Sulphate (SDS) is well studied using Electron Spin Resonance (ESR), circular dichroism (Rice et al., 2008) and NMR, particularly because it mimics the dissociation of phage particle in lipid bilayer during phage infection. The process of virion dissociation is a transition between two states: a sub-solubilization state where phage particles saturated with detergent molecules coexist with the detergent in solution and the solubilized state where coat protein is solubilized in detergent micelles (Stopar et al., 2003). At sub-solubilization states detergent molecules get inserted or wedged into the groves formed by pVIII monomers, which results in disruption of hydrophobic protein-protein interactions of neighboring pVIII molecules. Solubilization of protein in detergent is equilibrium between pVIII-pVIII interactions to pVIII-detergent interactions (Stopar et al., 1998). When critical ratio of detergent to phage is reached, even a single pVIII subunit displacement across the filament triggers a steric change. This increases the free energy of the surrounding pVIII molecules due to the exposure of their hydrophobic surfaces to the solvent resulting in cooperative dissociation of the virion (Ikehara et al., 1975; Stopar et al., 2002). Since full-length phage have 20 fold more pVIII subunits, hence presenting a greater surface area for detergent interaction than nanophage particles, the steric disbalance caused by SDS-pVIII interaction may be more pronounced in case of full-length phage particles than nanophage; which results in their rapid and complete disruption in the SDS under the conditions (70 °C) at which over half of the nanophage particles in the sample remain intact, as observed in time course experiment (Chapter 3 Section 3.3). Moreover, imperfections of pVIII packing due to mechanical bending and twisting, observed in the electron microscopic images of full-length phage, but not nanophage (Bennett, 2010) , may have conferred additional stability to nanophage in comparison to full-length phage virions. From the technological standpoint, this property may be of interest in nanotechnology or diagnostic applications that involve harsh conditions, such as introduction of chemical modifications or use at high temperature in detergent-containing environment

6.4 Helper-phage-free Production of Nanophage Particles

The nanophage preparations still contain residual helper phage particles (Chapter 3, and Section 3.3) which are not desirable in its applications outside of the laboratory containment. In order to attempt complete elimination of helper phage from the nanophage production system, a helper plasmid (pDH) was tested for production of the nanophage. The helper plasmid pDH was derived from helper phage VCSM13 by deletion of origin of replication and packaging signal. Upon transformation of cells carrying pDH with the nanophage-template plasmid pSS3, a high yield of nanophage particles was expected with no production of full-length helper phage particles in the system. However, no nanophage particles were detected by agarose gel electrophoresis when the helper plasmid system was used, contrary to the production system that used Rnano3 helper phage. Since the nanophage origin of replication is truncated relative to the wild-type f1 origin (it lacks the section II; Chapter 1 Figure 1.7), wild type pII initiates replication from this origin with a very low efficiency (1% relative to the full origin (Dotto et al., 1984). A compensatory mutation in pII sequence is required in order for replication to become efficient (Specthrie et al., 1992). This compensatory pII mutation is present in the Rnano and its derivatives (which are based on the helper phage R408). However, pII produced by pDH helper plasmid does not have this mutation and therefore it could not carry out replication from the microphage origin of replication. In order to test this hypothesis pII was overexpressed from a plasmid pNJB02 in addition to the pII production from helper plasmid pDH. Overexpression of pII indeed increased replication from the nanophage origin and resulted in production of nanophage, albeit at a low efficiency relative to the production using the helper phage.

Interestingly, a low level of phagemid particles derived from the plasmid that contains nanophage origin of replication was observed. The phagemid particles are replicated and assembled at a low efficiency due to deletion of the terminator portion of the nanophage-origin of replication (data not shown), allowing full circle of replication from the positive origin of replication. This phagemid was also identified, at a low frequency, when the Rnano and its derivatives were used for nanophage production and represents undesirable recombination product that contains antibiotic resistance

marker of the nanophage production plasmid. In conclusion, efficient replication of nanophage origin-carrying plasmid can be ensured by introducing *gII* from Rnano (R408) helper phage; this will eliminate helper phage and ensure high efficiency production and purification of the nanophage. Furthermore, to avoid recombination that converts the nanophage origin of replication into a phagemid origin, recombination pathway(s) that carry out this recombination need to be identified and a host strain with inactivated recombination genes will have to be used.

6.5 Investigation of Existing Nanophage Production System

The original nanophage production system published in 1992 indicated that only the helper phage R474 having a mutation in the promoter region of *gVIII* was able to produce a detectable quantity of nanophage. This mutation caused 10 % less pVIII production by this helper phage in comparison to wild type phage (Specthrie et al., 1992). Given that the length of the filamentous phage can be influenced by ratio of pVIII (stimulating elongation) to proteins at the virion caps which mediate initiation and termination of assembly (pVII/pIX or pIII/pVI, respectively) it was assumed that lowered pVIII production favors the packaging of the short nanophage particles over full-length helper phage by favoring termination of assembly over elongation. Because R474 also introduced a missense mutation in pVII, phagemid Rnano was designed, in which only pVIII production was lowered, by introducing an amber mutation in *gVIII* of a standard helper phage, R408. This amber mutation is suppressed with ~50% efficiency in strains containing suppressor *supE44* mutation (reading UAG stop codon as Gln) or *supD* (reading the UAG stop codon as Ser) (Bennett, 2010). It was concluded from the results that only Rnano produced detectable amount of nanophage whereas R408 failed to do so; instead it produced a strong extra band which was attributed to be the phagemid band produced due to conversion of nanophage plasmid in to a phagemid by recombination in nanophage origin of replication. However in the current study when helper phage R408-3 (R408 having multiple cloning site in *gIII*; but no *amber* mutation) was compared to Rnano3 (Rnano having multiple cloning site in *gIII*; have an amber mutation in *gVIII*) for nanophage production the results suggested otherwise. It was found that R408-3 was equally efficient in nanophage production as Rnano; therefore the hypothesis of less pVIII production favoring the

packaging of nanophage particles was not valid. The extra band observed in R408 preparations which was previously thought to be phagemid band is now identified as SDS-resistant nanophage particles band that failed to disassemble by detergent after heating at 70 ºC for 20 min (Chapter3, Section 3.4).

6.6 Applications of Nanophage

6.6.1 Applications in Diagnostic Tests ELISA and Dipstick

Filamentous phage have found extensive applications in the *in vitro* diagnostics in biomedical industry (Chapter 1, Section 1.7). A relatively new application of filamentous phage to detect the small molecules in a non-competitive anti-immunocomplex assay has been published (Gonzalez-Techera et al., 2007; González-Techera et al., 2007; Kim et al., 2009). The phage-displayed peptides were found to be superior to monoclonal antibodies derived by standard immunization protocols in detecting the changes in immune complexes upon binding of small molecules that cannot be detected by standard sandwich assays, because they cannot bind two different antibodies at the same time. Currently, availability of commercial phage display peptide libraries offers flexibility and cheap access to the technique in comparison to the production of specific monoclonal antibodies. This assay, named Phage Anti-immune complex Assay (PHAIA), was adapted to a simple dipstick format for onsite detection of the analytes. This application indicated the potential use of functionalized full-length phage particles in lateral flow devices such as dipstick for the affinity detection of specific ligands. The dip-stick assays involving the intact phage virion, however, are not used as yet outside the laboratory containment.

In this study I demonstrate the use of the nanophage particles carrying FnB domain as pIII fusion in a setup that corresponds to simple lateral flow dipstick device for the detection of dissolved fibronectin in sample solution. The assay was carried out using protocol listed in Chapter 2 Section 2.7, using a standard dipstick device that contains immobilized mouse monoclonal (mmAb) IgG1 antibody against human fibronectin sprayed at the test (T) line and anti-pVIII antibody sprayed at control (C) line. Phage particles having FnB domain as pIII fusion were expected to bind the anti-fibronectin antibody at the test line only when fibronectin is present in the test solution. However, results indicated a non-specific binding of both full-length and nanophage particles

carrying FnB domain, in the absence of added analyte (fibronectin) to test line containing fibronectin binding antibody (Chapter 4, Figure 4.5). Since control phage without FnB domain was not binding to the fibronectin antibody, this was indicative of binding due to the displayed FnB and not due to non-specific binding of the phage particles. It is known from literature that fibronectin binding protein Sfb1 from *Streptococcus pyogenes* exhibits a non-immune interaction with F(ab)'2 region of mouse IgGs, which is mediated by its fibronectin binding domain (Medina et al., 2000); since FnB domain is conserved in different fibronectin binding proteins it was concluded that FnB domain from serum opacity factor of *S. pyogenes* displayed on the surface of full-length and nanophage particles in this study was exhibiting a similar antigen-independent interaction. In order to verify this possibility binding of functionalized phage particles with three unrelated mouse monoclonal IgG antibodies was tested in dipsticks. Phage particles were not found to cross-react with any of them (data not shown). This eliminated the possibility of non-specific binding of FnB to the constant portion of antibodies; instead, it pointed to detection of the small amount of serum fibronectin that was co-purified with fibronectin-specific antibodies. This suggests an extremely high sensitivity of detection of analyte using the nanophage particles.

In order to overcome this problem, collagen was used as capture reagent on the test line to capture phage FnB-fibronectin complex. Collagen is known to bind fibronectin with high affinity and is used in sepharose columns to remove fibronectin from the serum samples (Balian et al., 1979; Engvall et al., 1978; Hayman and Ruoslahti, 1979; Ruoslahti et al., 1978). Collagen exhibited specific binding of phage to test line in presence of fibronectin only. Both full-length and nanophage particles exhibited specific binding to fibronectin via FnB domain that was displayed as pIII fusion. Control phage (Rnano3) did not bind to the collagen test line in presence or absence of fibronectin as expected. This indicated the potential for the use of functionalized nanophage particles as probes to detect soluble analyte in any sample solution.

Quantity of the analyte can be a critical parameter in dipstick assays; nanophage particles were also tested for the quantitative detection of fibronectin in sample solution in competitive as well as non-competitive assays. Difference in signal at the test line was found to be consistent with the difference in concentration of analyte in

the test solutions as indicated by the band density analysis. Both competitive and non-competitive assay showed quantitative correlation in the physiological range of fibronectin in human plasma that allows quantitation of fibronectin in unknown samples within the range of 7.81 ng – 500 ng. (Figure 4.8 and 4.9)

In conclusion, nanophage particles can be easily applied as detector probes in lateral flow dipstick devices for the detection of soluble ligands, offering full advantages associated with filamentous phage structure especially phage display. However both full-length and nanophage particles were not labeled to produce a visible signal, therefore western blotting was carried out to visualize the bound phage. It would be desirable to get a visible signal for onsite detection of the analytes that can be achieved by labeling the phage particles with visible dyes. Attempts were made to do labeling with (Uniblue A) but were unsuccessful due to high hydrophobicity of the dye (data not shown). In order to reduce the processing time of the dipsticks to visualize the bound phage at test line phage were labelled with FITC and detected by phosphorimager. It is already established from literature that phage clones labelled with FITC at major coat protein pVIII, retain the sensitivity and binding ability of the peptides expressed on pIII to the target ligand (Jaye et al., 2004). It was indeed observed as both nanophage and full-length phage demonstrated specific binding to the test line in presence of fibronectin in the test solution. Moreover, nanophage have an additional advantage of being non-infectious particles in comparison to full-length phage therefore they are much more likely to be approved by the regulatory authorities and consumers.

6.6.2 Application as Antigen Carriers

Owing to the phage display technology, filamentous phage can be engineered to display specific antigens on their surface to produce focused antibody response against the displayed peptide (Kneissel et al., 1999; van Houten et al., 2006). They are recognized as efficient vaccine carriers, particularly because of their low surface complexity, and highly ordered arrangement of the major coat protein pVIII, which provides opportunity for multiple display sites along the filament, providing high stimulation and crosslinking of the B-cell receptors in induction of immune response (Kneissel et al., 1999; van Houten et al., 2006). Moreover the antibody response against phage and the displayed peptide can be differentiated by a combination of

different immunogenetic assays; making it a model carrier to elicit and study immune system and antibody production against desired vaccine targets. Several studies have reported that immunization with whole phage particle carrying antigenic peptides was able to induce specific antibody response in animal models (Bastien et al., 1997; Di Marzo Veronese et al., 1994; Irving et al., 2001; Wang and Yu, 2004). Despite their effectiveness, the application of whole phage vaccine is restricted to the trial phases due to the fact that recombinant phage particles can pose an ecological threat owing to their ability of replication in gut *E. coli*, as well as horizontal gene transfer to other microbes and to the host.

The use of inactivated phage vaccines can be safer, however these inactivated phage particles are not as potent as the live antigen vaccines due to potential proteolysis or denaturation of antigen. Although it is relatively easy to construct non-infectious filamentous phage (Rakonjac and Model, 1998), this only eliminates infection of *E. coli*, whereas internalization into the mammalian cells, is not affected by this change. Due to these disadvantages the phage vaccine technology has not been employed to animals and humans post clinical trials. Since nanophage particles retain the complete display pattern of the full-length phage particles yet they are non-infectious and unable to replicate without a helper phage and have no coding potential in its 200 nt ssDNA circle(Bennett, 2010), they can be an ideal replacement to the whole phage vaccines.

A vaccine trial was conducted in this thesis with the aim of estimating nanophage ability to elicit antibody response against phage proteins as well as to test their ability to act as carriers for a bacterially-derived antigen, FnB domain, a 145-residue polypeptide recognized as a valid vaccine target from *S. pyogenes* (Guzman et al., 1999; Kawabata et al., 2001; Schulze et al., 2003). The antigen was displayed in a 5-copy setup at one of the ends of the nanophage particles (the length of the antigen prevented its display along the virion as a fusion to all copies of the major coat protein). The immune response to the phage (i.e. major coat protein) was used as an indicator of the nanophage potential as a carrier for peptide antigens as fusions to pVIII.

Antibody Response Against Phage Proteins

Five groups (I-V) of six BALB/c mice each were immunized with different vaccines. Group III mice were vaccinated with nanophage particles displaying FnB domain as a pIII fusion (Rnano3FnB nanophage). Since nanophage particles have proved to be more resistant to temperature and detergent treatments than full-length phage (this study Chapter 3, Section 3.3) they were predicted to be more stable vaccine carriers even after exposure to high temperatures, for example in comparison to liposomes or live vaccines which are clearly temperature-sensitive. The lack of refrigeration is a bottleneck for application of many vaccines in the remote areas and war zone. Because phage are very stable under non-refrigerated conditions, in this study the effect of prolonged exposure to tropical temperature (akin to "broken cold chain") on immunogenicity of the nanophage vaccine was tested. Even though it was not expected that the carrier (the phage) will be affected in any way, the testing was undertaken because the displayed antigen can still be affected by prolonged incubation at an increased temperature. In order to evaluate the effect of temperature on nanophage vaccine's immune potential group IV mice were immunized with the same vaccine as group III (nanophage displaying FnB domain), however instead of being constantly refrigerated, they were pre-incubated at 37 ºC for 48h. Positive control group was immunized with full-length phage particles displaying FnB domain, derived from the same production experiment as the nanophage particles and therefore expected to be identical in every other aspect except for the virion length. The negative control group (V) was vaccinated with PBS served as control in this set of experiment; whereas the control group (I) was vaccinated with full-length phage particles that do not display FnB domain.

All vaccines were administered without any adjuvant as it is established from the literature that phage have natural immune stimulation tendency and can generate strong antibody titres without any additional adjuvant (Greenwood et al., 1991; Willis et al., 1993). Adjuvant can produce undesired side-effects; hence it was a preferred option. Vaccines were administered through intraperitoneal route owing to the fact that intraperitoneal administration has been reported to induce good phage antibody response in mice (Yip et al., 2001). The immunization load between the full-length and the nanophage was adjusted to contain a similar number of FnB domains (antigens) per

dose (Chapter 5); The number of particles per inoculum was gauged in the middle of the range typically used in published full-length filamentous phage vaccine trials, whereas the number of nanophage was 10-fold higher, to account for difference in particle length (Delmastro et al., 1997).

Results indicated that both nanophage vaccine groups III and IV were able to generate a significant IgG serum antibody response against phage proteins, however this titre was significantly lower than full-length phage vaccine groups I and II. IgM response was significant for group I, II and III, whereas serum IgA response was at background levels for all groups. Serum IgG and IgM response of group II was higher than group I, however this difference was statistically non- significant. Since both groups were given equal number of phage particles this slight difference may have been due to the expressed peptide on group II Rnano3FnB phage. This is possible if expressed peptide has good opsonic activity as is the case of FnB domain; however the carrier effect cannot be accounted for with certainty as differences in antibody titres were not statistically significant. The immunogenic activity of filamentous phage is mostly due to the surface-exposed 12 residues at the N-terminus of pVIII (Kneissel et al., 1999). Given that the nanophage particles have ~20-fold lower number of pVIII molecules per virion in comparison to full-length phage, they were expected to produce a lower response against phage proteins due to less extensive crosslinking of antigen receptors on the surface of B cells. It was indeed observed as nanophage vaccine group immune response was significantly lower than full length page vaccine groups. This can be of particular advantage in the use of nanophage as vaccine carriers as it will generate less background against phage proteins.

Subtyping of the IgG response showed that IgG3 against phage was at background levels in all vaccine groups. The subtyping was also used as an indicator of the Th1-to-Th2 response skew. This analysis showed that groups III and IV had slightly higher IgG1 than IgG2a or IgG2b subtypes, indicating that immune response was skewed towards Th2. The IgG subtype profile in groups immunized with full-length phage vaccine groups was different, with the IgG2a response being higher than IgG1 and IgG2b, indicating a much stronger bias towards Th1 response in comparison to the nanophage vaccine. This is in agreement with the several reports that phage immune response is Th1 skewed (Henry et al., 2011; Prisco and De Berardinis, 2012; Tranum

Kaur, 2012). The IgG subtype switching indicates type of T helper-cell (1 or 2) response generated by the phage proteins which in turn indicates the type of effector molecules (cytokines) that play role in pathogen clearance and building of immune response. The initial line of defense induced by Th1 cells is pro-inflammatory that stimulates killing of invading pathogens as well as producing autoimmune responses (Berger, 2000; Deenick et al., 2005; Siegrist, 2008). However, excessive Th1 response caused by high levels of antigen dose can lead to uncontrolled tissue damage. In order to prevent damage this initial Th1 response should be balanced by Th2 response which is mainly anti-inflammatory. Therefore an ideal vaccine should produce a balanced Th1 and Th2 response. In the light of these findings the results shown here indicate that nanophage particles will be suitable as carriers since their immune response is more skewed towards Th2 in comparison to full length phage.

The type of T helper-cell response to vaccine preparations is dictated by the type of dendritic cells activated by innate immune response, which in turn is determined by the type of adjuvant as well as dose of the antigen (Siegrist, 2008). Since no adjuvant was used in this study (aside from potential trace amount of LPS derived from *E. coli*), dose remains the second important parameter. As indicated earlier, excessive Th1 response is triggered by a high dose of antigen. Although nanophage vaccine groups were given 10 fold excess of particles in comparison to full-length phage, still the animals immunized with the full-length phage particles received 2 fold excess of immunogenic determinants on pVIII than those immunized with the nanophage due to the 20:1 length ratio between the full-length phage particles and the nanophage (20:10=2). The full-length phage vaccine doses therefore contained about twice as much pVIII immunogenic epitopes on their surface relative to the nanophage vaccine doses, consistent with a the observed skew towards the Th1 responses. Furthermore, the 20-fold lower absolute number of epitopes per particle will result in much lower extent of the B-cell receptor crosslinking, which can in turn affected the overall antibody titre. This study presents the use of non-infectious nanophage particles as antigen carriers for the first time. It also indicates that nanophage particles hold immunogenic properties of phage coat proteins just like the full-length phage particles, including an ability to act as display scaffold, provide natural adjuvant activity as well as an ability to stimulate immune response.

The major coat protein immunogenicity is considered as a potential hurdle to a focused response to displayed antigens (van Houten et al., 2006), in particular one of the immune-dominant residues, Glu at position 2 (Glu2) of the mature pVIII (after the signal sequence cleavage). This was one of the pVIII residues that were mutated in a study that examined the role of the immune-dominant residues of pVIII in focusing the immune response to displayed antigen. In that study, Glu2 was replaced by Ala. Interestingly, the Rnano3 helper phage has the *amber* stop codon instead of the codon for Glu in position 2. In the *sup*D suppressor strain that is used for the nanophage production, serine is incorporated into pVIII at the position 2. Produced phage are recognized by commercial murine fd/f1-specific antibodies; hence this residue is not part of the epitope for those pVIII-specific antibodies. Whether Ser is less immunogenic than Glu remains to be examined, but this change may have influenced the phage-specific immune response in the vaccination trial.

Antibody Response Against Displayed Antigen FnB Domain of S. pyogenes

Both nanophage vaccine groups (III and IV) were tested for immune stimulation against the displayed peptide, FnB domain from serum opacity factor, a surface protein of *S. pyogenes*. Group II was vaccinated with the full-length phage displaying FnB domain. All three groups, II, III and IV, displayed FnB domain as fusion to pIII, theoretically in 5 copies per virion. Group I vaccinated with full-length phage carrying no antigen was used as negative control, to compare the specific immune response against FnB domain. The FnB domains from various fibronectin binding proteins of *S. pyogenes* are known to produce good immune response in a mouse model when administered through subcutaneous and intraperitoneal routes with standard adjuvants and carriers (Guzman et al., 1999; Kawabata et al., 2001; Ma et al., 2009; Schulze et al., 2003).

Only full-length phage vaccine group II was able to induce significant IgG titre against FnB domain. Group III vaccinated with nanophage particles displaying FnB domain produced some response against the expressed peptide, however it was statistically non-significant when compared to control (group I) as well as full-length phage displaying FnB domain (group II). Group IV vaccinated with FnB-displaying

nanophage incubated at 37 °C for 48 h did not show any increase in FnB domain specific antibodies over the negative controls (groups I and V). Serum IgM and IgA titres against expressed peptide were at background levels for all vaccination groups. This indicated that immune response was boosted to phage rather than the expressed peptide. It is known that large protein carriers with good immunogenic potential can suppresses the immune response against expressed peptides, particularly after repeated boosters a phenomenon called 'carrier effect' (Alexander et al., 2000; Schutze et al., 1989; Yip et al., 2001). Therefore nanophage particles were expected to produce greater response for expressed peptide because they have 20 fold less pVIII epitopes that will produce less phage antibodies, resulting in less suppression of the immune response to the expressed peptide rather than full-length phage particles as carrier. However, results were contrasting as full-length FnB-displaying particles (group II) produced a significant titre against expressed peptide, whereas the nanophage particles displaying FnB domain did not. This result indicates that carrier effect was not responsible for the observed profile of immune response in all vaccination groups.

The more likely reason for different response in this particular experiment is the uneven distribution of FnB domain in three vaccine groups due to proteolytic degradation. Western blotting showed that the majority of the FnB-pIII fusion in the nanophage samples was truncated, lacking the displayed FnB domain; whereas in the long phage about half of pIII lacked the displayed FnB domain (Chapter 5, Figure 5.14). The FnB domain is an intrinsically unfolded protein (IUP) prior to binding to fibronectin, and as such is highly susceptible to proteolysis (Bingham et al., 2008) . The cause of much more extensive degradation in the nanophage in comparison to full-length phage is consistent with a longer purification procedure in case of nanophage vaccine groups as they stay in culture supernatant one day more than full-length phage particles during their production (Chapter 2, Section 2.4.1). Although adding protease inhibitors to vaccine preparation is not possible due to the toxicity, adding these during preparation procedure is expected to improve the stability of displayed antigen(s).

Group IV nanophage that mimicked the cold chain disruption induced an IgG response that was even lower than that of group III. Given that group IV phage were incubated at 37 ºC for 48 h, trace proteases that are likely present in the preparation would have given a chance to further proteolyse FnB domain.

IgG subtype profile against FnB domains of both nanophage groups (II and III) showed overwhelmingly predominant IgG1 subclass, indicating a predominant Th2 response. Uneven IgG response to FnB in individual experimental animals is consistent with marginal immune response, possibly due to the low amount of applied antigen. The animals that did responded only showed significant IgG1 response out of all IgG subtypes. As this is the first class to which the response switches upon B-cell activation, it is very likely that this is an overall reflection of poor immune response rather than the Th1-Th2 skew. Moreover vaccination route may also play an important role in the immune response against any peptide (Siegrist, 2008).

Given that the FnB domain in this experiment was derived from the serum opacity factor (Rakonjac et al., 1995) which is also called streptococcal fibronectin binding protein II (SfbII; (Ramanujam et al.) and previous reports on FnB domain immunizations were carried out using the corresponding domains from another protein, streptococcal fibronectin binding protein I (SfbI), it was possible that the SOF (SfbII) FnB domain was intrinsically non-immunogenic, despite high conservation with the SfbI FnB domain. However, it was previously shown that the SOF is immunogenic, when applied through intraperitoneal route, the same route as used in the current study, ruling out this possibility (Courtney et al., 1999). A possibility cannot be excluded that the serum opacity factor FnB domain alone (without the rest of the protein) could be an unsuitable antigen for generation of strong antibody response. The fact that FnB domain was immunogenic when displayed on the surface of full-length phage particles argues against this possibility and in favor of low amount of antigen displayed on the nanophage preparation as a reason for weak immune response.

In conclusion, nanophage particles were effective in immune response stimulation against phage coat protein, however due to extensive peptide degradation their ability to generate antibody response to the displayed FnB domain could not be determined. Full length phage particles were able to produce significant immune response against phage coat proteins as well as FnB domain displayed as pIII fusion.

In order to fully assess the potential of the nanophage particles as vaccine carriers, antigen should be displayed along the length of the phage, at a high copy-number, either as a pVIII gene fusion or by chemical or enzymatic crosslinking. Use of protease inhibitors, protease deficient host cells or shortening the protocol by using helper

plasmid instead of helper phage, would also improve the yield and decrease proteolysis of displayed antigens.

6.7 Risk Assessment for Commercial Use of Nanophage

Since nanophage cannot be replicated in cells without the presence of a helper phage and they carry a small fragment of the DNA their use instead of full-length wild type filamentous phage in diagnostic and vaccine applications will remove the concern of increasing the virus load in the model organisms as well as antibiotic resistance gene transfer to the gut *E. coli*. However, whether nanophage can be regarded as completely safe for the human and animal application outside of the laboratory containment still needs to be established. They carry only 200 nt genome with no know bacterial antibiotic resistance gene marker but the fact that DNA fragments can be randomly taken up by *E. coli* cells and can get integrated in the genome still poses a low level of risk in its use. Since the gut *E. coli* populations may already carry full-length filamentous phage; infection of one such cell with the nanophage may result in their replication, however this will be an extremely rare event. Filamentous phage are known to rapidly disseminate in eukaryotes and can penetrate vasculature and tissues, however owing to the repetitive sequence of their coat protein they are usually eliminated from the eukaryotic body quickly due to a specific immune response; the same would be expected for the nanophage.

Functionalized nanophage will have less risk in comparison to genetically manipulated full-length filamentous phage as their phenotype will not be linked to their genotype and the risk of integrating the DNA in to the host cells will be eliminated. Nonetheless, functionalized nanophage may interact with other microbes in an unpredictable way that may incur a risk to the human/animal host or environment.

6.8 Conclusions

This thesis describes, for the first time, a proof-of-concept for a system for production and purification of functionalized nanophage – 50 nm protein-DNA complexes derived from filamentous bacteriophage.

The nanophage are more resistant to disruption by ionic detergent SDS at 70 °C than the full-length phage, making them suitable for nanotechnology applications that involve harsh conditions.

Preliminary investigation of nanophage performance in lateral flow assays and vaccines show that, with defined technical improvements, the nanophage technology could be suitable for extensive filamentous phage applications outside of laboratory containment.

6.9 Future Directions

This thesis identified the areas of future improvements of nanophage production system in order to make it suitable for large-scale applications and decrease the perceived risks inherent to the full-length phage, as listed below.

1. Replacing helper phage with a helper plasmid. This will include replacing pII replication protein in the current helper plasmid pDH, to allow replication from the nanophage origin.

2. Eliminating recombination within the nanophage origin of replication to eliminate the background of phagemid-like particles. This will be achieved by using recombination-deficient host strains.

3. Decreasing proteolysis of displayed antigens. This will be achieved by using *E. coli* strains with decreased proteolytic potential, using protease inhibitors in initial steps of purification and shortening the procedure (through use of helper plasmid or by using an entirely different rapid purification protocol).

4. Use in diagnostics will require a simple method for nanophage detection, using an easily quantifiable by spectrophotometric, electrochemical or other physicochemical method.

5. Use in vaccines, besides overcoming proteolysis (as stated in point 3.), will require display of antigen at high copy number along the length of the nanophage particles. In order to achieve this, another functionalizable surface will be added by modifying the system to allow display of proteins as fusions to major coat protein pVIII.

6. Multi-functionalization of the nanophage. It has been shown that in the full-length phage, pVII, pIX and pVI (besides pIII and pVIII), are suitable as display platforms, resulting in multi-functional particles. Therefore in the future, engineering of multiple display points into the nanophage production system would further increase the potential range of applications for the nanophage.

References

Alberts, B., Frey, L., and Delius, H. (1972). Isolation and characterization of *gene 5* protein of filamentous bacterial viruses. Journal Of Molecular Biology *68*, 139-152.

Alexander, J., del Guercio, M.F., Maewal, A., Qiao, L., Fikes, J., Chesnut, R.W., Paulson, J., Bundle, D.R., DeFrees, S., and Sette, A. (2000). Linear PADRE T helper epitope and carbohydrate B cell epitope conjugates induce specific high titer IgG antibody responses. J Immunol *164*, 1625-1633.

Arap, W., Pasqualini, R., and Ruoslahti, E. (1998). Cancer treatment by targeted drug delivery to tumor vasculature in a mouse model. Science *279*, 377-380.

Armstrong, J., Hewitt, J.A., and Perham, R.N. (1983). Chemical modification of the coat protein in bacteriophage fd and orientation of the virion during assembly and disassembly. EMBO Journal *2*, 1641-1646.

Armstrong, J., Perham, R.N., and Walker, J.E. (1981). Domain structure of bacteriophage fd adsorption protein. FEBS Lett *135*, 167-172.

Asano, S., Higashitani, A., and Horiuchi, K. (1999). Filamentous phage replication initiator protein gpII forms a covalent complex with the 5' end of the nick it introduced. Nucleic Acids Res *27*, 1882-1889.

Balian, G., Click, E.M., Crouch, E., Davidson, J.M., and Bornstein, P. (1979). Isolation of a collagen-binding fragment from fibronectin and cold-insoluble globulin. J Biol Chem *254*, 1429-1432.

Barbas III, C.F., Burton, D.R., Scott, J.K., and Silverman, G.J. (2001). Phage display: a laboratory manual (Cold Spring Harbor, New York, Cold Spring Harbor Laboratory Press).

Bass, S., Greene, R., and Wells, J.A. (1990). Hormone age: an enrichment method for variant proteins with altered binding properties. Proteins: structure, function and genetics *8*, 309-314.

Bastien, N., Trudel, M., and Simard, C. (1997). Protective immune responses induced by the immunization of mice with a recombinant bacteriophage displaying an epitope of the human respiratory syncytial virus. Virology *234*, 118-122.

Bauer, M., and Smith, G.P. (1988). Filamentous phage morphogenetic signal sequence and orientation of DNA in the virion and gene-V protein complex. Virology *167*, 166-175.

Bayan, N., Guilvout, I., and Pugsley, A.P. (2006). Secretins take shape. Mol Microbiol *60*, 1-4.

Beck, E., Sommer, R., Auerswald, E., Kurz, C., Zink, B., Osterburg, G., Schaller, H., Sugimoto, K., Sugisaki, H., and Okamoto, T. (1978). Nucleotide sequence of bacteriophage fd DNA. Nucleic Acids Research *5*, 4495-4504.

Beck, E., and Zink, B. (1981). Nucleotide sequence and genome organisation of filamentous bacteriophages f1 and fd. Gene *16*, 35-58.

Beekwilder, J., Rakonjac, J., Jongsma, M., and Bosch, D. (1999). A phagemid vector using the *E. coli* phage shock promoter facilitates phage display of toxic proteins. Gene *228*, 23-31.

Bennett, N. (2010). Unlocking the M13 (f1 and Fd) Virion: Investigation Into the Role of the PIII C-domain of F Specific Filamentous Bacteriophage in Infection : a Thesis Presented in Partial Fulfilment of the Requirements for the Degree of Doctor of Philosophy in Biochemistry at Massey University, Palmerston North, New Zealand.

Bennett, N.J. (2005). Unlocking the f1 (M13) virion: investigation into the role of pIII C domain of F specific filamentous bacteriophage in infection. In Institute of Molecular BioSciences (Palmerston North, New Zealand, Massey University).

Bennett, N.J., Gagic, D., Sutherland-Smith, A.J., and Rakonjac, J. (2011). Characterization of a Dual-Function Domain That Mediates Membrane Insertion and Excision of Ff Filamentous Bacteriophage. Journal of Molecular Biology *411*, 972-985.

Bennett, N.J., and Rakonjac, J. (2006). Unlocking of the filamentous bacteriophage virion during infection is mediated by the C domain of pIII. J Mol Biol *356*, 266-273.

Berardinis, P., Sartorius, R., Caivano, A., Mascolo, D., Domingo, G.J., GDel, P., Gaubin, M., Perham, R.N., Piatier-Tonneau, D., and Guardiola, J. (2003). Use of fusion proteins and procaryotic display systems for delivery of HIV-1 antigens: development of novel vaccines for HIV-1 infection. Current HIV Research *1*, 441-446.

Berger, A. (2000). Science commentary: Th1 and Th2 responses: what are they? BMJ: British Medical Journal *321*, 424.

Bhaviripudi, S., Qi, J., Hu, E.L., and Belcher, A.M. (2007). Synthesis, characterization, and optical properties of ordered arrays of III-nitride nanocrystals. Nano letters *7*, 3512-3517.

Bille, E., Zahar, J.R., Perrin, A., Morelle, S., Kriz, P., Jolley, K.A., Maiden, M.C., Dervin, C., Nassif, X., and Tinsley, C.R. (2005). A chromosomally integrated bacteriophage in invasive meningococci. The Journal of experimental medicine *201*, 1905-1913.

Bimboim, H., and Doly, J. (1979). A rapid alkaline extraction procedure for screening recombinant plasmid DNA. Nucleic Acids Research *7*, 1513-1523.

Bingham, R.J., Rudiño-Piñera, E., Meenan, N.A., Schwarz-Linek, U., Turkenburg, J.P., Höök, M., Garman, E.F., and Potts, J.R. (2008). Crystal structures of fibronectin-binding sites from Staphylococcus aureus FnBPA in complex with fibronectin domains. Proceedings of the National Academy of Sciences *105*, 12254-12258.

Blake, M.S., Johnsten, K.H., Russel-Jones, G.J., and Gotschlich, E.C. (1984). A rapid, sensitive method for detection of alkaline phosphatase-conjugated anti-antibody on Western Blots. Anal Biochem *136*, 175-179.

Blumer, K.J., Ivey, M.R., and Steege, D.A. (1987). Translational control of phage f1 gene expression by differential activities of the gene V, VII, IX and VIII initiation sites. J Mol Biol *197*, 439-451.

Blumer, K.J., and Steege, D.A. (1989). Recognition and cleavage signals for mRNA processing lie within local domains of the phage f1 RNA precursors. J Biol Chem *264*, 20770-20777.

Boeke, J.D., and Model, P. (1982). A procaryotic membrane anchor sequence: Carboxyl terminus if bacteriophage f1 gene III protein retains it in the membrane. Proc Natl Acad Sci USA *79*, 5200-5204.

Boeke, J.D., Model, P., and Zinder, N.D. (1982). Effects of bacteriophage f1 *gene III* protein on the host cell membrane. MolGenGenet *186*, 185-192.

Brigati, J.R., Samoylova, T.I., Jayanna, P.K., and Petrenko, V.A. (2008). Phage display for generating peptide reagents. Current Protocols in Protein Science, 18.19. 11-18.19. 27.

Brown, L.R., and Dowell, C. (1968). Replication of coliphage M-13 I. Effects on host cells after synchronized infection. Journal of Virology *2*, 1290-1295.

Brutlag, D., Schekman, R., and Kornberg, A. (1971). A possible role for RNA polymerase in the initiation of M13 DNA synthesis. Proceedings of the National Academy of Sciences *68*, 2826-2829.

Calendar, R., and Abedon, S.T. (2005). The bacteriophages (Oxford University Press).

Caro, L.G., and Schnös, M. (1966). The attachment of the male-specific bacteriophage f1 to sensitive strains of *E. coli*. Proc Natl Acad Sci USA *56*, 126-132.

Carter, P., Bedouelle, H., and Winter, G. (1985). Improved oligonudeotide site-directed rautagenesis using M13 vectors. Nucleic Acids Research *13*, 4431-4443.

Cascales, E., Buchanan, S.K., Duché, D., Kleanthous, C., Lloubes, R., Postle, K., Riley, M., Slatin, S., and Cavard, D. (2007). Colicin biology. Microbiology and Molecular Biology Reviews *71*, 158-229.

Caspar, D.L.D., and Makowski, L. (1981). The symmetries of filamentous phage particles. Journal of Molecular Biology *145*, 611-617.

Cavalieri, S.J., Neet, K.E., and Goldthwait, D.A. (1976). Gene 5 protein of bacteriophage fd: a dimer which interacts co-operatively with DNA. Journal of Molecular Biology *102*, 697-711.

Chang, C.N., Model, P., and Blobel, G. (1979). Membrane biogenesis: cotranslational integration of the bacteriophage f1 coat protein into an Escherichia coli membrane fraction. Proceedings of the National Academy of Sciences *76*, 1251-1255.

Chopin, M.-C., Rouault, A., Ehrlich, S.D., and Gautier, M. (2002). Filamentous phage active on the gram-positive bacterium Propionibacterium freudenreichii. Journal of bacteriology *184*, 2030-2033.

Clarke, M., Maddera, L., Harris, R.L., and Silverman, P.M. (2008). F-pili dynamics by live-cell imaging. Proceedings of the National Academy of Sciences *105*, 17978-17981.

Cleary, J.M., and Ray, D.S. (1981). Deletion analysis of the cloned replication origin region from bacteriophage M13. J Virol *40*, 197-203.

Click, E.M., and Webster, R.E. (1997). Filamentous phage infection: Required interactions with the TolA protein. J Bacteriol *179*, 6464-6471.

Click, E.M., and Webster, R.E. (1998). The TolQRA proteins are required for membrane insertion of the major capsid protein of the filamentous phage f1 during infection. Journal of bacteriology *180*, 1723-1728.

Courtney, H.S., Hasty, D.L., Li, Y., Chiang, H.C., Thacker, J.L., and Dale, J.B. (1999). Serum opacity factor is a major fibronectin-binding protein and a virulence determinant of M type 2 Streptococcus pyogenes. Molecular Microbiology *32*, 89-98.

Crissman, J.W., and Smith, G.P. (1984). Gene-III protein of filamentous phages: evidence for a carboxyl-terminal domain with a role in morphogenesis. Virology *132*, 445-455.

Cwirla, S.E., Peters, E.A., Barrett, R.W., and Dower, W.J. (1990). Peptides on phage: a vast library of peptides for identifying ligands. Proc Natl Acad Sci U S A *87*, 6378-6382.

Dabrowska, K., Switała-Jelen, K., Opolski, A., Weber-Dabrowska, B., and Gorski, A. (2005). Bacteriophage penetration in vertebrates. Journal of applied microbiology *98*, 7-13.

Davis, B.M., Lawson, E.H., Sandkvist, M., Ali, A., Sozhamannan, S., and Waldor, M.K. (2000). Convergence of the secretory pathways for cholera toxin and the filamentous phage, CTXΦ. Science *288*, 664-670.

Davis, N.G., Boeke, J.D., and Model, P. (1985). Fine-structure of a membrane Anchor Domain Journal Of Molecular Biology *181*, 111-121.

Davis, N.G., and Model, P. (1985). An artificial anchor domain: hydrophobicity suffices to stop transfer. Cell *41*, 607-614.

De Berardinis, P., and Haigwood, N.L. (2004). New recombinant vaccines based on the use of prokaryotic antigen-display systems. Expert review of vaccines *3*, 673-679.

de Wildt, R.M., Tomlinson, I.M., Ong, J.L., and Holliger, P. (2002). Isolation of receptor-ligand pairs by capture of long-lived multivalent interaction complexes. Proc Natl Acad Sci U S A *99*, 8530-8535.

Deenick, E.K., Hasbold, J., and Hodgkin, P.D. (2005). Decision criteria for resolving isotype switching conflicts by B cells. European journal of immunology *35*, 2949-2955.

Delacruz, V.F., Lal, A.A., and McCutchan, T.F. (1988). Immunogenicity and epitope mapping of foreign sequences via gnetically engineered filamentous phage. Journal of Biological Chemistry *263*, 4318-4322.

DeLano, W.L. (2006). The PyMOL molecular graphics system. DeLano Scientific, San Carlos, CA: USA

Delmastro, P., Meola, A., Monaci, P., Cortese, R., and Galfre, G. (1997). Immunogenicity of filamentous phage displaying peptide mimotopes after oral administration. Vaccine *15*, 1276-1285.

Deng, L.W., and Perham, R.N. (2002). Delineating the site of interaction on the pIII protein of filamentous bacteriophage fd with the F-pilus of *Escherichia coli*. J Mol Biol *319*, 603-614.

Dente, L., Cesareni, G., and Cortese, R. (1983). pEMBL: a new family of single stranded plasmids. Nucleic Acids Research *11*, 1645-1655.

Deprez, C., Lloubès, R., Gavioli, M., Marion, D., Guerlesquin, F., and Blanchard, L. (2005). Solution structure of the *E.coli* TolA C-terminal domain reveals conformational changes upon binding to the phage g3p N-terminal domain. Journal of Molecular Biology *346*, 1047-1057.

Devlin, J.J., Panganiban, L.C., and Devlin, P.E. (1990). Random peptide libraries: a source of specific protein binding molecules. Science *249*, 404-406.

Di Marzo Veronese, F., Willis, A.E., Boyer-Thompson, C., Appella, E., and Perham, R.N. (1994). Structural mimicry and enhanced immunogenicity of peptide epitopes displayed on filamentous bacteriophage: the V3 loop of HIV-1 gp120. Journal of molecular biology *243*, 167-172.

Dotto, G.P., Enea, V., and Zinder, N.D. (1981). Functional analysis of bacteriophage intergenic region. Virology *114*, 463-473.

Dotto, G.P., Horiuchi, K., and Zinder, N.D. (1984). The origin of DNA replication of bacteriophage f1 and its interaction with the phage gene II protein. Adv Exp Med Biol *179*, 185-191.

Dotto, G.P., and Zinder, N.D. (1983). The morphogenetic signal of bacteriophage f1. Virology *130*, 252-256.

Dotto, G.P., and Zinder, N.D. (1984). Increased intracellular concentration of an initiator protein markedly reduces the minimal sequence required for initiation of DNA synthesis. Proceedings of the National Academy of Sciences *81*, 1336-1340.

Eckert, B., Martin, A., Balbach, J., and Schmid, F.X. (2005). Prolyl isomerization as a molecular timer in phage infection. Nature structural & molecular biology *12*, 619-623.

Endemann, H., and Model, P. (1995). Location of filamentous phage minor coat proteins in phage and in infected cells. Journal of Molecular Biology *250*, 495-506.

Enea, V., and Zinder, N.D. (1982). Interference resistant mutants of phage f1. Virology *122*, 222-226.

Engvall, E., Bell, M., and Ruoslahti, E. (1981). Affinity chromatography of collagen on collagen-binding fragments of fibronectin. Collagen and related research *1*, 505.

Engvall, E., Ruoslahti, E., and Miller, E. (1978). Affinity of fibronectin to collagens of different genetic types and to fibrinogen. The Journal of experimental medicine *147*, 1584-1595.

Eriksson, F., Culp, W.D., Massey, R., Egevad, L., Garland, D., Persson, M.A., and Pisa, P. (2007). Tumor specific phage particles promote tumor regression in a mouse melanoma model. Cancer immunology, immunotherapy *56*, 677-687.

Eriksson, F., Tsagozis, P., Lundberg, K., Parsa, R., Mangsbo, S.M., Persson, M.A., Harris, R.A., and Pisa, P. (2009). Tumor-specific bacteriophages induce tumor destruction through activation of tumor-associated macrophages. The Journal of Immunology *182*, 3105-3111.

Feng, J.-n. (2000). Studies of the assembly/export proteins and energy requirements for filamentous phage assembly (The Rockefeller University).

Feng, J.N., Model, P., and Russel, M. (1999). A trans-envelope protein complex needed for filamentous phage assembly and export. Mol Microbiol, 745-755.

Frenkel, D., Dewachter, I., Van Leuven, F., and Solomon, B. (2003). Reduction of β-amyloid plaques in brain of transgenic mouse model of Alzheimer's disease by EFRH-phage immunization. Vaccine *21*, 1060-1065.

Frenkel, D., and Solomon, B. (2002). Filamentous phage as vector-mediated antibody delivery to the brain. Proceedings of the National Academy of Sciences *99*, 5675-5679.

Fulford, W., and Model, P. (1984). Gene X of bacteriophage f1 is required for phage DNA synthesis: Mutagenesis of in-frame overlapping genes. Journal of molecular biology *178*, 137-153.

Fulford, W., and Model, P. (1988a). Bacteriophage f1 DNA replication genes: II. The roles of gene V protein and gene II protein in complementary strand synthesis. Journal of Molecular Biology *203*, 39-48.

Fulford, W., and Model, P. (1988b). Regulation of bacteriophage f1 DNA replication: I. New functions for genes II and X. Journal of Molecular Biology *203*, 49-62.

Gailus, V., and Rasched, I. (1994). The adsorption protein of bacteriophage fd and its neighbour minor coat protein build a structural entity. European Journal of Biochemistry *222*, 927-931.

Gao, C., Mao, S., Kaufmann, G., Wirsching, P., Lerner, R.A., and Janda, K.D. (2002). A method for the generation of combinatorial antibody libraries using pIX phage display. Proc Natl Acad Sci U S A *99*, 12612-12616.

Gao, C., Mao, S., Lo, C.H., Wirsching, P., Lerner, R.A., and Janda, K.D. (1999). Making artificial antibodies: a format for phage display of combinatorial heterodimeric arrays. Proc Natl Acad Sci U S A *96*, 6025-6030.

Gaubin, M., Fanutti, C., Mishal, Z., Durrbach, A., De Berardinis, P., Sartorius, R., Del Pozzo, G., Guardiola, J., Perham, R.N., and Piatier-Tonneau, D. (2003). Processing of filamentous bacteriophage virions in antigen-presenting cells targets both HLA class I and class II peptide loading compartments. DNA and cell biology *22*, 11-18.

Geider, K., and Kornberg, A. (1974). Conversion of the M13 viral single strand to the double-stranded replicative forms by purified proteins. Journal of Biological Chemistry *249*, 3999-4005.

Goffinet, M., Chinestra, P., Lajoie-Mazenc, I., Medale-Giamarchi, C., Favre, G., and Faye, J.-C. (2008). Identification of a GTP-bound Rho specific scFv molecular sensor by phage display selection. BMC Biotechnology *8*, 34.

Gonzalez-Techera, A., Kim, H.J., Gee, S.J., Last, J.A., Hammock, B.D., and Gonzalez-Sapienza, G. (2007). Polyclonal antibody-based noncompetitive immunoassay for small analytes developed with short peptide loops isolated from phage libraries. Anal Chem *79*, 9191-9196.

González-Techera, A., Vanrell, L., Last, J.A., Hammock, B.D., and González-Sapienza, G. (2007). Phage Anti-Immune Complex Assay: general strategy for noncompetitive immunodetection of small molecules. Analytical Chemistry *79*, 7799-7806.

Gonzalez, M.D., Lichtensteiger, C.A., Caughlan, R., and Vimr, E.R. (2002). Conserved filamentous prophage in *Escherichia coli* O18: K1: H7 and Yersinia pestis biovar orientalis. Journal of bacteriology *184*, 6050-6055.

Goodrich, A.F., and Steege, D.A. (1999). Roles of polyadenylation and nucleolytic cleavage in the filamentous phage mRNA processing and decay pathways in *Escherichia coli*. RNA *5*, 972-985.

Grabowska, A., Jennings, R., Laing, P., Darsley, M., Jameson, C., Swift, L., and Irving, W. (2000). Immunisation with phage displaying peptides representing single epitopes of the glycoprotein G can give rise to partial protective immunity to HSV-2. Virology *269*, 47-53.

Grant, R., Lin, T., Konigsberg, W., and Webster, R. (1981a). Structure of the filamentous bacteriophage fl. Location of the A, C, and D minor coat proteins. Journal of Biological Chemistry *256*, 539-546.

Grant, R.A., Lin, T.-C., Webster, R.E., and Konigsberg, W. (1981b). Structure of filamentous bacteriophage: isolation, characterization, and localization of the minor coat proteins and orientation of the DNA. Progress in clinical and biological research *64*, 413.

Gray, C.P., Sommer, R., Polke, C., Beck, E., and Schaller, H. (1978). Structure of the orgin of DNA replication of bacteriophage fd. Proceedings of the National Academy of Sciences *75*, 50-53.

Gray, C.W. (1989). Three-dimensional structure of complexes of single-stranded DNA-binding proteins with DNA. Ike and fd gene 5 proteins form left-handed helices with single-stranded DNA. J Mol Biol *208*, 57-64.

Gray, C.W., Brown, R.S., and Marvin, D.A. (1979). Direct visualization of adsorption protein of fd phage. J Supramol Str *1979*, 91-91.

Gray, C.W., Brown, R.S., and Marvin, D.A. (1981). Adsorption complex of filamentous fd virus. J Mol Biol *146*, 621-627.

Greenstein, D., and Horiuchi, K. (1989). Double-strand cleavage and strand joining by the replication initiator protein of filamentous phage f1. J Biol Chem, 12627-12632

Greenstein, D., Zinder, N.D., and Horiuchi, K. (1988). Integration host factor interacts with the DNA replicatin enhancer of filamentous phage f1. Proc Natl Acad *85*, 6262-6266.

Greenwood, J., Hunter, G.J., and Perham, R.N. (1991). Regulation of filamentous bacteriophage length by modification of electrostatic interactions between coat protein and DNA. J Mol Biol, 223-227

Greenwood, J., Willis, A.E., and Perham, R.N. (1991). Multiple display of foreign peptides on a filamentous bacteriophage. Peptides from Plasmodium falciparum circumsporozoite protein as antigens. Journal of Molecular Biology *220*, 821-827.

Griffiths, A.D., Malmqvist, M., Marks, J.D., Bye, J.M., Embleton, M.J., McCafferty, J., Baier, M., Holliger, K.P., Gorick, B.D., Hughes-Jones, N.C., *et al.* (1993). Human anti-self antibodies with high specificity from phage display libraries. Embo J *12*, 725-734.

Guy-Caffey, J.K., Rapoza, M.P., Jolley, K.A., and Webster, R.E. (1992). Membrane localization and topology of a viral assembly protein. J Bacteriol *174*, 2460-2465.

Guzman, C.A., Talay, S.R., Molinari, G., Medina, E., and Chhatwal, G.S. (1999). Protective immune response against Streptococcus pyogenes in mice after intranasal vaccination with the fibronectin binding protein SfbI. Journal of Infectious Diseases *179*, 901-906.

Haigh, N.G., and Webster, R.E. (1999). The pI and pXI assembly proteins serve separate and essential roles in filamentous phage assembly. Journal of Molecular Biology *293*, 1017-1027.

Harlow, E. (1999). Using antibodies: a laboratory manual In (Cold Apring Harbor N.Y, Cold Spring Harbor Laboratory Press).

Hashemi, H., Bamdad, T., Jamali, A., Pouyanfard, S., and Mohammadi, M.G. (2010). Evaluation of humoral and cellular immune responses against HSV-1 using genetic immunization by filamentous phage particles: A comparative approach to conventional DNA vaccine. Journal of Virological Methods *163*, 440-444.

Hayman, E.G., and Ruoslahti, E. (1979). Distribution of fetal bovine serum fibronectin and endogenous rat cell fibronectin in extracellular matrix. The Journal of cell biology *83*, 255-259.

Heilpern, A.J., and Waldor, M.K. (2003). pIIICTX, a predicted CTXphi minor coat protein, can expand the host range of coliphage fd to include Vibrio cholerae. J Bacteriol, 1037-1044.

Hemminga, M.A., Sanders, J.C., Wolfs, C.J.A.M., and Spruijt, R.B. (1993). Chapter 8 Lipid-protein interactions involved in bacteriophage M13 infection. In New Comprehensive Biochemistry, A. Watts, ed. (Elsevier), pp. 191-212.

Henry, K.A., Murira, A., van Houten, N.E., and Scott, J.K. (2011). Developing strategies to enhance and focus humoral immune responses using filamentous phage as a model antigen. Bioengineered *2*, 275-283.

Higashitani, A., Higashitani, N., and Horiuchi, K. (1997). Minus-strand origin of filamentous phage versus transcriptional promoters in recognition of RNA polymerase. Proceedings of the National Academy of Sciences *94*, 2909-2914.

Higashitani, N., Higashitani, A., Guan, Z.W., and Horiuchi, K. (1996). Recognition mechanisms of the minus-strand origin of phage f1 by *Escherichia coli* RNA polymerase. Genes to Cells *1*, 829-841.

Hill, D.F., Short, N.J., Perham, R.N., and Petersen, G.B. (1991). DNA sequence of the filamentous bacteriophage Pf1. J Mol Biol *218*, 349-364.

Hoffmann-Berling, H., and Mazé, R. (1964). Release of male-specific bacteriophages from surviving host bacteria. Virology *22*, 305-313.

Hofschneider, P.H., and Preuss, A. (1963). M13 bacteriophage liberation from intact bacteria as revealed by electron microscopy. J Mol Biol *7*, 450-451.

Hohn, B., Von Schütz, H., and Marvin, D.A. (1971). Filamentous bacterial viruses: II. Killing of bacteria by abortive infection with fd. Journal of Molecular Biology *56*, 155-165.

Holliger, P., Riechmann, L., and Williams, R.L. (1999). Crystal structure of the two N-terminal domains of g3p from filamentous phage fd at 1.9 A: evidence for conformational lability. J Mol Biol *288*, 649-657.

Hoogenboom, H.R., de Bruïne, A.P., Hufton, S.E., Hoet, R.M., Arends, J.-W., and Roovers, R.C. (1998). Antibody phage display technology and its applications. Immunotechnology *4*, 1-20.

Horabin, J.I., and Webster, R.E. (1986). Morphogenesis of f1 filamentous bacteriophage: increased expression of gene I inhibits bacterial growth. Journal of Molecular Biology *188*, 403-413.

Horabin, J.I., and Webster, R.E. (1988). An amino acid sequence which directs membrane insertion causes loss of membrane potential. Journal Of Biological Chemistry *263*, 11575-11583.

Horiuchi, K. (1997). Initiation mechanisms in replication of filamentous phage DNA. Genes to Cells *2*, 425-432.

Houimel, M., and Dellagi, K. (2009). Peptide mimotopes of rabies virus glycoprotein with immunogenic activity. Vaccine *27*, 4648-4655.

Huang, J.a., Wang, L., Firth, S., Phelps, A., Reeves, P., and Holmes, I. (2000). Rotavirus VP7 epitope mapping using fragments of VP7 displayed on phages. Vaccine *18*, 2257-2265.

Huang, S., Yang, H., Lakshmanan, R., Johnson, M., Chen, I., Wan, J., Wikle, H., Petrenko, V., Barbaree, J., and Cheng, Z. (2008). The effect of salt and phage concentrations on the binding sensitivity of magnetoelastic biosensors for Bacillus anthracis detection. Biotechnology and bioengineering *101*, 1014-1021.

Huang, Y., Chiang, C.Y., Lee, S.K., Gao, Y., Hu, E.L., De Yoreo, J., and Belcher, A.M. (2005). Programmable assembly of nanoarchitectures using genetically engineered viruses. NANO LETT *5*, 1429-1434.

Hufton, S.E., Moerkerk, P.T., Meulemans, E.V., de Bruine, A., Arends, J.W., and Hoogenboom, H.R. (1999). Phage display of cDNA repertoires: the pVI display system and its applications for the selection of immunogenic ligands. J Immunol Methods *231*, 39-51.

Hunter, G.J., Rowitch, D.H., and Perham, R.N. (1987). Interactions between DNA and coat protein in the structure and assembly of filamentous bacteriophage fd. Nature *327*, 252-254.

Iannolo, G., Minenkova, O., Petruzzelli, R., and Cesareni, G. (1995). Modifying filamentous phage capsid: limits in the size of the major capsid protein. J Mol Biol *248*, 835-844.

Ikehara, K., Utiyama, H., and Kurata, M. (1975). Studies on the structure of filamentous bacteriophage fd: II. All-or-none disassembly in guanidine-HCl and sodium dodecyl sulfate. Virology *66*, 306-315.

Irving, M.B., Pan, O., and Scott, J.K. (2001). Random-peptide libraries and antigen-fragment libraries for epitope mapping and the development of vaccines and diagnostics. Current opinion in chemical biology *5*, 314-324.

Ivey-Hoyle, M., and Steege, D.A. (1989). Translation of phage f1 gene VII occurs from an inherently defective initiation site made functional by coupling. Journal of Molecular Biology *208*, 233-244.

Ivey-Hoyle, M., and Steege, D.A. (1992). Mutational analysis of an inherently defective translation initiation site. Journal of Molecular Biology *224*, 1039-1054.

Jacobson, A. (1972). The role of F pili in the penetration of bacteriophage f1. JVirol, 835-843.

Jankovic, D., Collett, M.A., Lubbers, M.W., and Rakonjac, J. (2007). Direct selection and phage display of a Gram-positive secretome. Genome biology *8*, R266.

Jaye, D.L., Geigerman, C.M., Fuller, R.E., Akyildiz, A., and Parkos, C.A. (2004). Direct fluorochrome labeling of phage display library clones for studying binding specificities: applications in flow cytometry and fluorescence microscopy. Journal of immunological methods *295*, 119-127.

Jespers, L.S., De Keyser, A., and Stanssens, P.E. (1996). LambdaZLG6: a phage lambda vector for high-efficiency cloning and surface expression of cDNA libraries on filamentous phage. Gene *173*, 179-181.

Jespers, L.S., Messens, J.H., De Keyser, A., Eeckhout, D., Van den Brande, I., Gansemans, Y.G., Lauwereys, M.J., Vlasuk, G.P., and Stanssens, P.E. (1995). Surface expression and ligand-based selection of cDNAs fused to filamentous phage gene VI. Biotechnology (N Y) *13*, 378-382.

Ji, X., Oh, J., Dunker, A.K., and Hipps, K.W. Effects of relative humidity and applied force on atomic force microscopy images of the filamentous phage fd. 165-176, 1998 May.

Kawabata, S., Kunitomo, E., Terao, Y., Nakagawa, I., Kikuchi, K., Totsuka, K.I., and Hamada, S. (2001). Systemic and mucosal immunizations with fibronectin-binding protein FBP54 induce protective immune responses against Streptococcus pyogenes challenge in mice. Infection and Immunity *69*, 924-930.

Kay, B.K., Winter, J., and McCafferty, J. (1996). Phage display of peptides and proteins: a laboratory manual (Academic Press).

Kazmierczak, B.I., Mielke, D.L., Russel, M., and Model, P. (1994). pIV, a filamentous phage protein that mediates phage export across the bacterial cell envelope, forms a multimer. Journal of Molecular Biology *238*, 187-198.

Khatoon, H., Iyer, R.V., and Iyer, V.N. (1972). A new filamentous bacteriophage with sex-factor specificity. Virology *48*, 145-155.

Kim, A.Y., and Blaschek, H.P. (1991). Isolation and characterization of a filamentous viruslike particle from *Clostridium acetobutylicum* NCIB 6444. Journal of bacteriology *173*, 530-535.

Kim, H.J., Ahn, K.C., Gonzalez-Techera, A., Gonzalez-Sapienza, G.G., Gee, S.J., and Hammock, B.D. (2009). Magnetic bead-based phage anti-immunocomplex assay (PHAIA) for the detection of the urinary biomarker 3-phenoxybenzoic acid to assess human exposure to pyrethroid insecticides. Anal Biochem *386*, 45-52.

Kim, M.H., Hines, J.C., and Ray, D.S. (1981). Viable deletions of the M13 complementary strand origin. Proceedings of the National Academy of Sciences *78*, 6784-6788.

King, A.M., Adams, M.J., and Lefkowitz, E. (2011). Virus taxonomy: ninth report of the International Committee on Taxonomy of Viruses, Vol 9 (Elsevier).

Kneissel, S., Queitsch, I., Petersen, G., Behrsing, O., Micheel, B., and Dubel, S. (1999). Epitope structures recognised by antibodies against the major coat protein (g8p) of filamentous bacteriophage fd (*Inoviridae*). Journal of Molecular Biology *288*, 21-28.

Konings, R., Hulsebos, T., and Van den Hondel, C.A. (1975). Identification and characterization of the in vitro synthesized gene products of bacteriophage M13. Journal of Virology *15*, 570-584.

Krebber, C., Spada, S., Desplancq, D., Krebber, A., Liming, G., and Pluckthun, A. (1997). Selectively-infective phage (SIP): a mechanistic dissection of a novel in vivo selection for protein-ligand interactions. J Mol Biol *268*, 607-618.

Krogh, A., Larsson, B., Von Heijne, G., and Sonnhammer, E.L. (2001). Predicting transmembrane protein topology with a hidden Markov model: application to complete genomes. Journal of molecular biology *305*, 567-580.

Kuo, T.-T., Lin, Y.-H., Huang, C.-M., Chang, S.-F., Dai, H., and Feng, T.-Y. (1987). The lysogenic cycle of the filamentous phage Cflt from *Xanthomonas campestris pv. citri*. Virology *156*, 305-312.

La Farina, M., Izzo, V., Duro, G., Barbieri, R., Costa, M.A., and Mutolo, V. (1987). Intragenomic recombination between homologous regions of genes II and IV promotes formation of bacteriophage f1 miniphages. Nucleic Acids Research *15*, 7190-7190.

Laemmli, U.K. (1970). Cleavage of structural proteins during the assembly of the head of bacteriophage T4. Nature *227*, 680-685.

Larocca, D., Kassner, P.D., Witte, A., Ladner, R.C., Pierce, G.F., and BAIRD, A. (1999). Gene transfer to mammalian cells using genetically targeted filamentous bacteriophage. The FASEB journal *13*, 727-734.

Lee, S.-M., Lee, E.-J., Hong, H.-Y., Kwon, M.-K., Kwon, T.-H., Choi, J.-Y., Park, R.-W., Kwon, T.-G., Yoo, E.-S., and Yoon, G.-S. (2007). Targeting bladder tumor cells in vivo and in the urine with a peptide identified by phage display. Molecular cancer research *5*, 11-19.

Lee, S., Mao, C., Flynn, C., and Belcher, A. (2002). Ordering of quantum dots using genetically engineered viruses. Science *296*, 892-895.

Linderoth, N.A., Simon, M.N., and Russel, M. (1997). The filamentous phage pIV multimer visualized by scanning transmission electron microscopy. Science *278*, 1635-1638.

Loeb, T. (1960). Isolation of a bacteriophage specific for the F+ and Hfr mating types of *Escherichia coli* K-12. Science *131*, 932-933.

Lopez, J., and Webster, R.E. (1983). Morphogenesis of filamentous bacteriophage f1: orientation of extrusion and production of polyphage. Virology *127*, 177-193.

Lopez, J., and Webster, R.E. (1985). Assembly site of bacteriophage f1 corresponds to adhesion zones between the inner and outer membranes of the host cell. J Bacteriol *163*, 1270-1274.

Lowman, H.B., Bass, S.H., Simpson, N., and Wells, J.A. (1991). Selecting high-affinity binding proteins by monovalent phage display. Biochemistry *30*, 10832-10838.

Lubkowski, J., Hennecke, F., Pluckthun, A., and Wlodawer, A. (1998). The structural basis of phage display elucidated by the crystal structure of the N-terminal domains of g3p. Nat Struct Biol *5*, 140-147.

Lubkowski, J., Hennecke, F., Pluckthun, A., and Wlodawer, A. (1999). Filamentous phage infection: crystal structure of g3p in complex with its coreceptor, the C-terminal domain of TolA. Structure Fold Des *15*, 711-272.

Ma, C.Q., Li, C.H., Wang, X.R., Zeng, R.H., Yin, X.L., Feng, H.D., and Wei, L. (2009). Similar ability of FbaA with M protein to elicit protective immunity against group A streptococcus challenge in mice. Cellular & Molecular Immunology *6*, 73-77.

Makowski, L. (1994). Phage display: structure, assembly and engineering of filamentous bacteriophage M13. Current opinion in structural biology *4*, 225-230.

Makowski, L., and Russel, M. (1997). Structure and assembly of filamentous bacteriophage. In Structural Biology of Viruses, W. Chiu, R.M. Burnett, and R.L. Garcelas, eds. (New York, Oxford University Press, Inc.), pp. 352-380.

Mao, C., Flynn, C., Hayhurst, A., Sweeney, R., Qi, J., Georgiou, G., Iverson, B., and Belcher, A. (2003). Viral assembly of oriented quantum dot nanowires. Proc Natl Acad Sci U S A *100*, 6946-6951.

Mao, C., Solis, D., Reiss, B., Kottmann, S., Sweeney, R., Hayhurst, A., Georgiou, G., Iverson, B., and Belcher, A. (2004). Virus-based toolkit for the directed synthesis of magnetic and semiconducting nanowires. Science *303*, 213-217.

Marciano, D.K., Russel, M., and Simon, S.M. (1999). An aqueous channel for filamentous phage export. Science *284*, 1516-1519.

Marciano, D.K., Russel, M., and Simon, S.M. (2001). Assembling filamentous phage occlude pIV channels. Proc Natl Acad Sci USA *98*, 9359-9364.

Marvin, D. (1990). Model-building studies of *Inovirus*: genetic variations on a geometric theme. International journal of biological macromolecules *12*, 125-138.

Marvin, D. (1998a). Filamentous phage structure, infection and assembly. Current opinion in structural biology *8*, 150-158.

Marvin, D., and Hohn, B. (1969). Filamentous bacterial viruses. Bacteriological reviews *33*, 172.

Marvin, D.A. (1978). Structure of the filamentous phage virion. In The Single-Stranded DNA-Phages, D.T. Denhardt, D. Dressler, and D.S. Ray, eds. (Cold Spring Harbor, N. Y., Cold Spring Harbor Laboratory Press), pp. 583-603.

Marvin, D.A. (1998b). Filamentous phage structure, infection and assembly. Current opinion in structural biology *8*, 150-158.

Marvin, D.A., and Hoffmann-Berling, H. (1963). A fibrous DNA phage (fd) and a spherical RNA phage (fr) specific for male strains of *E. coli* II. Physical charecteristics. Z Naturforsch B *18*, 884-893.

Marvin, D.A., Welsh, L.C., Symmons, M.F., Scott, W.R.P., and Straus, S.K. (2006). Molecular structure of fd (f1, M13) filamentous bacteriophage refined with respect to X-ray fibre diffraction and solid-state NMR Data supports specific models of phage assembly at the bacterial membrane. Journal of Molecular Biology *355*, 294-309.

McCafferty, J., Griffiths, A.D., Winter, G., and Chiswell, D.J. (1990). Phage antibodies: filamentous phage displaying antibody variable domains. Nature *348*, 552-554.

McLeod, S.M., Kimsey, H.H., Davis, B.M., and Waldor, M.K. (2005). CTXφ and *Vibrio cholerae*: exploring a newly recognized type of phage–host cell relationship. Molecular Microbiology *57*, 347-356.

Mead, D.A.K., B (1988). Chimeric single-stranded DNA phage-plasmid clonning vectors, In Vectors: A survey of molecular cloning vectors and their uses, R.L. Rodriquez, Denhardt, D.T., Eds.;Butterworths:Boston ed.

Medina, E., Schulze, K., Chhatwal, G.S., and Guzman, C.A. (2000). Nonimmune interaction of the SfbI protein of *Streptococcus pyogenes* with the immunoglobulin G F(ab')(2) fragment. Infect Immun *68*, 4786-4788.

Meselson, M., and Stahl, F.W. (1958). The replication of DNA in *Escherichia coli*. Proceedings of the National Academy of Sciences *44*, 671-682.

Meyer, T.F., and Geider, K. (1982). Enzymatic synthesis of bacteriophage fd viral DNA. Nature *296*, 828 - 832.

Meynell, G.G., and Lawn, A.M. (1968). Filamentous phages specific for the I sex factor. Nature *217*, 1184-1186.

Michel, B., and Zinder, N.D. (1989). Invitro binding of the bacteriophage f1-gene V-protein to the gene-II RNA-operator and its DNA analog Nucleic Acids Research *17*, 7333-7344.

Minenkova, O.O., Ilyichev, A.A., Kishchenko, G.P., and Petrenko, V.A. (1993). Design of specific immunogens using filamentous phage as the carrier. Gene *128(1)*, 85-88.

Mintz, P.J., Kim, J., Do, K.-A., Wang, X., Zinner, R.G., Cristofanilli, M., Arap, M.A., Hong, W.K., Troncoso, P., and Logothetis, C.J. (2002). Fingerprinting the circulating repertoire of antibodies from cancer patients. Nature biotechnology *21*, 57-63.

Model, P., and Russel, M. (1988). Filamentous Bacteriophage. In The Bacteriophages, R. Calendar, ed. (New York, Plenum Publishing), pp. 375-456.

Model, P., and Zinder, N.D. (1974). *In vitro* synthesis of bacteriophage f1 proteins. Journal Of Molecular Biology *83*, 231-251.

Mooij, M.J., Drenkard, E., Llamas, M.A., Vandenbroucke-Grauls, C.M., Savelkoul, P.H., Ausubel, F.M., and Bitter, W. (2007). Characterization of the integrated filamentous

phage *Pf5* and its involvement in small-colony formation. Microbiology *153*, 1790-1798.

Mullis, K., Faloona, F., Scharf, S., Saiki, R., Horn, G., and Erlich, H. (1986). Specific enzymatic amplification of DNA in vitro: the polymerase chain reaction. Paper presented at: Cold Spring Harb Symp Quant Biol.

Newman, J., Swinney, H.L., and Day, L.A. (1977). Hydrodynamic properties and structure of fd virus. Journal of Molecular Biology *116*, 593-603.

Oey, J.L., and Knippers, R. (1972). Properties of the isolated gene 5 protein of bacteriophage fd. Journal of Molecular Biology *68*, 125-138.

Oliver, A.W., Bogdarina, I., Schroeder, E., Taylor, I.A., and Kneale, G.G. (2000). Preferential binding of fd gene 5 protein to tetraplex nucleic acid structures. Journal of molecular biology *301*, 575.

Opalka, N., Beckmann, R., Boisset, N., Simon, M.N., Russel, M., and Darst, S.A. (2003). Structure of the filamentous phage pIV multimer by cryo-electron microscopy. J Mol Biol *325*, 461-470.

Opella, S.J., Zeri, A.C., and Park, S.H. (2008). Structure, dynamics, and assembly of filamentous bacteriophages by nuclear magnetic resonance spectroscopy. Annual Review of Physical Chemistry *59*, 635-657.

Parmley, S.F., and Smith, G.P. (1988). Antibody-selectable filamentous fd phage vectors - affinity purification of target genes. Gene *73*, 305-318.

Pratt, D., and Erdahl, W.S. (1968). Genetic control of bacteriophage M13 DNA synthesis. Journal of molecular biology *37*, 181-200.

Pratt, D., Laws, P., and Griffith, J. (1974). Complex of bacteriophage M13 single-stranded DNA and gene 5 protein. Journal of Molecular Biology *82*, 425-439.

Pratt, D., Tzagoloff, H., and Beaudoin, J. (1969). Conditional lethal mutants of the small filamentous coliphage M13: II. Two genes for coat proteins. Virology *39*, 42-53.

Prisco, A., and De Berardinis, P. (2012). Filamentous bacteriophage fd as an antigen delivery system in vaccination. International Journal of Molecular Sciences *13*, 5179-5194.

Rakonjac, J. (2001). Filamentous bacteriophages: biology and applications. In eLS (John Wiley & Sons, Ltd).

Rakonjac, J., Bennett, N.J., Spagnuolo, J., Gagic, D., and Russel, M. (2011). Filamentous bacteriophage: biology, phage display and nanotechnology applications. Current issues in molecular biology *13*, 51.

Rakonjac, J., and Conway, J.F. (2006). Bacteriophages: self-assembly and applications. Molecular Bionanotechnology, 153-190.

Rakonjac, J., Feng, J.N., and Model, P. (1999). Filamentous phage are released from the bacterial membrane by a two-step mechanism involving a short C-terminal fragment of pIII. Journal of Molecular Biology *289*, 1253-1265.

Rakonjac, J., Jovanovic, G., and Model, P. (1997). Filamentous phage infection-mediated gene expression: construction and propagation of the *gIII* deletion mutant helper phage R408d3. Gene *198*, 99-103.

Rakonjac, J., and Model, P. (1998). The roles of pIII in filamentous phage assembly. J Mol Biol *282*, 25-41.

Rakonjac, J.V., Robbins, J.C., and Fischetti, V.A. (1995). DNA sequence of the serum opacity factor of group A streptococci: identification of a fibronectin-binding repeat domain. Infection and immunity *63*, 622-631.

Ramanujam, P., Tan, W.S., Nathan, S., and Yusoff, K. Novel peptides that inhibit the propagation of Newcastle disease virus. 981-993, 2002 May.

Rapoza, M.P., and Webster, R.E. (1993). The filamentous bacteriophage assembly proteins require the bacterial SecA protein for correct localisation to the membrane. J Bacteriol *175*, 1856-1859.

Rapoza, M.P., and Webster, R.E. (1995). The products of *gene I* and the overlapping in-frame *gene XI* are required for filamentous phage assembly. J Mol Biol *248*, 627-638.

Rasmussen, U.B., Schreiber, V., Schultz, H., Mischler, F., and Schughart, K. (2002). Tumor cell-targeting by phage-displayed peptides. Cancer gene therapy *9*, 606-612.

Rebar, E.J., and Pabo, C.O. (1994). Zinc finger phage: affinity selection of fingers with new DNA-binding specificities. Science *263*, 671-673.

Rice, S.A., Tan, C.H., Mikkelsen, P.J., Kung, V., Woo, J., Tay, M., Hauser, A., McDougald, D., Webb, J.S., and Kjelleberg, S. (2008). The biofilm life cycle and virulence of *Pseudomonas aeruginosa* are dependent on a filamentous prophage. The ISME journal *3*, 271-282.

Riechmann, L., and Holliger, P. (1997). The C-Terminal Domain of TolA Is the Coreceptor for Filamentous Phage Infection of *E. coli*. Cell *90*, 351-360.

Roberts, B.L., Markland, W., Ley, A.C., Kent, R.B., White, D.W., Guterman, S.K., and Ladner, R.C. (1992). Directed evolution of a protein: selection of potent neutrophil elastase inhibitors displayed on M13 fusion phage. Proc Natl Acad Sci U S A *89*, 2429-2433.

Roth, T.A., Weiss, G.A., Eigenbrot, C., and Sidhu, S.S. (2002). A minimized M13 coat protein defines the requirements for assembly into the bacteriophage particle. Journal of Molecular Biology *322*, 357-367.

Rowitch, D.H., Hunter, G.J., and Perham, R.N. (1988). Variable electrostatic interaction between DNA and coat protein in filamentous bacteriophage assembly Journal Of Molecular Biology *204*, 663-674.

Ruoslahti, E., Vuento, M., and Engvall, E. (1978). Interaction of fibronectin with antibodies and collagen in radioimmunoassay. Biochimica et Biophysica Acta (BBA)-Protein Structure *534*, 210-218.

Russel, M. (1991). Filnmentous phage assembly. Molecular Microbiology *5*, 1607-1613.

Russel, M., and Model, P., ed. (2006). Filamentous Phage, Second edn (New York, (Oxford University Press, Inc.)).

Russel, M., Kidd, S., and Kelley, M.R. (1986). An improved filamentous helper phage for generating single-stranded plasmid DNA. Gene *45*, 333-338.

Russel, M., Lowman, H.B., and Clackson, T. (2004). Introduction to phage biology and phage display. Practical Approach to Phage Display, 1-26.

Russel, M., and Model, P. (1982). Filamentous phage pre-coat is an integral membrane protein: analysis by a new method of membrane preparation. Cell *28*, 177-184.

Russel, M., and Model, P. (1989). Genetic analysis of the filamentous bacteriophage packaging signal and of the proteins that interact with it. Journal of Virology *63*, 3284-3295.

Russel, M., Whirlow, H., Sun, T.P., and Webster, R.E. (1988). Low-frequency infection of F^- bacteria by transducing particles of filamentous bacteriophages J Bacteriol *170*, 5312-5316.

Salstrom, J.S., and Pratt, D. (1971). Role of coliphage M13 *gene 5* in single-stranded DNA production. Journal of Molecular Biology *61*, 489-501.

Sambrook, J., Fritsch, E.F., and Maniatis, T. (1989). Molecular cloning, Vol 2 (Cold spring harbor laboratory press New York).

Samuelson, J.C., Jiang, F., Yi, L., Chen, M., de Gier, J.W., Kuhn, A., and Dalbey, R.E. (2001). Function of YidC for the insertion of M13 procoat protein in *Escherichia coli*: translocation of mutants that show differences in their membrane potential dependence and Sec requirement. J Biol Chem *276*, 34847-34852.

Sartorius, R., Bettua, C., D'Apice, L., Caivano, A., Trovato, M., Russo, D., Zanoni, I., Granucci, F., Mascolo, D., and Barba, P. (2011). Vaccination with filamentous bacteriophages targeting DEC-205 induces DC maturation and potent anti-tumor T-cell responses in the absence of adjuvants. European journal of immunology *41*, 2573-2584.

Schaller, H., Voss, H., and Gucker, S. (1969). Structure of the DNA of bacteriophage fd: II. Isolation and characterization of a DNA fraction with double strand-like properties. Journal of Molecular Biology *44*, 445-458.

Schier, R., Marks, J.D., Wolf, E.J., Apell, G., Wong, C., McCartney, J.E., Bookman, M.A., Huston, J.S., Houston, L.L., Weiner, L.M., *et al.* (1995). *In vitro* and *in vivo* characterization of a human anti-c-erbB-2 single-chain Fv isolated from a filamentous phage antibody library. Immunotechnology *1*, 73-81.

Schulze, K., Medina, E., Chhatwal, G.S., and Guzman, C.A. (2003). Stimulation of long-lasting protection against Streptococcus pyogenes after intranasal vaccination with non adjuvanted fibronectin-binding domain of the SfbI protein. Vaccine *21*, 1958-1964.

Schulze, K., Medina, E., Talay, S.R., Towers, R.J., Chhatwal, G.S., and Guzmán, C.A. (2001). Characterization of the domain of fibronectin-binding protein I of Streptococcus pyogenes responsible for elicitation of a protective immune response. Infection and immunity *69*, 622-625.

Schutze, M.P., Deriaud, E., Przewlocki, G., and LeClerc, C. (1989). Carrier-induced epitopic suppression is initiated through clonal dominance. J Immunol *142*, 2635-2640.

Schwarz-Linek, U., Höök, M., and Potts, J.R. (2006). Fibronectin-binding proteins of Gram-positive cocci. Microbes and Infection *8*, 2291-2298.

Scott, J.K., and Smith, G.P. (1990). Searching for peptide ligands with an epitope library. Science *249*, 386-390.

Siegel, D.L., Chang, T.Y., Russell, S.L., and Bunya, V.Y. (1997). Isolation of cell surface-specific human monoclonal antibodies using phage display and magnetically-activated cell sorting: applications in immunohematology. Journal of immunological methods *206*, 73-85.

Siegel, D.L., Stowell, C., and Dzik, W. (2003). Diagnostic and therapeutic applications of phage display technology. Stowell Ch and Dzik W Emerging Technologies in Transfusion Medicine American Association of Blood Bank, Bethesda, Maryland.

Siegrist, C.-A. (2008). Vaccine immunology. Vaccines Saunders.

Silverman, P.M. (1997). Towards a structural biology of bacterial conjugation. Molecular Microbiology *23*, 423-429.

Smith, G.P. (1985). Filamentous fusion phage: novel expression vectors that display cloned antigens on the virion surface. Science *228*, 1315-1317.

Smith, G.P., and Petrenko, V.A. (1997). Phage display. Chemical reviews *97*, 391-410.

Spada, S., Krebber, C., and Pluckthun, A. (1997). Selectively infective phage (SIP). Biological Chemistry *378*, 445-456.

Specthrie, L., Bullitt, E., Horiuchi, K., Model, P., Russel, M., and Makowski, L. (1992). Construction of a microphage variant of filamentous bacteriophage. J Mol Biol, 720-724.

Stengele, I., Bross, P., Garces, X., Giray, J., and Rasched, I. (1990). Dissection of functional domains in phage fd adsorption protein - discrimination between attachment and penetration sites. J Mol Biol *212*, 143-149.

Stopar, D., Spruijt, R.B., Wolfs, C.J., and Hemminga, M.A. (1998). Mimicking initial interactions of bacteriophage M13 coat protein disassembly in model membrane systems. Biochemistry *37*, 10181-10187.

Stopar, D., Spruijt, R.B., Wolfs, C.J., and Hemminga, M.A. (2002). Structural characterization of bacteriophage M13 solubilization by amphiphiles. Biochimica et Biophysica Acta (BBA)-Protein Structure and Molecular Enzymology *1594*, 54-63.

Stopar, D., Spruijt, R.B., Wolfs, C.J.A.M., and Hemminga, M.A. (2003). Protein–lipid interactions of bacteriophage M13 major coat protein. Biochimica et Biophysica Acta (BBA) - Biomembranes *1611*, 5-15.

Stump, M., and Steege, D. (1996). Functional analysis of filamentous phage f1 mRNA processing sites. RNA *2*, 1286.

Sun, T., and Webster, R.E. (1986). fii, a bacterial locus required for filamentous phage infection and its relation to colicin-tolerant tolA and tolB. Journal of bacteriology *165*, 107-115.

Takeya, K., and Amako, K. (1966). A rod-shaped Pseudomonas phage. Virology *28*, 163-165.

Tomasini-Johansson, B., and Mosher, D.F. (2009). Plasma fibronectin concentration in inbred mouse strains. Thrombosis and haemostasis *102*, 1278.

Tranum Kaur, N.N., Olla Wasfi, Katlyn Sheldon, Shawn Wettig, and Roderick Slavcev (2012). Immunocompatibility of bacteriophages as nanomedicines. Journal of Nanotechnology *2012*, 13.

Tseng, Y.H., Lo, M.C., Lin, K.C., Pan, C.C., and Chang, R.Y, and (1990). Characterization of filamentous bacteriophage phi Lf from *Xanthomonas campestris pv. campestris*. J Gen Virol *71* 1881-1884.

Ulivieri, C., Citro, A., Ivaldi, F., Mascolo, D., Ghittoni, R., Fanigliulo, D., Manca, F., Baldari, C.T., Pira, G.L., and Del Pozzo, G. (2008). Antigenic properties of HCMV peptides displayed by filamentous bacteriophages vs. synthetic peptides. Immunology letters *119*, 62-70.

Val, M.E., Bouvier, M., Campos, J., Sherratt, D., Cornet, F., Mazel, D., and Barre, F.-X. (2005). The single-stranded genome of phage CTX is the form used for integration into the genome of *Vibrio cholerae*. Molecular cell *19*, 559-566.

van Houten, N.E., Henry, K.A., Smith, G.P., and Scott, J.K. (2010). Engineering filamentous phage carriers to improve focusing of antibody responses against peptides. Vaccine *28*, 2174-2185.

van Houten, N.E., Zwick, M.B., Menendez, A., and Scott, J.K. (2006). Filamentous phage as an immunogenic carrier to elicit focused antibody responses against a synthetic peptide. Vaccine *24*, 4188-4200.

van Wezenbeek, P.M., Hulsebos, T.J., and Schoenmakers, J.G. (1980). Nucleotide sequence of the filamentous bacteriophage M13 DNA genome: comparison with phage fd. Gene *11*, 129-148.

Vieira, J., and Messing, J. (1982). The pUC plasmids, an M13mp7-derived system for insertion mutagenesis and sequencing with synthetic universal primers. Gene *19*, 259-268.

Vieira, J., and Messing, J. (1987). Production of single-stranded plasmid DNA. Methods in Enzymology *153*, 3-11.

Vos, W.L., Nazarov, P.V., Koehorst, R., Spruijt, R.B., and Hemminga, M.A. (2009). From 'I' to 'L'and back again: the odyssey of membrane-bound M13 protein. Trends in Biochemical Sciences *34*, 249-255.

Waldor, M.K., and Mekalanos, J.J. (1996). Lysogenic conversion by a filamentous phage encoding cholera toxin. Science *272*, 1910-1914.

Wan, Y., Wu, Y., Zhou, J., Zou, L., Liang, Y., Zhao, J., Jia, Z., Engberg, J., Bian, J., and Zhou, W. (2005). Cross-presentation of phage particle antigen in MHC class II and endoplasmic reticulum marker-positive compartments. European journal of immunology *35*, 2041-2050.

Wang, G., Sun, M., Fang, J., Yang, Q., Tong, H., and Wang, L. (2006). Protective immune responses against systemic candidiasis mediated by phage-displayed specific epitope of *Candida albicans* heat shock protein 90 in C57BL/6J mice. Vaccine *24*, 6065-6073.

Wang, L.-F., and Yu, M. (2004). Epitope identification and discovery using phage display libraries: applications in vaccine development and diagnostics. Current drug targets *5*, 1-15.

Webb, J.S., Lau, M., and Kjelleberg, S. (2004). Bacteriophage and phenotypic variation in *Pseudomonas aeruginosa* biofilm development. Journal of bacteriology *186*, 8066-8073.

Webster, R.E. (1991). The *tol* gene products and the import of macromolecules into *Escherichia coli*. Mol Microbiol *5*, 1001-1011.

Webster, R.E., and Lopez, J. (1985). Structure and assembly of the class I filamentous bacteriophage. In Virus structure and assembly, S. Casjens, ed. (Boston, Jones and Bartlett), pp. 235-267.

Weller, M., Wiedemann, P., Heimann, K., and Zilles, K. (1988). Fibronectin quantification in plasma and vitreous by a noncompetitive ELISA technique. Documenta ophthalmologica *69*, 341-351.

Wickner, W. (1975). Asymmetric orientation of a phage coat protein in cytoplasmic membrane of *E. coli*. Proc Natl Acad Sci USA *72*, 4749-4753.

Willis, A.E., Perham, R.N., and Wraith, D. (1993). Immunological properties of foreign peptides in multiple display on a filamentous bacteriophage. Gene *128*, 79-83.

Wrighton, N.C., Farrell, F.X., Chang, R., Kashyap, A.K., Barbone, F.P., Mulcahy, L.S., Johnson, D.L., Barrett, R.W., Jolliffe, L.K., and Dower, W.J. (1996). Small peptides as potent mimetics of the protein hormone erythropoietin. Science *273*, 458-463.

Yang, Q., Su, Q.p., Wang, G.y., Wen, D.z., Zhang, Y.h., Bao, H.z., and Wang, L. (2007). Production of hybrid phage displaying secreted aspartyl proteinase epitope of *Candida albicans* and its application for the diagnosis of disseminated candidiasis. Mycoses *50*, 165-171.

Yip, Y.L., Smith, G., and Ward, R.L. (2001). Comparison of phage pIII, pVIII and GST as carrier proteins for peptide immunisation in Balb/c mice. Immunology Letters *79*, 197-202.

Yoon, K.Y., Tan, W.S., Tey, B.T., Lee, K.W., and Ho, K.L. (2013). Native agarose gel electrophoresis and electroelution: A fast and cost-effective method to separate the small and large hepatitis B capsids. Electrophoresis *34*, 244-253.